NOAA Technical Memorandum ERL AOML-46

AUSTRALIAN TROPICAL CYCLONES KERRY AND ROSA, FEBRUARY - MARCH 1979

Robert C. Sheets
Greg Holland

Atlantic Oceanographic and Meteorological Laboratories
Miami, Florida
May 1981

oaa NATIONAL OCEANIC AND ATMOSPHERIC ADMINISTRATION / Environmental Research Laboratories

NOAA Technical Memorandum ERL AOML-46

AUSTRALIAN TROPICAL CYCLONES KERRY AND ROSA, FEBRUARY - MARCH 1979

Robert C. Sheets

National Hurricane Research Laboratory
Coral Gables, Florida

Greg Holland

Bureau of Meteorology
Department of Science and Technology
Melborne, Australia

Atlantic Oceanographic and Meteorological Laboratories
Miami, Florida
May 1981

UNITED STATES DEPARTMENT OF COMMERCE
Malcolm Baldrige, Secretary

NATIONAL OCEANIC AND ATMOSPHERIC ADMINISTRATION
James P. Walsh, Acting Administrator

Environmental Research Laboratories
Joseph O. Fletcher, Acting Director

NOTICE

The Environmental Research Laboratories do not approve, recommend, or endorse any proprietary product or proprietary material mentioned in this publication. No reference shall be made to the Environmental Research Laboratories or to this publication furnished by the Environmental Research Laboratories in any advertising or sales promotion which would indicate or imply that the Environmental Research Laboratories approve, recommend, or endorse any proprietary product or proprietary material mentioned herein, or which has as its purpose an intent to cause directly or indirectly the advertised product to be used or purchased because of this Environmental Research Laboratories publication.

CONTENTS

AUSTRALIAN TROPICAL CYCLONES KERRY AND ROSA, FEBRUARY - MARCH 1979

Robert C. Sheets and Greg Holland

Abstract

The first known flights by highly instrumented research aircraft into southern hemisphere tropical cyclones were made into Australian Tropical Cyclones Kerry and Rosa of 1979. Three flights were made into Kerry and one into Rosa with one of NOAA's P-3 research aircraft. Data collected during these unique flights are presented along with a brief discussion of the major features of the structures of these storms as revealed by these data sets. In addition, brief summaries of the life cycles of these storms are given and the general synoptic-scale features influencing their behavior are outlined.

1. INTRODUCTION

This report is unique in that it describes a series of special missions into Australian area tropical cyclones. During February and March 1979, a highly instrumented research aircraft operated by NOAA'S Research Facilities Center (RFC), along with scientists from NOAA'S National Hurricane Research Laboratory (NHRL), visited Australia. The aircraft and research teams visited Darwin, Townsville, Brisbane, Sydney, Canberra, and Melborne. Research missions were flown into Tropical Cyclones Kerry and Rosa.

The purpose of this document is to present selected data sets, as recorded on the research aircraft during these tropical cyclone missions, primarily in unanalyzed form, to enable researchers to assess the quality and quantity of data available from these flights. The data are available for scientific research through the Director, National Hurricane Research Laboratory, AOML, Gables One Tower, 1320 South Dixie Highway, Miami, Florida 33146.

The prevailing climatology of the region is outlined together with brief summaries of the life cycles of Tropical Cyclones Kerry and Rosa. In addition, major features of the structure of Cyclone Kerry, as revealed by the aircraft data, are discussed. Much more detailed studies of synoptic-scale influences, storm characteristics, and boundary-layer processess in Cyclone Kerry are under way in collaboration between United States and Australian scientists. The results of these studies will be presented in other reports.

2. SYNOPTIC FEATURES

2.1 Prevailing Situation

The monthly mean streamline analyses for February at the gradient (900-m) and 200-mb) levels are shown in figures 2a and 2b. At the gradient level, there is a well-developed northwesterly monsoonal flow in near-equatorial regions. The monsoonal shearline lies over northern Australia, with depressions just south of Darwin and in the eastern Coral Sea. A heat low persists to the southwest of Darwin. The subtropical ridge lies south of the Australian continent and easterly flow prevails south of 15°-20°S. At the 200-mb level, a well-developed anticyclone is centered above the low-level monsoonal disturbance over northern Australia. The subtropical ridge extends further south over Western Australia than the Coral Sea and is at its most southerly seasonal position. Outflow from the anticyclone extends into the westerlies over northern Australia and across the equator into the Northern Hemisphere through the Coral Sea-Papua, New Guinea region. Marked divergence is apparent above the surface-level depression over the Solomon Islands.

The prevailing gradient-level flow for early February 1979 was fairly typical, though the monsoonal shear zone over northern Australia was quite tenuous and the mean depression over the Coral Sea appeared to have shifted considerably eastward. The upper flow was also generally similar to the mean, except the closed anticyclone center moved eastward away from the continent during part of the month. This was consistent with the weak monsoonal activity over northern Australia.

Sea surface temperatures were up to 2°C higher than average in the region enclosed by 175°E-175°W and 0°S-35°S. Lower- than-average values occurred in the eastern Coral Sea during January and February. These were possibly the factors that caused the anomolously eastward position of the low-level depression. Definitely, in January and early February, there was good evidence from the Japanese Geostationary Meteorological Satellite (GMS) imagery of higher-than-normal convective activity and cloudiness east of 175°E and reduced activity over the Coral Sea. An ITCZ-type cloud band extended along 5°-10°S eastward to 160°W; normally it would have been in the Northern Hemisphere at these longitudes. There was also markedly reduced convection and cloudiness over northern Australia during January and February.

2.2 Tropical Cyclone Kerry

The generally disturbed area east of the Solomons had spawned three tropical cyclones before Kerry. They were Gordon, Henry and Judith (fig. 1). Gordon and Henry reached severe tropical cyclone (hurricane) intensity while moving almost directly southward. Judith, which at best just barely reached severe tropical cyclone (hurricane) intensity, moved on a

southwest course. One cyclone formed east of 170°W after Kerry. The detailed, erratic, path of Tropical Cyclone Kerry is shown in figure 3 and the satellite-derived estimates of central pressure and maximum winds (following Dvorak, 1975) are shown in figures 4 (operational values) and 5 (postanalysis values).

Kerry can be traced back to a low that became evident near 5°S-170°E on February 7. At first it was poorly organized, but by February 10 some cyclonic curvature could be detected in the convection. By February 13 (fig. 6a) the system was displaying consistent organization and appeared to be intensifying. At 0000 GMT on the 13th, Nandi issued the first cyclone warning.

The gradient-level analysis (fig. 7a) shows a well-developed tropical depression with strong cyclonic shear to the south and a westward-extending convergence band between cross equatorial and Southern Hemispheric flows. At 200 mb (fig. 8a) a divergent anticyclone was over the surface cyclone with outflow "channels" into both the easterlies and the westerlies. The satellite imagery indicates a well-organized system with a band of convection extending westward and evidence of cirrus outflow. Estimated central pressure and maximum winds at 0600 GMT were 998 mb and 21 m s^{-1} (fig. 5).

Kerry intensified steadily during February 13, 14, and 15 (figs. 6a-c), while moving west-southwest at 5-10 s^{-1}; by 0000 GMT on the 15th the storm had reached severe tropical cyclone (hurricane) intensity. A well-organized upper level outflow and a strong influx of moisture in the low levels was present at this time (figs. 6c, 7b, and 8b). A central pressure of 978 mb and maximum winds at 35-40 m s^{-1} were estimated (fig. 5). However, further intensification was delayed as Kerry crossed the Solomon Islands (fig. 3). Maximum observed winds in the islands were 20 m s^{-1} at about 70 km south of the cyclone. But widespread destruction and loss of life were experienced, indicating that much stronger winds were present.

After moving southwest away from the Solomons, Kerry again intensified steadily (figs. 5 and 6d-g). It recurved to the southeast, then back towards the southwest. It is very difficult to ascertain a steering mechanism for this early movement and the subsequent highly erratic movement towards the Australian coast. The initial recurvature may have been associated with a passage of a weak middle-to-upper level trough to the south, and the subsequent movement to the west may have been caused by the blocking action of an anticyclone that developed in the low to middle levels over the Tasman Sea. However, the only definitive statement that can be made is that there was no clearly defined steering mechanism. This is consistent with the erratic movement of Kerry.

A maximum estimated intensity of 954 mb and 55 m s^{-1} was obtained on February 19 (fig. 5). By February 20 the cloud features were becoming less well-organized (fig. 6h) and the cyclone was considered to be decaying on February 21 (Fig. 6i)

when the first reconnaissance flight was made. At 0600 GMT the cyclone was estimated to have a central pressure of 975 mb and maximum wind speed of 50 m s^{-1} (fig. 5). From the reconnaissance flight, however, the storm was found to be more intense, with measured winds of 63 m s^{-1} and a central pressure of 958 mb. The cloud features also indicated further filling on February 22 (fig. 6j), whereas the aircraft reconnaissance still gave a central pressure of 957 mb and increased maximum winds of 70 m s^{-1}. The 0000 GMT gradient and 200-mb wind analyses for February 21 and 22 are shown in figures 7c and 7d, and 8c and 8d respectively.

From February 19 to 26 (figs. 6 g-n), Kerry progressively weakened as it moved slowly and erratically around a large loop, during which it crossed its own track on at least three occasions. This weakening may be attributed to the cyclone moving over cool water left from upwelling during a previous passage, an effect which has been described by Brand (1970) and Black (1979). Possible further factors were the interaction with an upper level trough in the westerlies and a tongue of dry air that appeared to move around the west and northwest sides of the cyclone in this period. These are common features of decaying tropical cyclones in the Australian region. During the aircraft reconnaissance flights on February 21 and 22, the presence of dry, low-level air and suppressed convection in the northwest quadrant was obvious. This condition is also subtantiated by the satellite-observed cloud structure (figs. 6j and 6k).

Kerry continued to weaken while moving erratically towards the coast and came within range of the Mackay and Rockhampton Plessey WF44 weather watch radars on February 27. For the remainder of its lifetime Kerry was under continuous surveillance by these radars and those in Townsville and Cairns. The track during this period was determined mainly from time-lapse movies (at 2-min intervals) of the Mackay and Townsville radars. The synoptic situation at landfall is illustrated in figures 7e and 8e.

A sequence of Plan Position Indicator (PPI) radar photographs is shown in figures 9a-c for the period when Kerry approached the coast, crossed the Whitsunday Islands, and made landfall near Mackay. These radar pictures show outer bands on February 27 and a relatively weak vortex, with the eye becoming quite ragged as the center passed over the coastline at about 0400 GMT on March 1 just south of Bowen. Wind speeds > 30 m s^{-1} were recorded and widespread damage, especially from flooding and coastal erosion, was experienced.

Kerry did not remain long over land, but soon moved northward over the Great Barrier Reef and reintensified just east of Townsville. This reintensification is shown by the sequence of radar photographs in figures 10a-d, which depict the formation of a well-defined eye with two main spiral bands converging into the southwest and westerly quadrants. The cyclone became quasi-stationary on March 3 and became more organized, with up to five

spiral bands to the east and south of the center. The maximum satellite-estimated intensity was 988 mb and 28 m s^{-1} at 0600 GMT on March 3 (fig. 5.).

Late on March 3 Kerry accelerated to the southeast, weakened rapidly, and decayed over the ocean on March 6. A low-level reconnaissance around 2300 GMT on March 3 recorded a central pressure of 993 mb and maximum winds of 33 m s^{-1}. At about 0700 GMT on March 4, a commercial Boeing 747 overflying the cyclone at 12,000 m observed an 18°C temperature rise. This was followed by a return to ambient temperatures over a distance of only 13 km! The synoptic situation for 0000 GMT on March 4, 1979, is illustrated in figures 7f and 8f.

Kerry set a number of records for the Australian region. Besides being the first cyclone to be reconnoitered by an instrumented research aircraft, it was the longest-lived and most erratic eastern region cyclone and had the highest observed wind speed in the Australian region. Kerry's total lifetime was 27 days, of which a record 20 days were at cyclone intensity. It is difficult to objectively describe "erratic" behavior, but Kerry underwent at least 11 major changes of direction, which far exceeds the number of changes found during previous observations. The highest winds observed by the aircraft were 70 m s^{-1} at 540 m altitude in the southwest quadrant on February 22. Before this time, the highest observation was a 1-s wind gust of 68 m s^{-1} recorded at an altitude of 30 m at Onslow in Western Australia; the highest for the eastern region was a 1-s gust of 56 m s^{-1} recorded at an altitude of 30 m at Willis Island (fig. 1) in 1957.

2.3 Tropical Cyclone Rosa

Tropical Cyclone Rosa was the third cyclone to develop in the Gulf of Carpentaria in the 1978-79 season. The previous cyclones, Greta and Peter, are shown in figure 1. Rosa was first detected as an area of enhanced convection southwest of the developing Tropical Cyclone Kerry on February 11. This may have been associated with a perturbation in the low-level easterly flow, but lack of data precludes any confirmation. The convective area moved quickly westward towards the southeastern tip of Papua, New Guinea. By 1100 GMT on the 13th, a ship observation indicated a possible surface perturbation, and by 0000 GMT on the 14th a surface depression had formed. The subsequent track is given in figures 11a and 11b along with selected, estimated, minimum sea-level pressures.

Little, if any, intensification occurred as the system moved at 5-10 m s^{-1} across the Coral Sea and Cape York Peninsula. After crossing Cape York Peninsula, Rosa began a meandering path around the Gulf of Carpentaria. It intensified slightly on the 19th and 20th and weakened on the 21st before reintensifying into a tropical cyclone from February 22 thought 24. The analyses for February 21 and 22 (figs. 7c and 7d; 8c and 8d) and the satellite

picture for February 21 (fig. 6j) indicate a well-developed low-level depression with an influx of tropical air from the Arafura Sea. The depression was overlaid by an upper level anticyclone and there was evidence of divergent flow into the westerlies. The cyclone intensified rapidly on the 24th and 25th and reached a maximum (estimated from satellite) intensity of 970 mb with 45 m s^{-1} winds at 0400 GMT on February 26 as it crossed the coast (fig. 12). The synoptic situation for February 26 and 27 is shown in figures 13 and 14. The planned aircraft reconnaissance pattern could not be accomplished as the cyclone crossed the coast while the aircraft approached. However, a major portion of the pattern was completed and maximum winds of 40 m s^{-1} were recorded in the left rear quadrant. A minimum sea-level pressure (MSLP) of 974 mb was obtained from a dropsonde. (It is uncertain whether this represents the lowest pressure.) The maximum observed surface wind was 25 m s^{-1} about 60 km to the south of Rosa.

Rosa continued rapidly westward across northern Australia. It decayed very slowly and maintained a good organization and gale force winds for a number of days

3. FLIGHT DATA

3.1 Introduction

The flight data are displayed in two basic formats. These are plan views of the aircraft position relative to the storm center with superimposed wind speeds and directions versus time and profiles of selected elements plotted versus radial distance from the storm center. The arrangement of figures is such that a plan view for a given level is followed by radial profiles of selected elements that correspond to the flight legs displayed on the plan view. All data are plotted relative to the center of the storm rather than relative to geographical positions.

The plan views contain positions and winds at 1-min intervals, as well as wind directions (nearest 10°) and speeds (meters per second) listed at 2-min intervals. For instance, the wind speed and direction observed at 0550 Z on February 21, 1979, (fig. 16) is coded as 545, which means the wind was from 150° (between 145° to 154°) at 45 m s^{-1}. The elements shown in profile form are plotted at a frequency of one observation every 10 s.

The standard elements plotted out are defined as follows:

1) Azimuth. Radial direction, in degrees, of the aircraft position (observation point) from the storm center. (North is 360°.)

2) Vertical Wind Speed. Speed (meters per second) of the vertical component of the wind as measured by the Inertial

Navigation System (INS) and angle of attack (vertical angle of wind relative to the aircraft).

3) Adjusted "D" Value. A measure of pressure computed as the actual altitude (Radar Altitude) of a given pressure surface minus the altitude of that same pressure surface in the U.S. Standard Atmosphere (Pressure Altitude) where values are adjusted to a constant reference level or pressure. That is, adjusted "D" value = RA-PA plotted in meters.

4) Adjusted Temperature. Free-air temperature in degrees centigrade adjusted to the reference level, from an assumed lapse rate of $6.5°C\ km^{-1}$*.

5) Adjusted Dewpoint. Free-air dew point in degrees centigrade adjusted to the reference level, from an assumed lapse rate of $6.5°C\ km^{-1}$*.

6) Relative Wind Speed. Wind speed in meters per second relative to the storm center. That is, the translational component caused by storm motion is subtracted from the measured wind.

7) Actual Wind Speed. Observed wind speed in meters per second.

In addition, some selected digitized PPI radar data are presented from the lower fuselage radar and the nose radar. Because of sea clutter and mechanical problems (the lower fuselage radar was unstabilized during the flights on February 21 and 22) it was necessary to composite data. Also, most of the lower fuselage radar data collected at middle and upper levels are unusable.

Another instrument problem existed that involved temperature measurement. Fortunately, this problem appeared to be initiated only when saturation conditions were encountered at temperatures colder than -5° or -6°C. Apparently deicing equipment features failed to keep the temperature sensor free of ice or liquid water. The result is that temperatures appear colder than actual. At times it appears easy to determine when the temperature was incorrect; that is, when the temperature suddenly became much colder than the dew point temperature at the time saturation conditions were first encountered. However, it is difficult to determine when or if the sensor recovered after drier or warmer conditions were encountered. With these factors in mind, users must exercise caution when referring to the temperatures in these data sets at the upper levels for flights on February 21, 22, and 26. However, much of the temperature data recorded at these levels appear to be correct. Therefore, we have included all of the profiles in this document, but have

* Temperatures and dew points are usually only adjusted over small vertical distances, which generally results in negligible errors from possible differences in assumed and actual lapse rates.

indicated the regions where, in our opinion, the values are incorrect or, at a minimum, quite questionable. To assist the casual user, we have included an estimated smooth profile for regions of incorrect or highly questionable temperature values. These smooth profiles were arrived at by constructing vertical profiles of temperature at radial distances of 25, 50, 75 and 100 km along each radial leg of the pattern. That is, temperature values at the 540-m, and 500-, 400- or 450-mb levels were plotted on thermodynamic charts. Values at the upper level were then adjusted, if necessary, based upon moist adiabatic ascent, or other lapse rates indicated by the lower level measurements and/or dew point temperatures. The resulting estimated smooth temperature profile for these questionable areas is indicated by the bold dashed line. The resultant values should not be taken as absolute correct values, but should only be used as first-guess estimates.

The next question that arises is, What other elements depicted are affected by erroneous temperature measurements? The answer is winds, since True Air Speed (TAS) measurements are temperature-dependent. Fortunately, < 2% errors in the TAS are generated by temperature errors of ± 10 °C at the average airspeeds and temperatures encountered at the levels where the temperature data are in question. Furthermore, this TAS error has only a minimal effect on wind directions normal to the aircraft track as generally encountered on radial passes through the storm center. That is, 10°C temperature errors would result in < ± 1 m s^{-1} and ± 2 m s^{-1} wind speed errors for winds normal to the flight track at 30 m s^{-1} and 80 m s^{-1}, resectively. However, if the wind direction is parallel to the flight track, the error in the TAS is reflected totally in the wind speed. That is, a 10°C temperature error at approximately the 270°A level would result in approximately a 3 m s^{-1} TAS and wind speed error, which, of course, would represent a 10 % error for a 30 m s^{-1} wind. However, the wind speed profiles presented in this document are for radial passes and errors caused by these erroneous temperatures should be minimal.

3.2 Kerry - February 21, 1979

The mission into Tropical Cyclone Kerry on February 21, 1979, included completion of patterns at altitudes of 500 m, and 500 and 400 mb. As noted in the synoptic-scale discussion, the storm had apparently decreased in strength (based upon satellite evaluations) from peak intensities on February 19. The minimum sea-level pressure at the time of this mission was approximately 958 mb. A PPI digitized radar analysis (fig. 15) shows that most of the deep convection was located on the eastern side of the storm at the time of this mission. A large eye (about 85 km diameter) was open to the northwest and there was very little convection west of the eye. However, low-level wind speeds > 50 m s^{-1} were observed over a large area out to radial distances of 100 km; wind speeds > 45 m s^{-1} extended outward to 150 km southwest of the storm center (fig. 16). Temperatures were

approximately 4°C warmer in the eye at this level than in the eyewall or at larger radial distances. Although the flight was quite turbulent at this level, vertical winds rarely reached 4 m s^{-1}. Figures 16 through 25 show data collected during the approximately 2 h and 20 min required to complete the low-level pattern.

Figures 26 through 35 show data collected at the 500-mb level. Wind speeds on the south and west sides of the storm (region of minimal convection) were considerably less than those recorded at the lower level. Also, peak winds were observed to be at large distances from the storm center and often remained nearly constant from the peak wind outward to the end of each radial pass. Temperature rises in the eye of the storm of near 8°C were recorded on each pass through the storm center, with air on the west and southwest side being much warmer and drier than for comparable regions on the east side. Vertical winds, again, were generally small.

Figures 36 through 45 show data collected at the 450- and 400-mb levels. The features briefly discussed for the 500-mb level were also generally present at these higher levels. However, vertical winds on the east side of the storm approached 5 m s^{-1} occasionally as compared with much smaller values at lower levels. In addition, considerable icing occurred in the northeast part of the storm, causing the aircraft to lose altitude. The result was that the final pass through the storm was near the 450-mb level, rather than the 400-mb level as for the other two passes. This factor should be noted when one compares observations from the three passes. Also, possible errors in temperatures at these upper levels, as discussed in section 3.1, should be noted.

3.3 Kerry - February 22, 1979

When the research aircraft penetrated the storm on February 22, Tropical Cyclone Kerry was in nearly the same position as it was on the previous day. Also, the storm structure appeared remarkably similar. Figure 46 shows a radar composite of Kerry from 0552 Z to 0637 Z on February 22, 1979. The eye of the storm continued to be quite large and open to the west. There was very little convection on the west side of the storm. The eastern half of the storm appeared to be more active than for the 21st. However, as mentioned, the lower fuselage radar was unstabilized on these two days and direct comparisons are subject to question.

Figures 47 through 56 show data collected near the 500-m level. The minimum sea-level pressure, again, was near 957 mb, and there were extensive areas of wind speeds > 50 m s^{-1}. Turbulent motion was quite strong at this level and vertical winds were larger on this day than for the 21st. Also, peak winds in the southwest quadrant exceeded 60 m s^{-1}, which was slightly stronger than for the previous day.

Figures 57 through 66 show data collected at the 500-mb level. Again, major decreases in wind with height can be noted for the western side of the storm, whereas the eastern sectors (region of convection) showed greater consistencies of wind with height. The center of the storm was quite warm as compared with its surroundings, but, in contrast to the structure observed on the 21st, it was not quite as asymmetric in its distribution.

Figures 67 through 76 show data recorded at the 500- and 450-mb levels. Storm characteristics at this and the lower level were similar to those of the previous day. Heavy icing in the northeast sector of the storm caused a loss of altitude, resulting in the northeast-to-southwest pass being made at 450 mb, as compared with 400 mb for the other two passes at the upper level.

3.4 Kerry - March 1, 1979

Kerry, in a much weakened state, made landfall on the northeast coast of Australia near Mackay on March 1. The NOAA research aircraft was returning to Townsville from a mission in Darwin at this time. One quick pass was made into the storm before the aircraft landed at Townsville. In figure 77, the digitized PPI radar shows a single large, but relatively weak, rainband at this time. Figures 78 through 80 show data recorded on the passes into and out of the storm. Comparisons of these data with those shown for February 21 and 22 show the degree to which the storm had, fortunately, weakened before landfall.

3.5 Kerry - March 4, 1979

Kerry moved northward over the open water north of Townsville and started to reintensify. A single-level research mission was scheduled into the storm at this time. Figure 81 shows a PPI radar composite, made during this mission, which depicts some semblance of a partial eye wall and some rainbands. Figures 82 through 91 show data collected at the 500-m level during this mission. A well-formed, though quite asymmetric, circulation system is depicted with maximum wind speeds nearing hurricane force (33 m s^{-1}). The minimum sea-level pressure was near 993 mb.

3.6 Rosa - February 26, 1979

Tropical Cyclone Rosa formed in the Gulf of Carpenteria, as mentioned. The storm was moving west-southwest and the eye was just crossing the southwest coast of the Gulf of Carpenteria by the time the research aircraft approached. Therefore, no complete penetrations of the eye were made (RFC policy is not to penetrate storms over land), although each pass entered the eyewall at each of the two levels (500 m and 450 mb) where the data were collected.

Figure 92 shows a PPI radar composite of Rosa from of 0410 Z to 0450 Z on February 26, 1979. A well-organized storm with major rainbands and a closed eyewall is depicted. The eye diameter was 30 km, with the most intense convection located on the eye's west side.

Figures 93 through 102 show data collected near the 500-m level during these missions. Wind speeds > 45 m s^{-1} were observed on the side of the storm. A minimum pressure of near 983 mb was recorded at the closest point of penetration to the storm center. However, a dropwindsonde, which may have drifted closer to the storm center, gave a minimum reading of 974 mb. Also, when pressure/wind relationships developed in the Atlantic are used, a sustained wind of 95 kt corresponds to a minimum sea-level pressure of 966 mb (Kraft, 1961). Estimates using Pacific data would result in a minimum sea-level pressure of 959 mb (Atkinson and Holliday, 1977). Estimates from satellite imagery (Dvorak, 1975) gave 970 mb.

Figures 103 through 109 show data collected at the 450-mb level on long radial legs northeast and east-southeast of the storm center and short legs west-northwest of the center. The wind speed profiles are quite flat at this level, with maxima near 30 m s^{-1}.

4. SUMMARY

The first flights by highly instrumented research aircraft into southern hemisphere tropical cyclones were made into Australian-area Tropical Cyclones Kerry and Rosa of 1979. The internal structures of these storms were well documented. Complete multiple-level data sets were collected on February 21 and 22 in Kerry; more limited data sets were obtained on March 1 and 3 for Kerry and on February 26 for Rosa. These data sets are presented here in graphical form.

5. ACKNOWLEDGMENTS

Many groups and individuals were involved in coordinating this program, collecting the data illustrated in this report, and preparing that data for publication. Paramount among those, of course were the participating crews and staffs of the Research Facilities Center, National Hurricane Research Laboratory and the Australian Bureau of Meteorology. In addition, outstanding support and participation was received from the Royal Australian Air Force (RAAF) and James Cook University. Special recognition goes to Dr. Wilmot Hess and Mr. Merlin Williams of NOAA/ERL for originating the plan for this mission, and to Dr. Robert Brook, Australian Bureau of Meteorology, who prepared the draft mission plan. Dr. Brook also assisted in developing schedules, along with Dr. C.B. Emmanuel of RFC and the two authors. Special

meteorological support was received from Mr. Ray Wilkie and his staff of the Brisbane office, Mr. Rex Falls and his staff of the Darwin office, and Mr. John McGann and his staff of the Australian Bureau of Meteorology at Townsville. In addition, Dr. Tom Keenan of the Research and Development Branch of the Bureau of Meteorology gave assistance for several facets of this paper.

Finally, the authors wish to dedicate this paper to the memory of Mr. James McCory, who worked so diligently and resourcefully during these and many other missions during his tenure at RFC and NHRL. The work of people such as Jim, behind the scenes, often goes unrecognized; yet without their contributions such programs would not be possible.

6. REFERENCES

Atkinson, G. D., and C. R. Holliday (1977): Tropical cyclone minimum sea-level pressure/maximum sustained wind relationship for the western North Pacific. Mon. Wea. Rev., 105, pp. 421-427.

Black, P. G. (1979): Ocean response to moving tropical cyclones. Pres., Workshop on the Mechanisms of Cyclones-NOAA/Austr. Bur. Meteor/James Cook University of North Queensland, Feb. 28 - March 2, 1979, Townsville, Australia.

Brand, S. (1970): Effects on a tropical cyclone of cooler surface waters due to upwelling and mixing produced by a prior tropical cyclone. J. Appl. Meteor., 10, 865-874.

Dvorak, V. F. (1975): Tropical cyclone intensity analysis and forecasting from satellite imagery. Mon. Wea Rev., 103, 420-430.

Kraft, R. H. (1961): The hurricane's central pressure and highest wind. Mar. Wea. Log, 5, 157.

Appendix

Illustrations

Figure

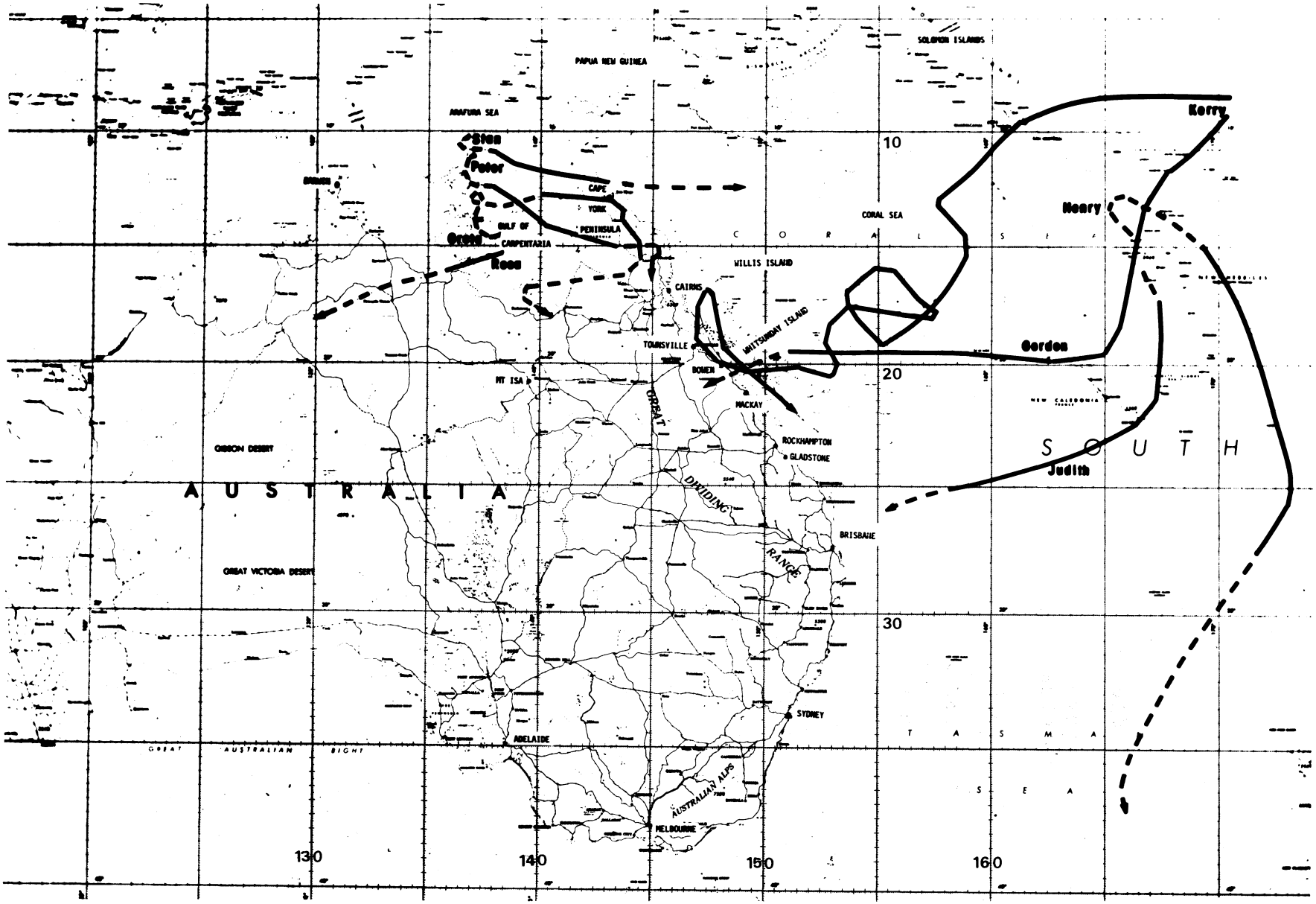

Figure 1. Geographical/topographical map of Australia and surrounding area with superimposed tracks of 1979 tropical cyclones. Solid lines indicate stages of tropical cyclone (tropical storm) intensity ($\geq$ 17 m s^{-1} or 34 kt) and dashed lines depict pre- or post-tropical cyclone stages.

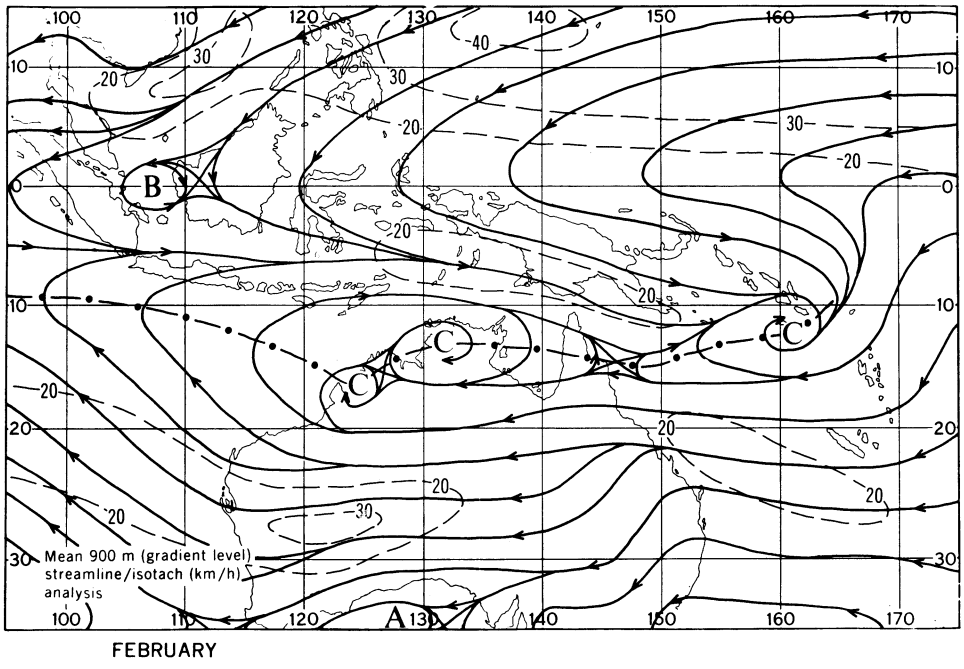

a.

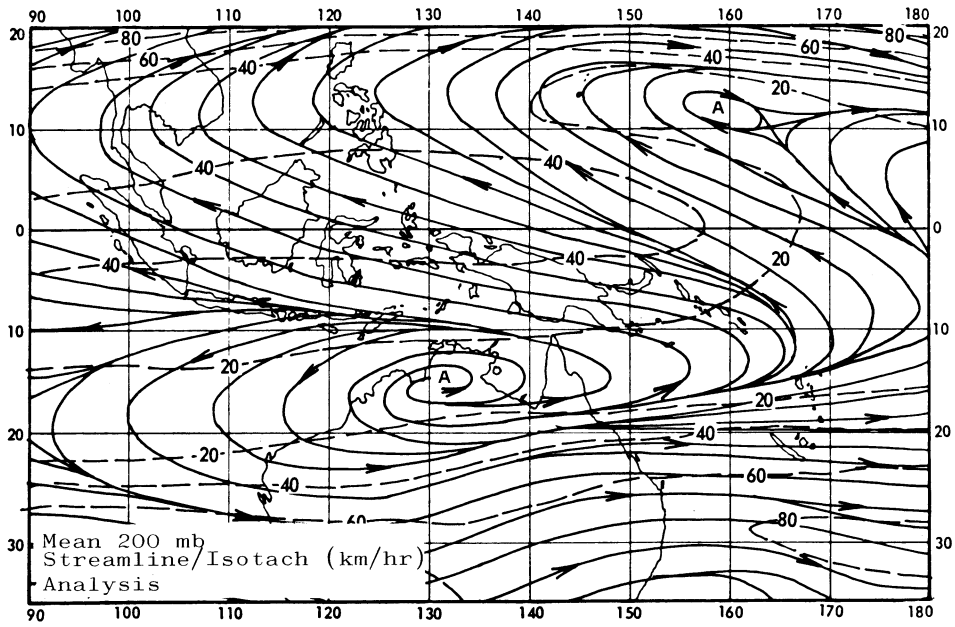

b.

Figure 2. Australian-area February mean streamline and isotach analysis at the (a) gradient (900-m) and (b) 200-mb levels.

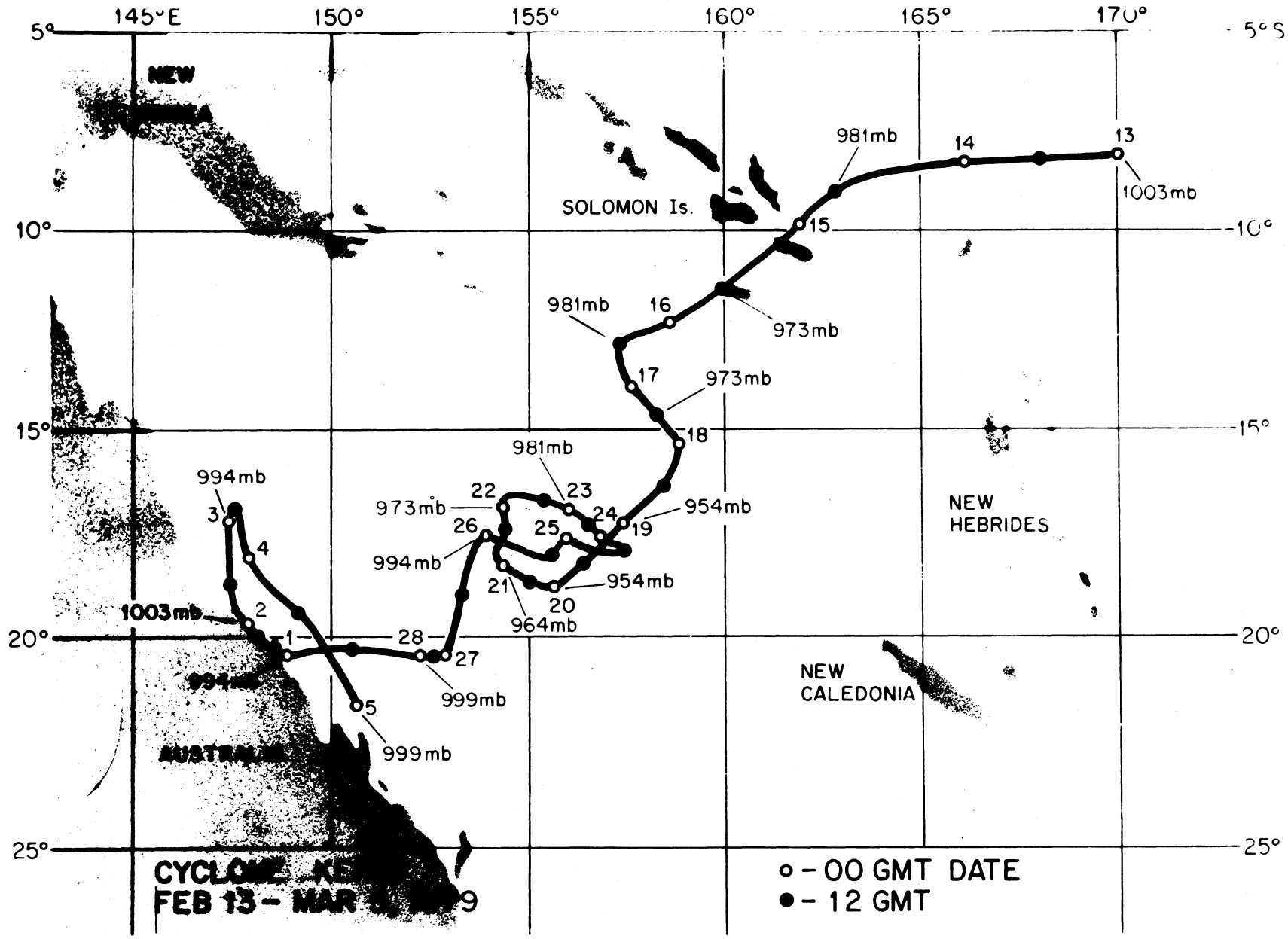

Figure 3. Detailed track of Tropical Cyclone Kerry with selected, superimposed, estimated Minimum Sea Level Pressures (MSLP).

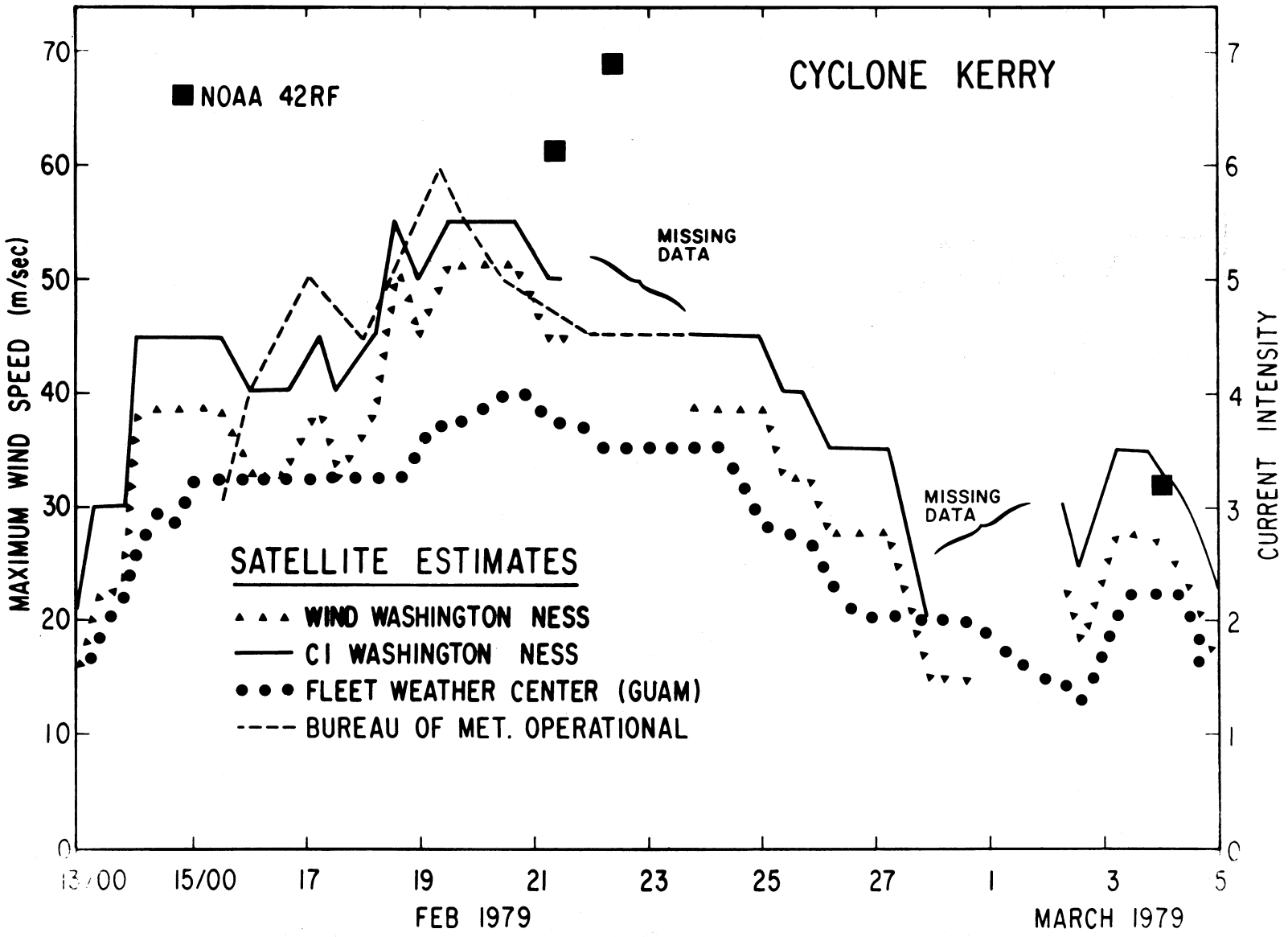

Figure 4. Operationally derived estimates of Tropical Cyclone Kerry maximum wind speeds.

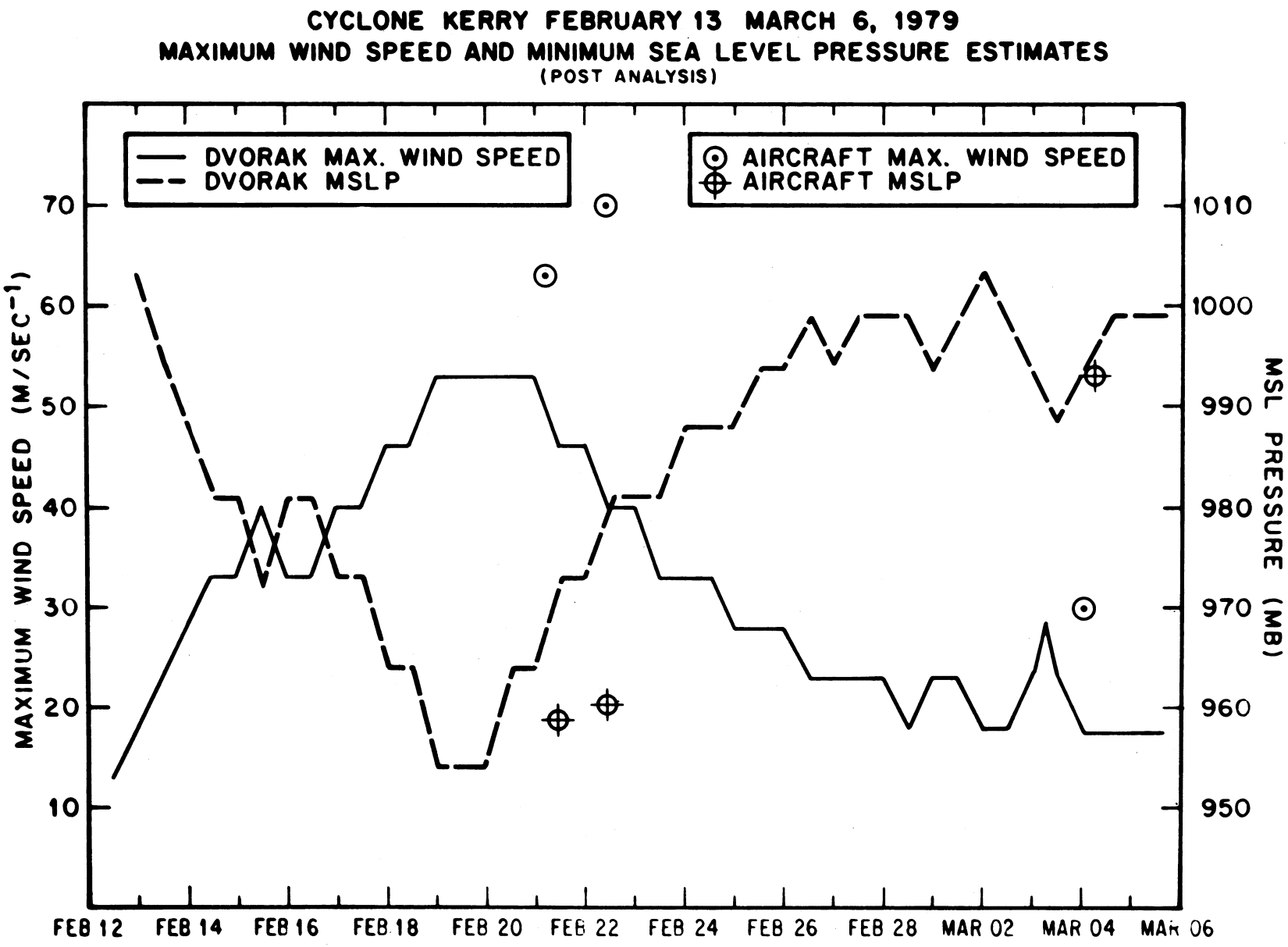

Figure 5. Bureau of Meteorology postanalysis of Tropical Cyclone Kerry maximum wind speeds and MSLP.

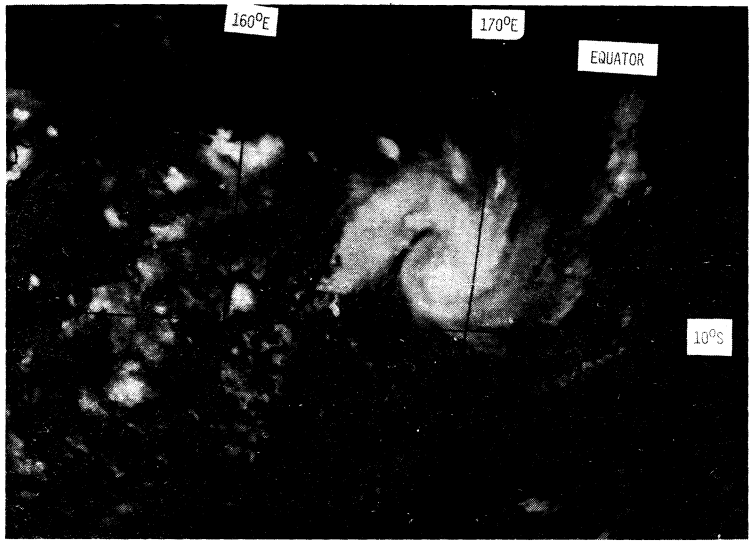

a.

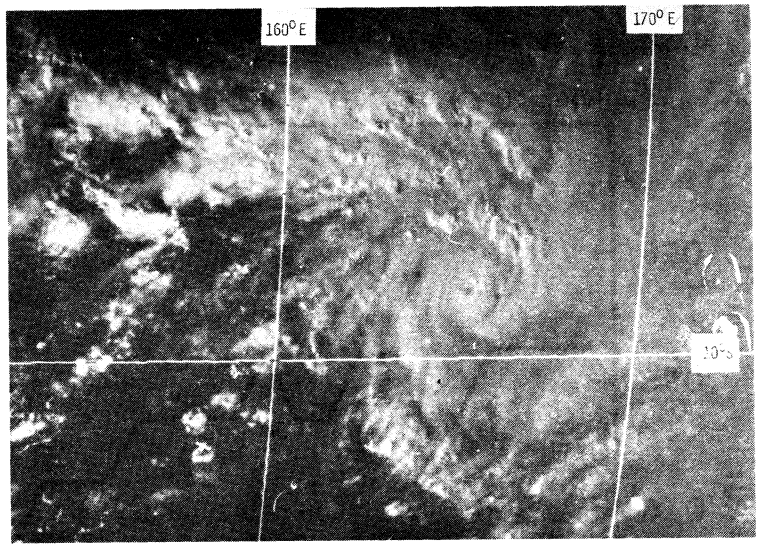

b.

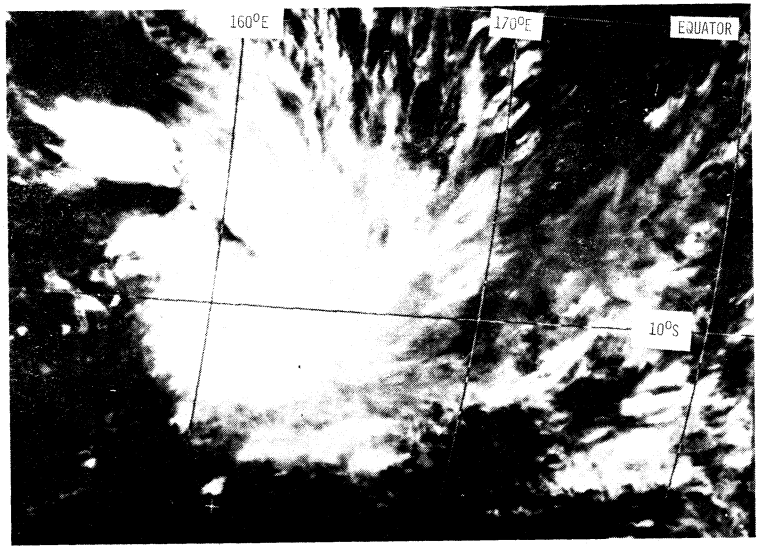

c.

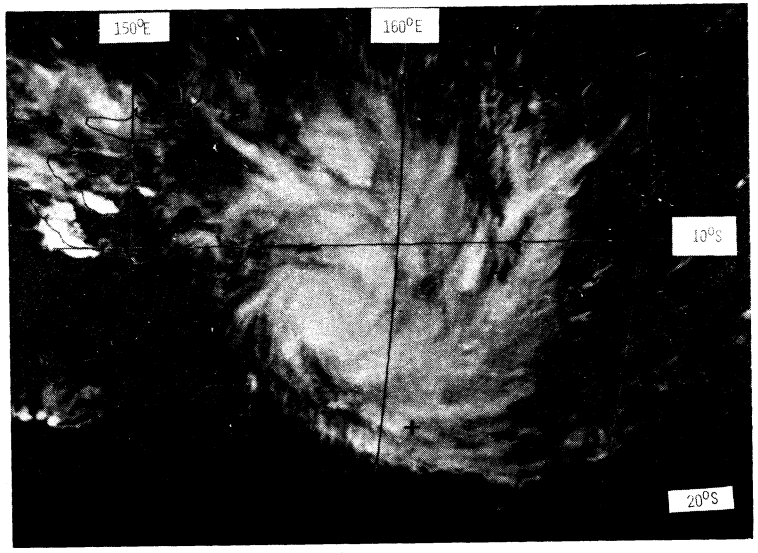

d.

Figure 6. Japanese Geosynchronous Meteorological Satellite (GMS) pictures of Tropical Cyclone Kerry at 0600 GMT on (a) February 13, (b) February 14, (c) February 15, and (d) February 16, 1979.

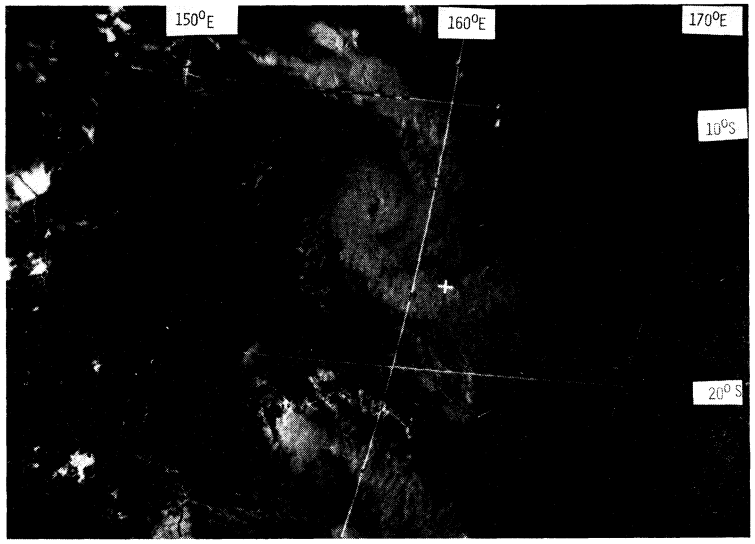

e.

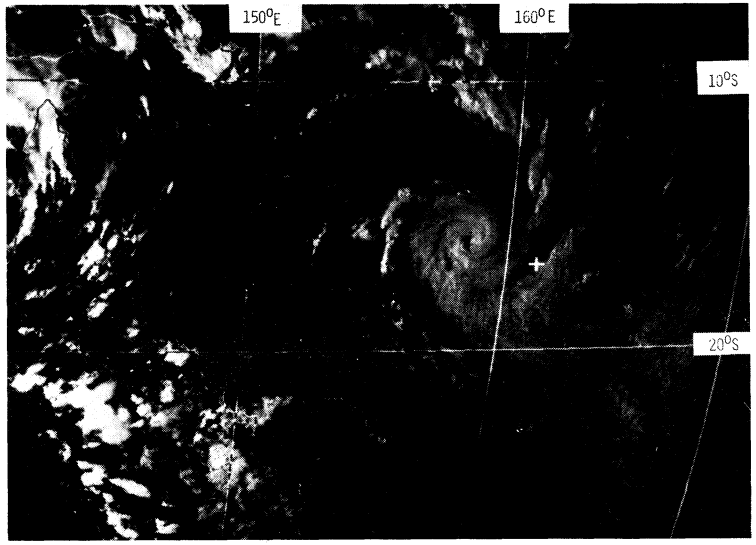

f.

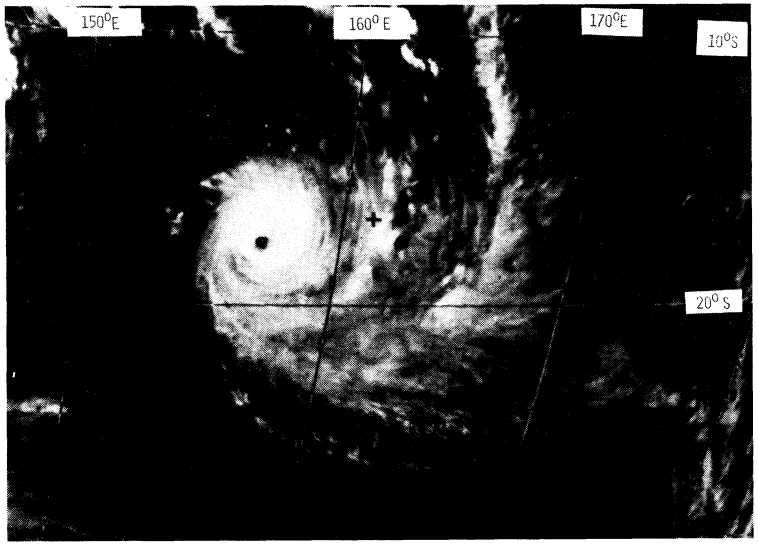

g.

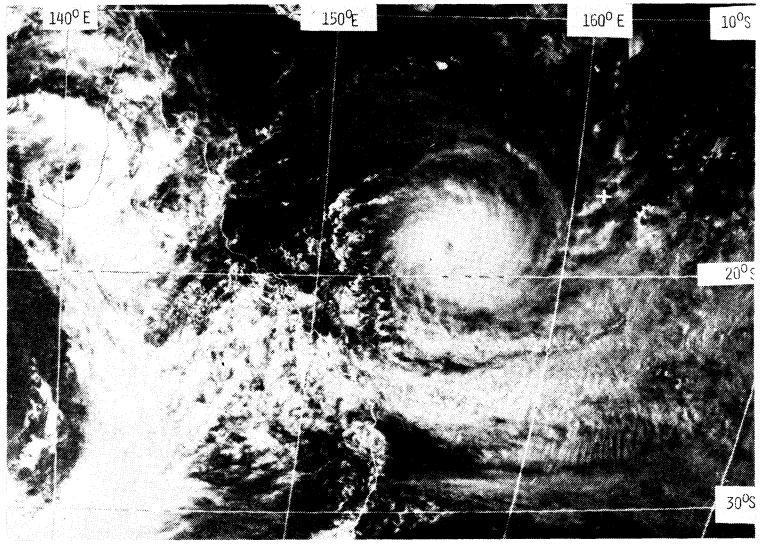

h.

Figure 6. Japanese Geosynchronous Meteorological Satellite (GMS) pictures of Tropical Cyclone Kerry at 0600 GMT on (e) February 17, (f) February 18, (g) February 19, and (h) February 20, 1979.

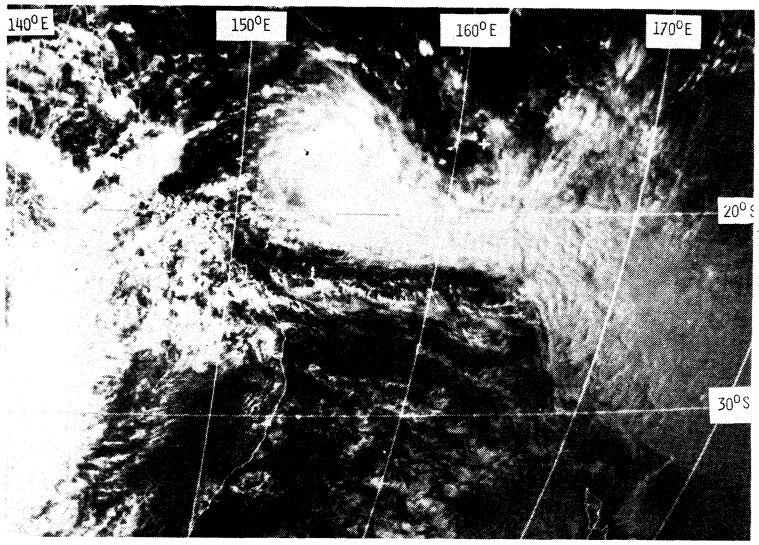

i.

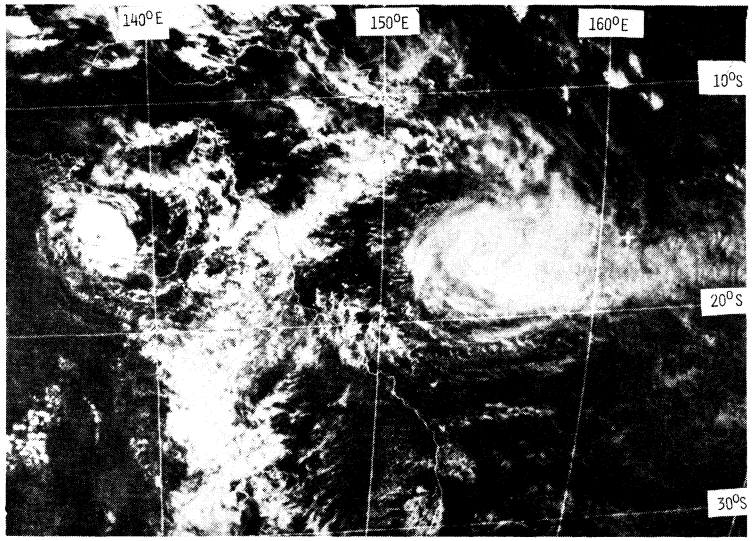

j.

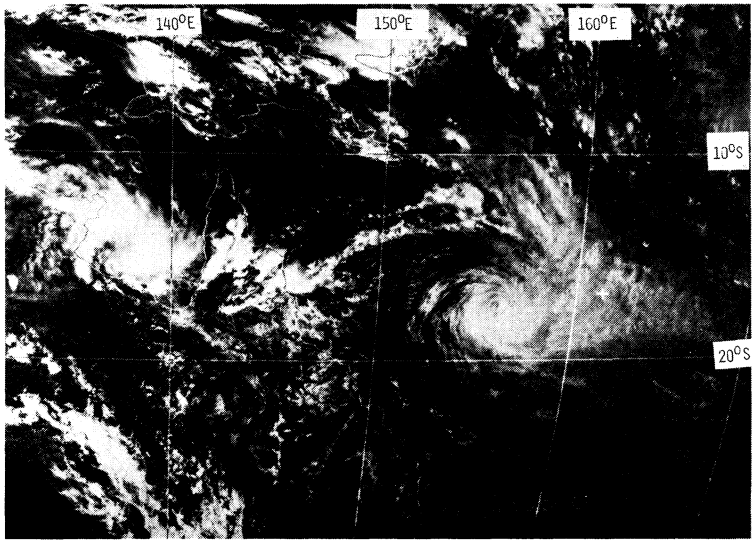

k.

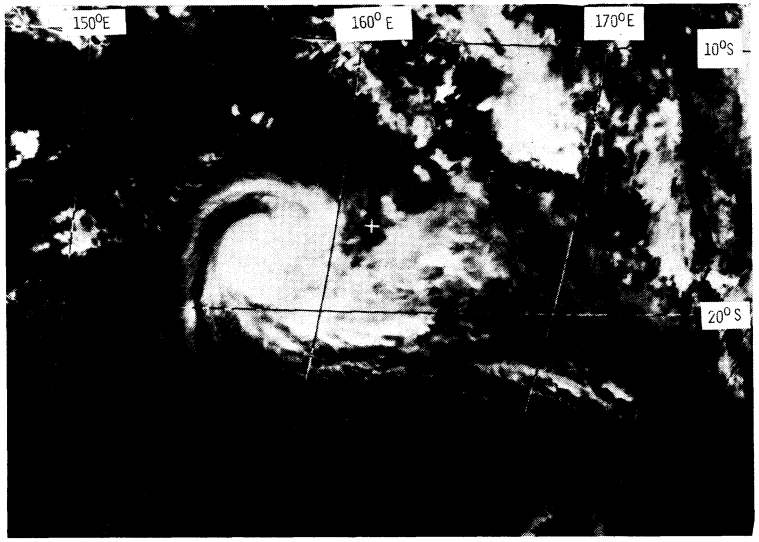

l.

Figure 6. Japanese Geosynchronous Meteorological Satellite (GMS) pictures of Tropical Cyclone Kerry at 0600 GMT on (i) February 21, (j) February 22, (k) February 23, and (l) February 24, 1979.

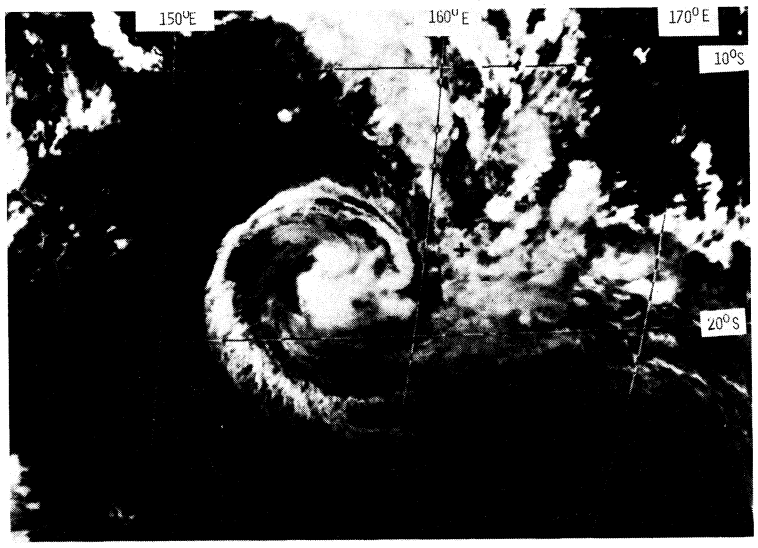

m.

n.

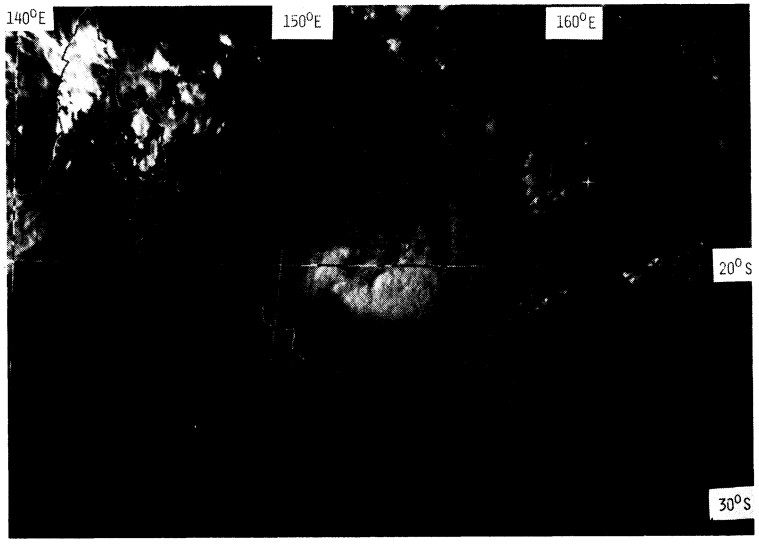

o.

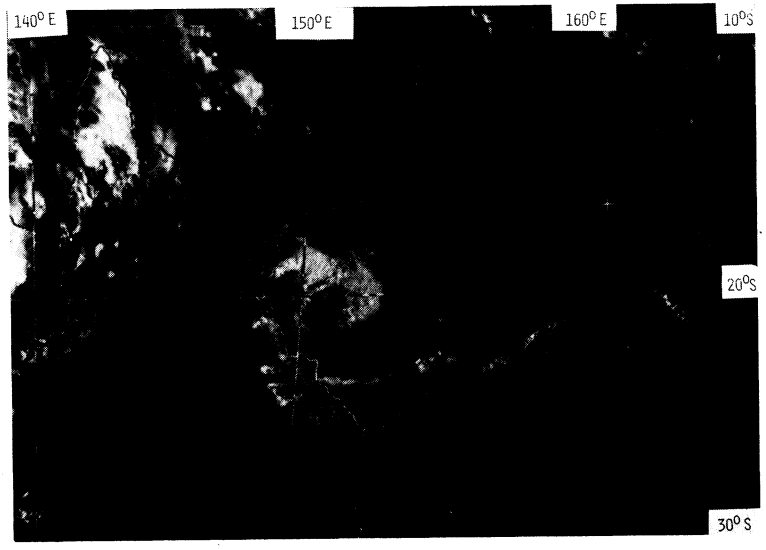

p.

Figure 6. Japanese Geosynchronous Meteorological Satellite (GMS) pictures of Tropical Cyclone Kerry at 0600 GMT on (m) February 25, (n) February 26, (o) February 27, and (p) February 28, 1979.

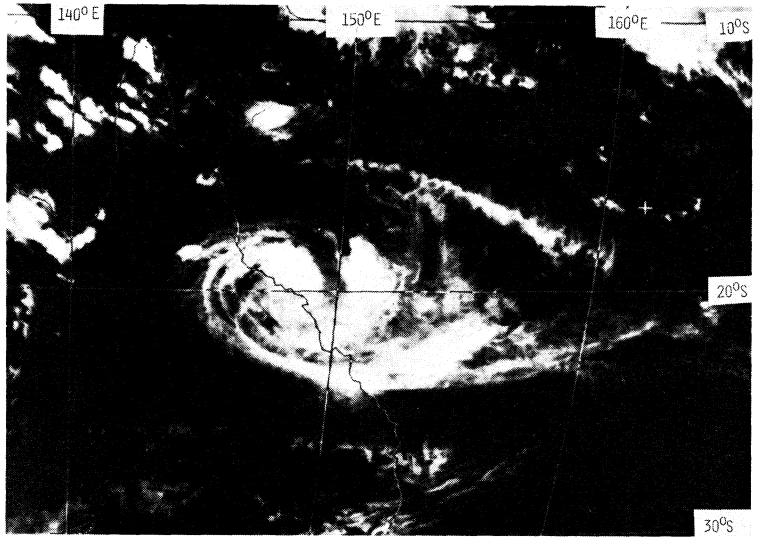

q.

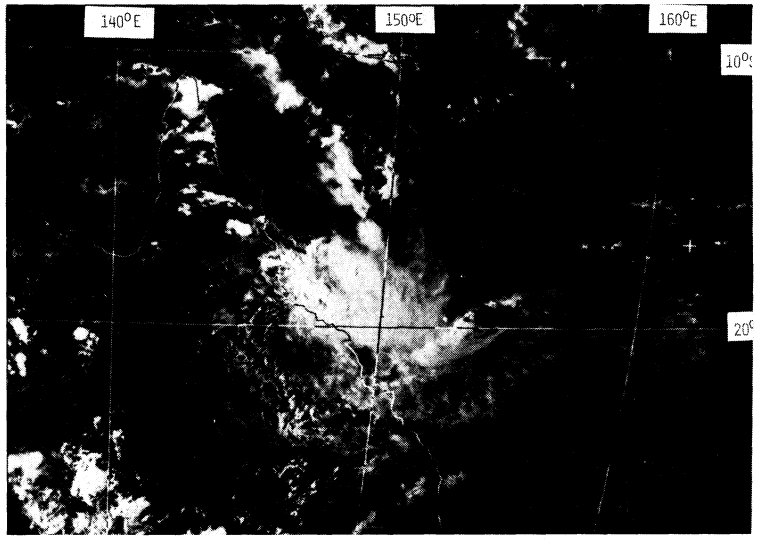

r.

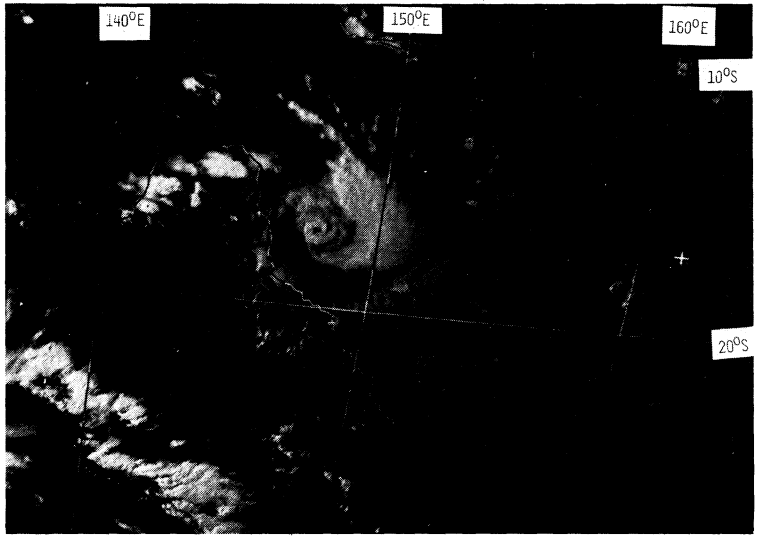

s.

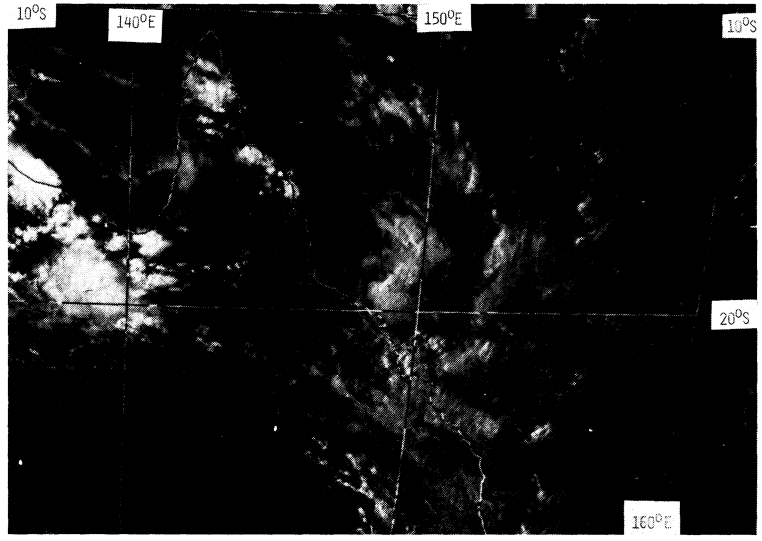

t.

Figure 6. Japanese Geosynchronous Meteorological Satellite (GMS) pictures of Tropical Cyclone Kerry at 0600 GMT on (q) March 1, (r) March 2, (s) March 3, and (t) March 4, 1979.

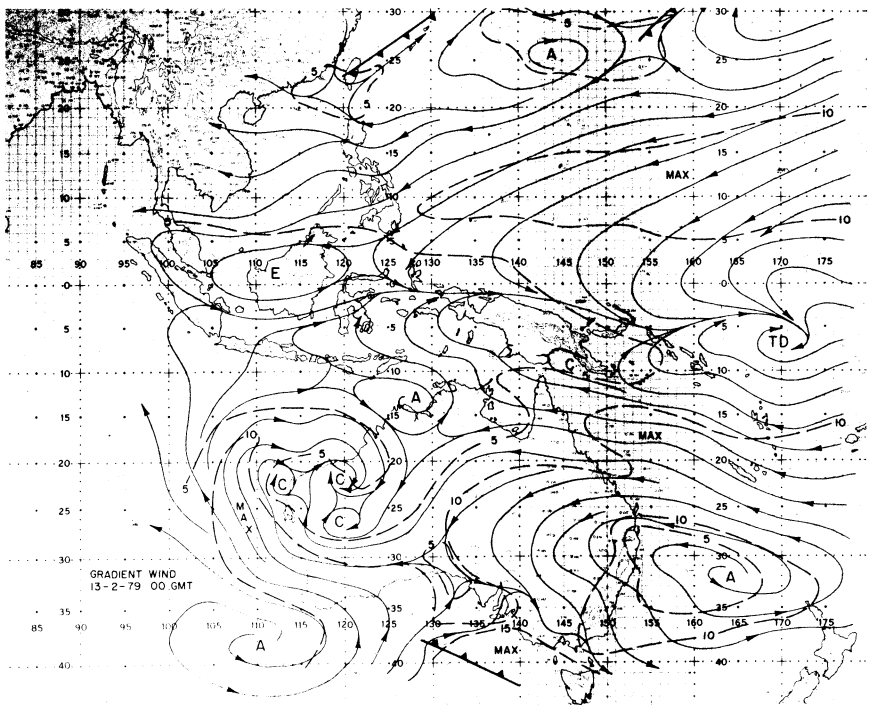

a.

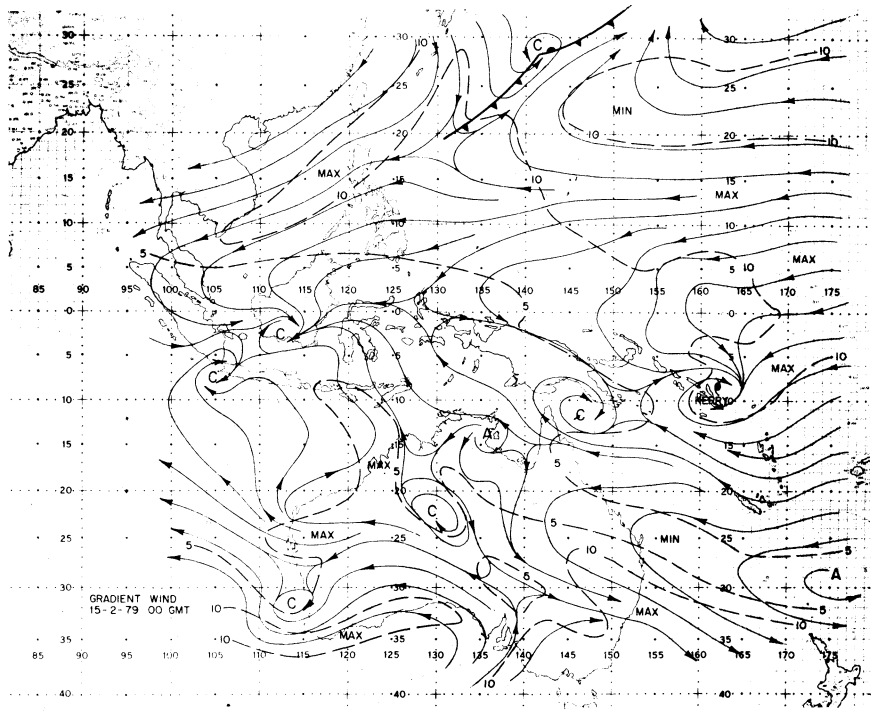

b.

Figure 7. Streamline and isotach analyses of the gradient wind level (900 m) for the Australian region at 0000 GMT on (a) February 13, and (b) February 15, 1979.

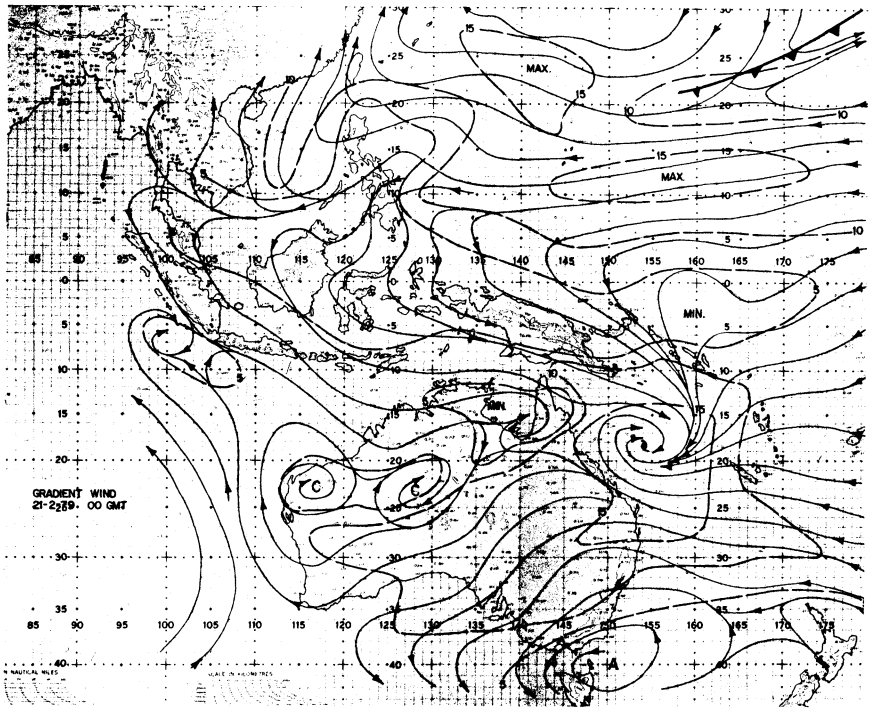

c.

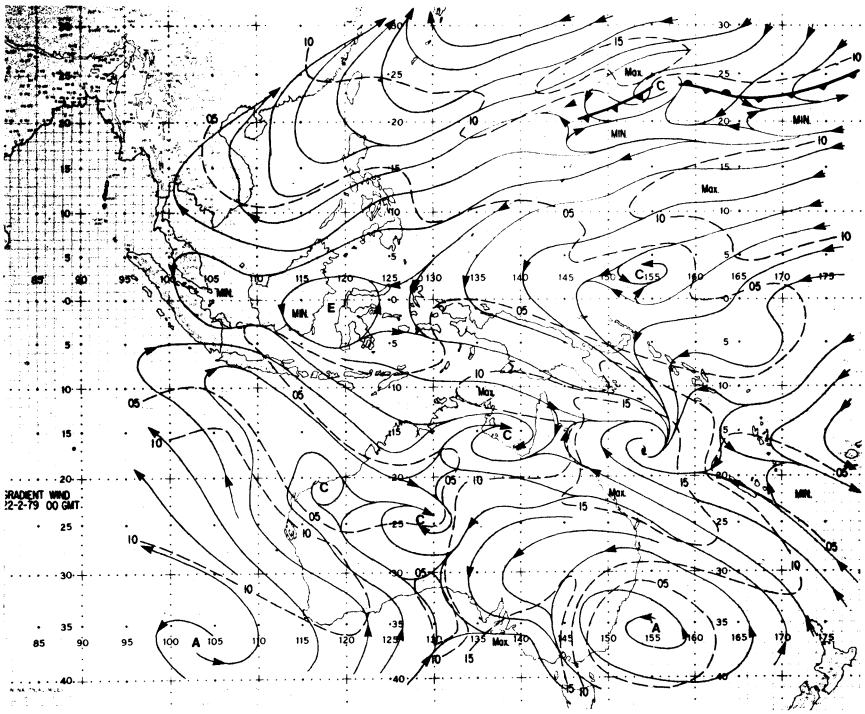

d.

Figure 7. Streamline and isotach analyses of the gradient wind level (900 m) for the Australian region at 0000 GMT on (c) February 21, and (d) February 22, 1979.

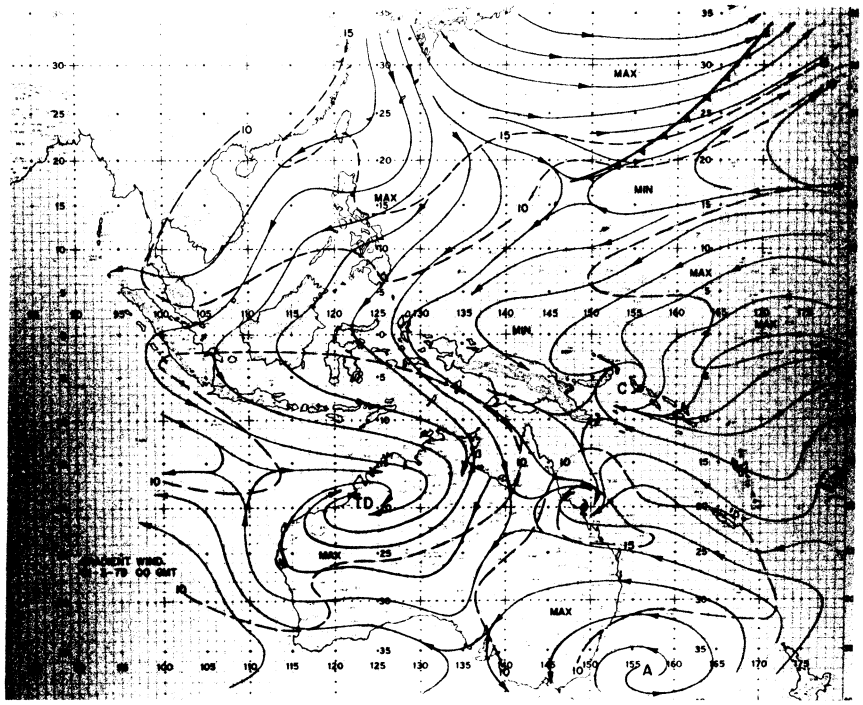

e.

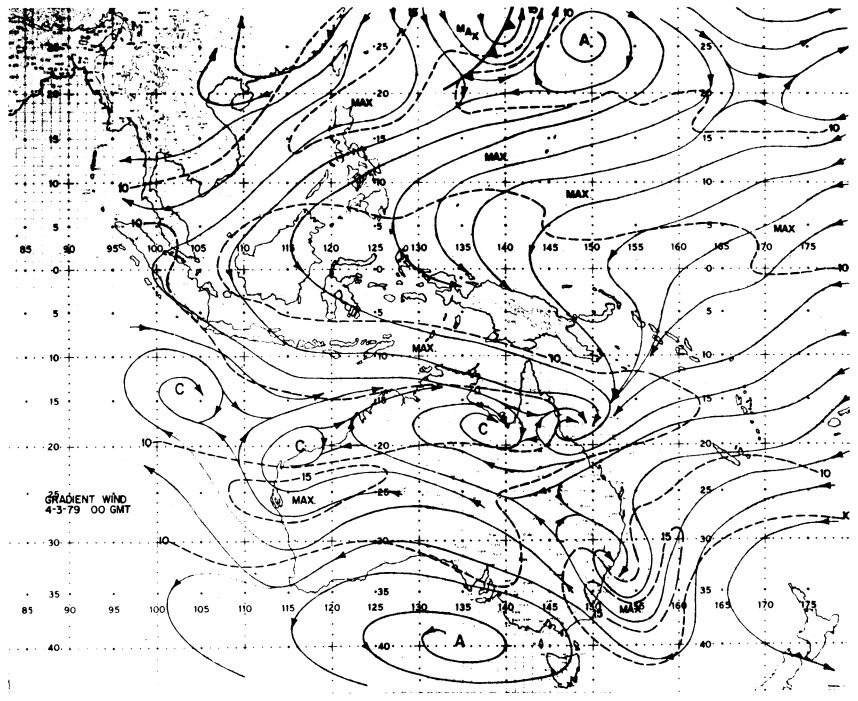

f.

Figure 7. *Streamline and isotach analyses of the gradient wind level (900 m) for the Australian region at 0000 GMT on (e) March 1, and (f) March 4, 1979.*

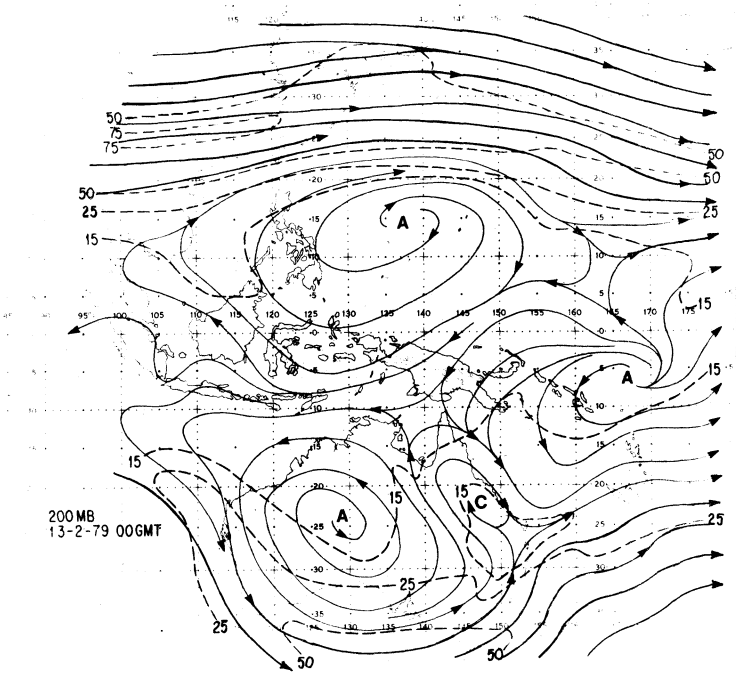

a.

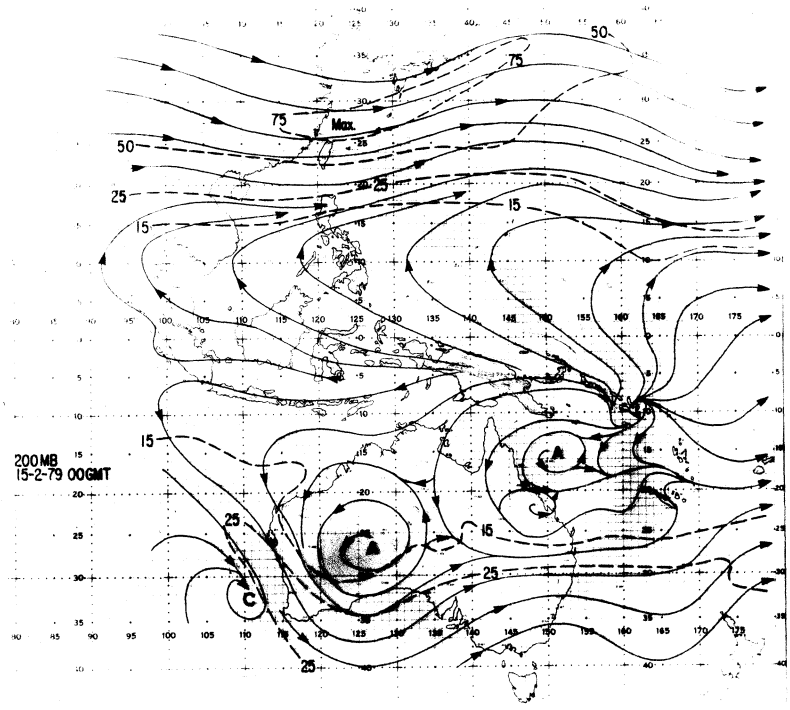

b.

Figure 8. Streamline and isotach analyses for the 200-mb level for the Australian region at 0000 GMT on (a) February 13, and (b) February 15, 1979.

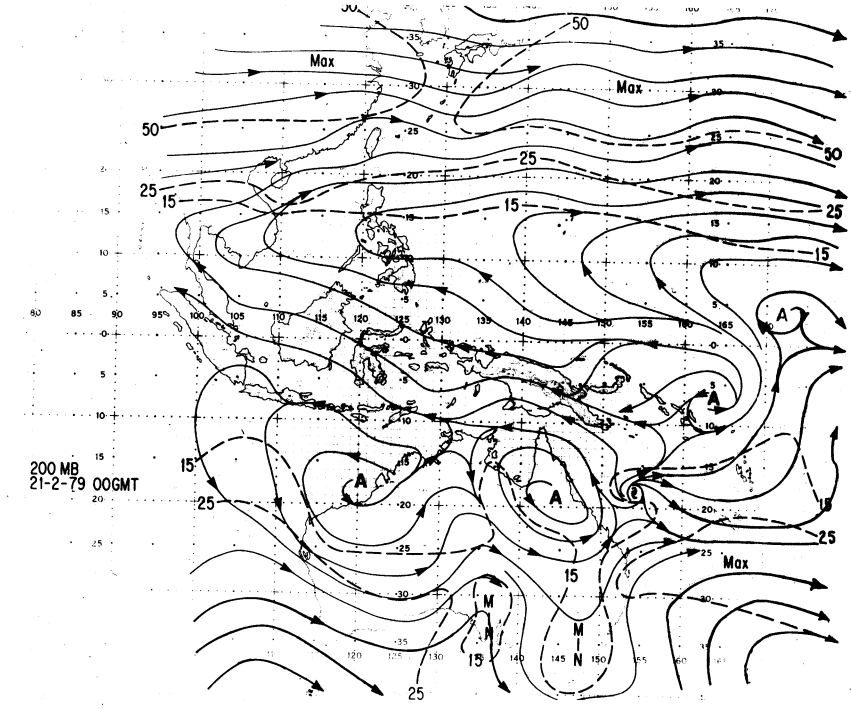

c.

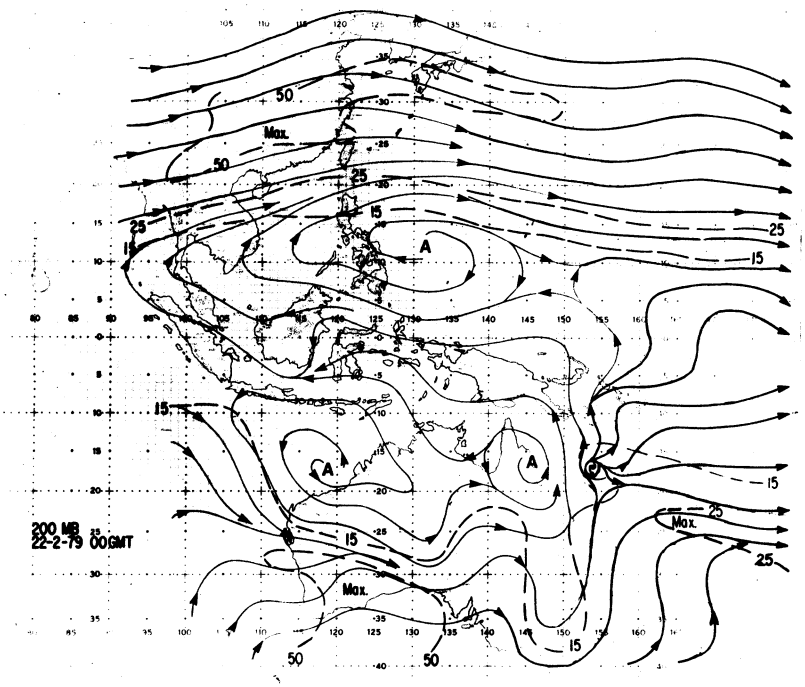

d.

Figure 8. Streamline and isotach analyses for the 200-mb level for the Australian region at 0000 GMT on (c) February 21, and (d) February 22, 1979.

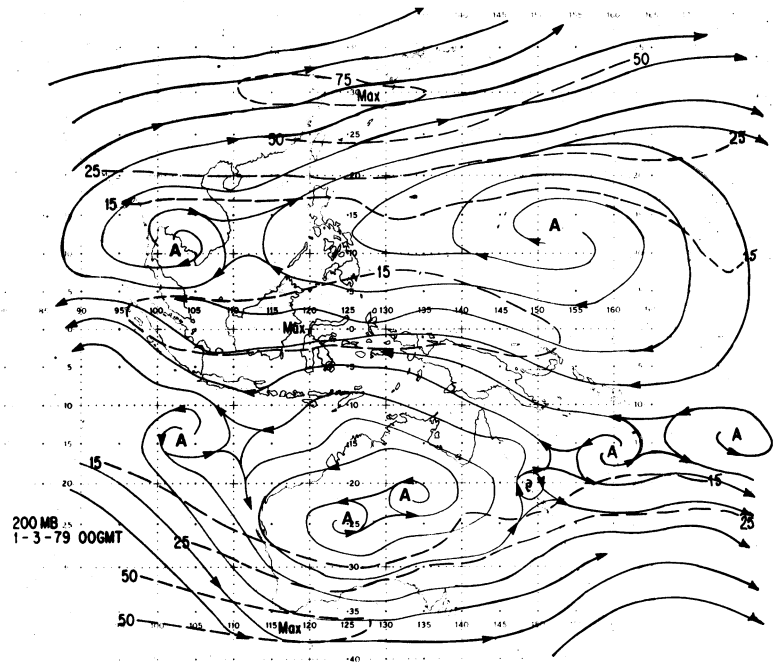

e.

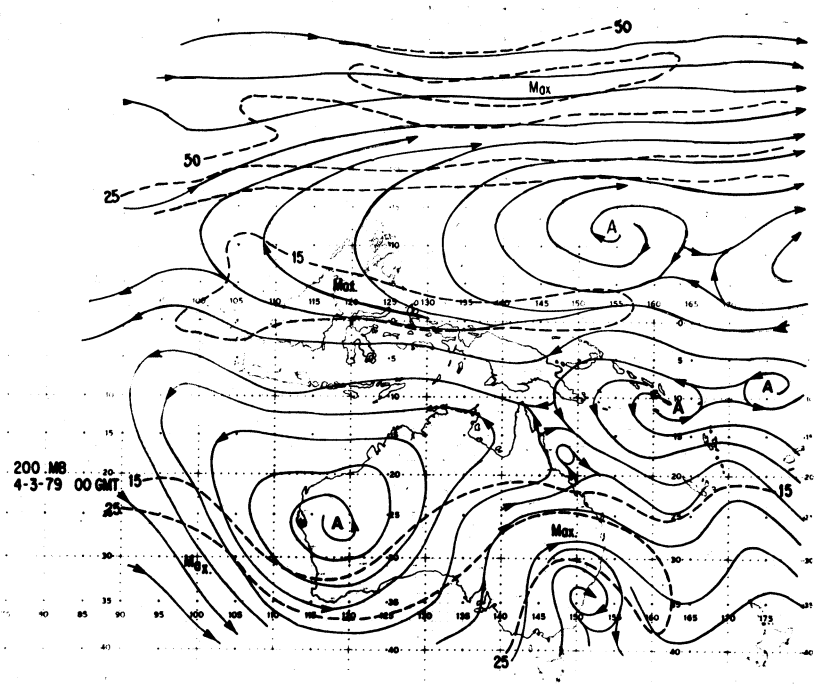

f.

Figure 8. Streamline and isotach analyses for the 200-mb level for the Australian region at 0000 GMT on (e) March 1, and (f) March 4, 1979.

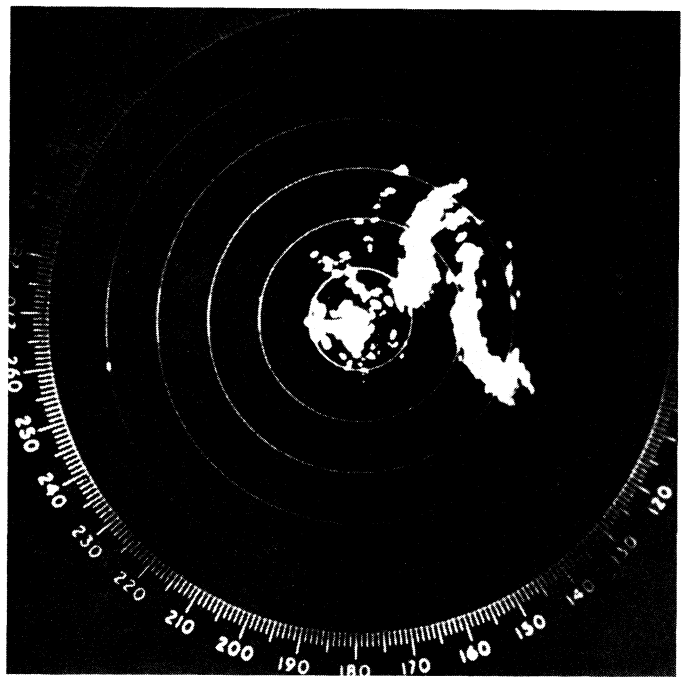

a.

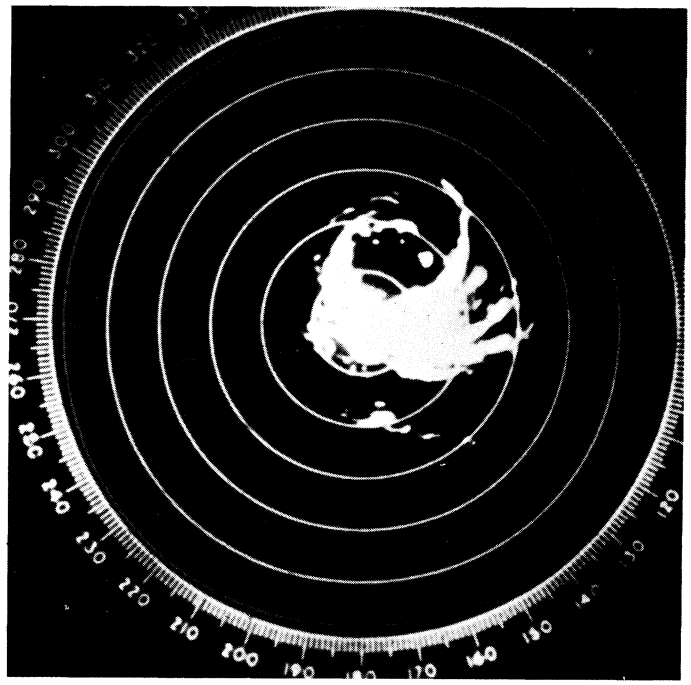

b.

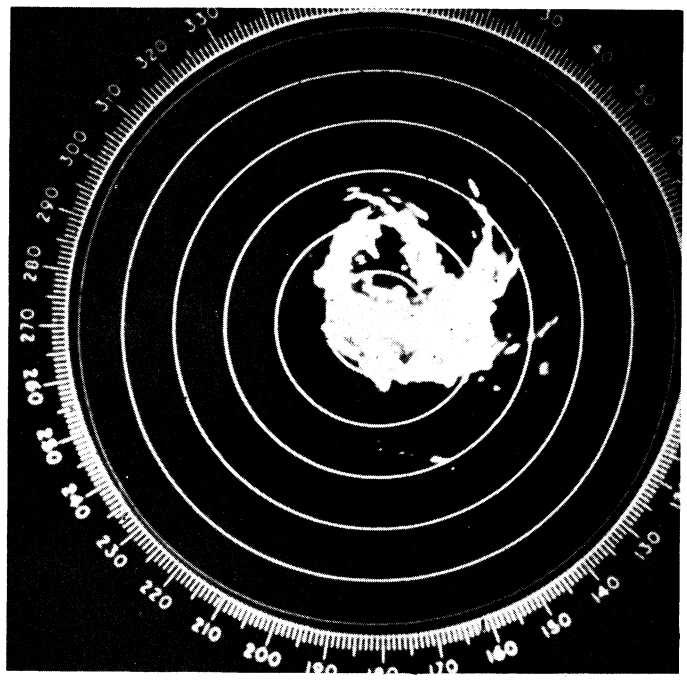

c.

Figure 9. Plan Position Indicator (PPI) radar depictions of Tropical Cyclone Kerry as recorded at Mackay at (a) 1830 GMT, February 27, (b) 2059 GMT, February 28, and (c) 2200 GMT, February 28, 1979.

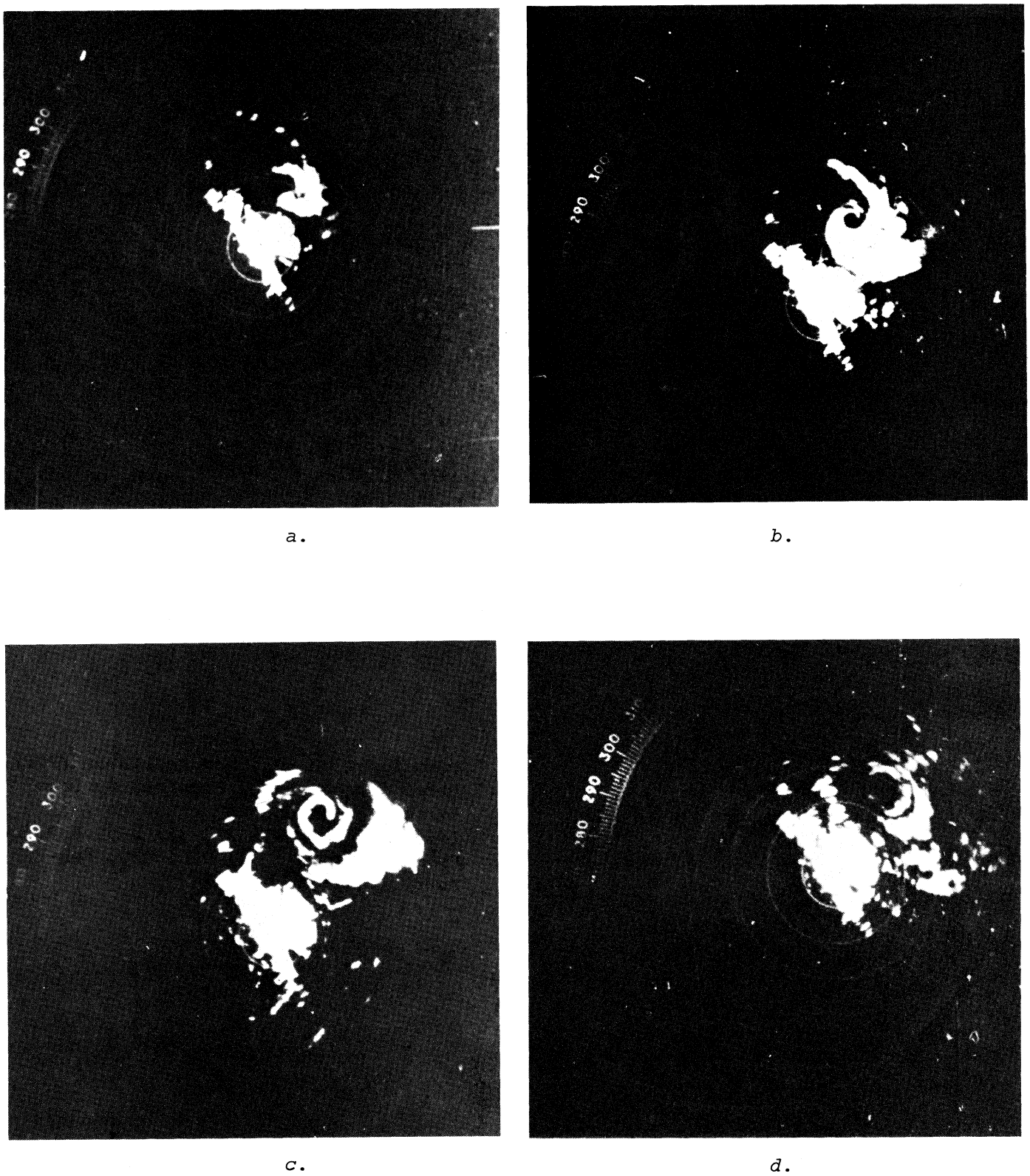

a. b.

c. d.

Figure 10. PPI radar depictions of Tropical Cyclone Kerry as recorded at Townsville at (a) 1326 GMT, March 2, (b) 1750 GMT, March 2, (c) 0306 GMT, March 3, and (d) 2312 GMT, March 3, 1979.

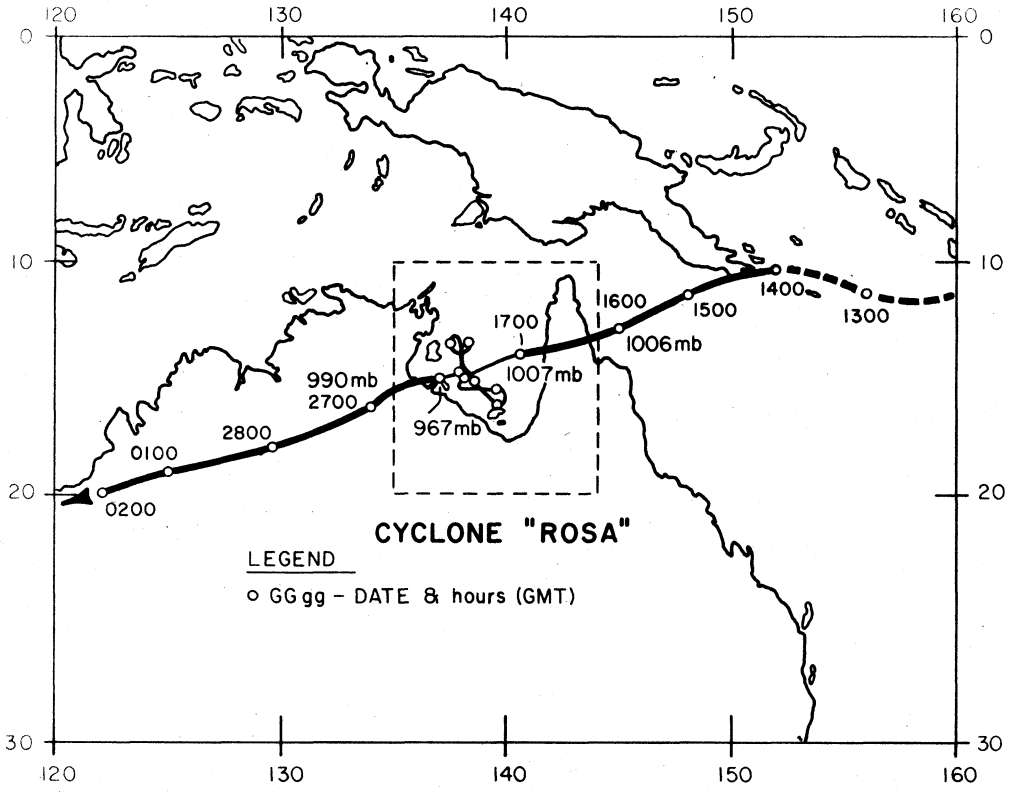

a.

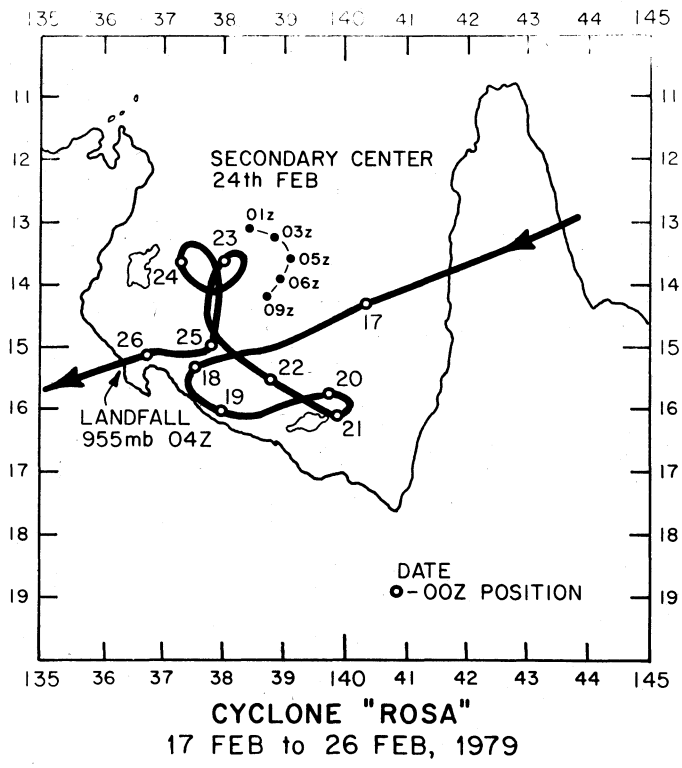

b.

Figure 11. Tropical Cyclone Rosa storm track and estimated MSLP's for (a) overall smoothed track and (b) detailed track in Gulf of Carpentaria.

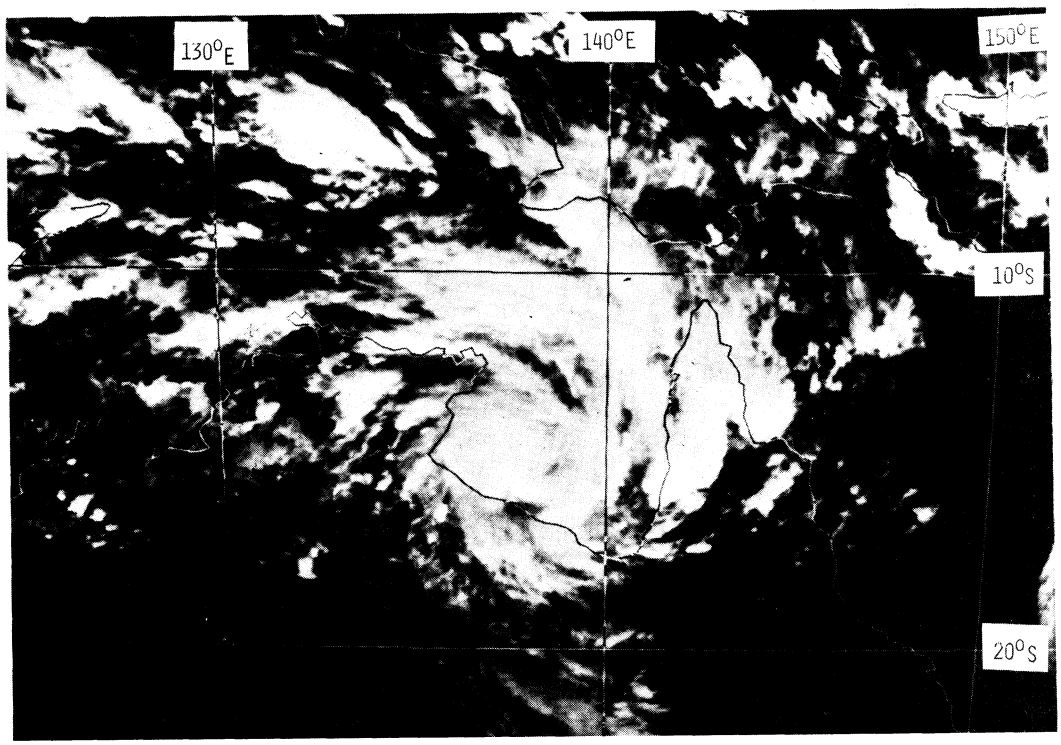

a.

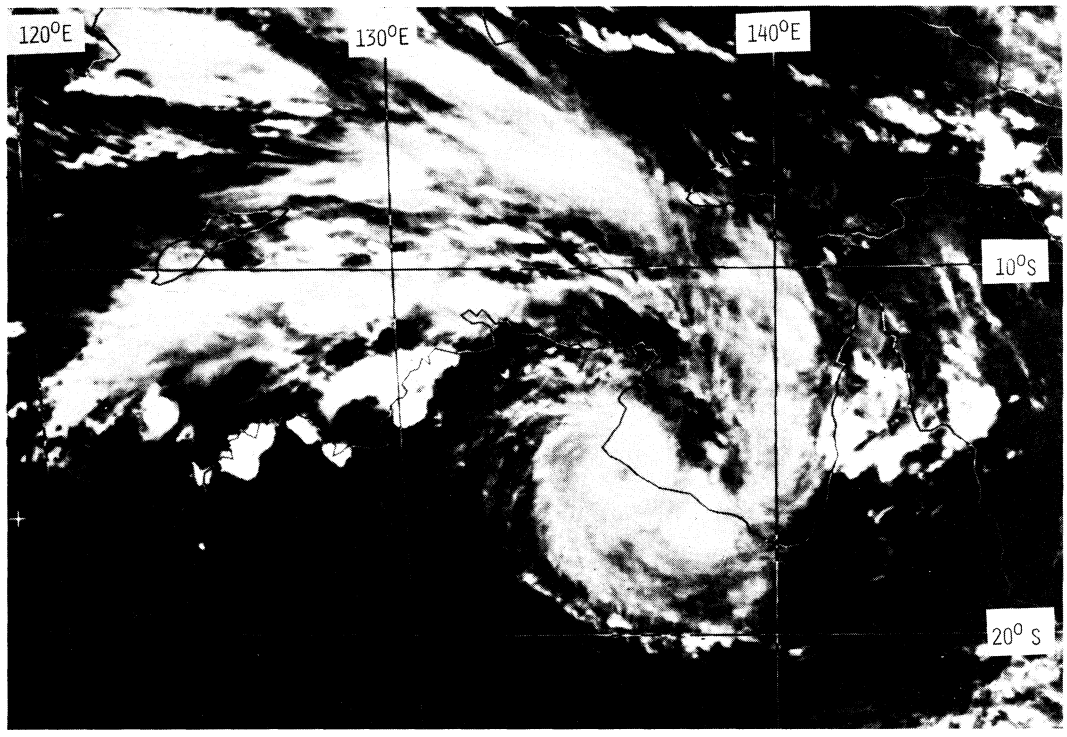

b.

Figure 12. Japanese Geosynchronous Meteorological Satellite (GMS) picture of Tropical Cyclone Rosa at 0600 GMT on (a) February 25 and (b) February 26, 1979.

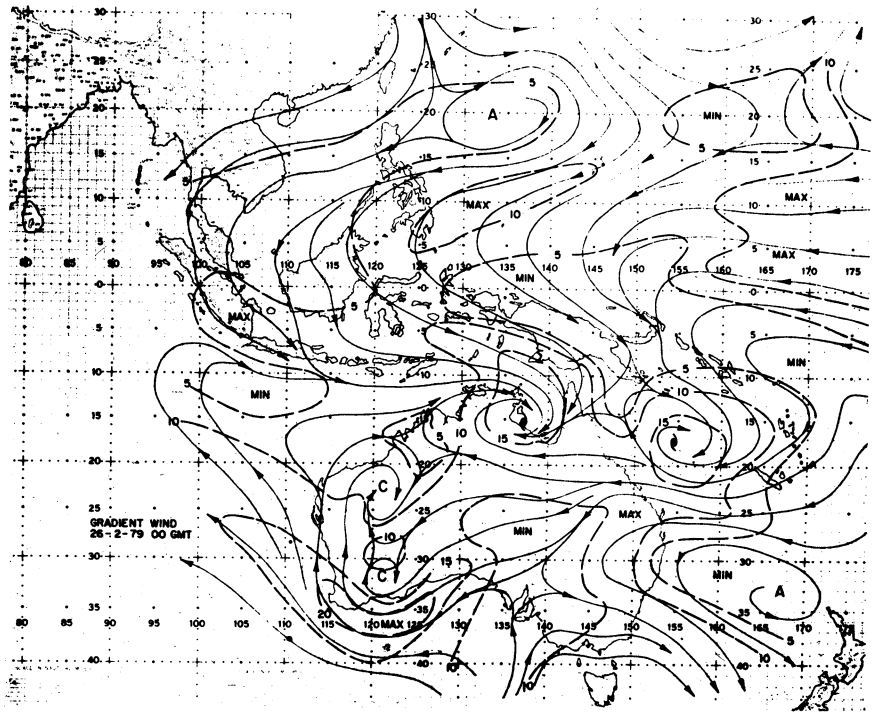

a.

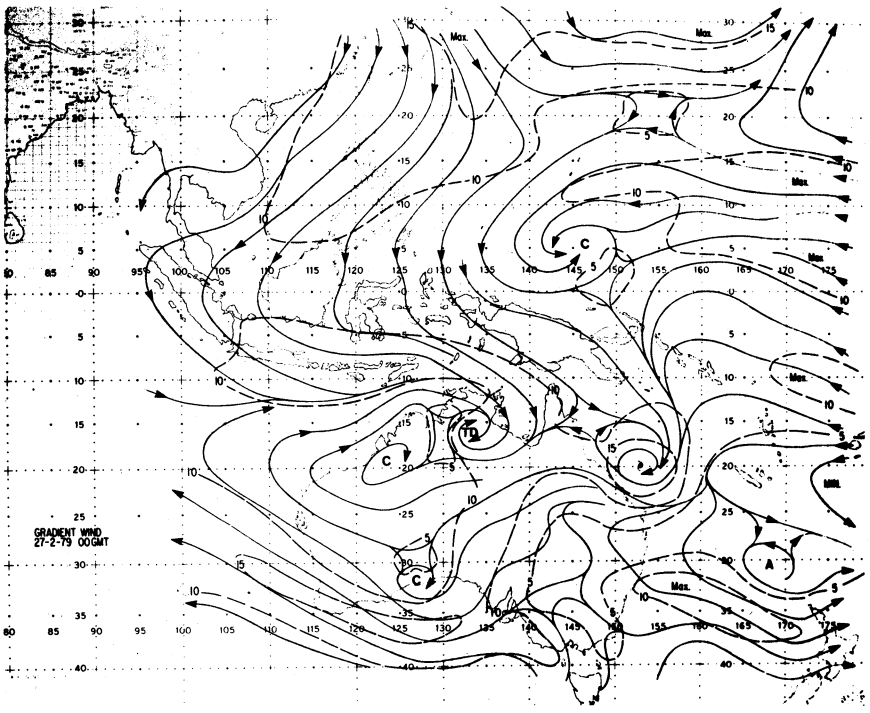

b.

Figure 13. Streamline and isotach analyses of the gradient wind level (900 m) for the Australian region at 0000 GMT on (a) February 26 and (b) February 27, 1979.

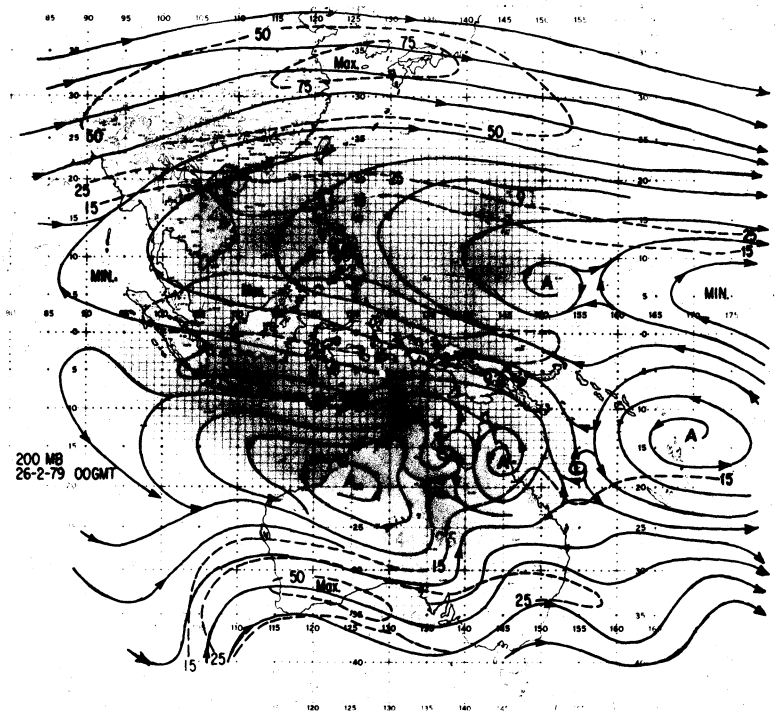

a.

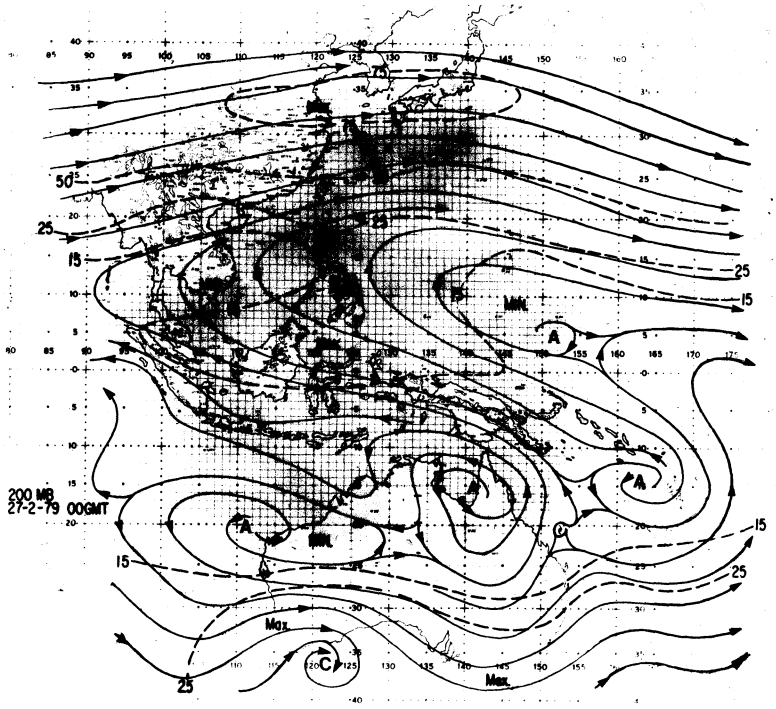

b.

Figure 14. Streamline and isotach analyses of the 200-mb-level winds for the Australian region at 0000 GMT on (a) February 26 and (b) February 27, 1979.

Figure 15. Digitized Plan Position Indicator radar depiction of Tropical Cyclone Kerry composited from 0600 Z to 0720 Z on February 21, 1979.

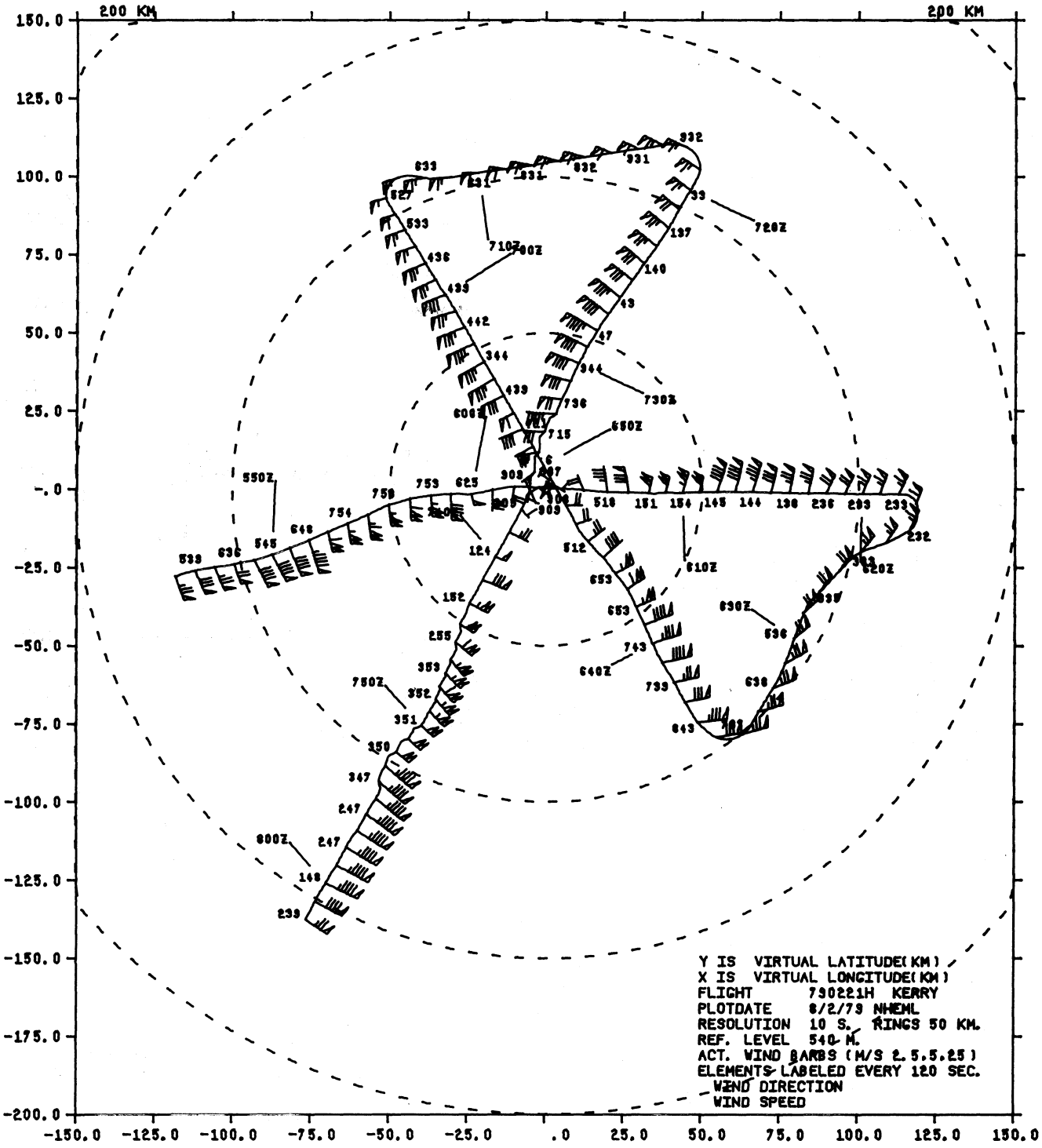

Figure 16. Plan view of aircraft position and actual wind relative to the center of Tropical Cyclone Kerry on February 21, 1979, from 0545 Z to 0802 Z and at an altitude of 540 m.

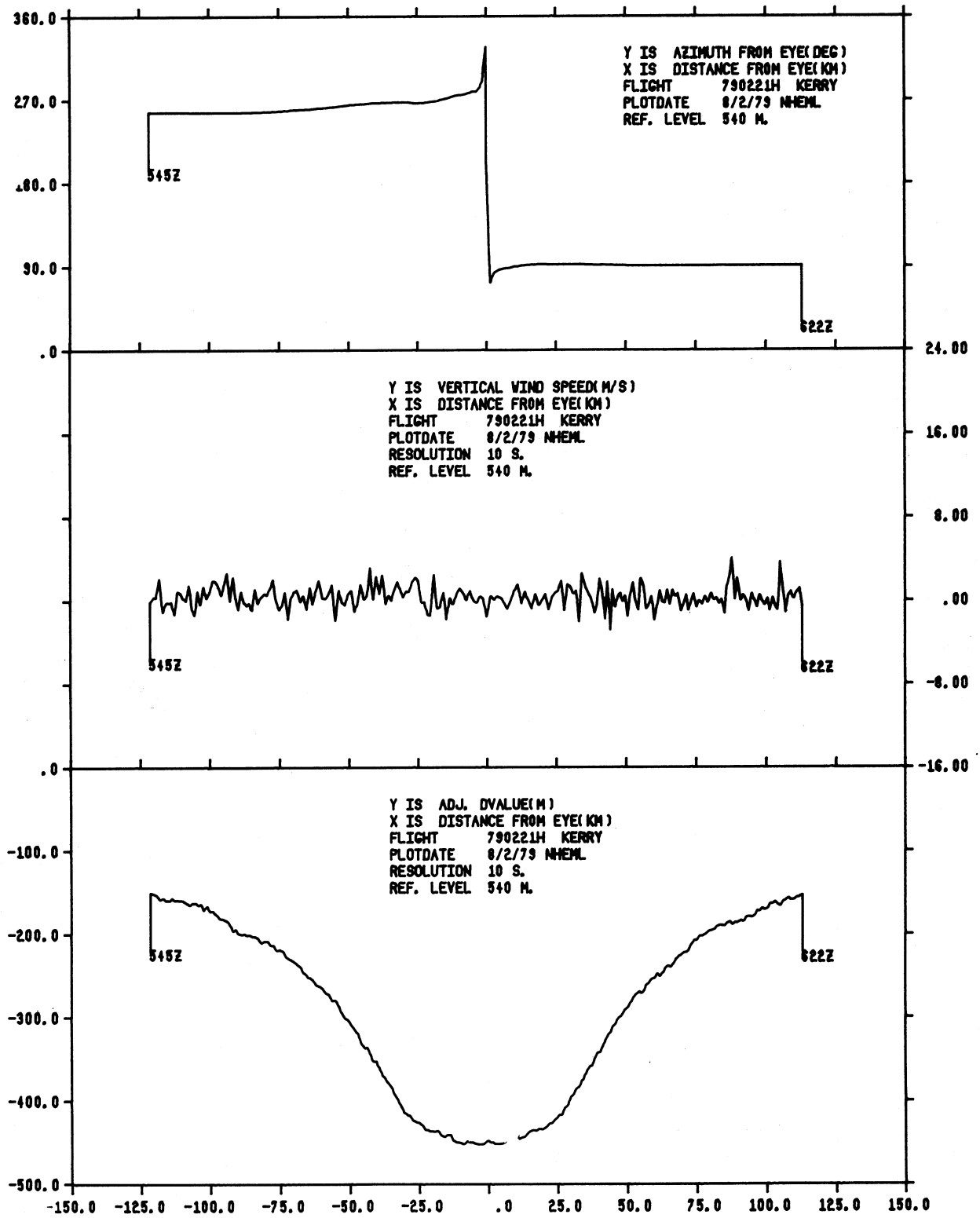

Figure 17. Profiles of the aircraft position in degrees from the center (top), vertical wind speed in meters per second (middle), and adjusted "D" value in meters (bottom) plotted as a function of radial distance in kilometers from the storm center. Profiles are for the west-to-east pass from 0545 Z to 0622 Z shown in figure 16. Adjusted values refer to a pressure altitude of 540 m (950 mb).

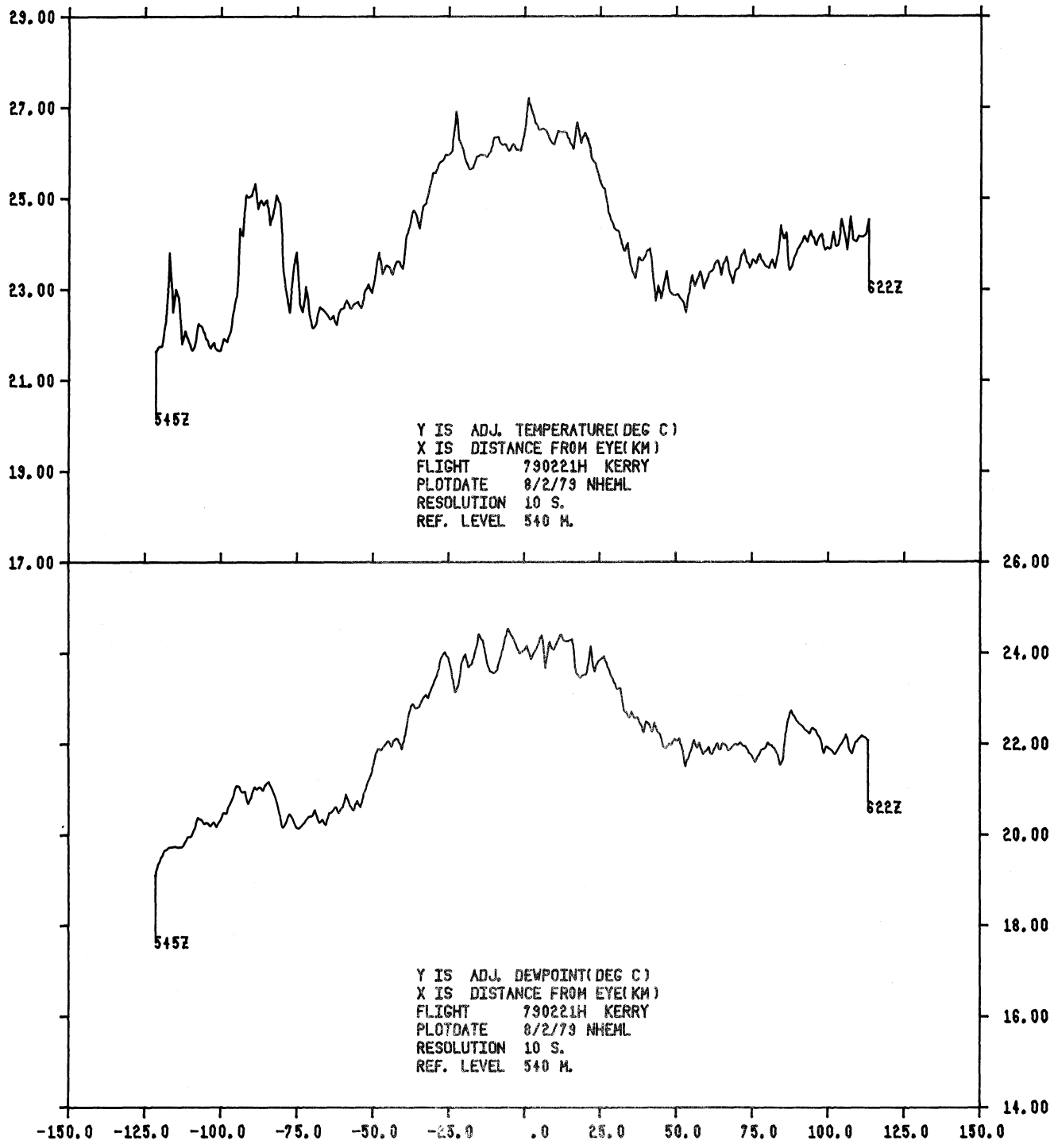

Figure 18. Same as figure 17, except for adjusted temperatures (top) and adjusted dew point temperatures (bottom) in degrees centigrade.

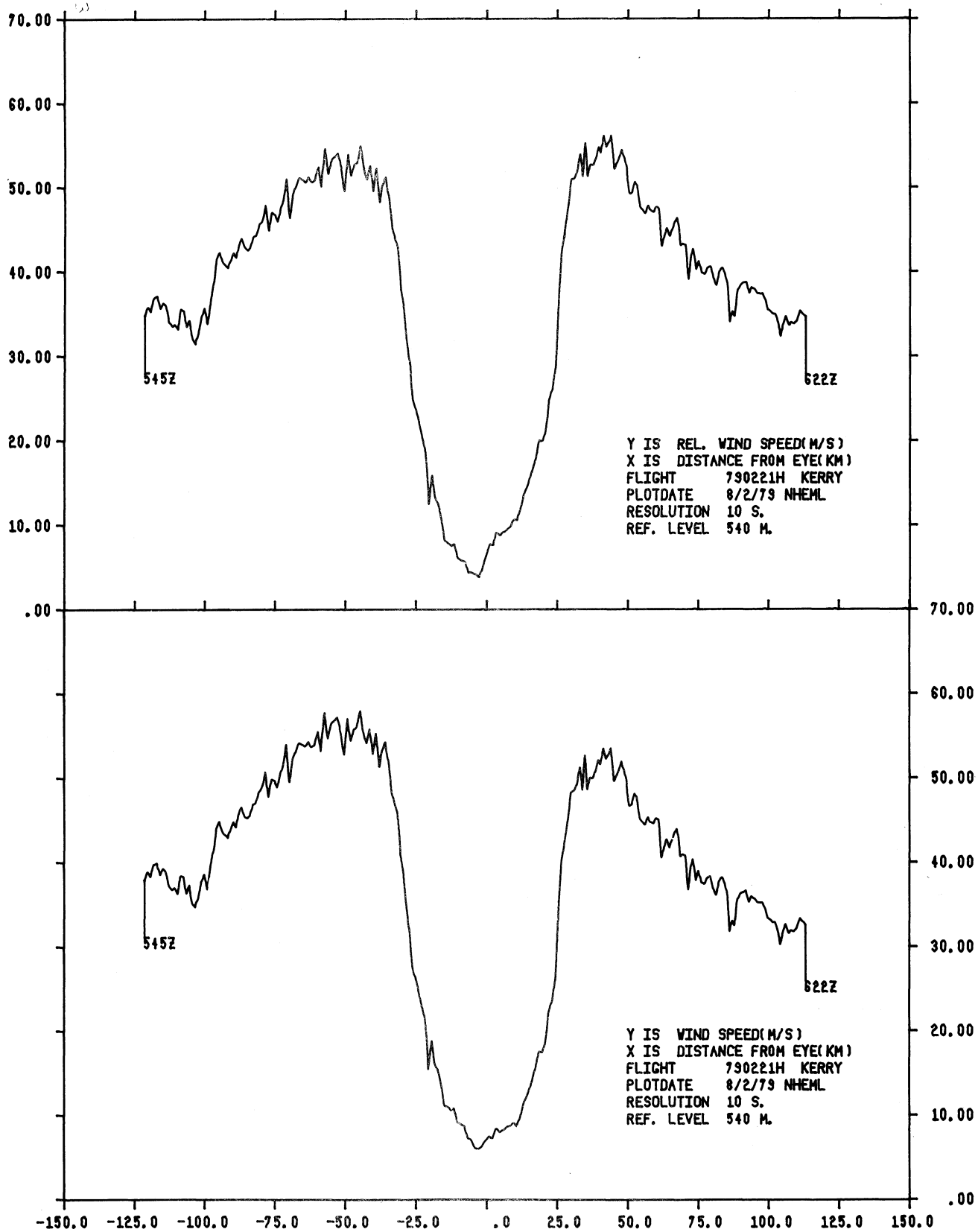

Figure 19. Same as figure 17, except for relative wind speed (top) and actual wind speed (bottom) in meters per second.

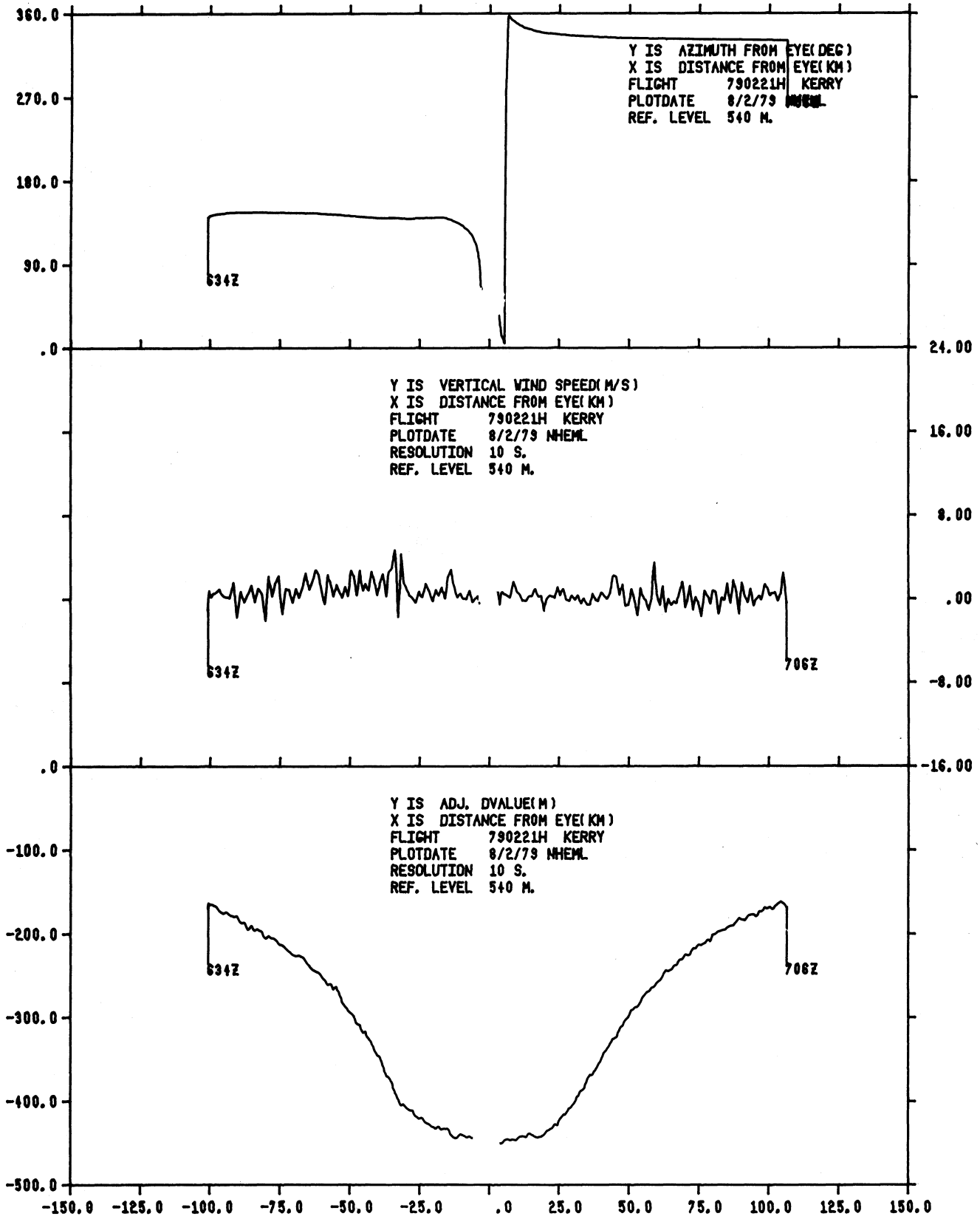

Figure 20. Same as figure 17, except for southeast-to-northwest pass in figure 16 from 0634 Z to 0706 Z.

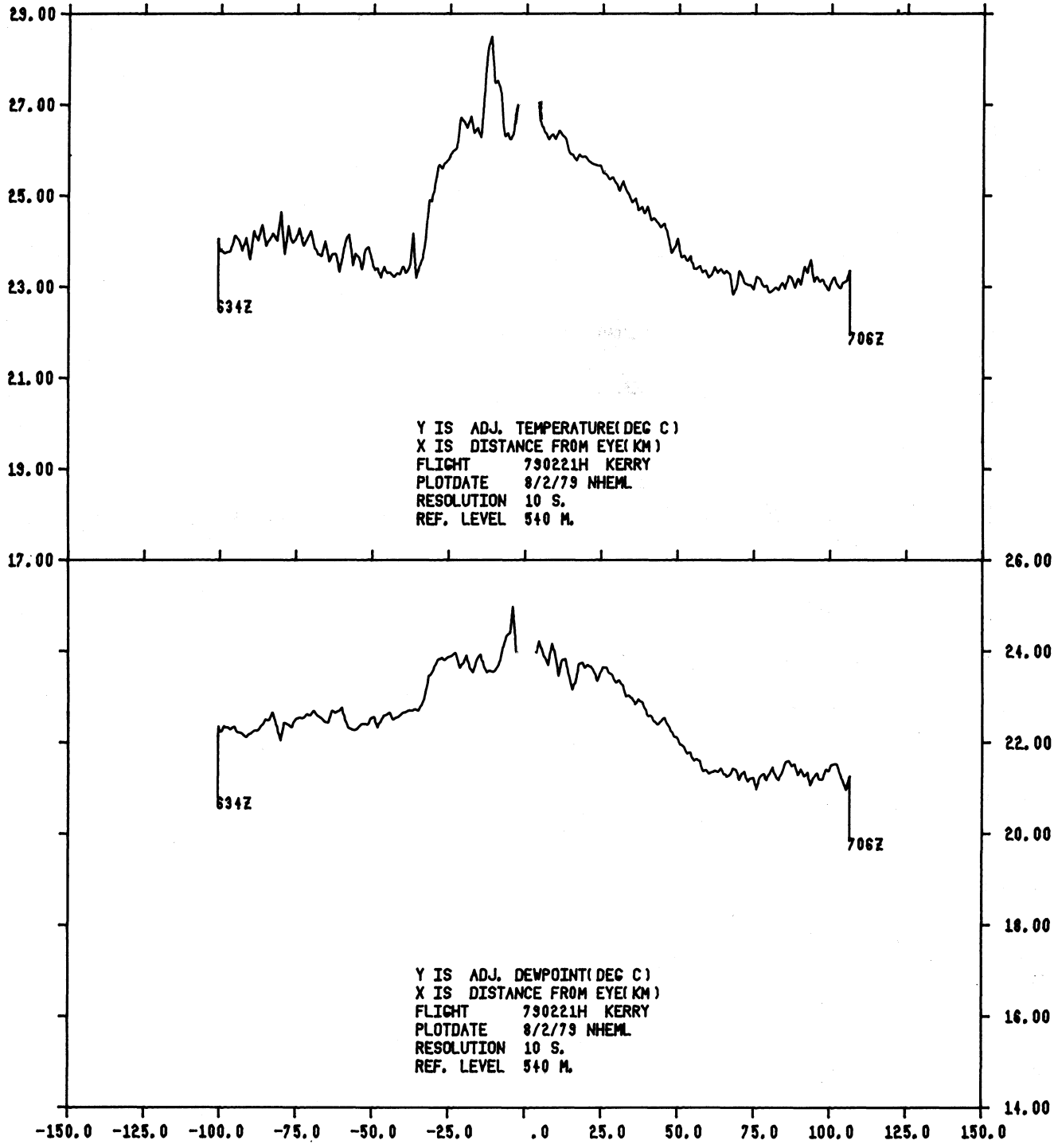

Figure 21. Same as figure 20, except for adjusted temperatures (top) and adjusted dew point temperatures (bottom).

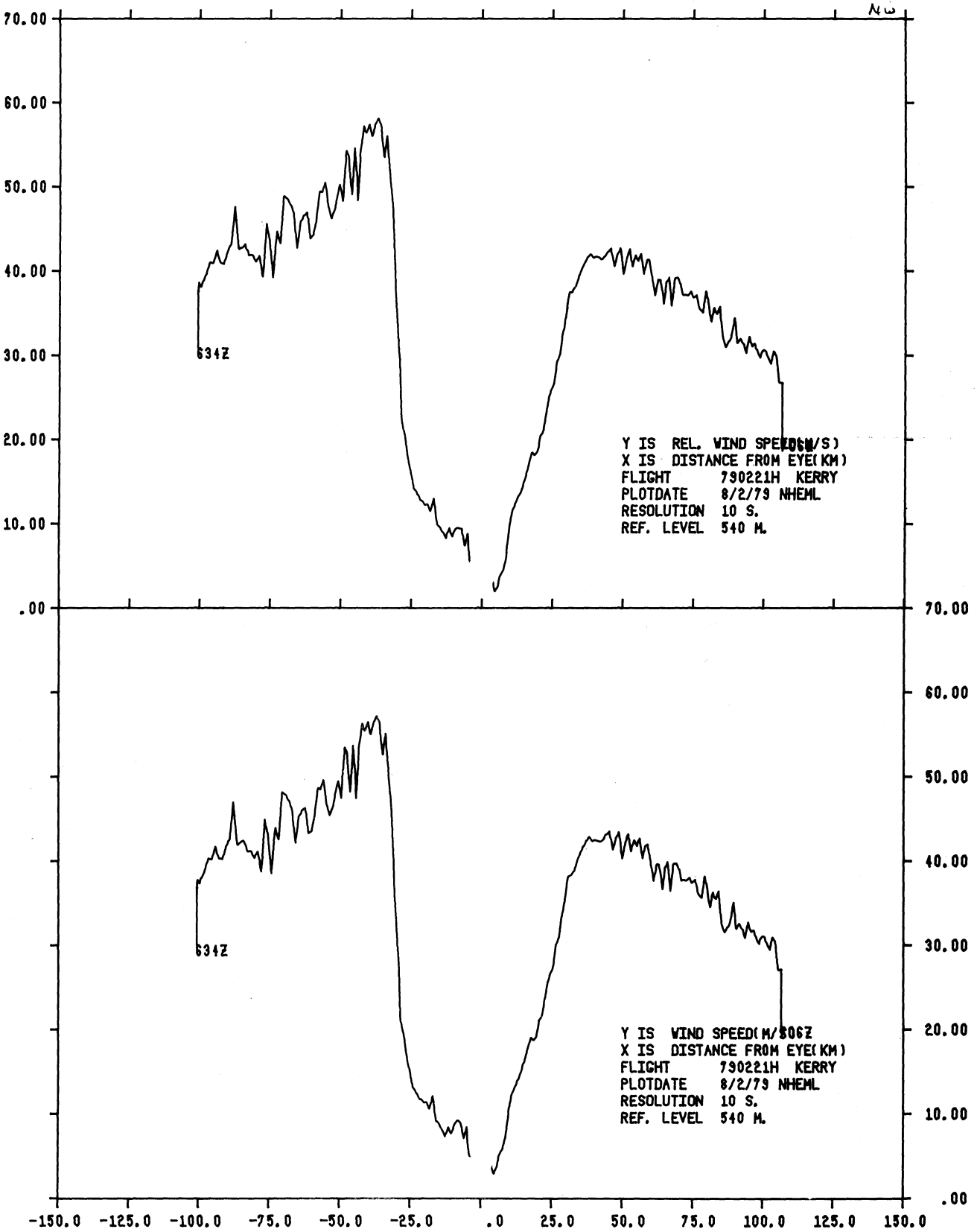

Figure 22. Same as figure 20, except for relative wind speed (top) and actual wind speed (bottom).

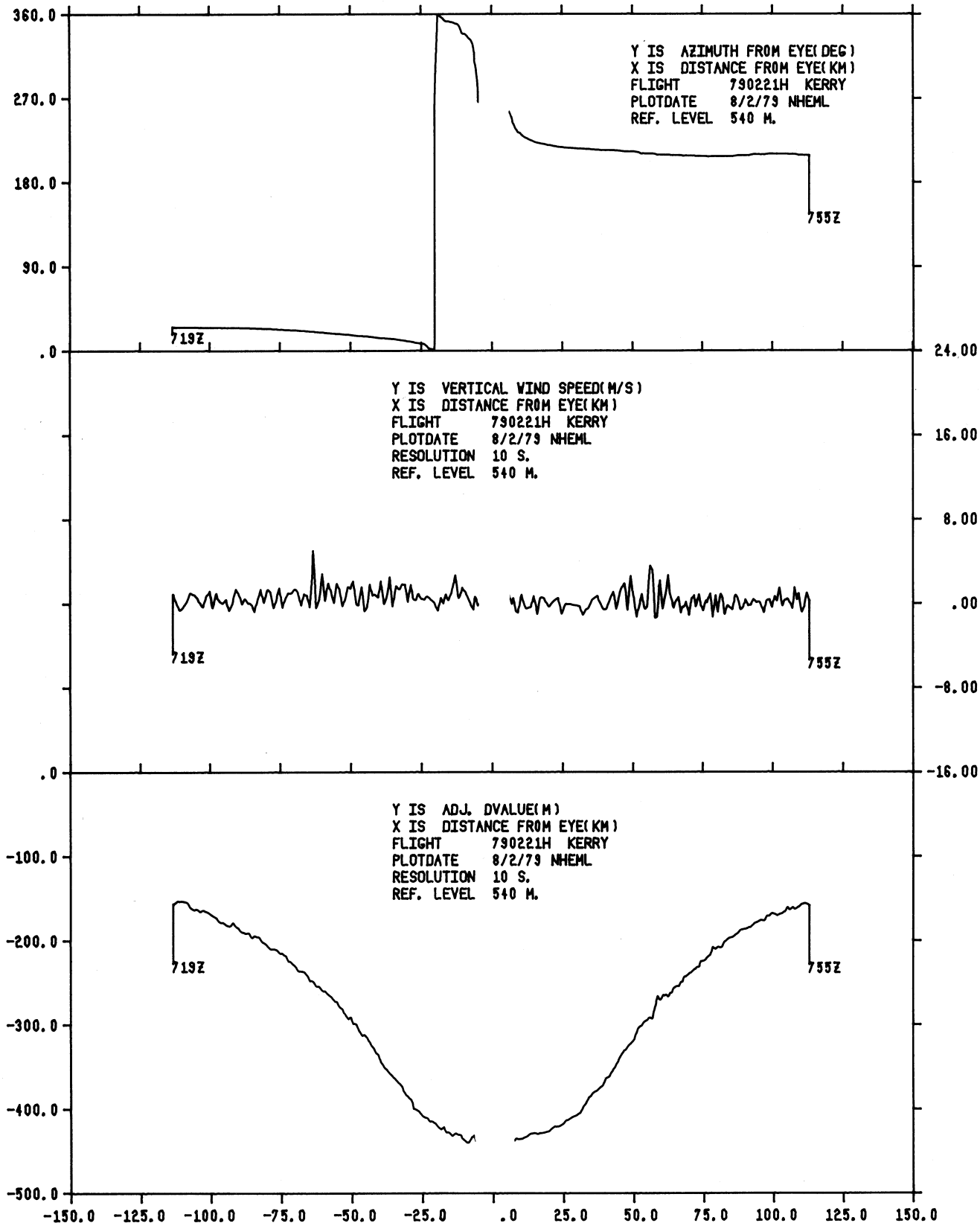

Figure 23. Same as figure 17, except for northeast-to-southwest pass in figure 16 from 0719 Z to 0755 Z.

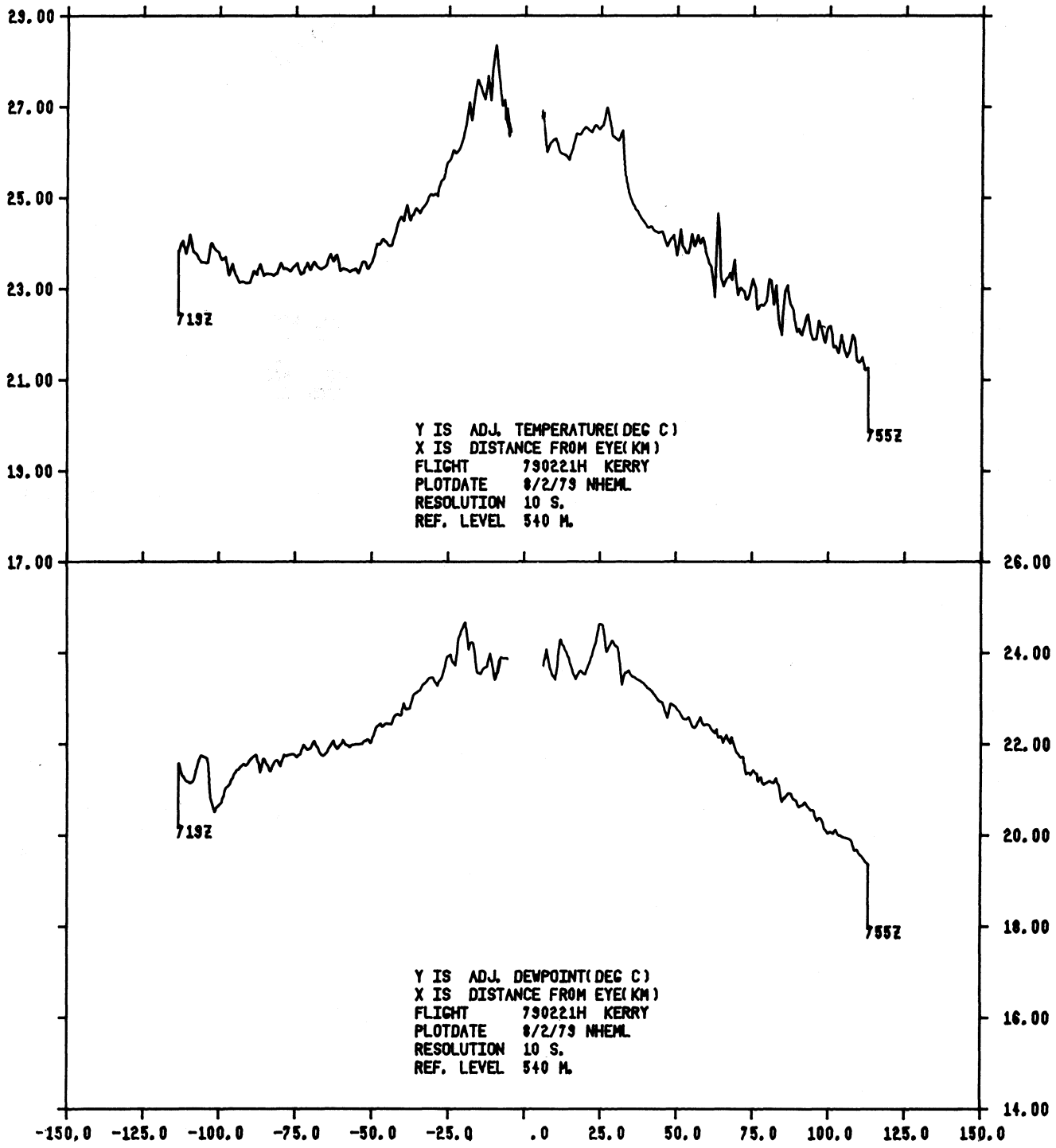

Figure 24. Same as figure 23, except for adjusted temperatures (top) and adjusted dew point temperatures (bottom).

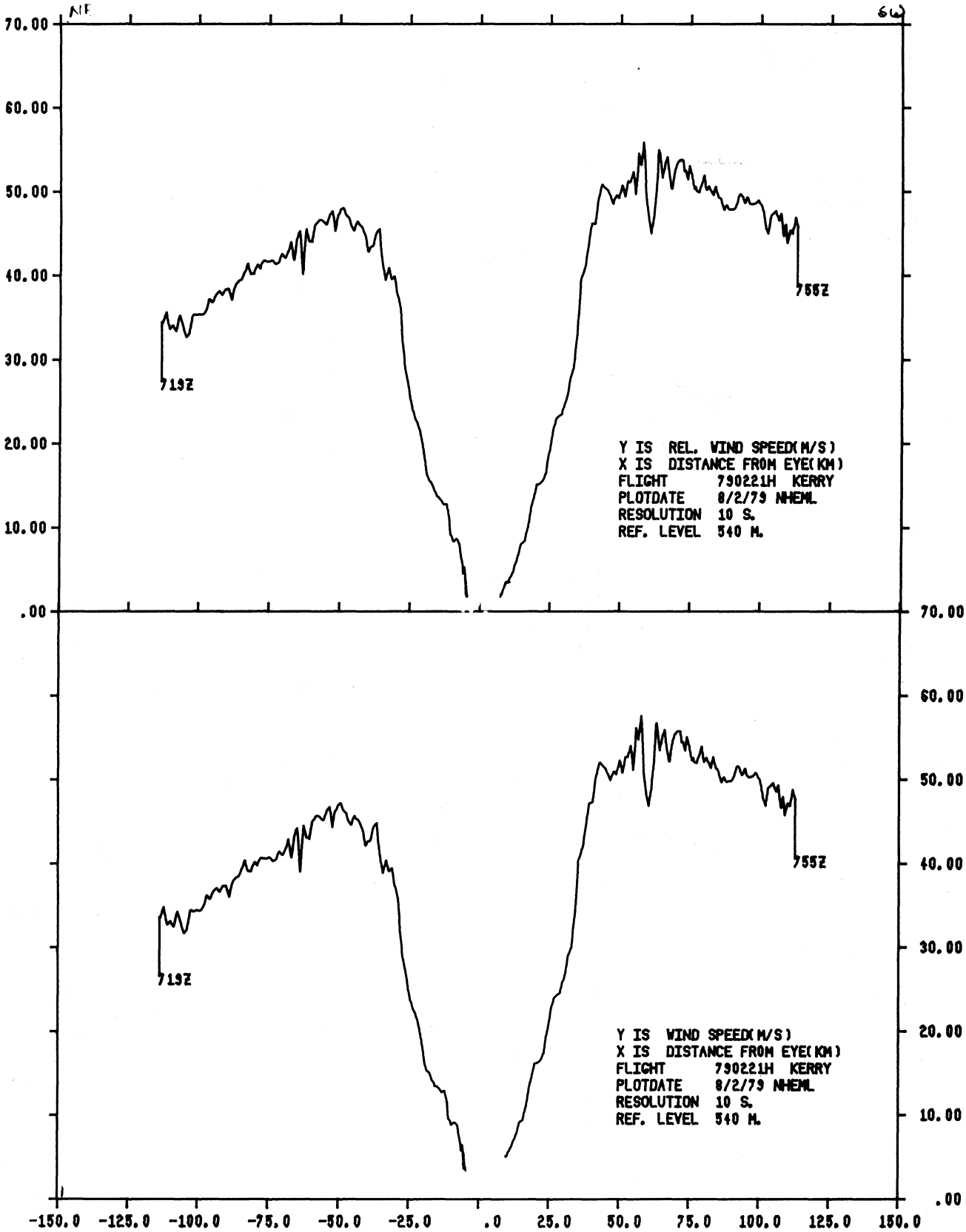

Figure 25. Same as figure 23, except for relative wind speed (top) and actual wind speed (bottom).

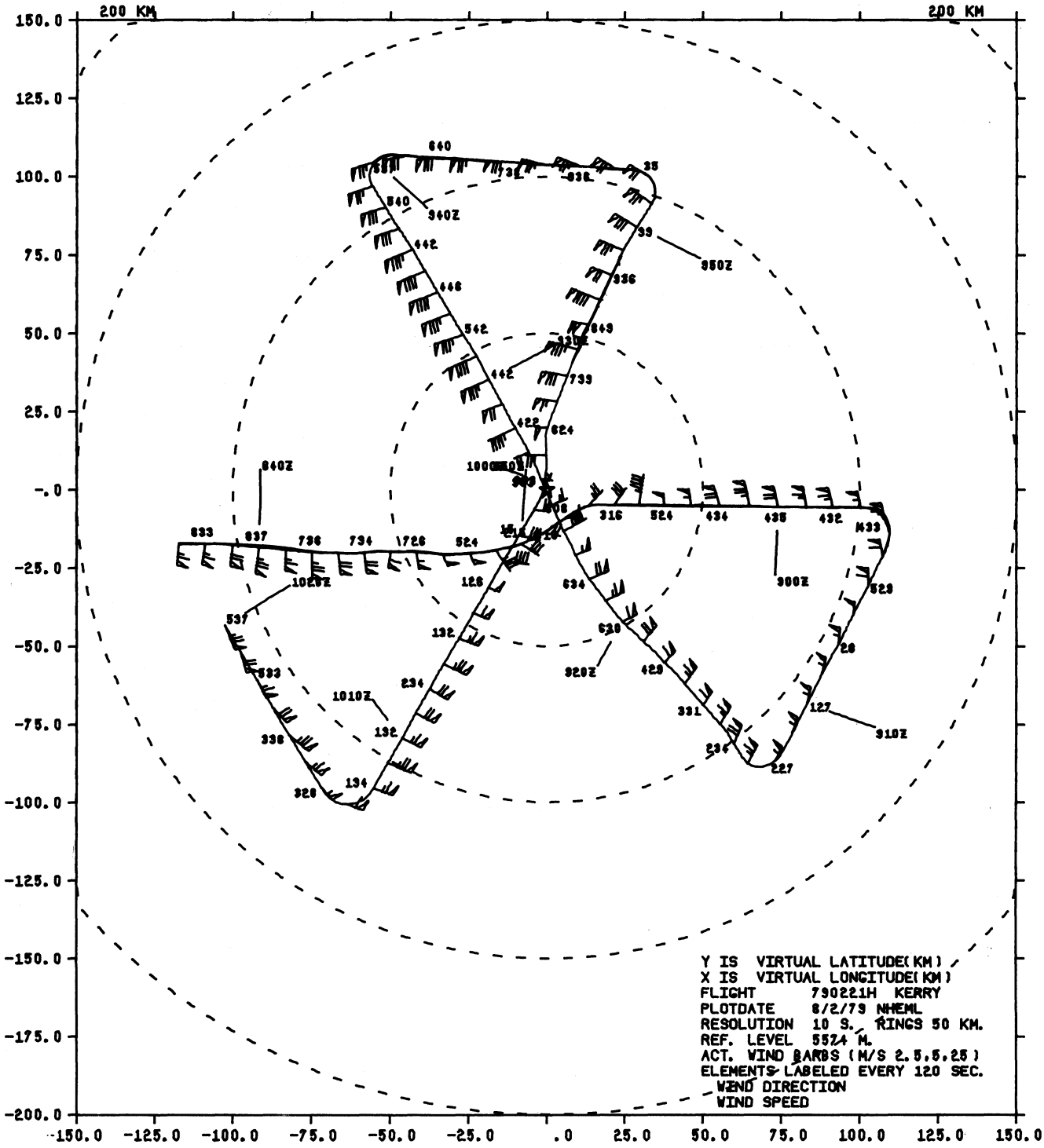

Figure 26. Plan view of aircraft position and actual winds relative to the center of Tropical Cyclone Kerry from 0837 Z to 1120 Z on February 21, 1979, and at a reference pressure altitude of 5574 m (500 mb).

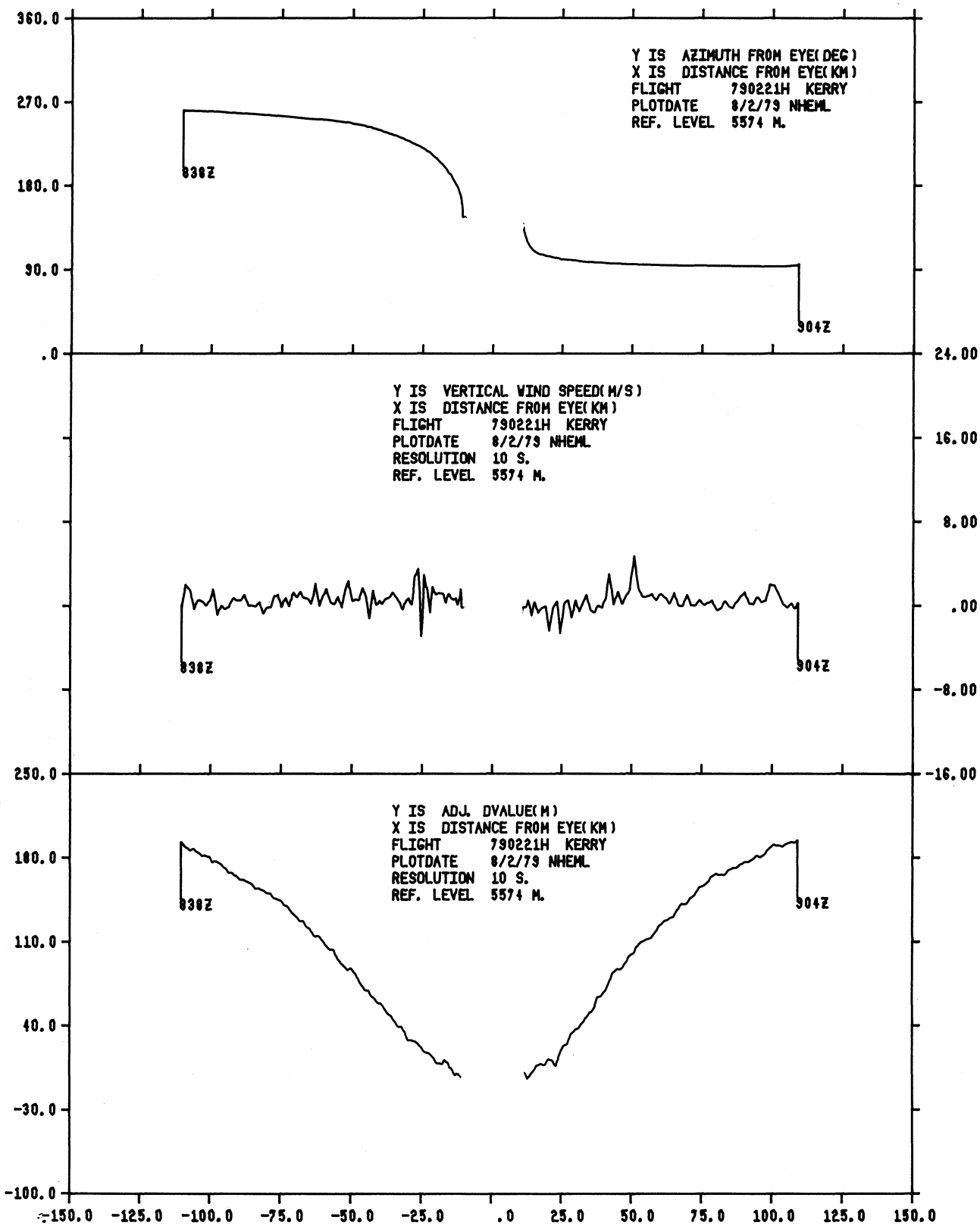

Figure 27. Profiles of the aircraft position (observation point) from the storm center in degrees (top), vertical wind (middle), and adjusted "D" value (bottom) versus radial distance from the storm center. Profiles correspond to the west-to-east pass in figure 26 from 0838 Z to 0904 Z.

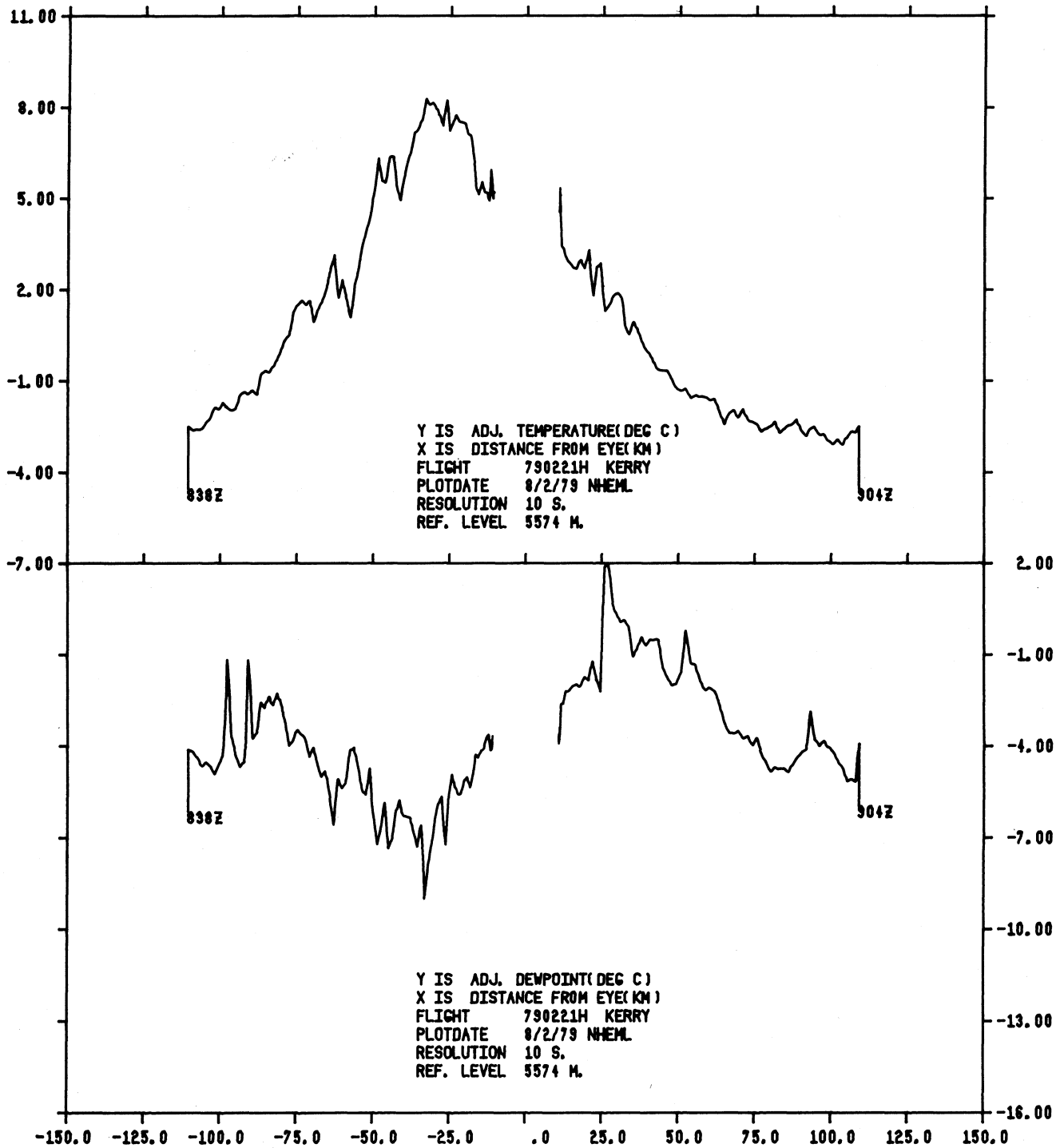

Figure 28. Same as figure 27, except for adjusted temperatures (top) and adjusted dew point temperatures (bottom).

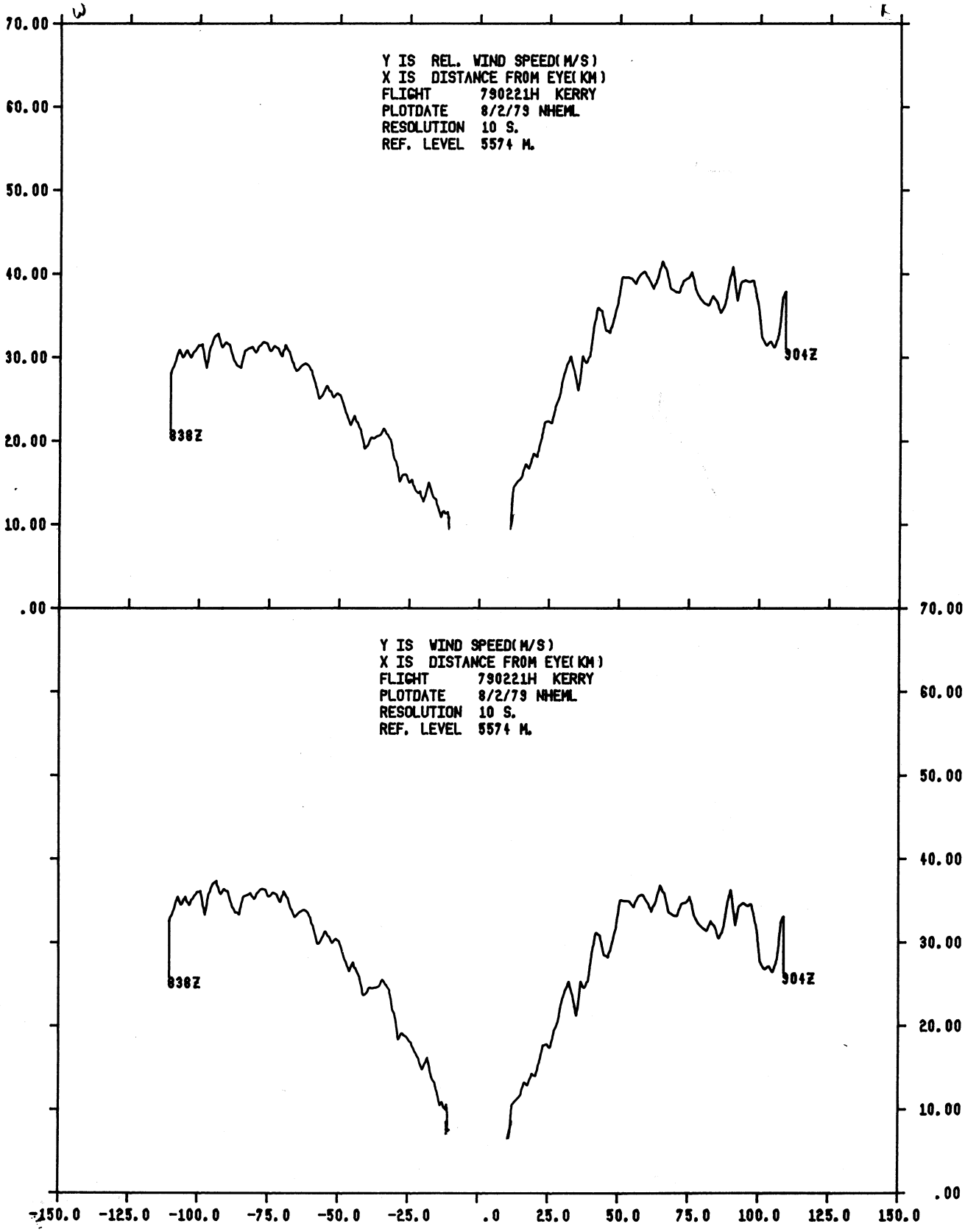

Figure 29. Same as figure 27, except for relative wind speed (top) and actual wind speed (bottom).

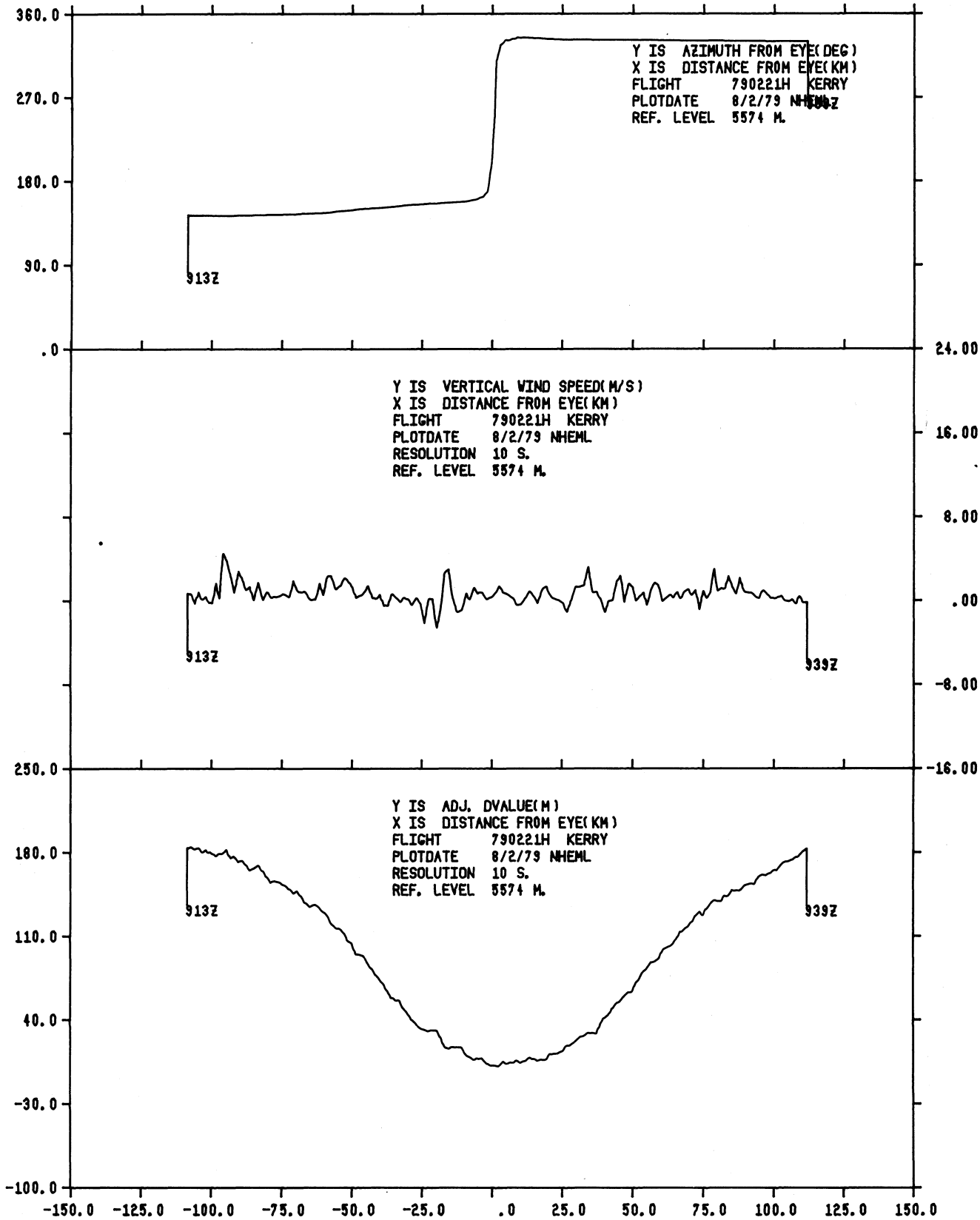

Figure 30. Same as figure 27, except for southeast-to-northwest pass in figure 26 from 0913 Z to 0939 Z.

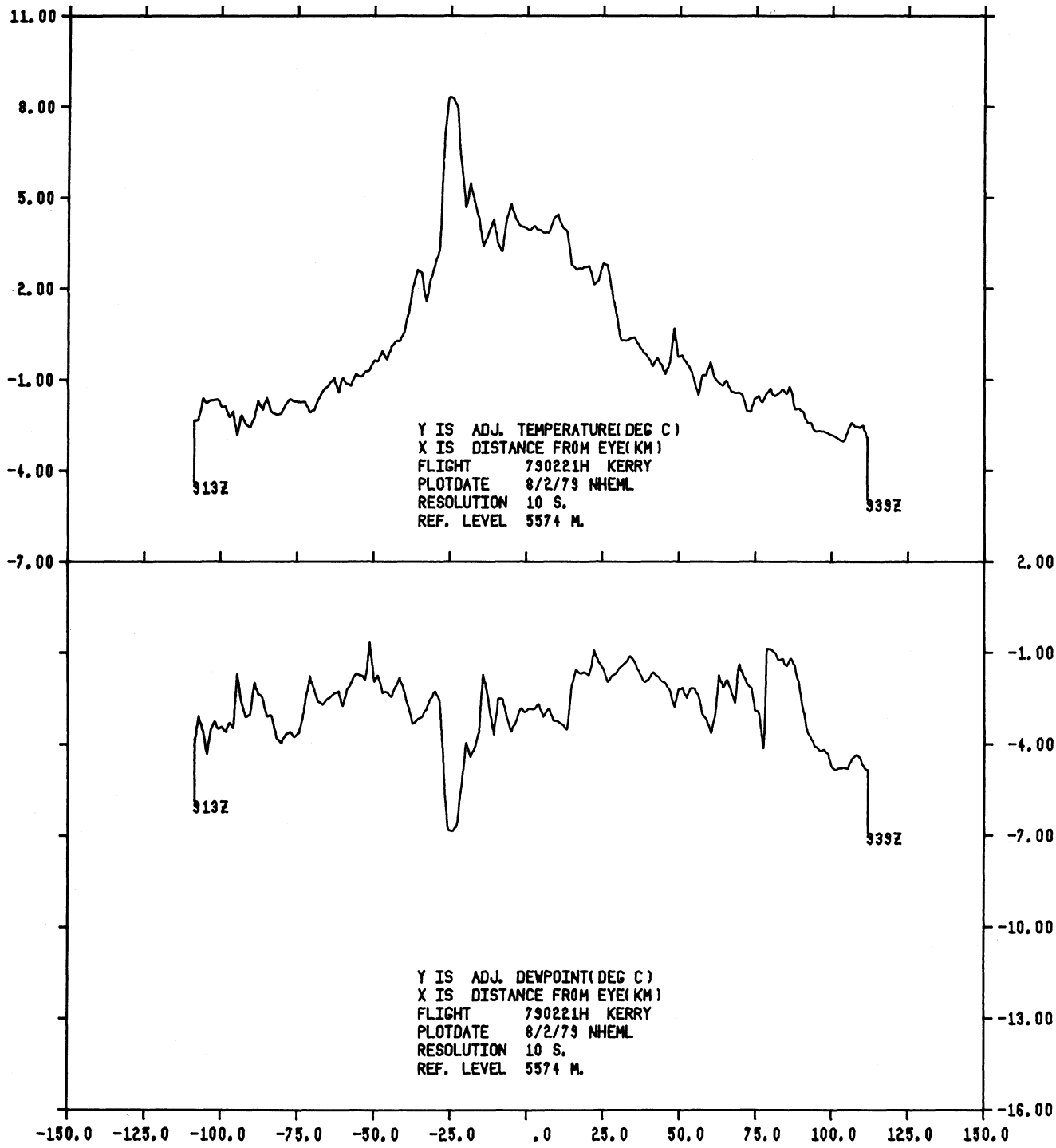

Figure 31. Same as figure 30, except for adjusted temperatures (top) and adjusted dew point temperatures (bottom).

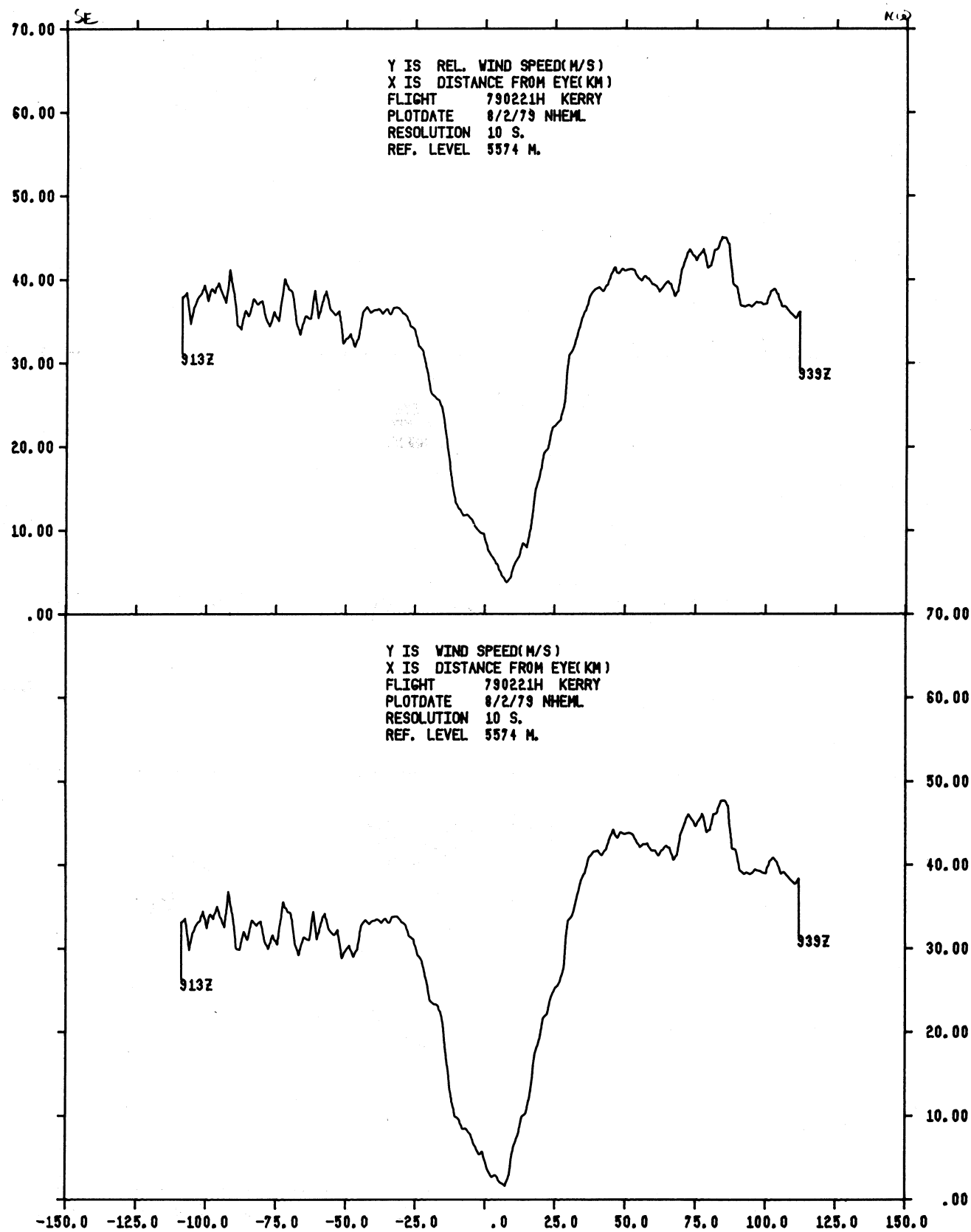

Figure 32. Same as figure 30, except for relative wind speed (top) and actual wind speed (bottom).

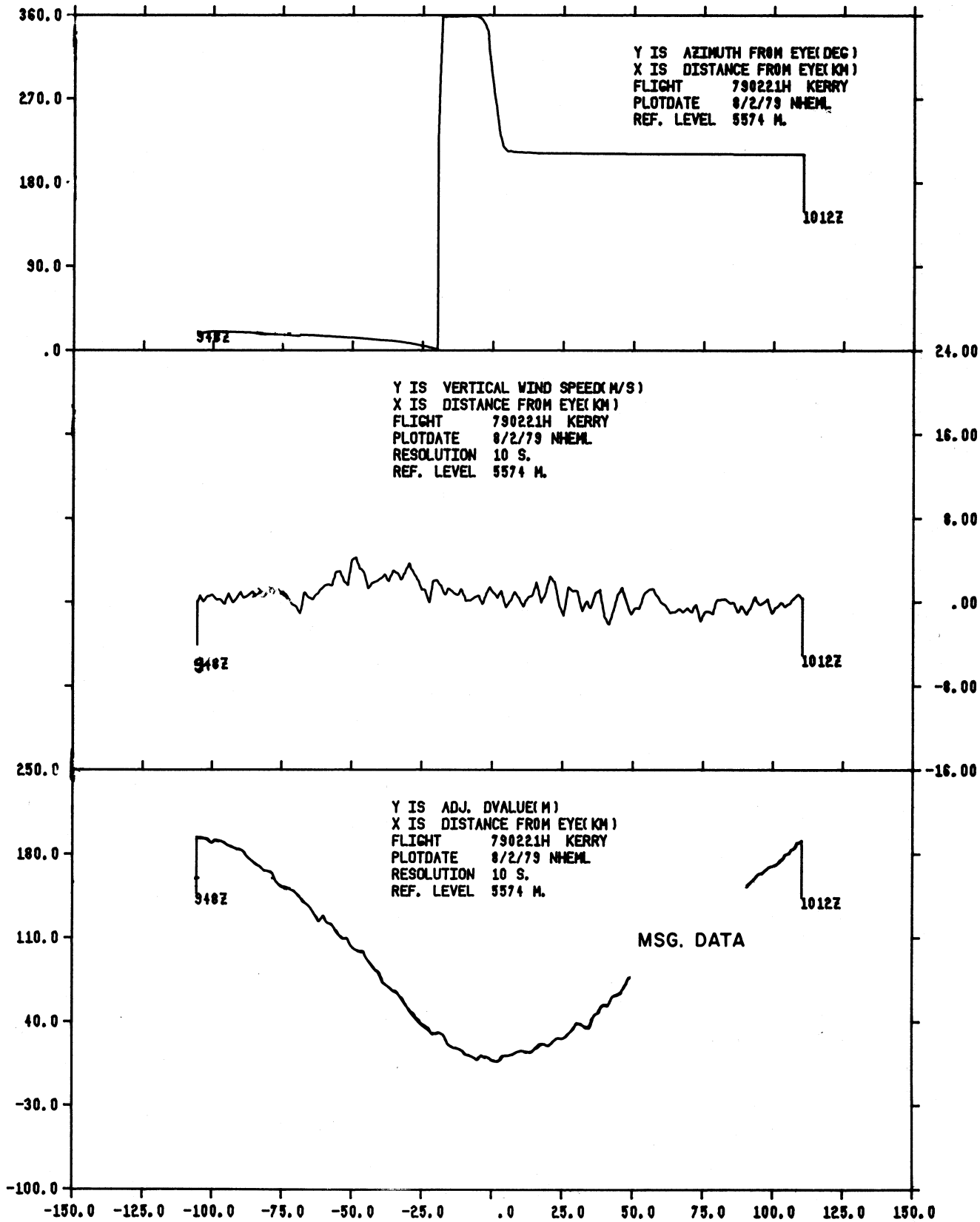

Figure 33. Same as figure 27, except for northeast-to-southwest pass in figure 26 from 0948 Z to 1012 Z.

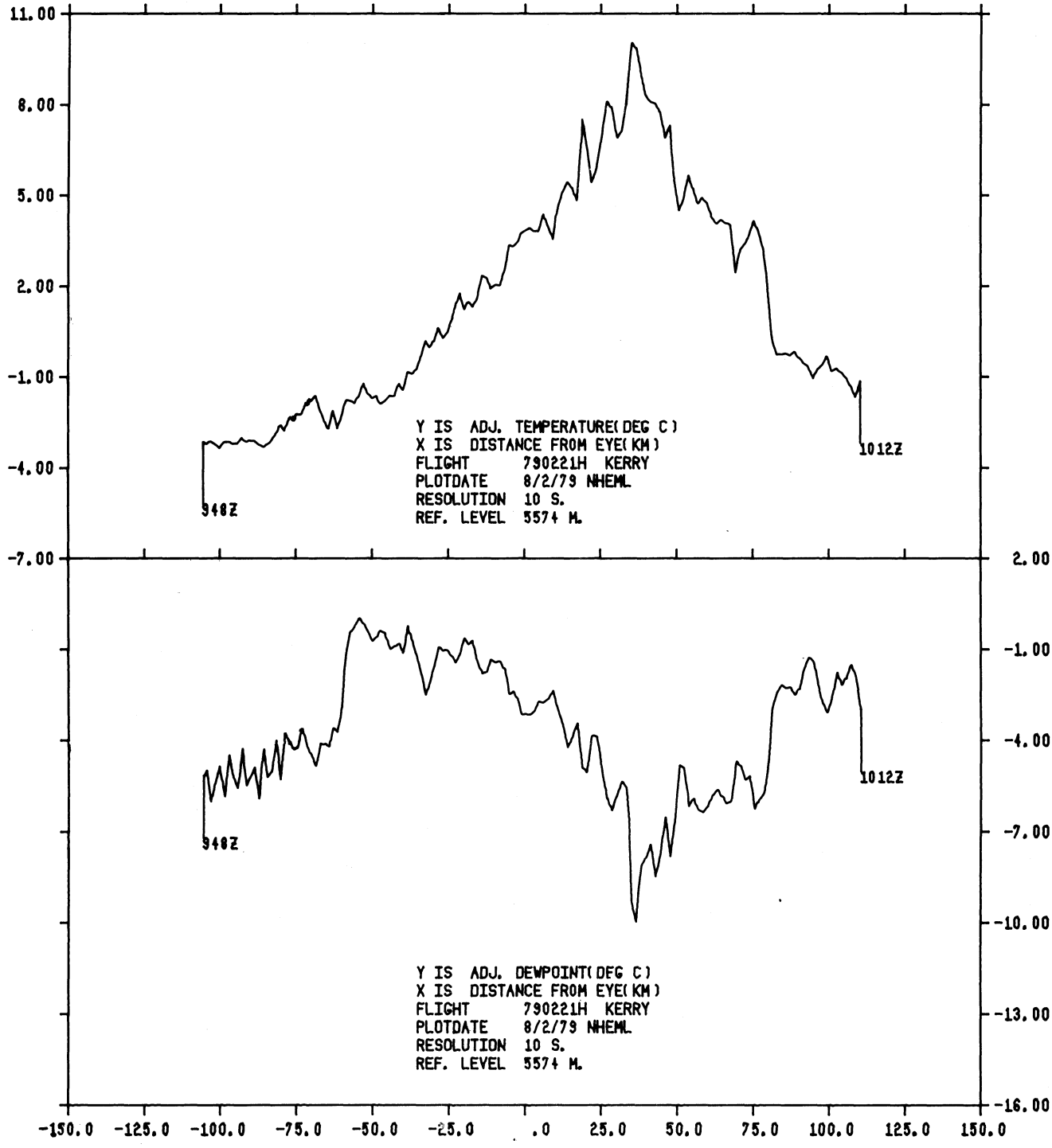

Figure 34. Same as figure 33, except for adjusted temperatures (top) and adjusted dew point temperatures (bottom).

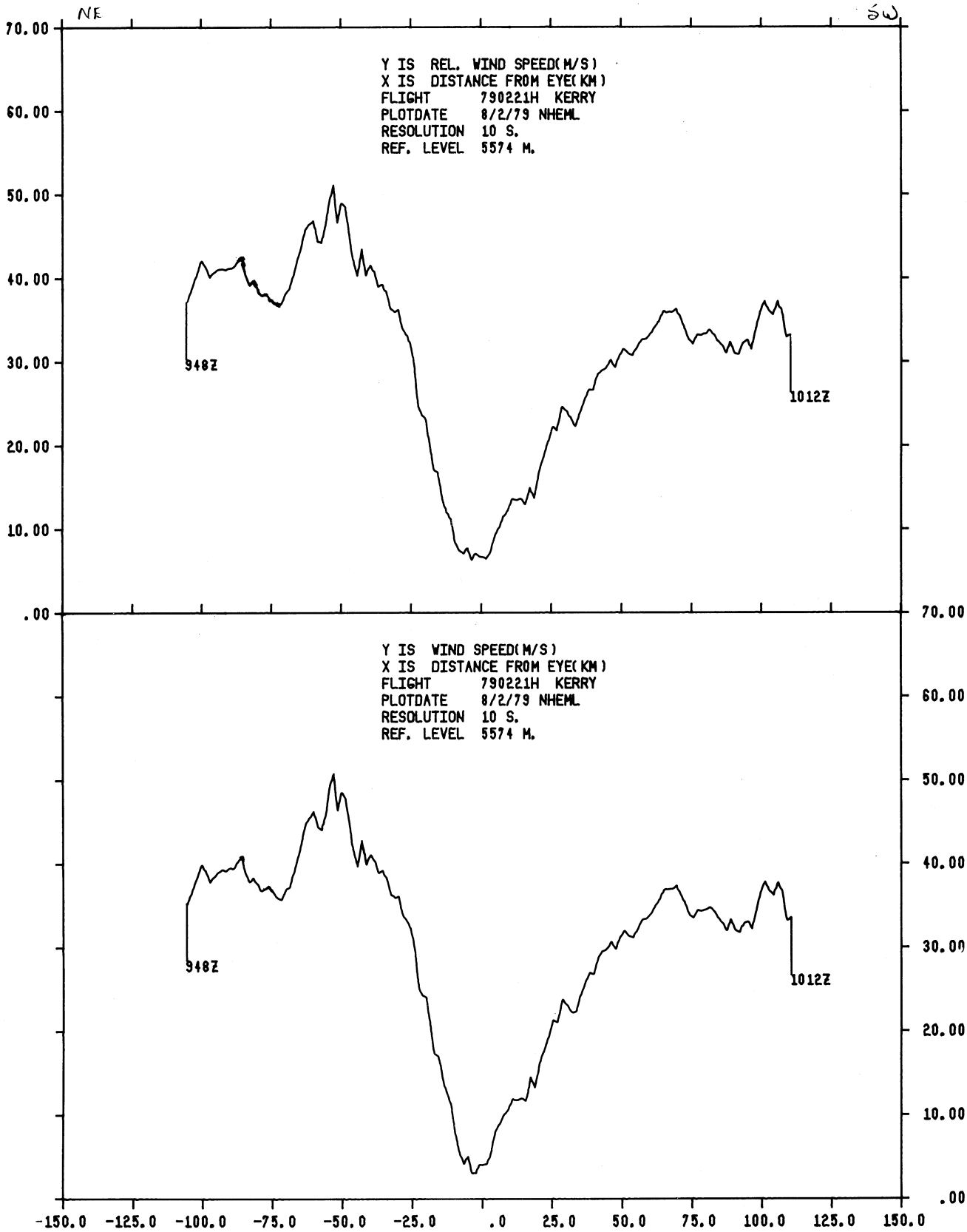

Figure 35. Same as figure 33, except for relative wind speed (top) and actual wind speed (bottom).

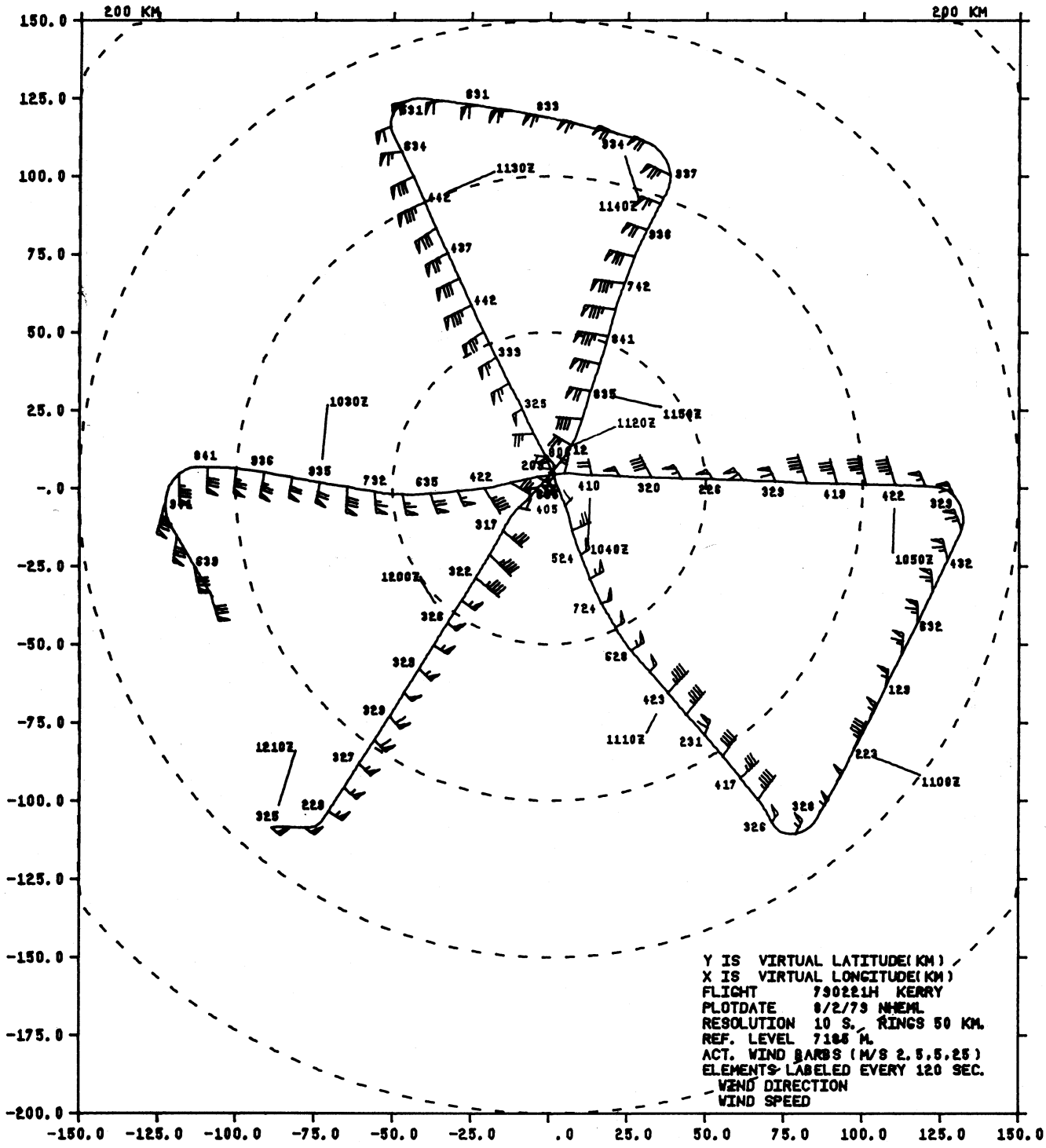

Figure 36. Plan view of aircraft position and actual winds relative to the center of Tropical Cyclone Kerry from 1021 Z to 1210 Z on February 21, 1979, and at a reference pressure altitude of 7185 m (400 mb).

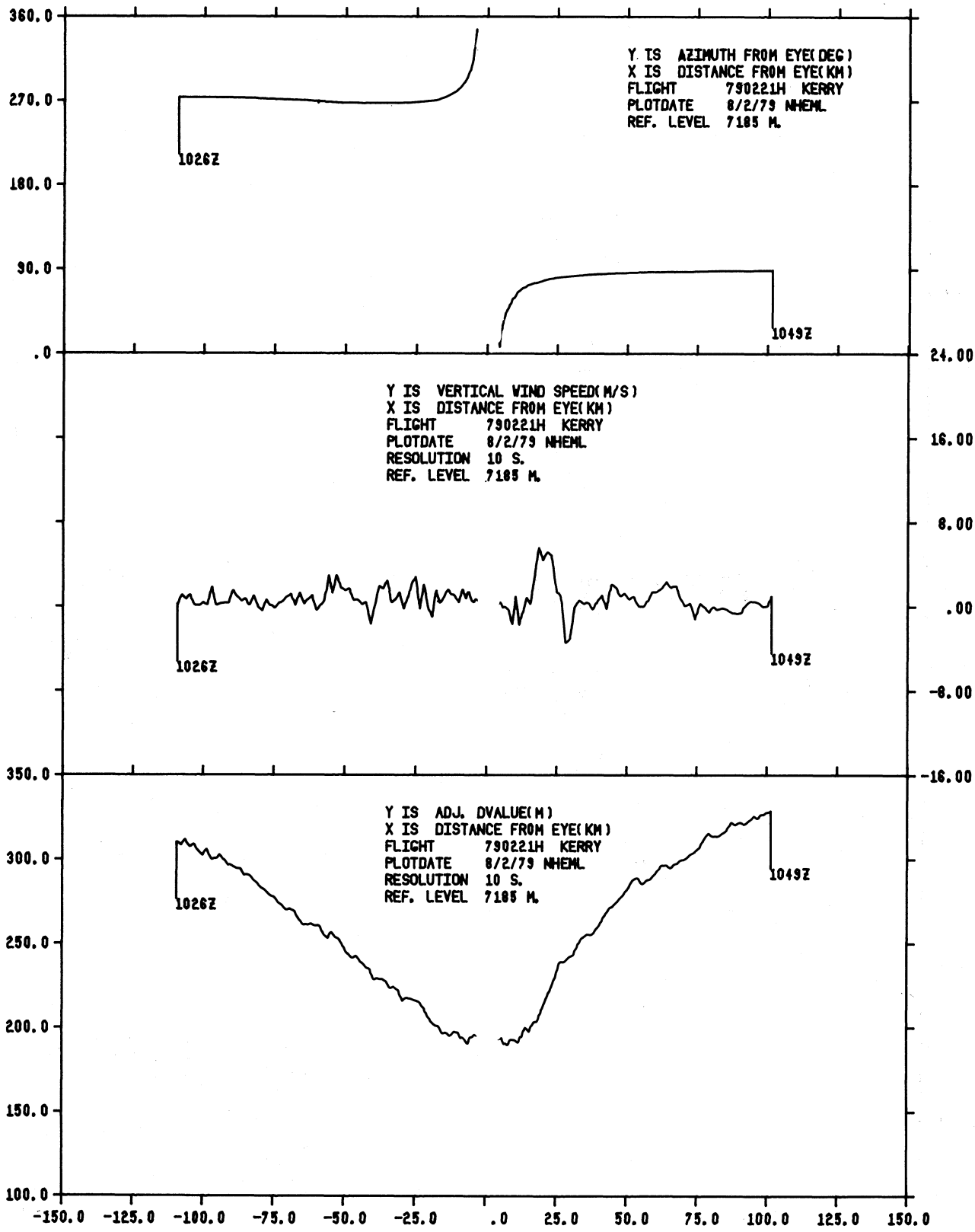

Figure 37. Profiles of the aircraft position (observation point) from the storm center in degrees (top), vertical wind (middle), and adjusted "D" value (bottom) versus radial distance from the storm center. Profiles correspond to the west-to-east pass in figure 36 from 1026 Z to 1049 Z.

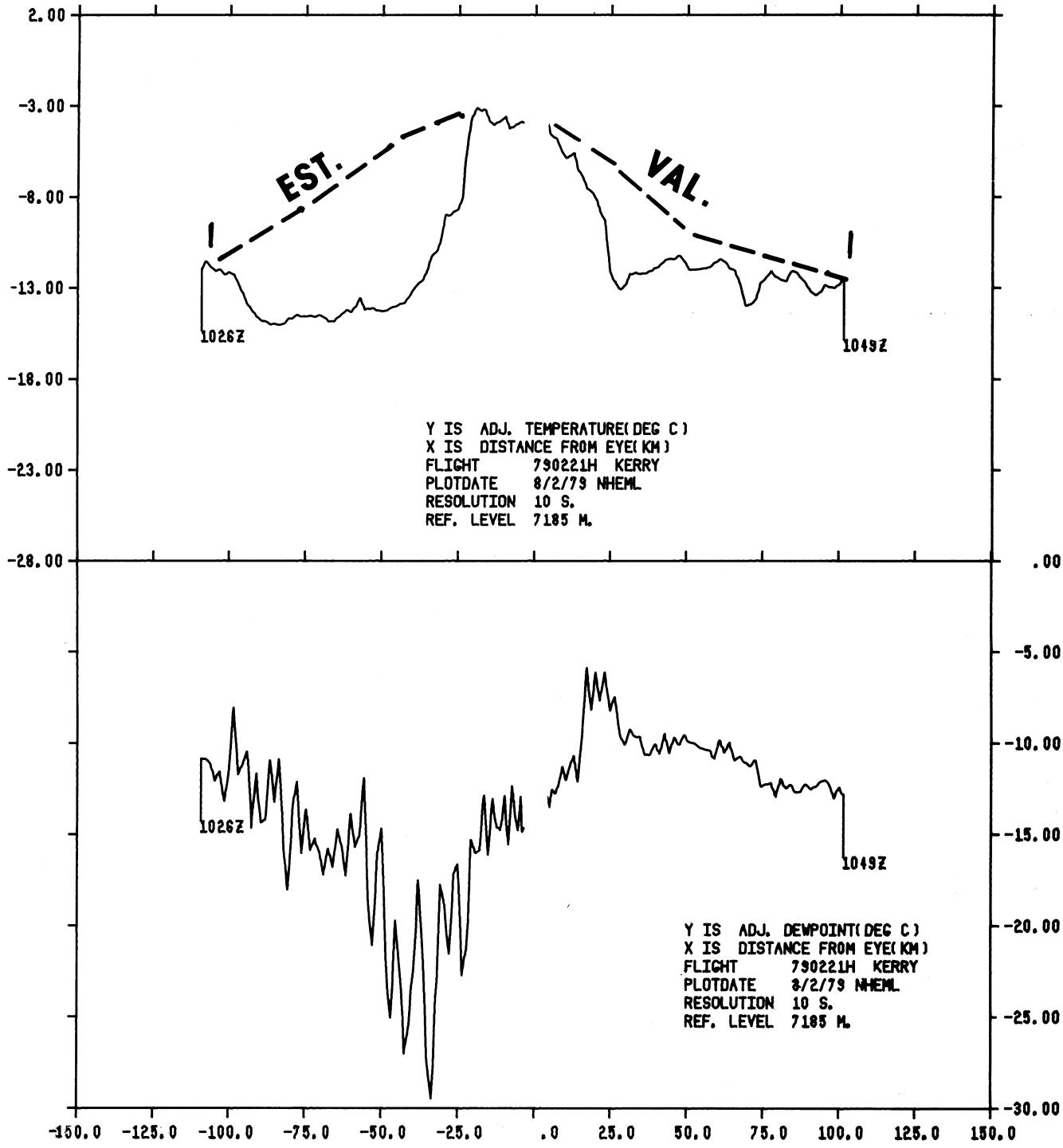

Figure 38. Same as figure 37, except for adjusted temperatures (top) and adjusted dew point temperatures (bottom). (Note comments in section 3.1.)

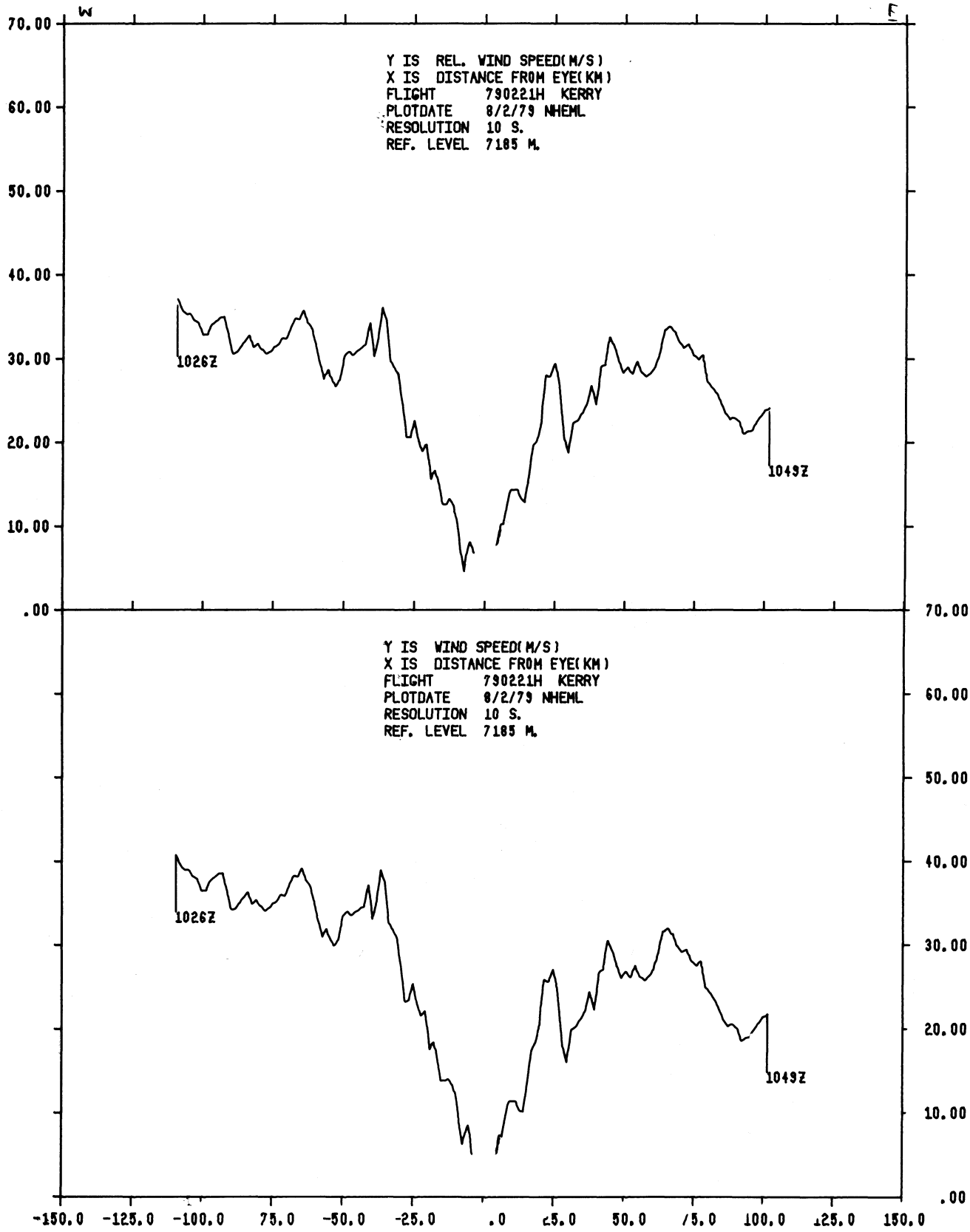

Figure 39. Same as figure 37, except for relative wind speed (top) and actual wind speed (bottom).

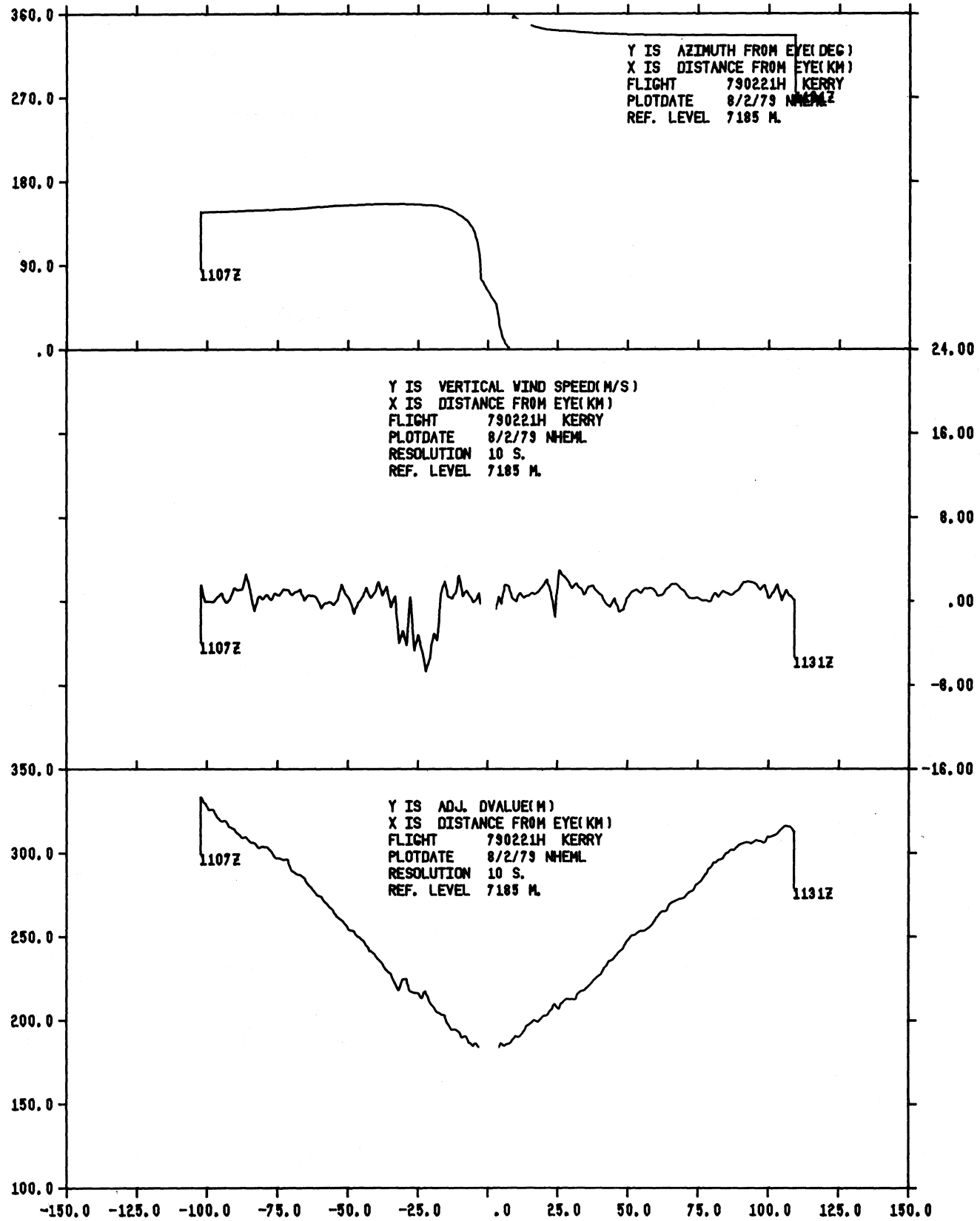

Figure 40. Same as figure 37, except for southeast-to-northwest pass in figure 36 from 1107 Z to 1131 Z.

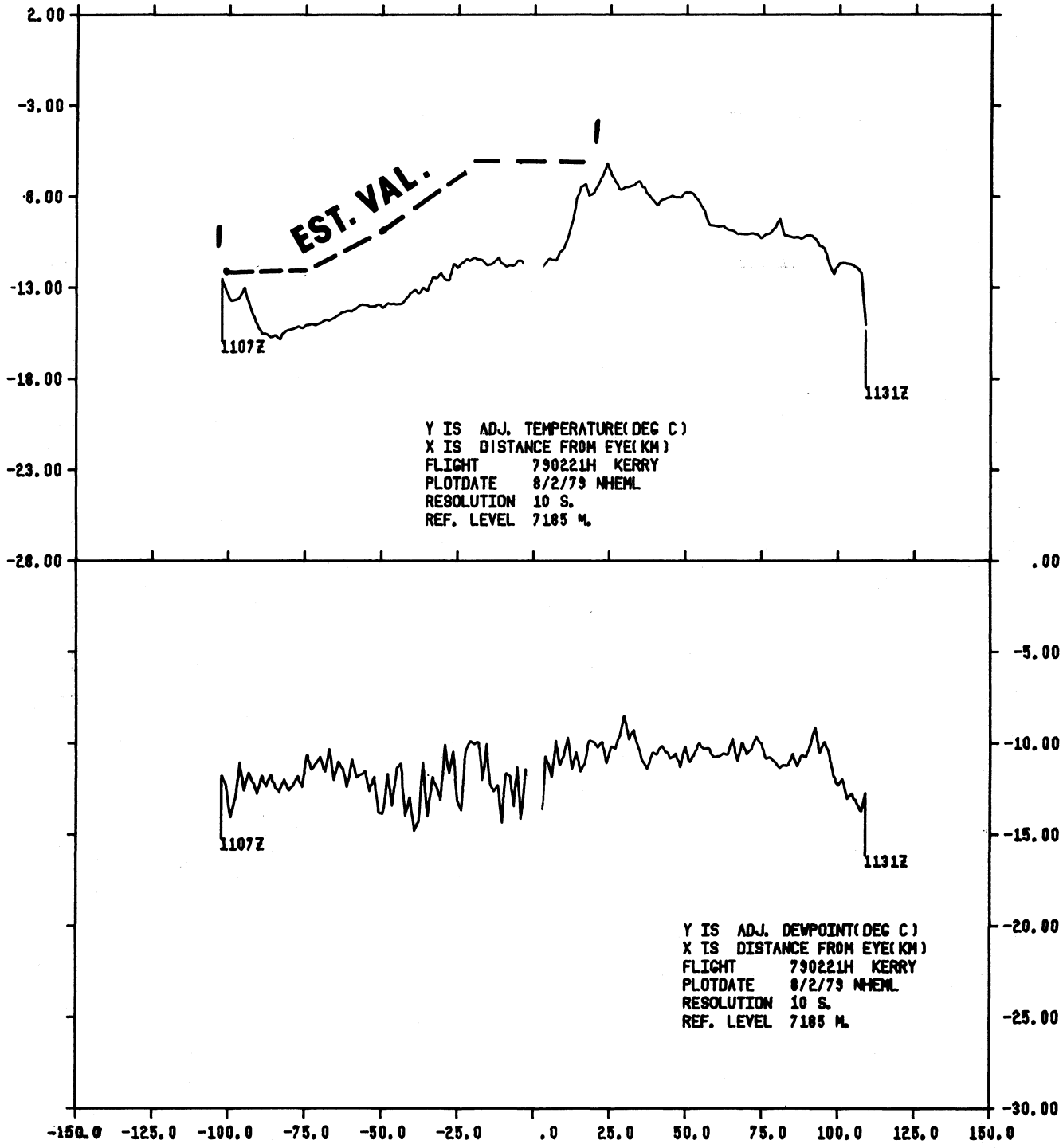

Figure 41. Same as figure 40, except for adjusted temperatures (top) and adjusted dew point temperatures (bottom). (Note comments in section 3.1.)

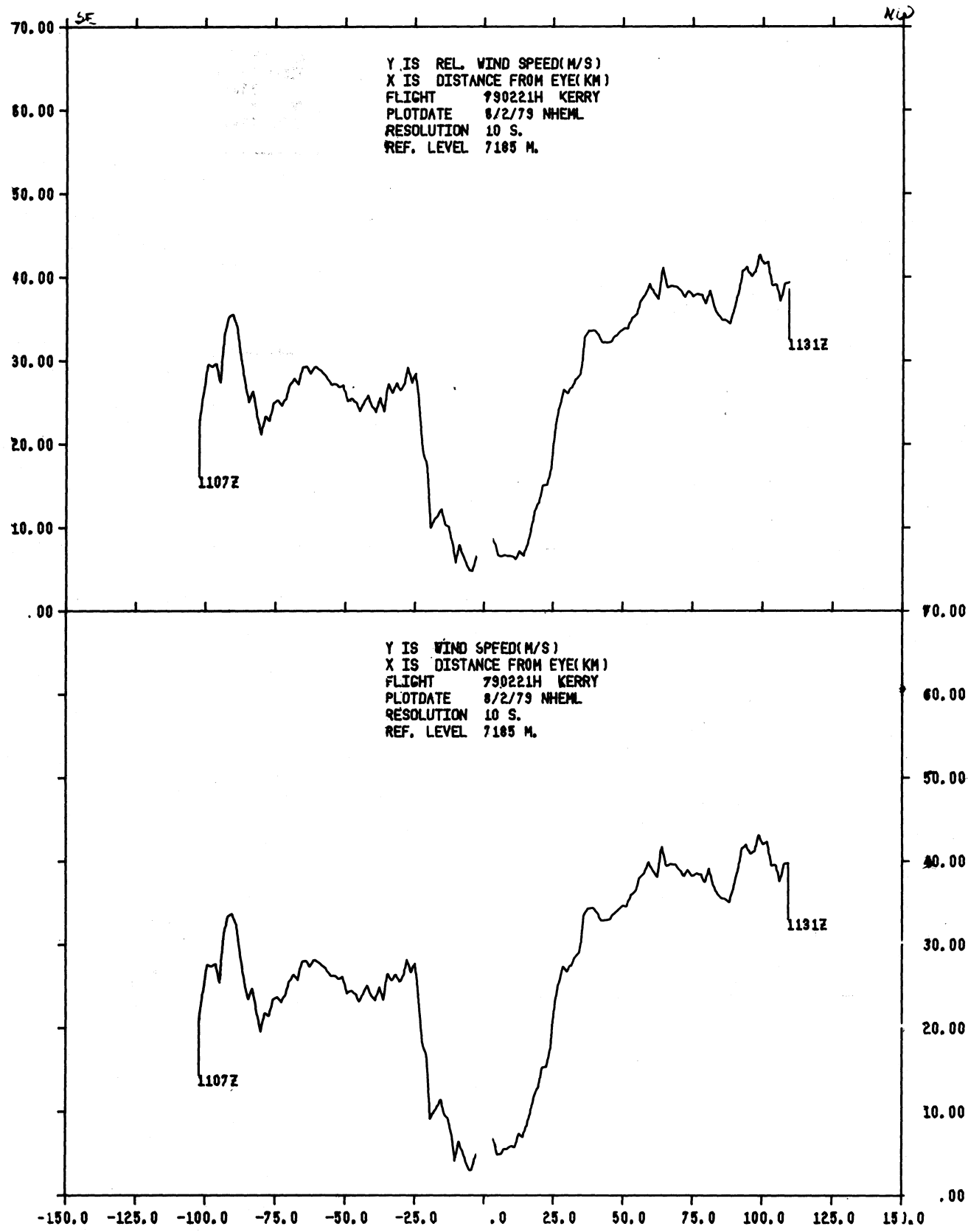

Figure 42. Same as figure 40, except for relative wind speed (top) and actual wind speed (bottom).

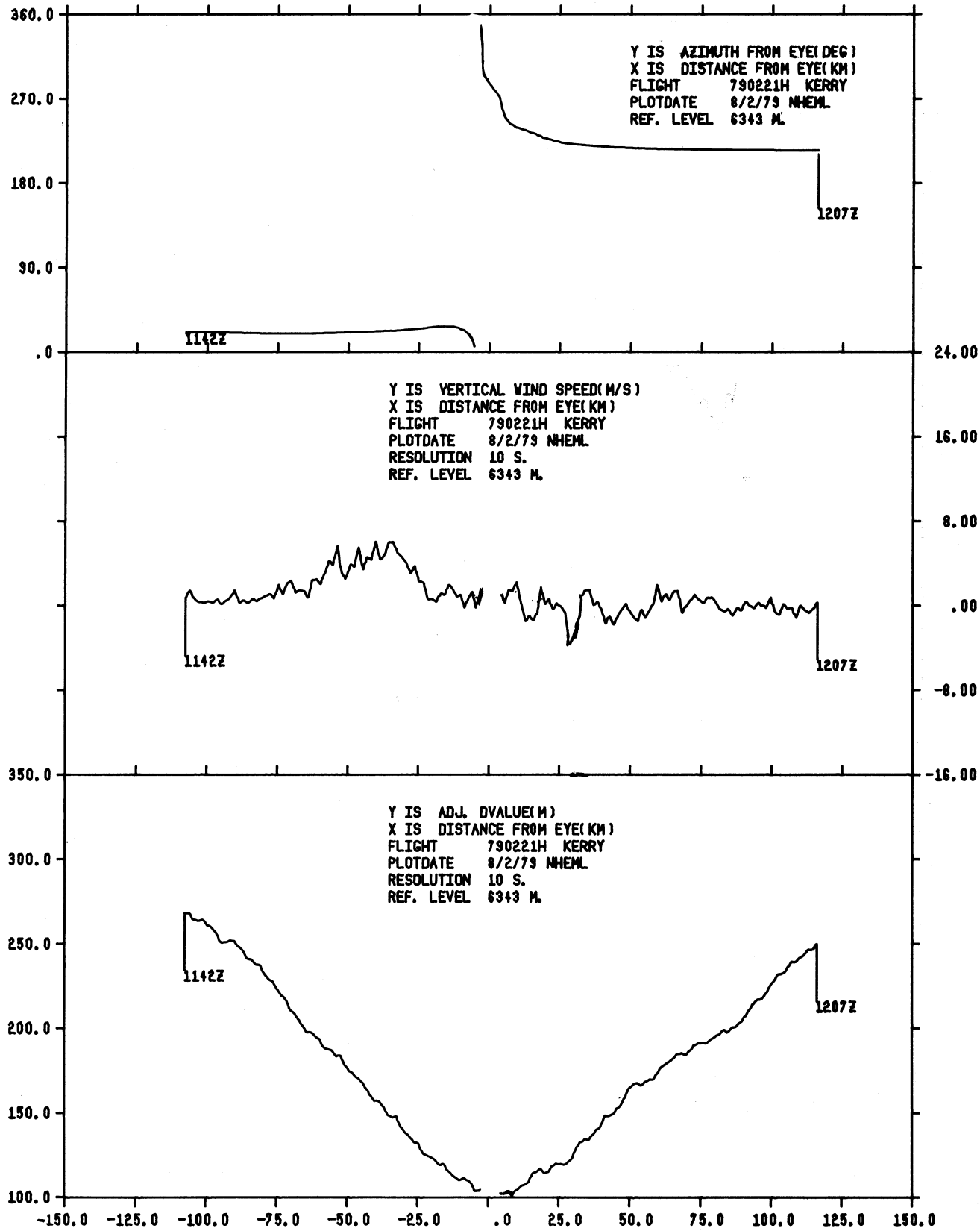

Figure 43. Same as figure 37, except for northeast-to-southwest pass in figure 36 from 1142 Z to 1207 Z and a reference pressure altitude of 6343 m (450 mb).

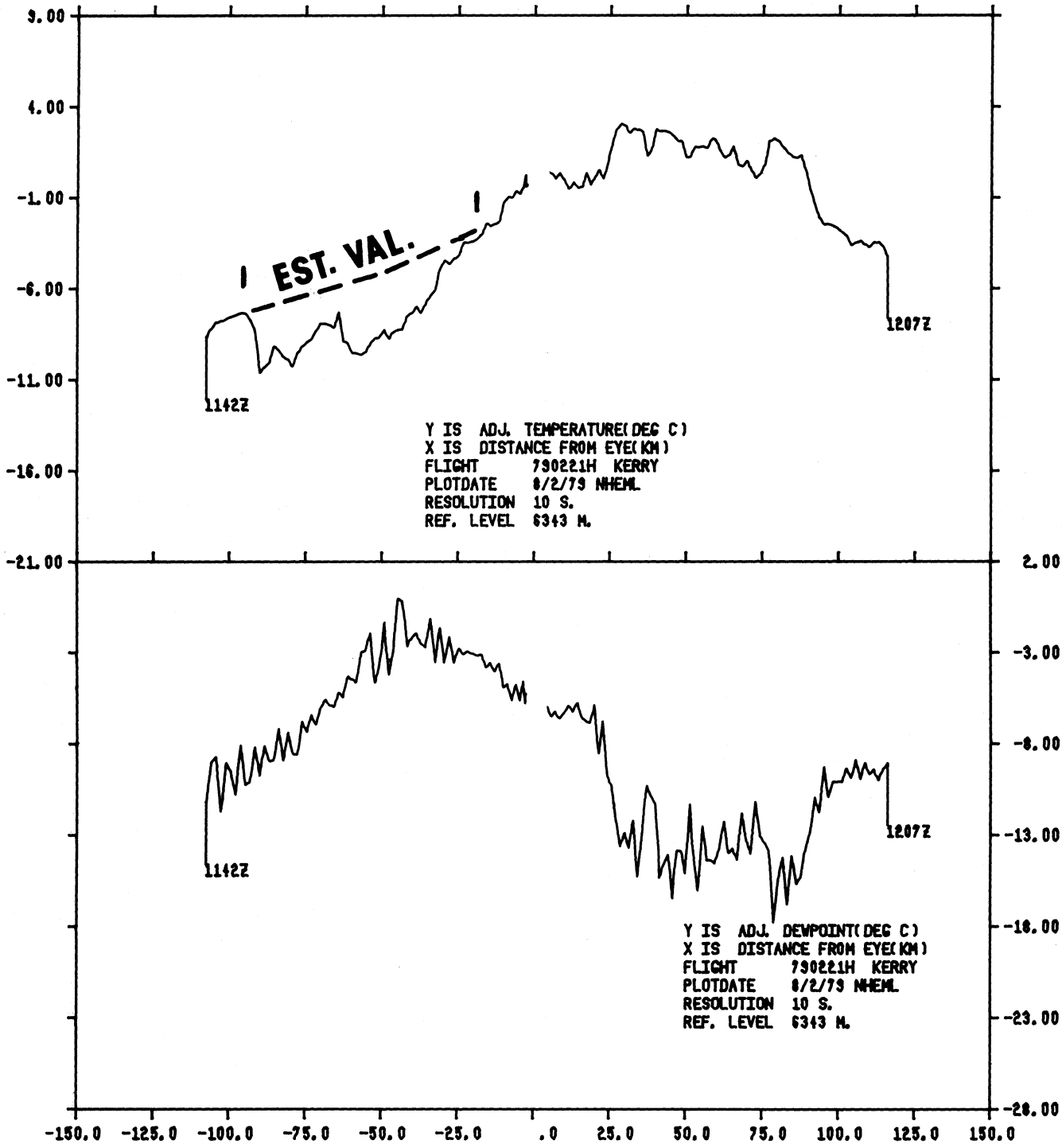

Figure 44. Same as figure 43, except for adjusted temperatures (top) and adjusted dew point temperatures (bottom). (Note comments in section 3.1.)

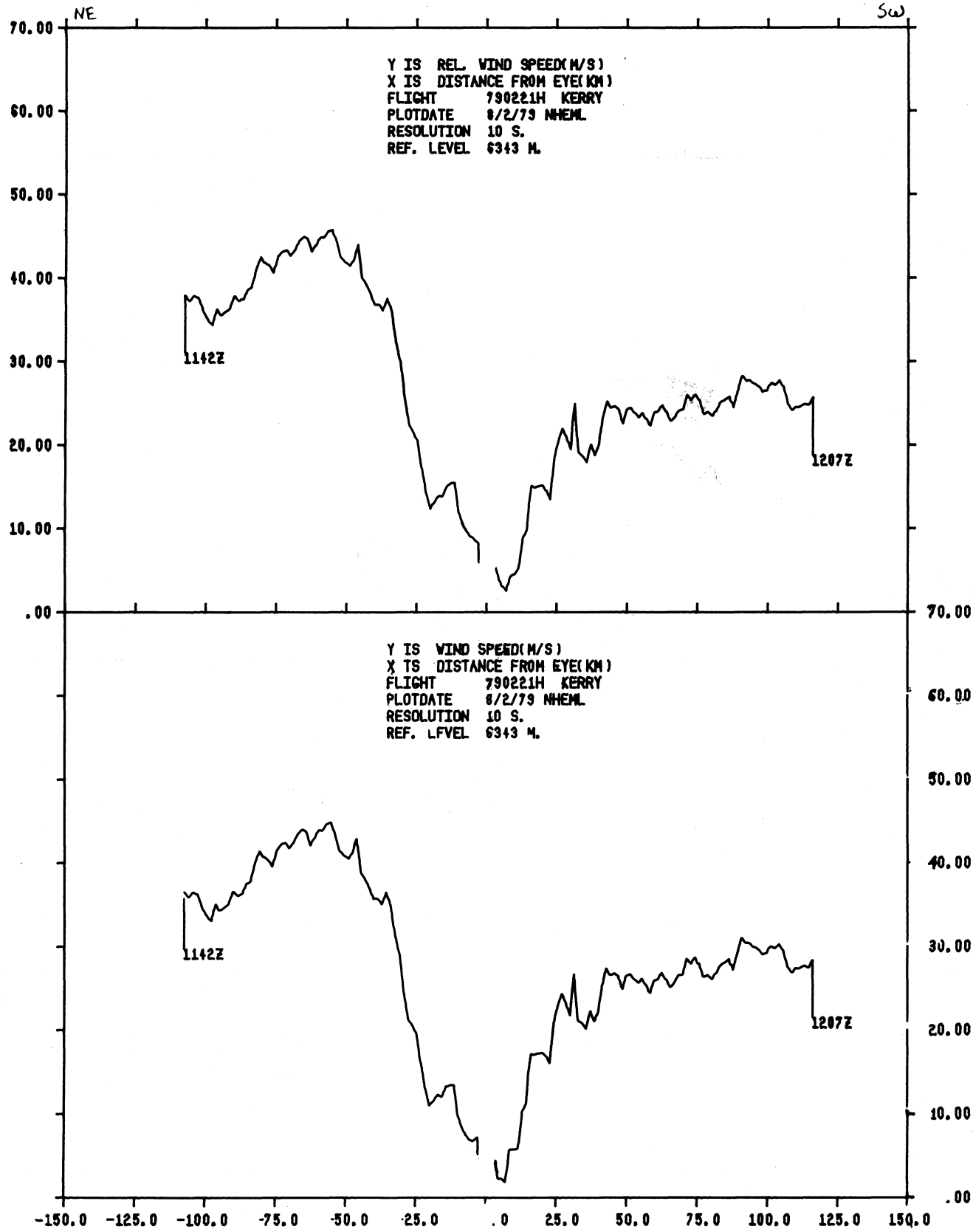

Figure 45. Same as figure 43, except for relative wind speed (top) and actual wind speed (bottom).

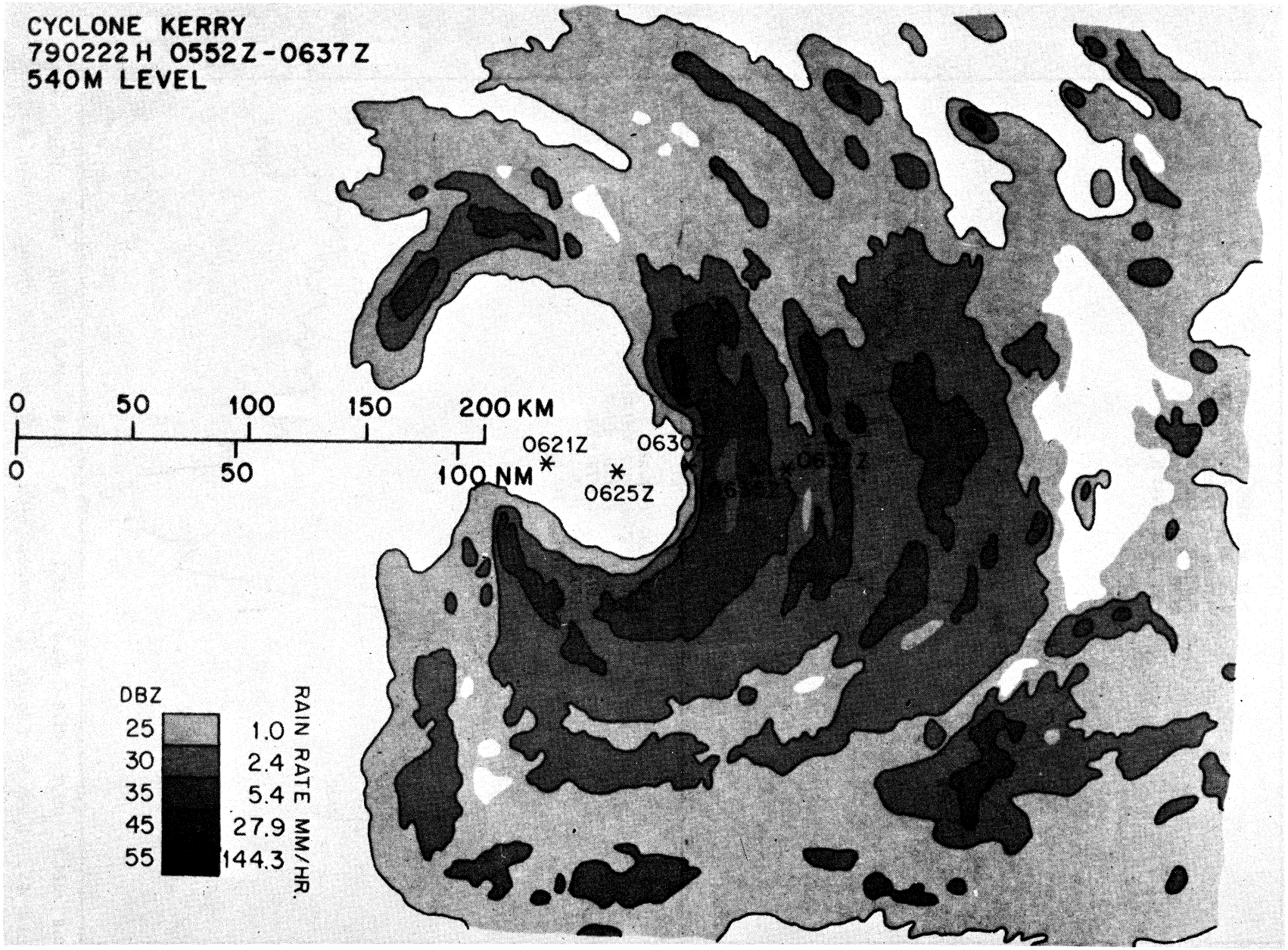

Figure 46. Digitized Plan Position Indicator radar depiction of Tropical Cyclone Kerry composited from 0552 Z to 0637 Z on February 22, 1979.

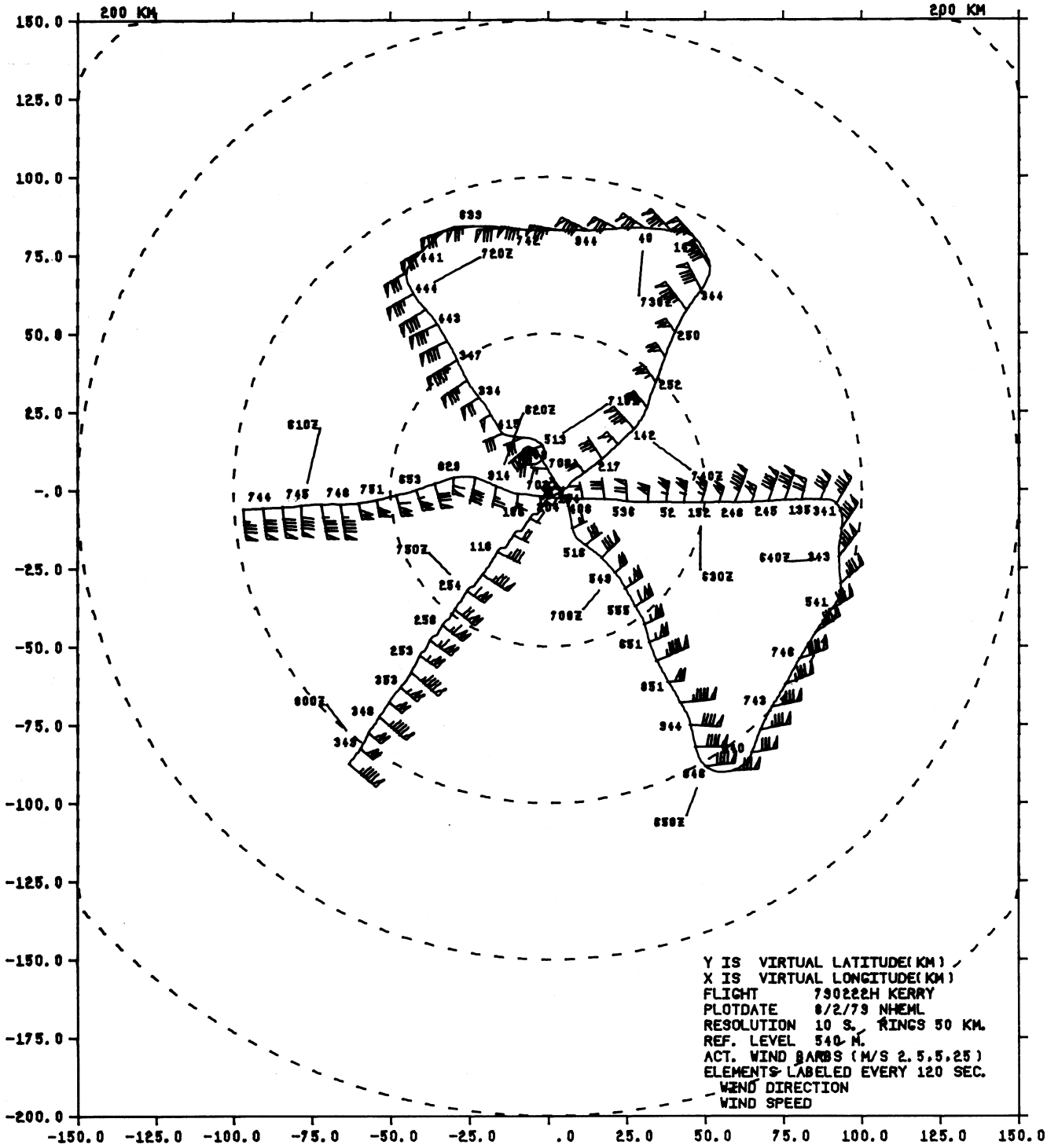

Figure 47. Plan view of aircraft position and actual winds relative to the center of Tropical Cyclone Kerry from 0607 Z to 0801 Z on February 22, 1979, and at an altitude of 540 m.

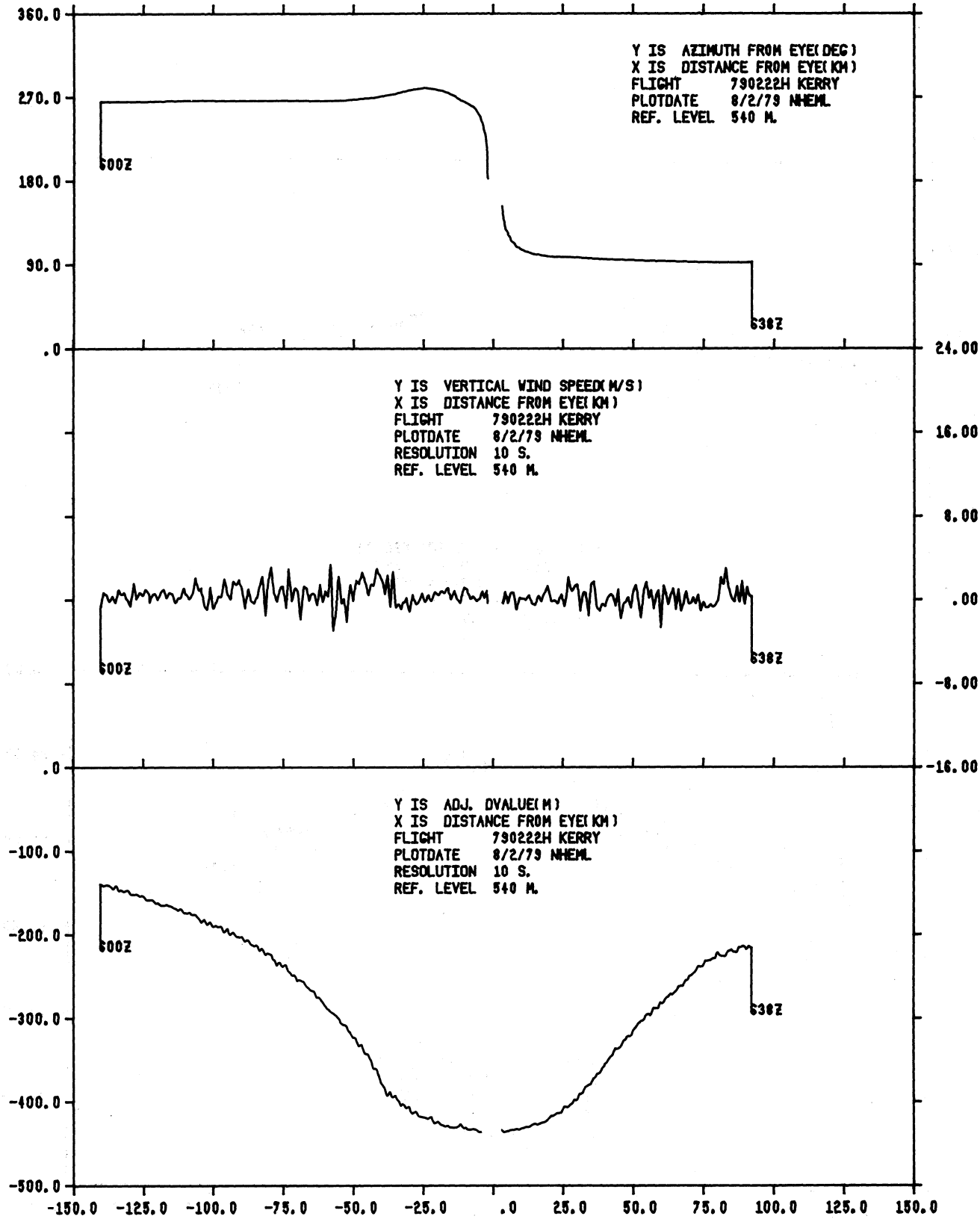

Figure 48. Profiles of the aircraft position (observation point) from the storm center in degrees (top), vertical wind (middle), and adjusted "D" value (bottom) versus radial distance from the storm center. Profiles correspond to the west-to-east pass in figure 47 from 0600 Z to 0638 Z with a reference pressure altitude of 540 m (950 mb).

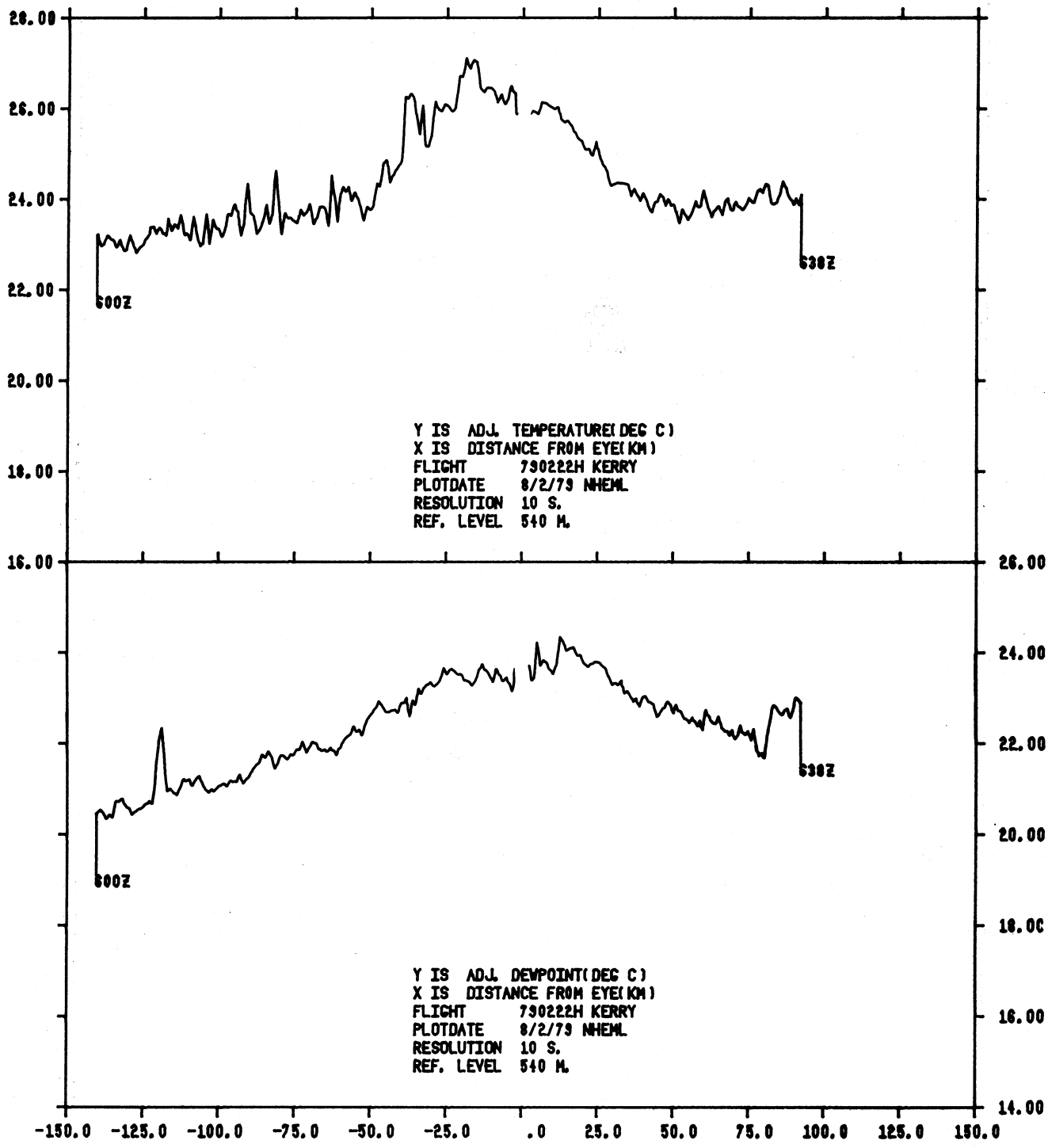

Figure 49. Same as figure 48, except for adjusted temperatures (top) and adjusted dew point temperatures (bottom).

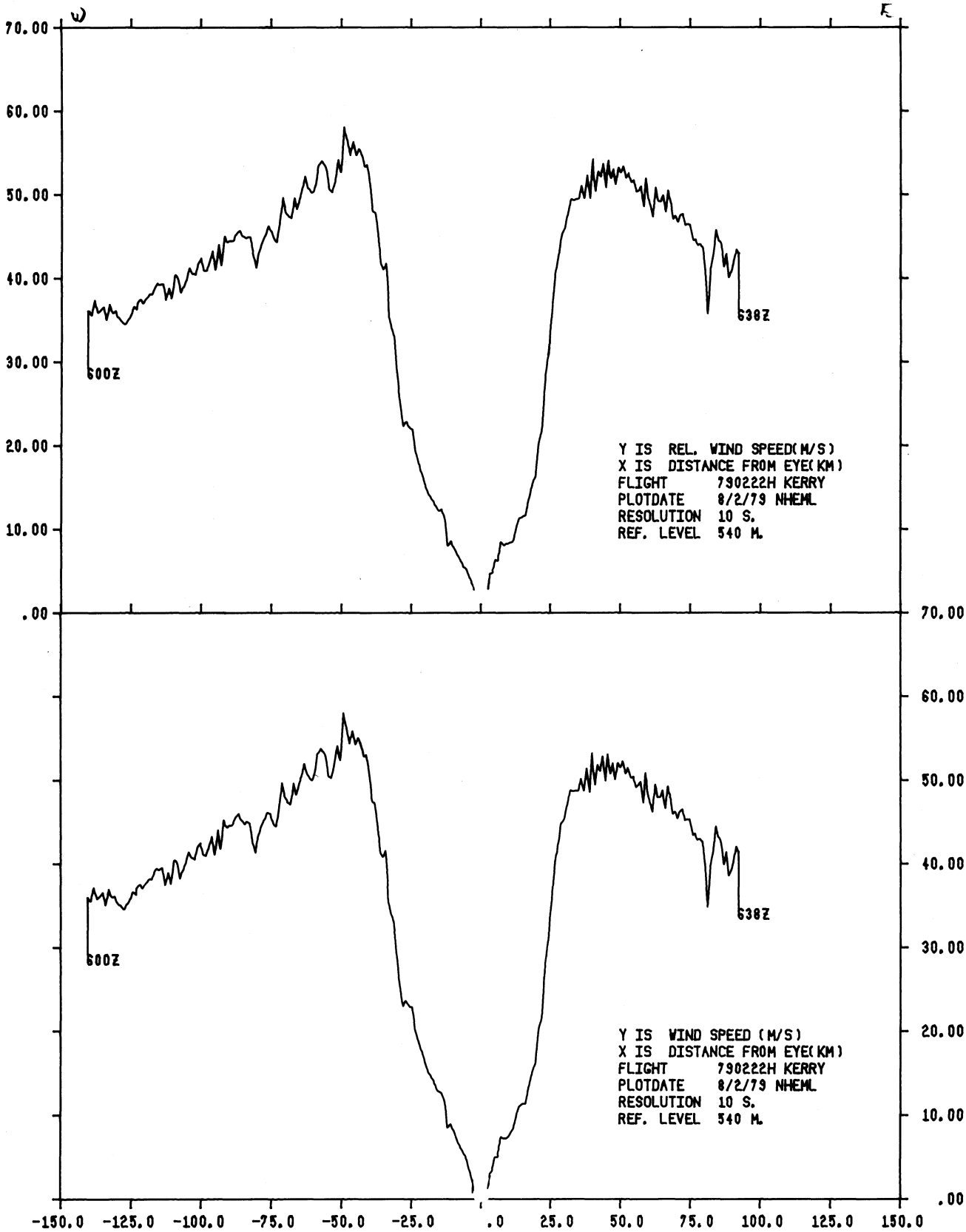

Figure 50. Same as figure 48, except for relative wind speed (top) and actual wind speed (bottom).

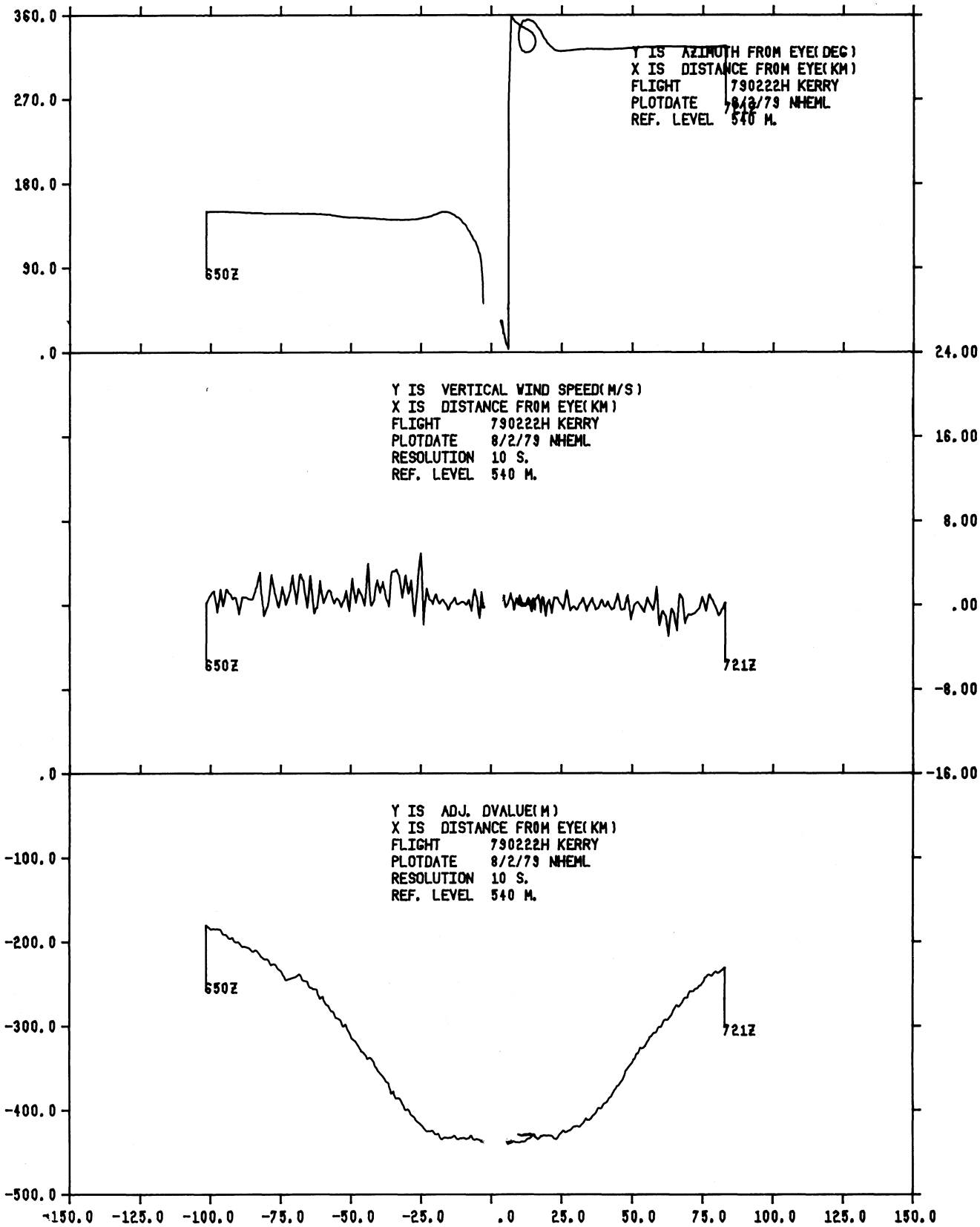

Figure 51. Same as figure 48, except for the southeast-to-northwest pass in figure 47 from 0650 Z to 0721 Z.

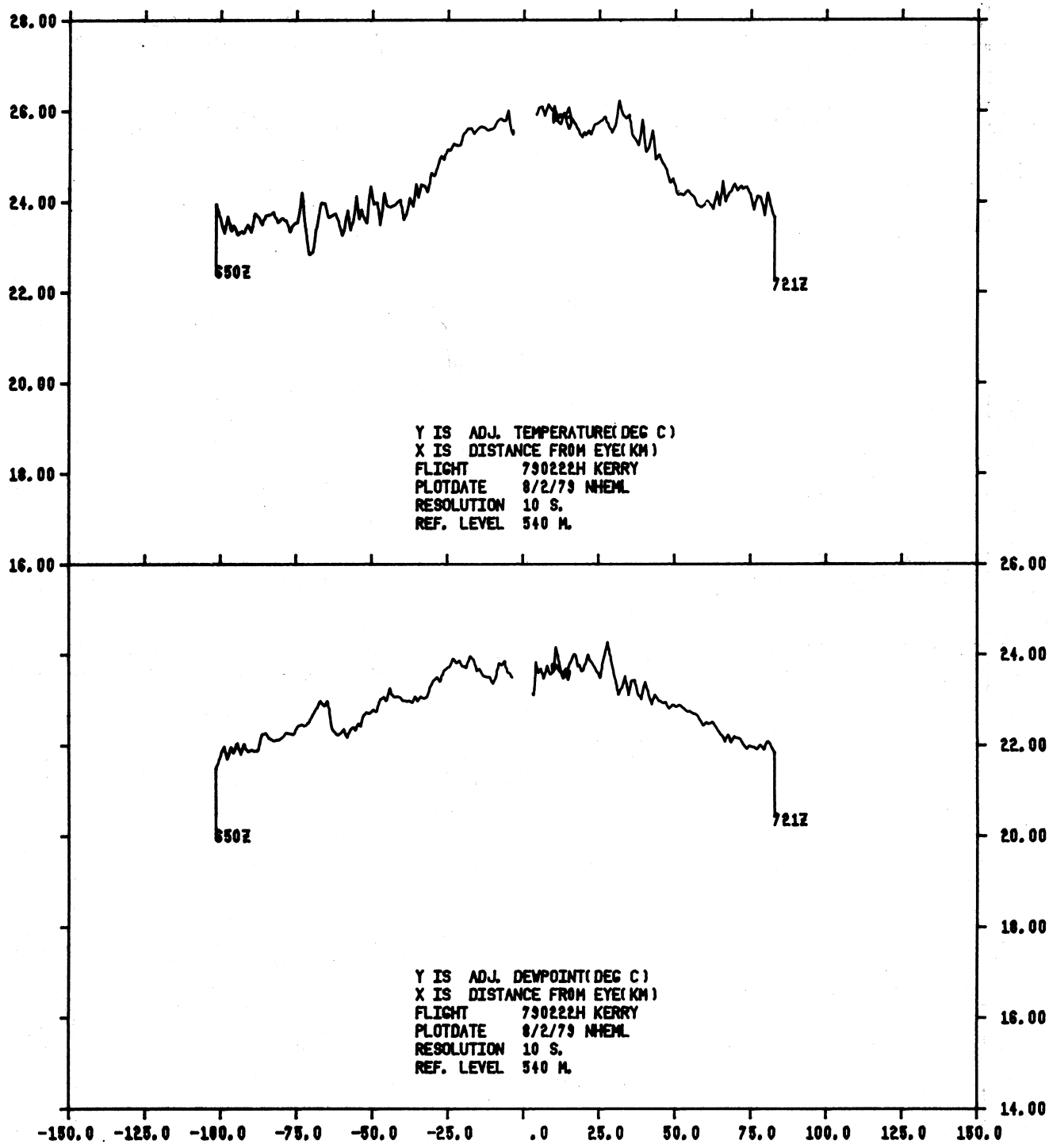

Figure 52. Same as figure 51, except for adjusted temperatures (top) and adjusted dew point temperatures (bottom).

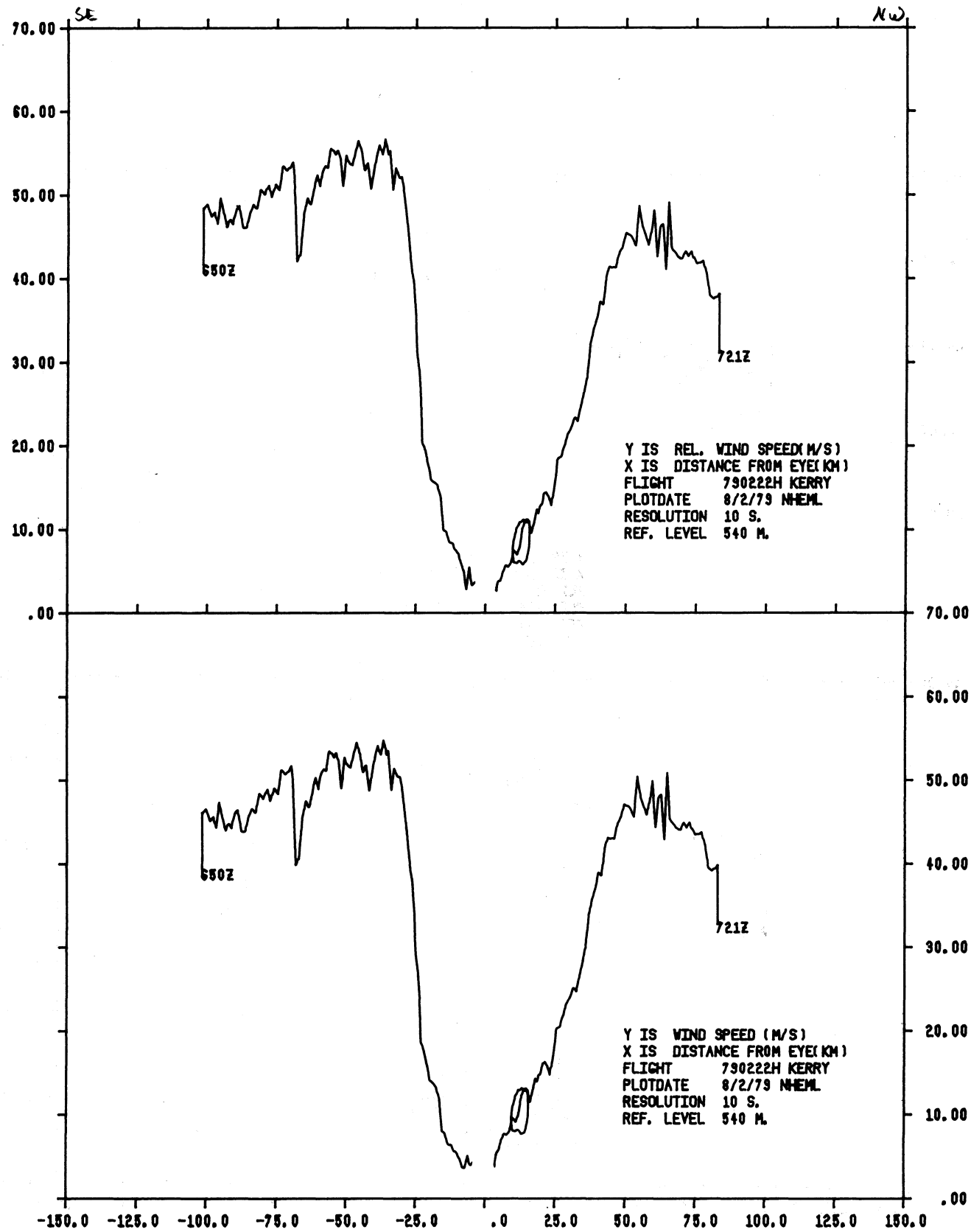

Figure 53. Same as figure 51, except for relative wind speed (top) and actual wind speed (bottom).

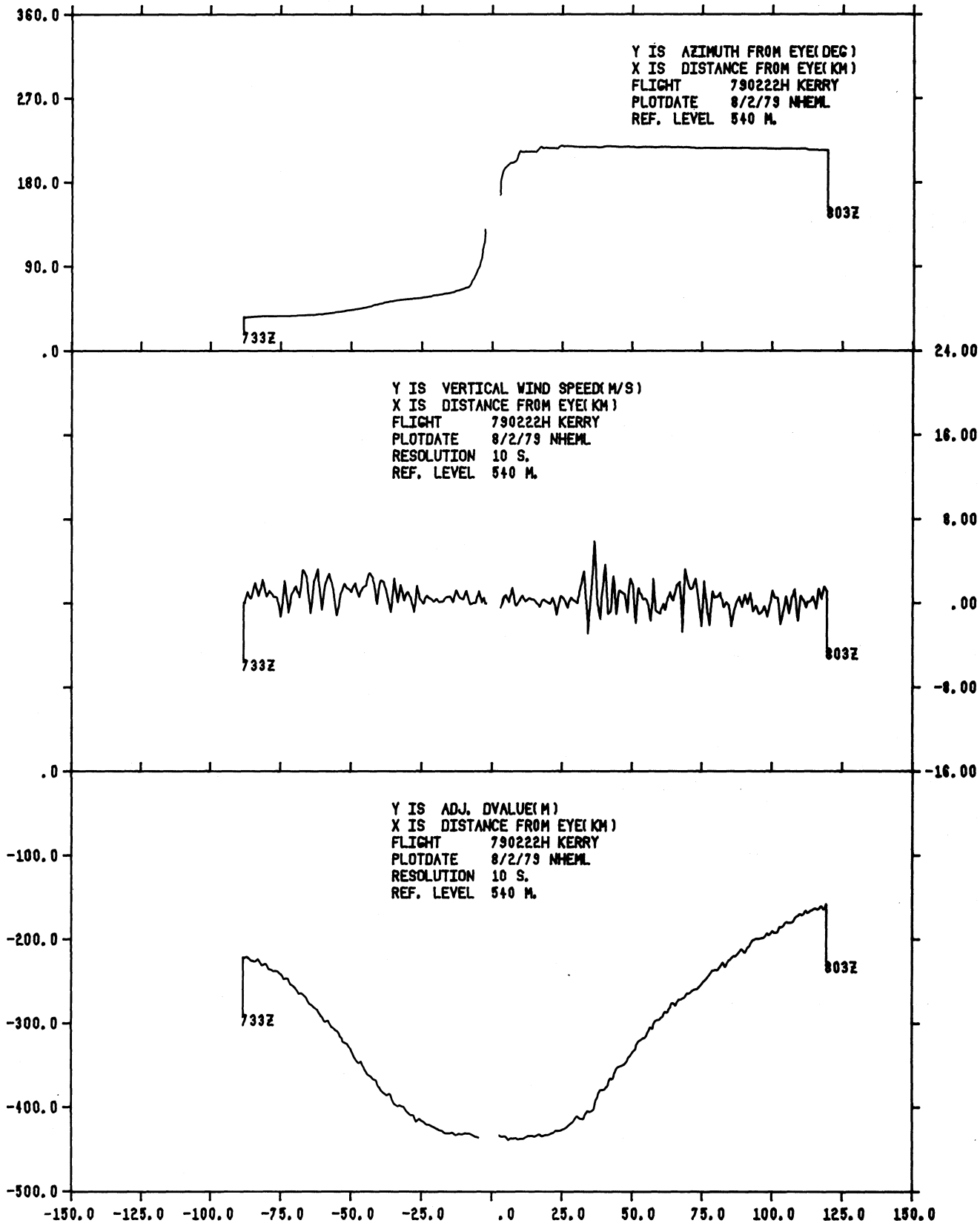

Figure 54. Same as figure 48, except for northeast-to-southwest pass in figure 47 from 0733 Z to 0803 Z.

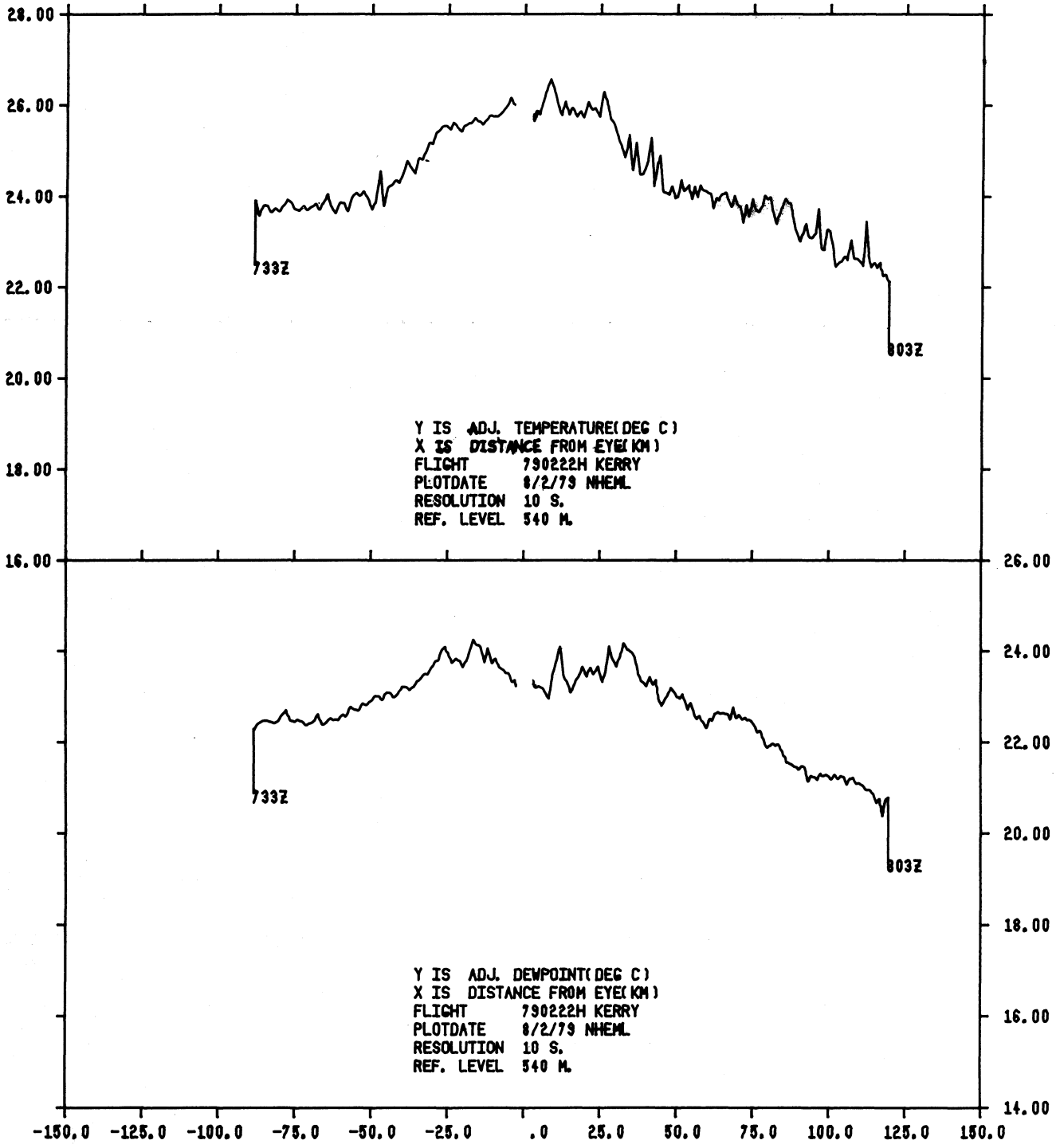

Figure 55. Same as figure 54, except for adjusted temperatures (top) and adjusted dew point temperatures (bottom).

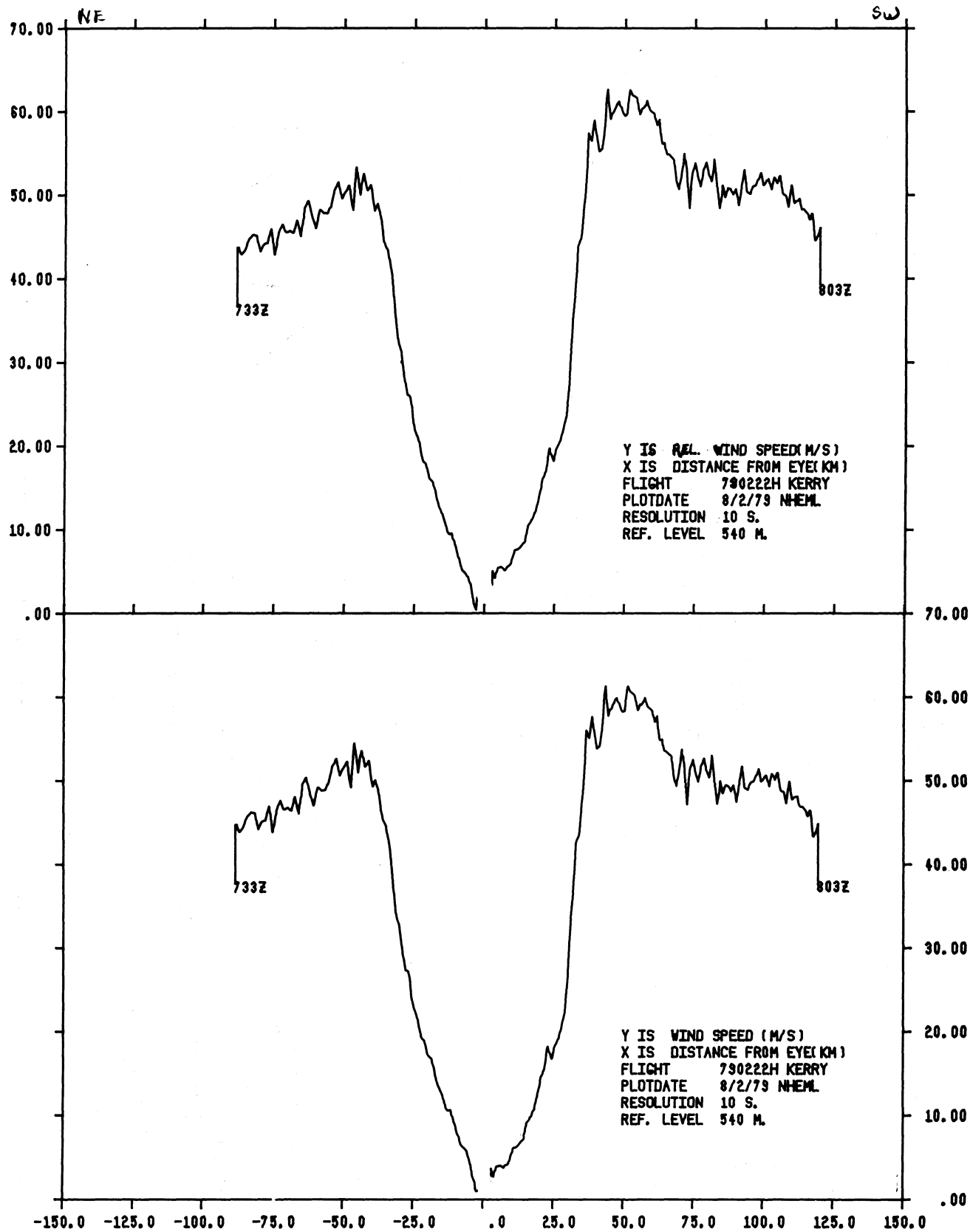

Figure 56. Same as figure 54, except for relative wind speed (top) and actual wind speed (bottom).

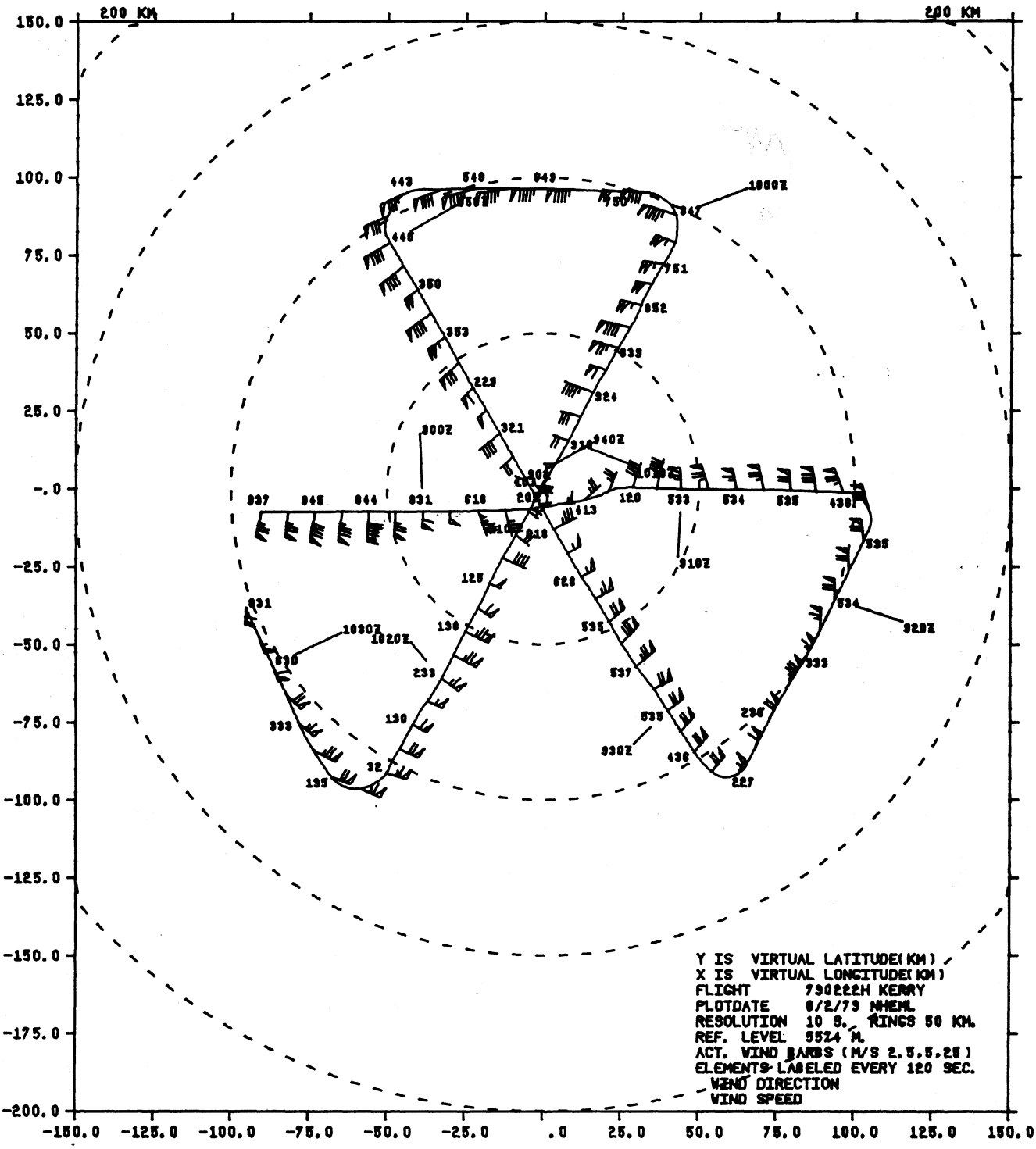

Figure 57. Plan view of aircraft position and actual winds relative to the center of Tropical Cyclone Kerry from 0854 Z 1032 Z on February 22, 1979, and a reference pressure altitude of 5574 m (500 mb).

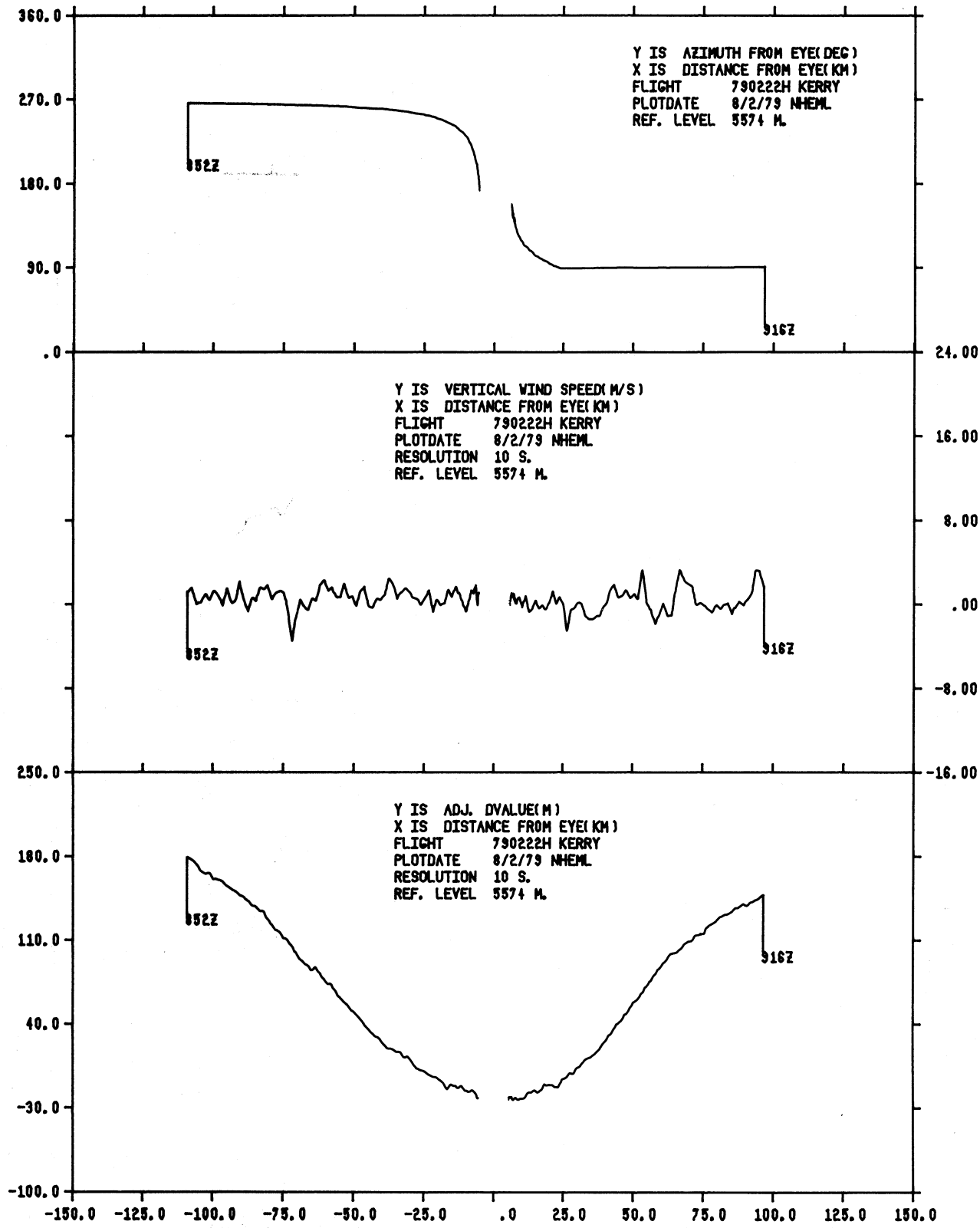

Figure 58. Profiles of the aircraft position (observation point) from the storm center in degrees (top), vertical wind (middle), and adjusted "D" value (bottom) versus radial distance. Profiles correspond to the west-to-east pass in figure 57 from 0852 Z to 0916 Z.

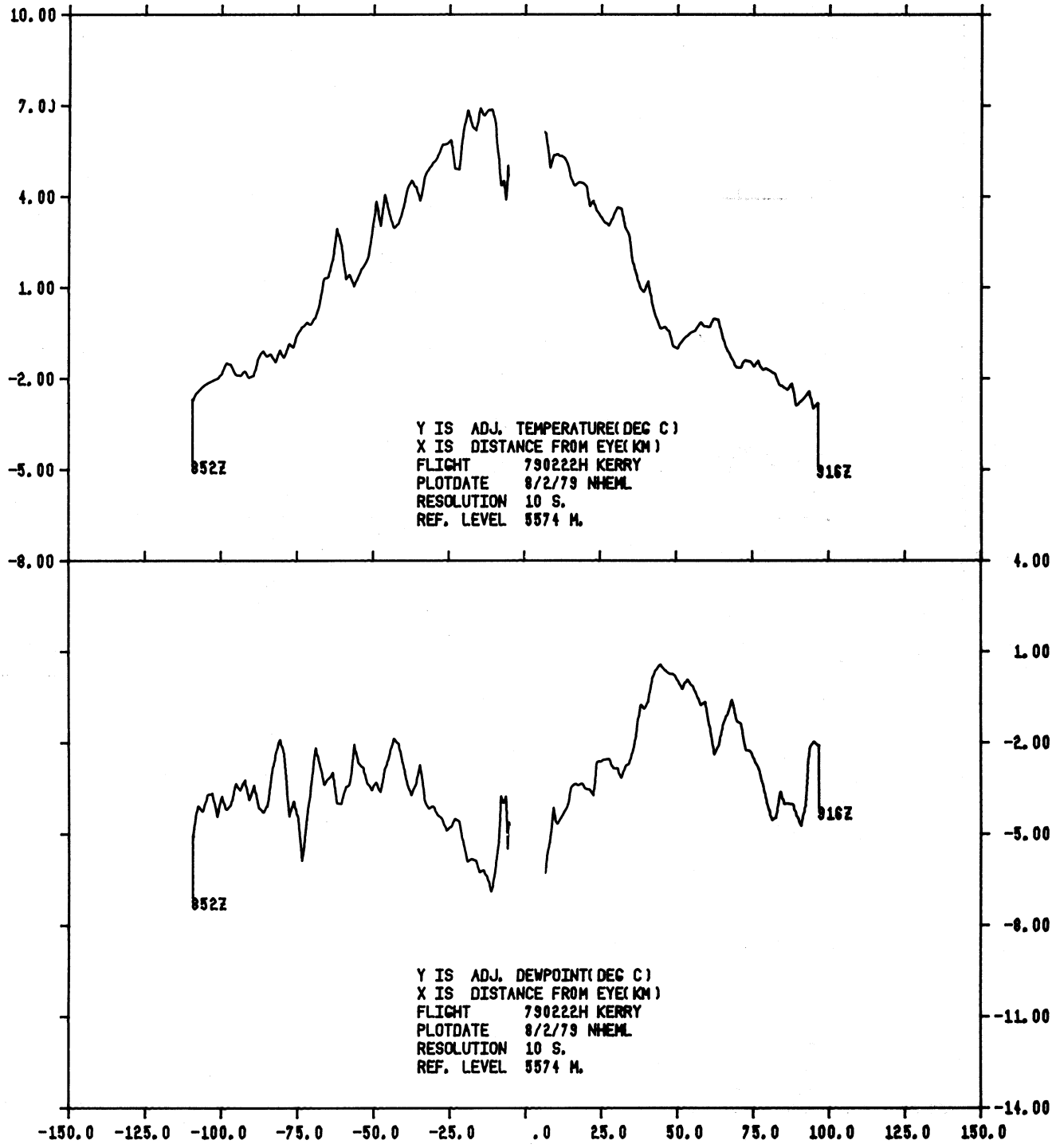

Figure 59. Same as figure 58, except for adjusted temperatures (top) and adjusted dew point temperatures (bottom).

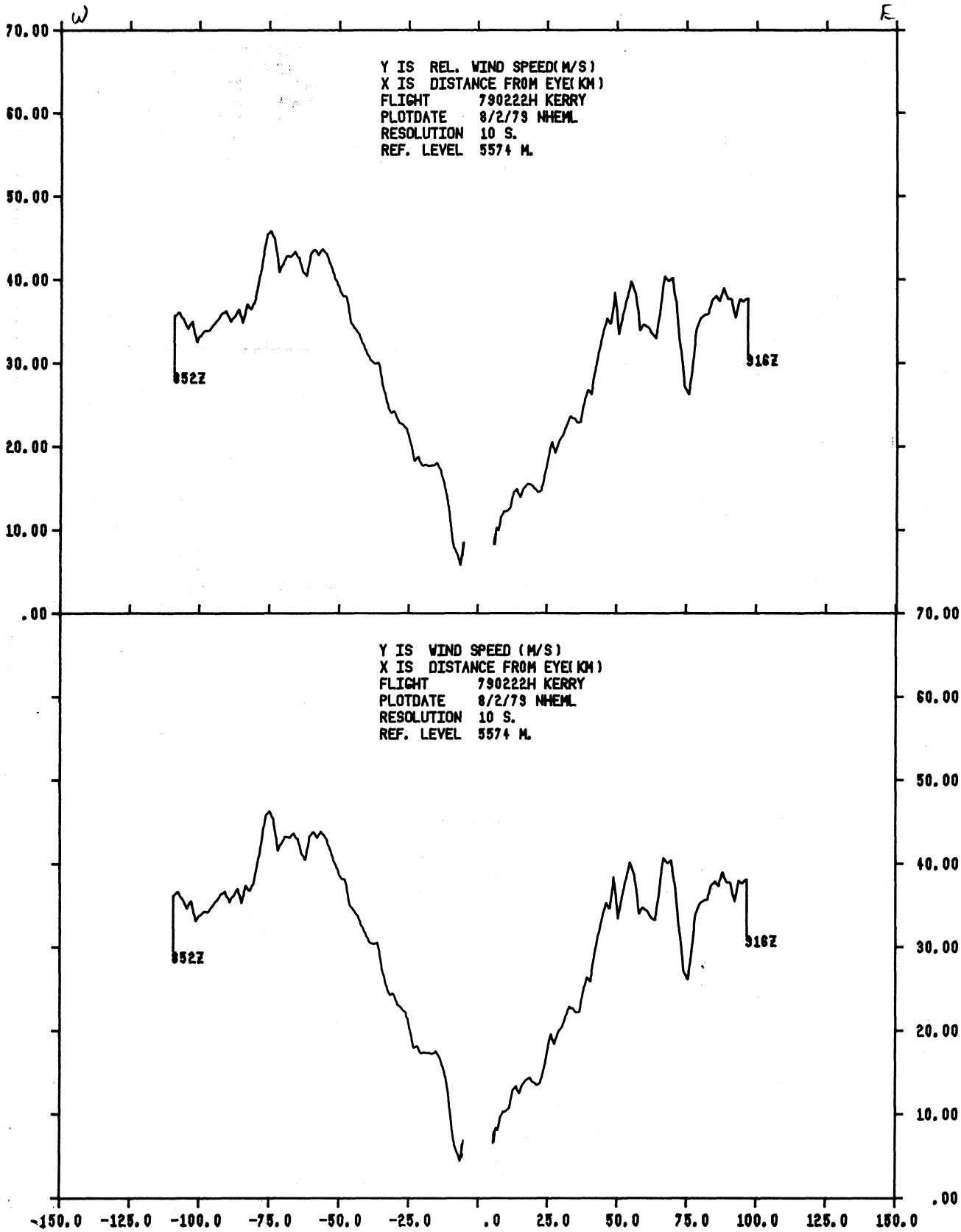

Figure 60. Same of figure 59, except for relative wind speed (top) and actual wind speed (bottom).

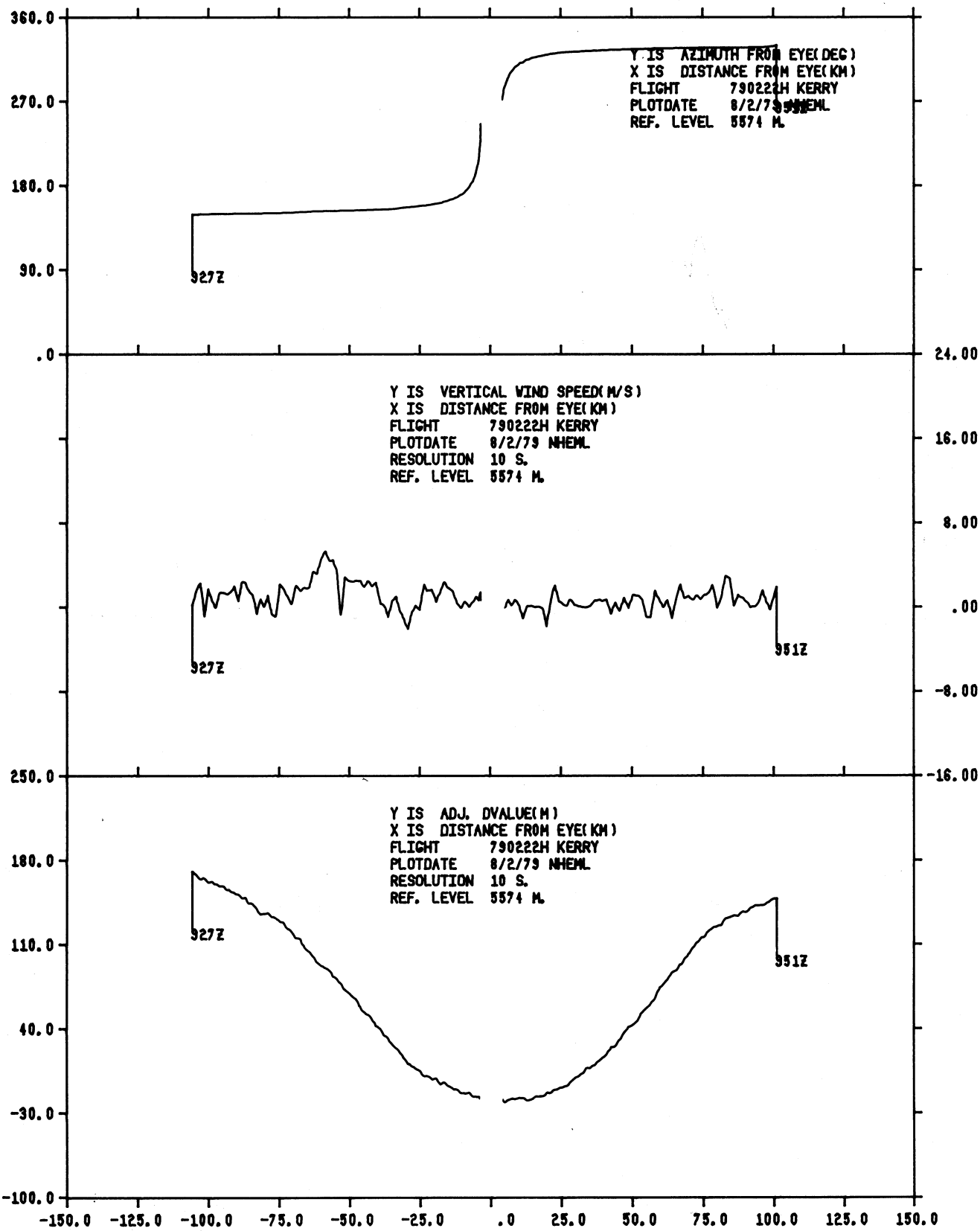

Figure 61. Same as figure 58, except for southeast-to-northwest pass in figure 57 from 0927 Z to 0951 Z.

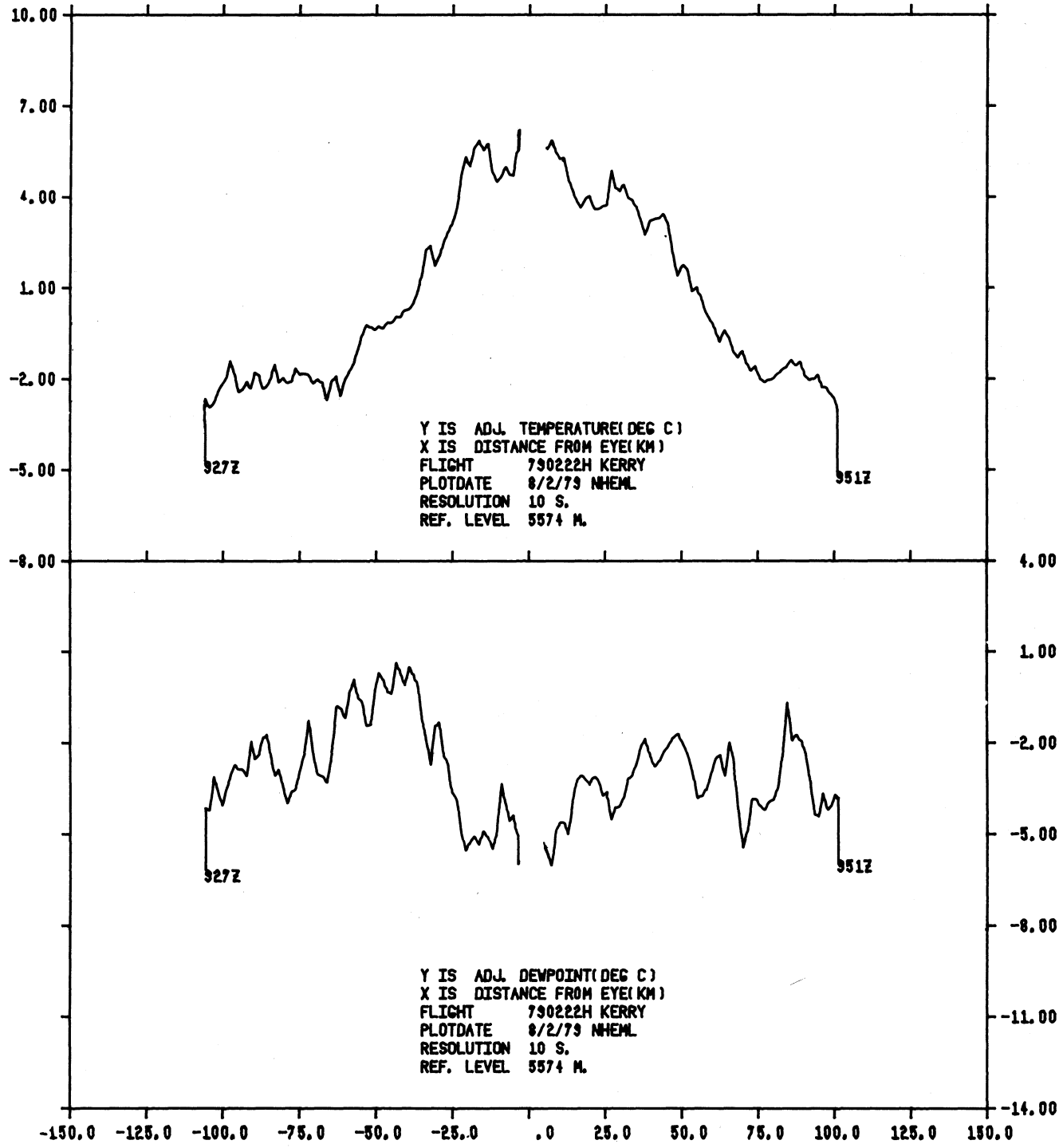

Figure 62. Same as figure 61, except for adjusted temperatures (top) and adjusted dew point temperatures (bottom).

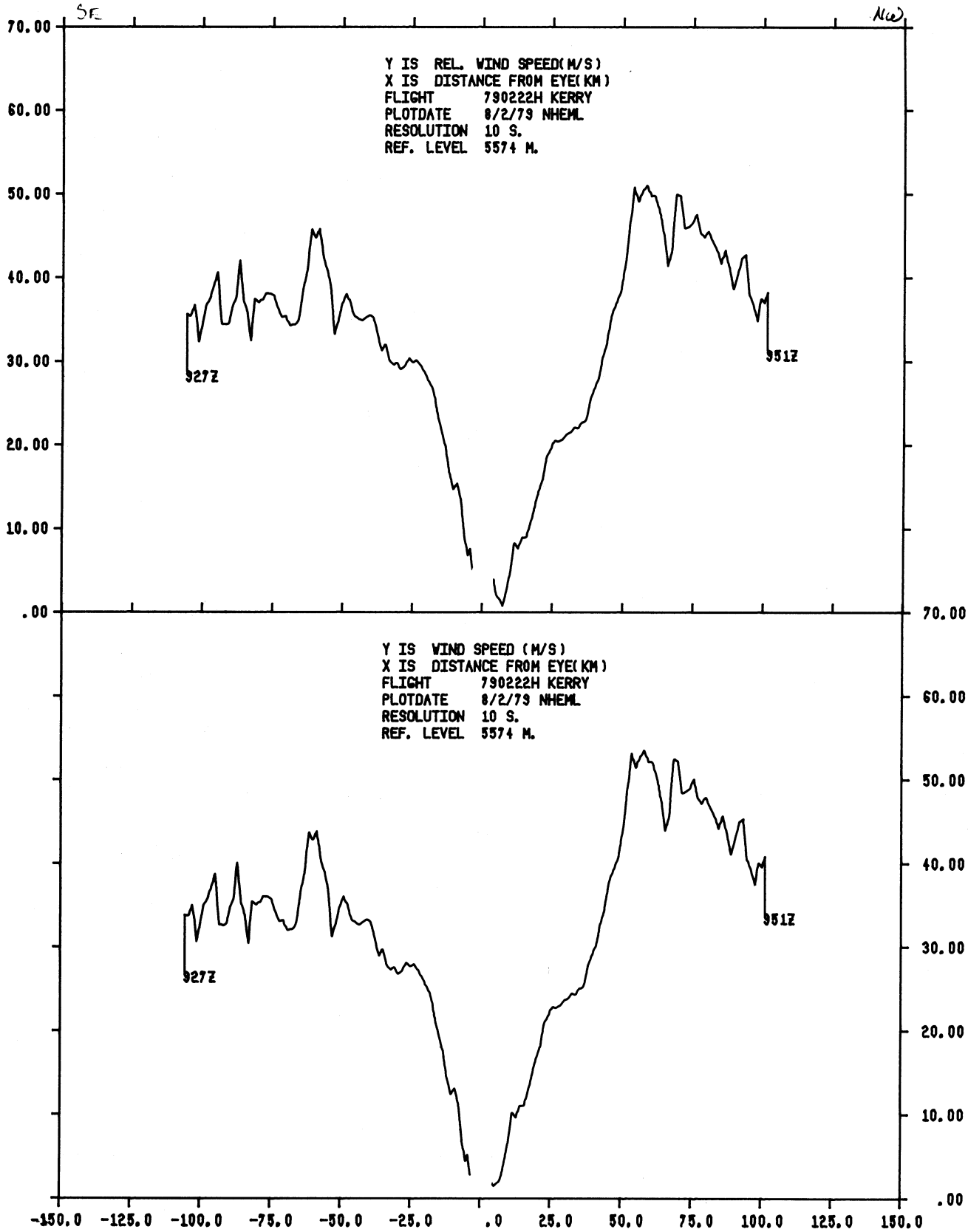

Figure 63. Same as figure 61, except for relative wind speed (top) and actual wind speed (bottom).

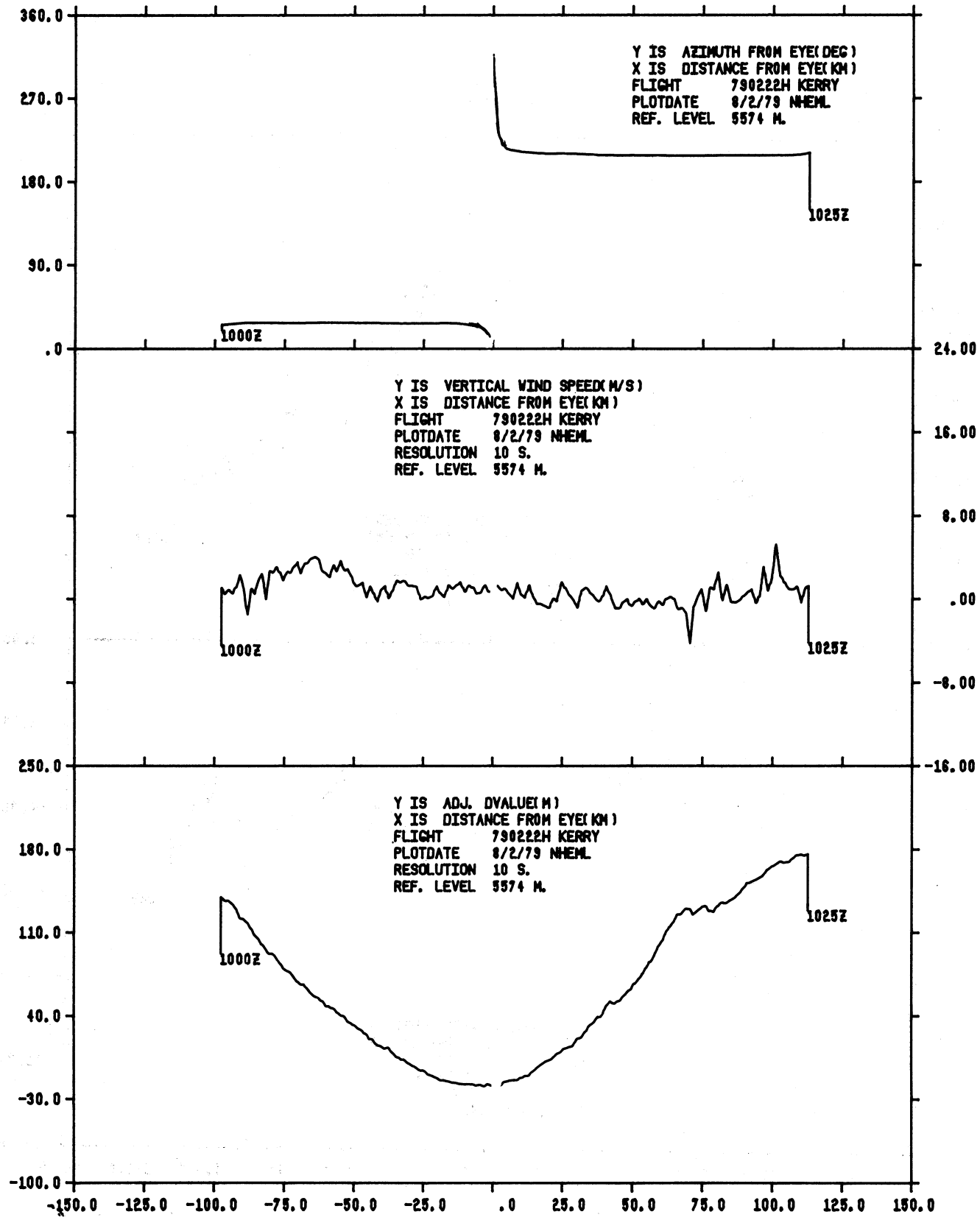

Figure 64. Same as figure 58, except for northeast-to-southwest pass in figure 57 from 1000 Z to 1025 Z.

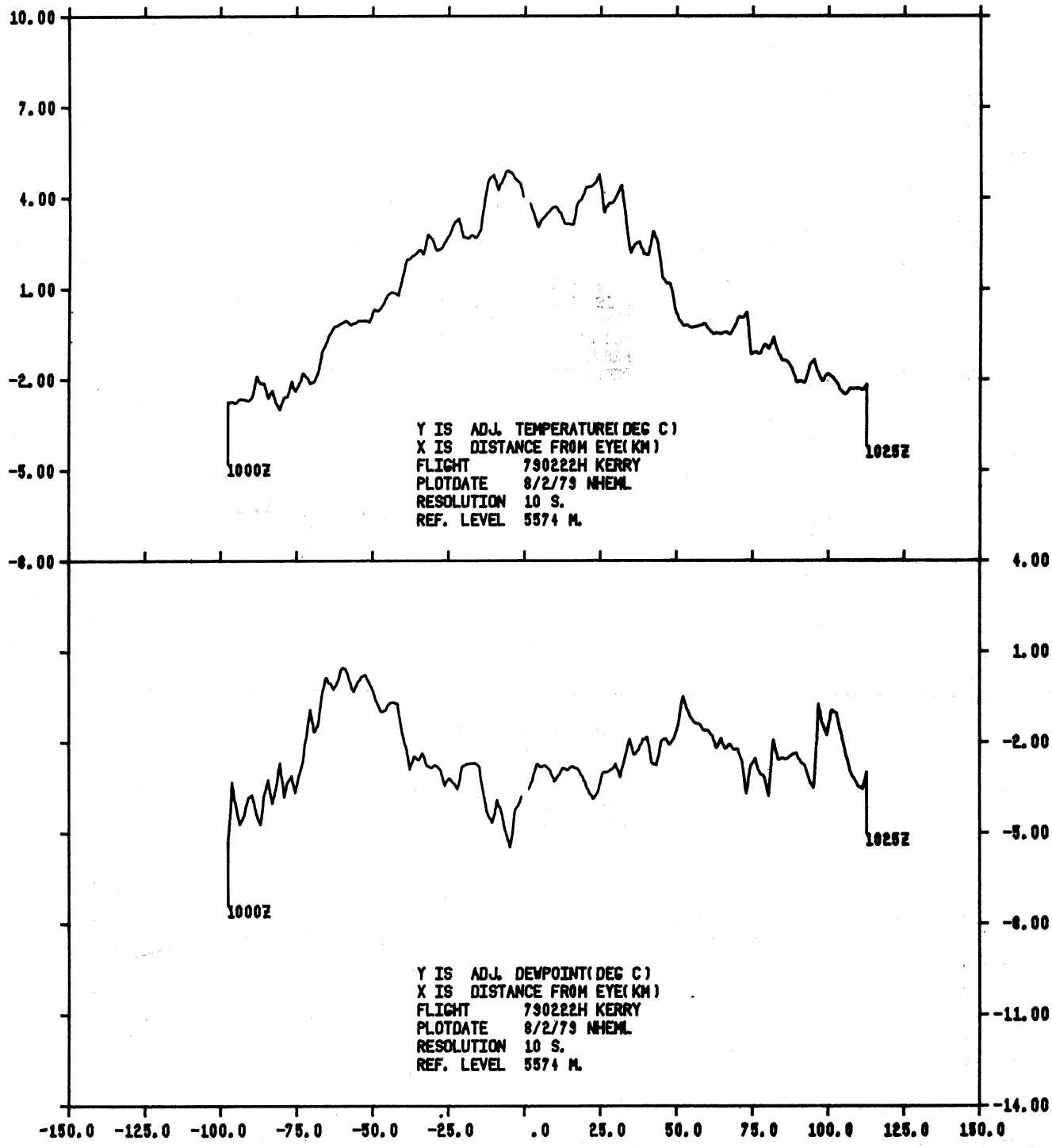

Figure 65. Same as figure 64, except for adjusted temperatures (top) and adjusted dew point temperatures (bottom).

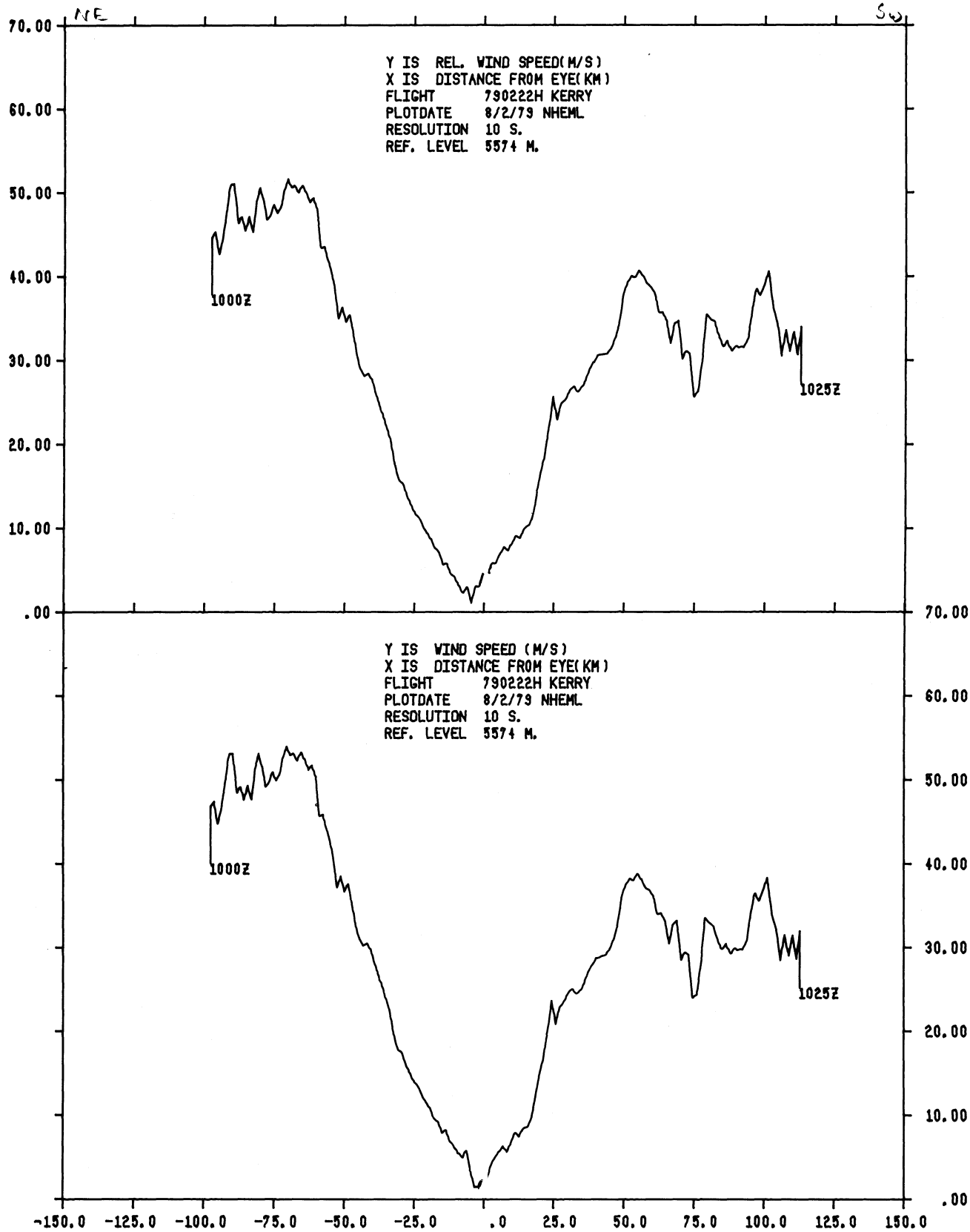

Figure 66. Same as figure 64, except for relative wind speed (top) and actual wind speed (bottom).

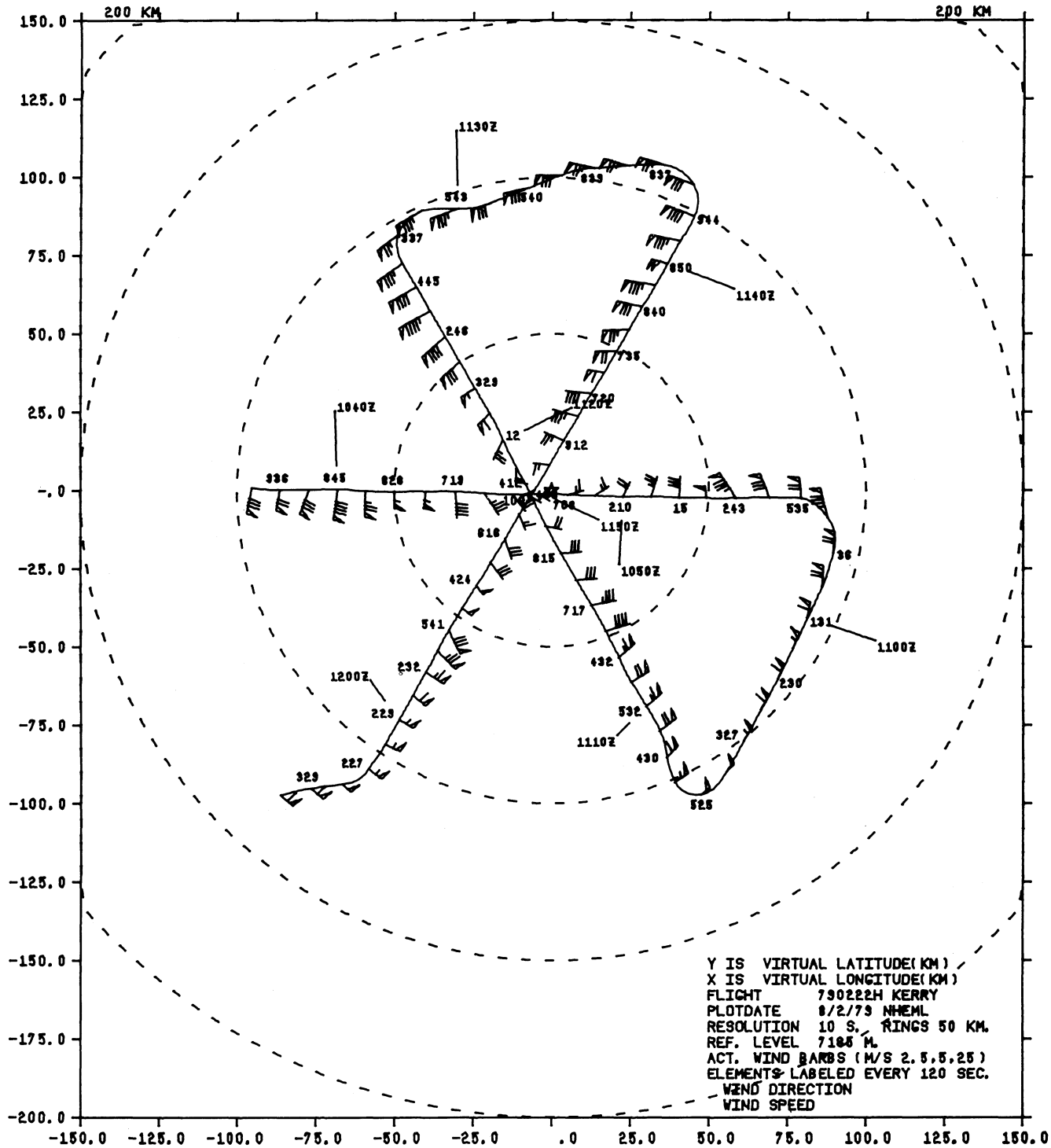

Figure 67. Plan view of aircraft position and actual winds relative to the center of tropical Cyclone Kerry from 1037 Z to 1205 Z on February 2, 1979, and a reference pressure altitude of 7185 m (400 mb).

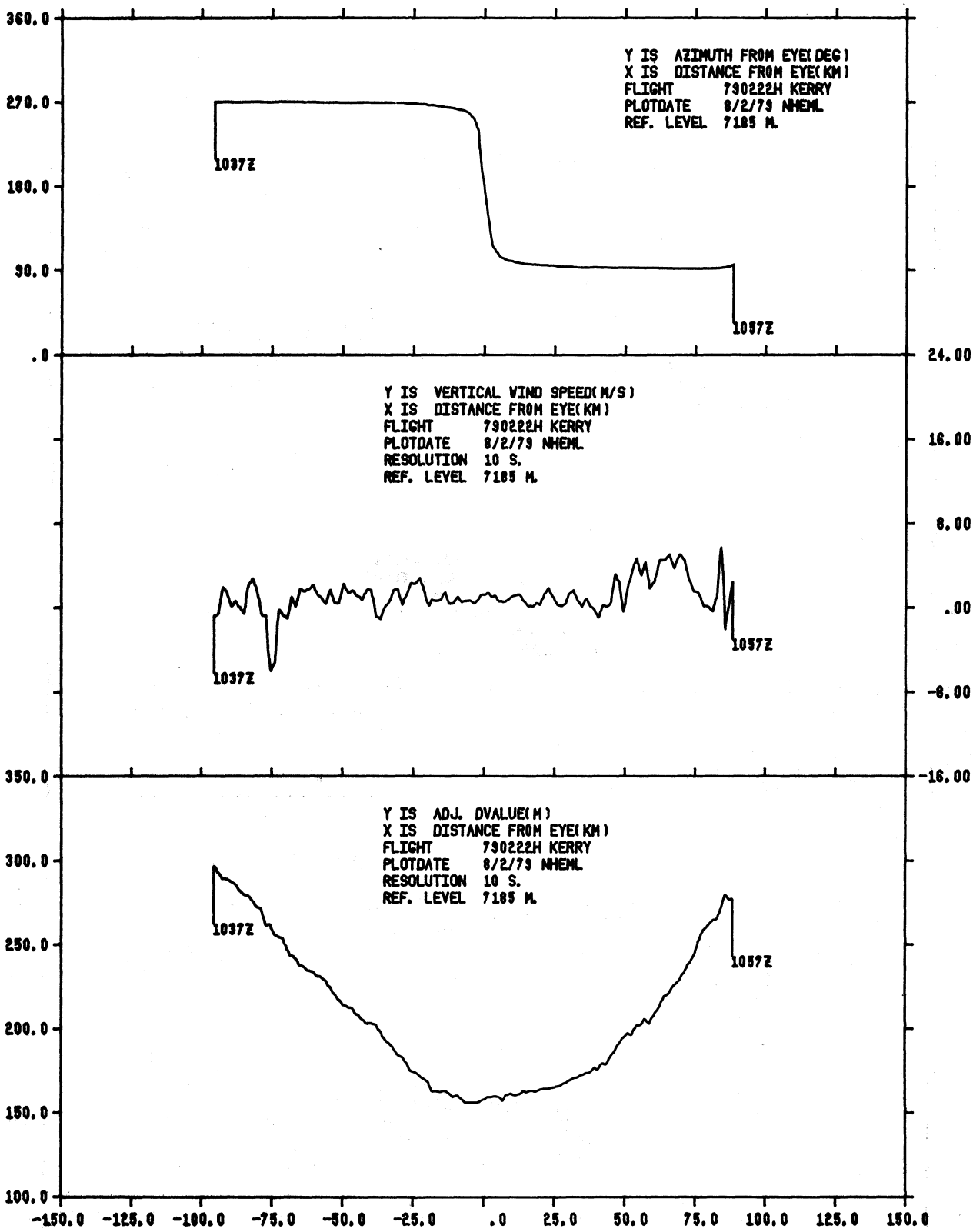

Figure 68. Profiles of the aircraft position (observation point) from the storm center in degrees (top), vertical wind (middle), and adjusted "D" value (bottom) versus radial distance. Profiles correspond to the west pass in figure 67 from 1037 Z to 1057 Z.

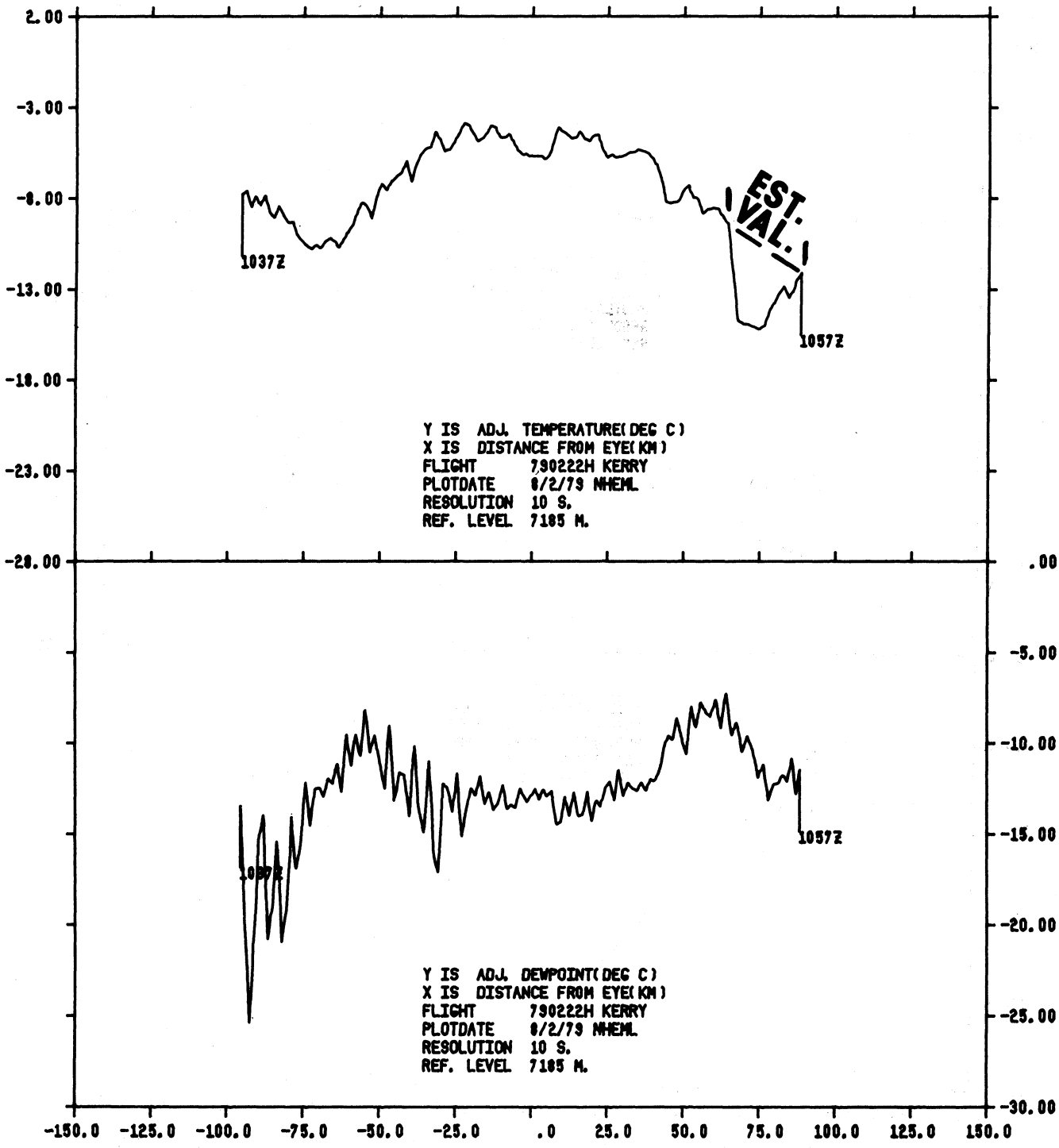

Figure 69. Same as figure 68, except for adjusted temperatures (top) and adjusted dew point temperatures (bottom). (Note comments in section 3.1.)

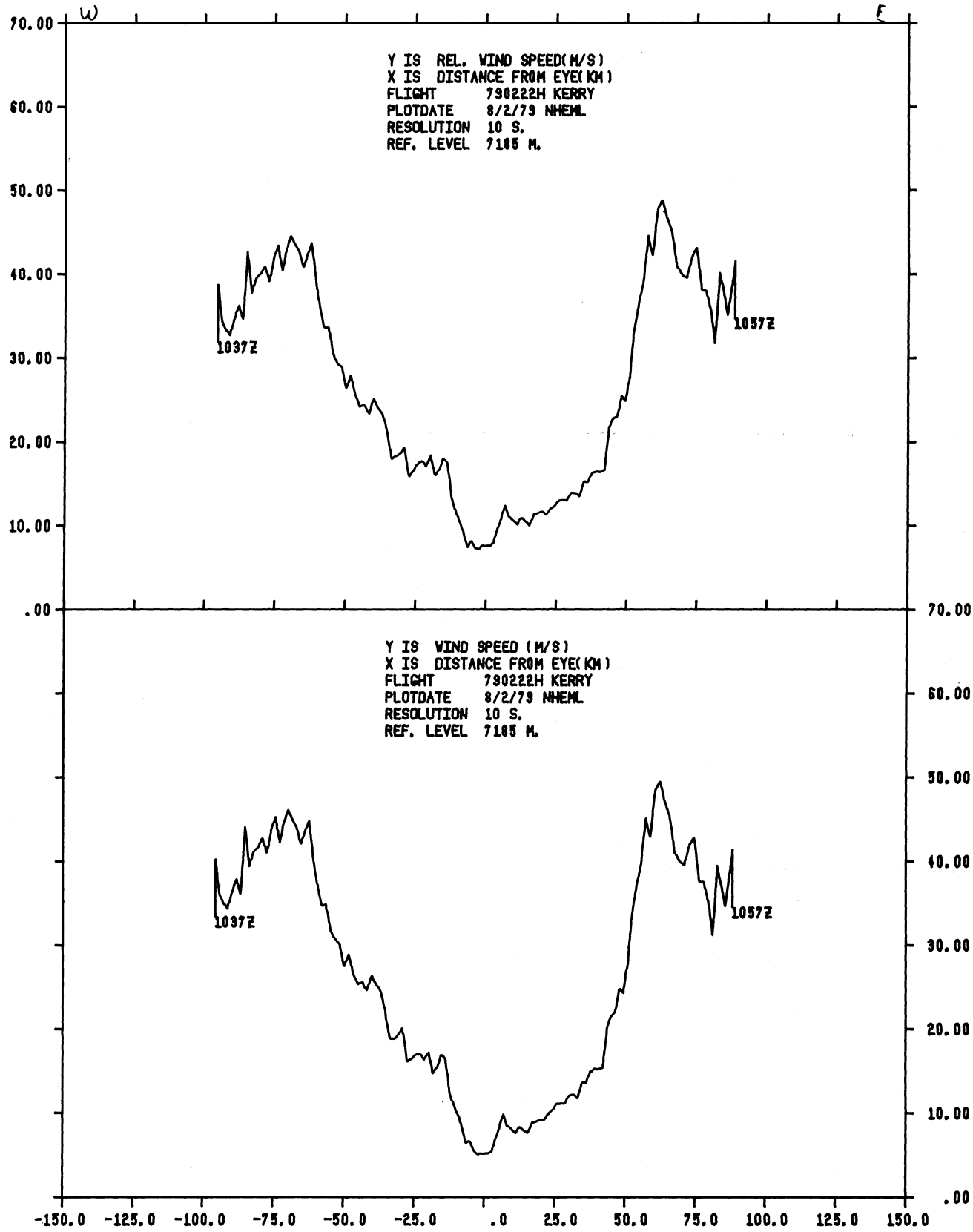

Figure 70. Same as figure 68, except for relative wind speed (top) and actual wind speed (bottom).

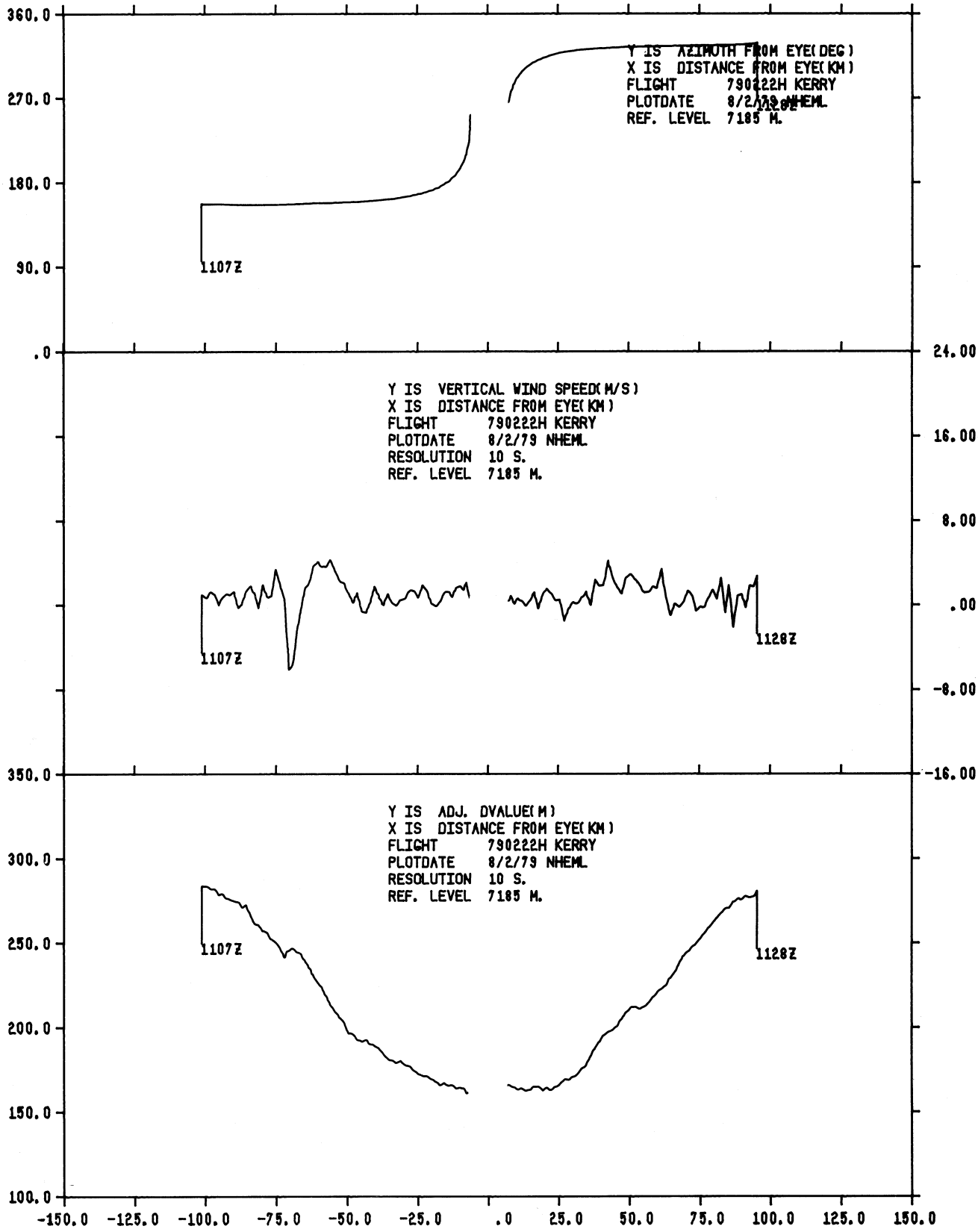

Figure 71. Same as figure 68, except for southeast-to-northwest pass in figure 67 from 1107 Z to 1128 Z.

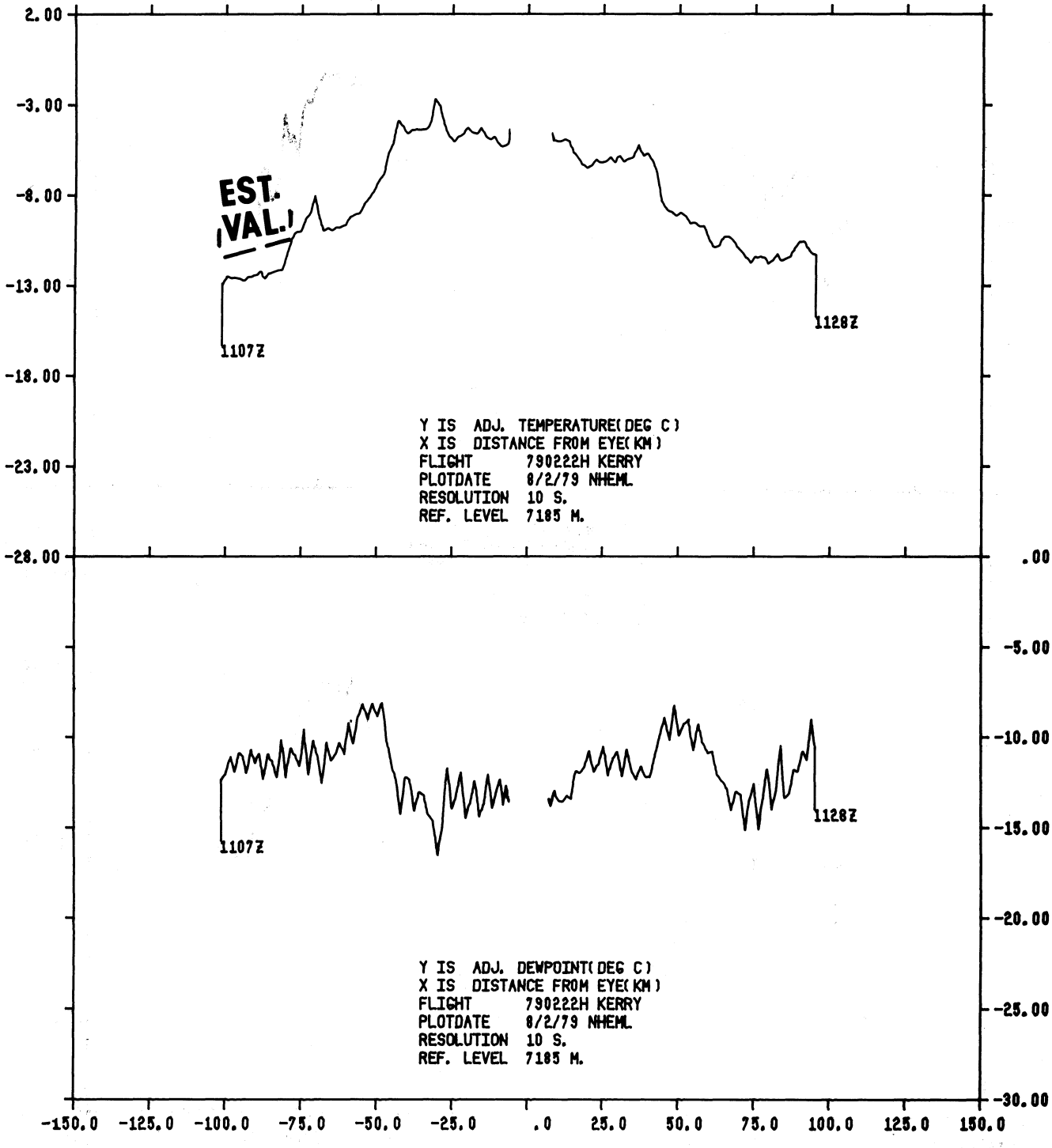

Figure 72. Same as figure 71, except for adjusted temperatures (top) and adjusted dew point temperatures (bottom). (Note comments in section 3.1.)

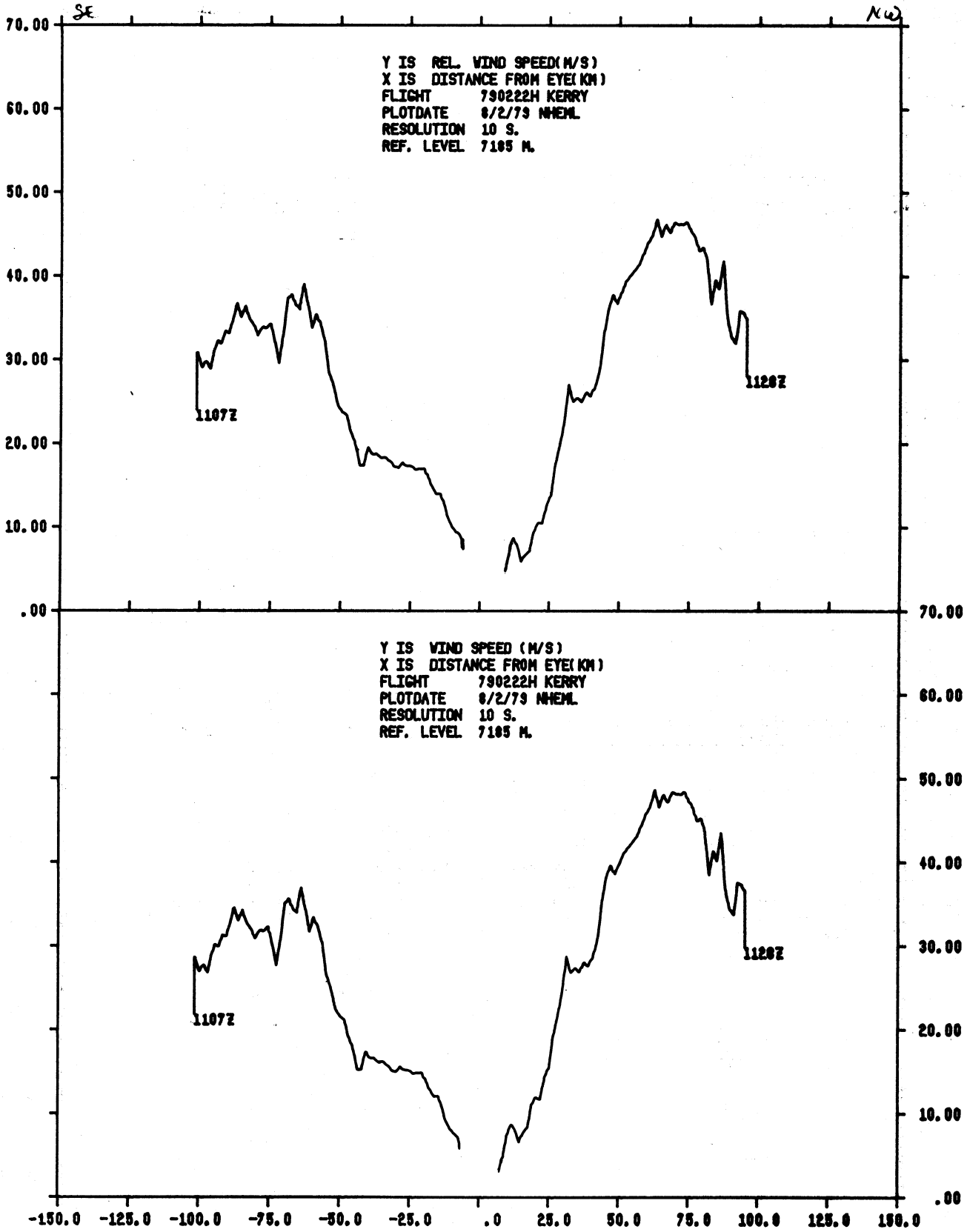

Figure 73. Same as figure 71, except for relative wind speed (top) and actual wind speed (bottom).

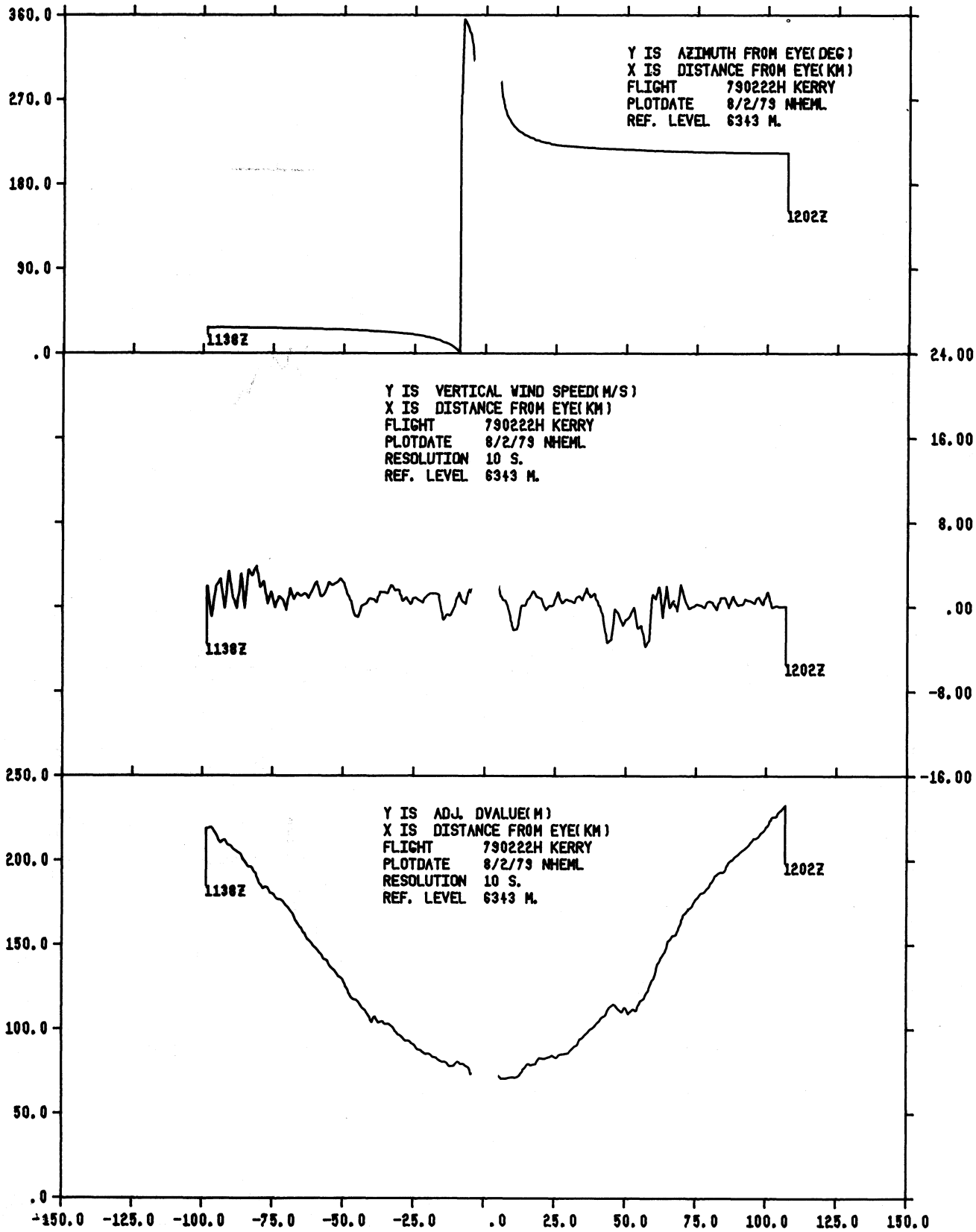

Figure 74. Same as figure 68, except for northeast-to-southwest pass in figure 67 from 1138 Z to 1202 Z and a reference pressure altitude of 6343 m (450 mb).

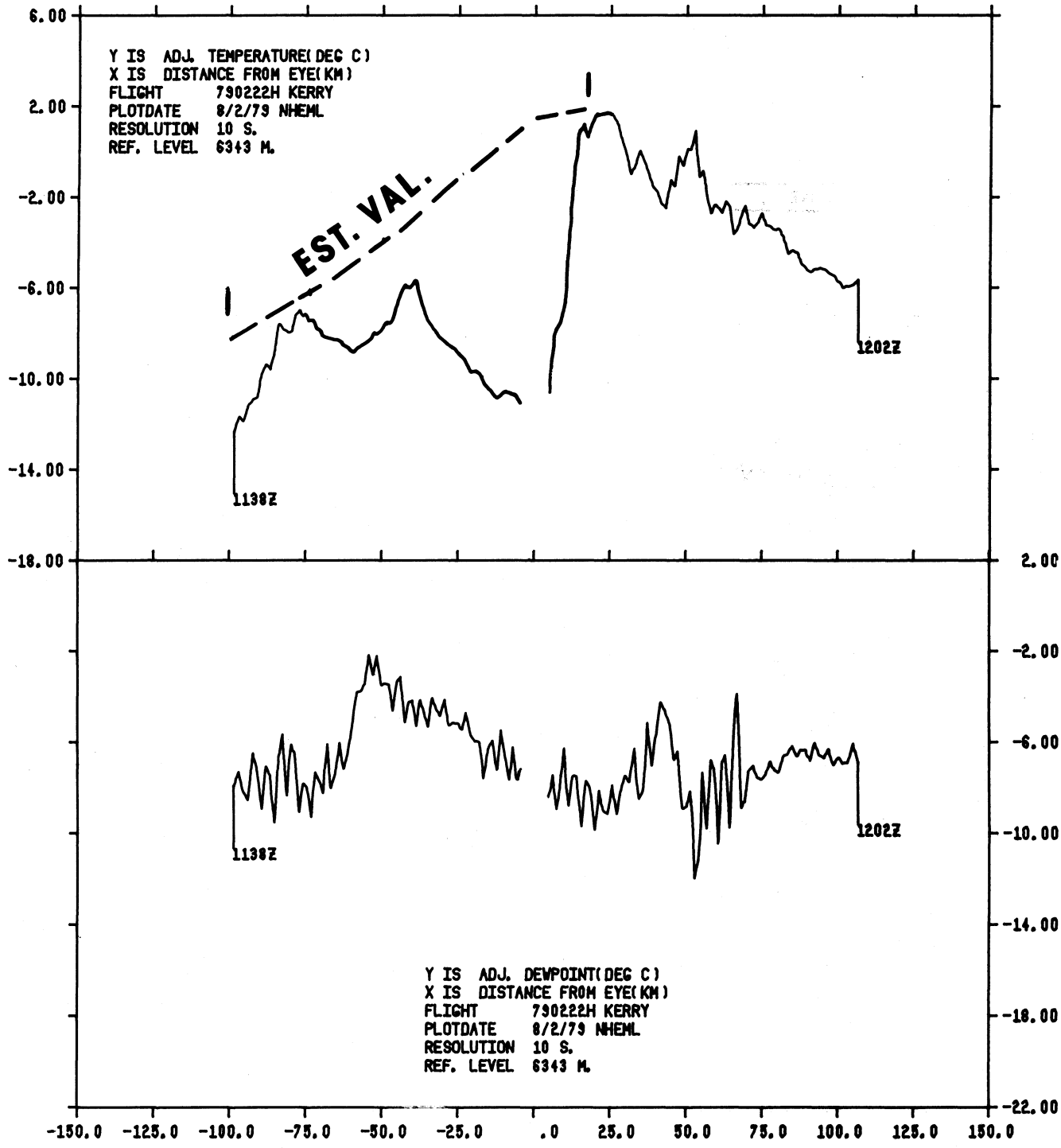

Figure 75. Same as figure 74, except for adjusted temperatures (top) and adjusted dew point temperatures (bottom). (Note comments in section 3.1.)

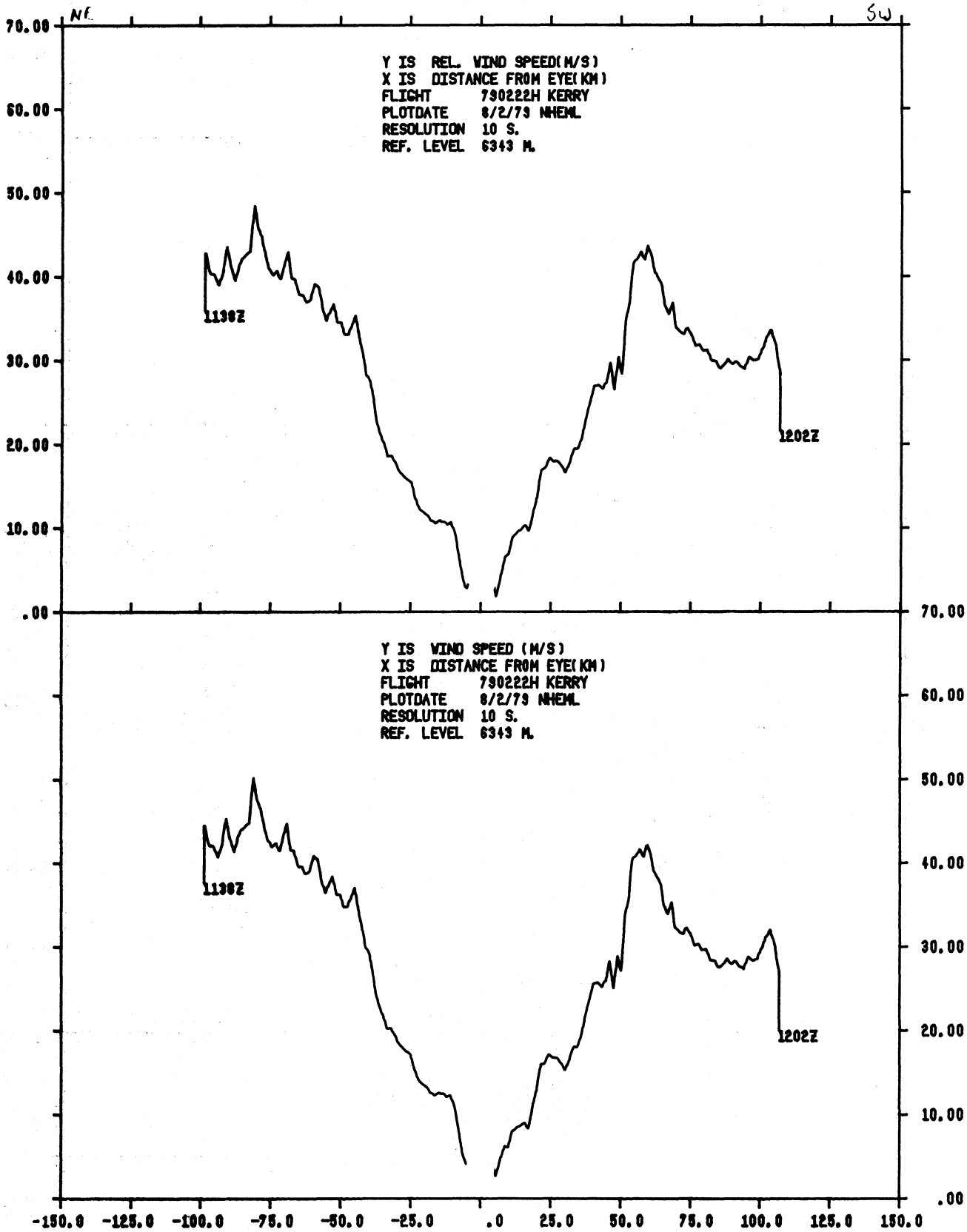

Figure 76. Same as figure 74, except for relative wind speed (top) and actual wind speed (bottom).

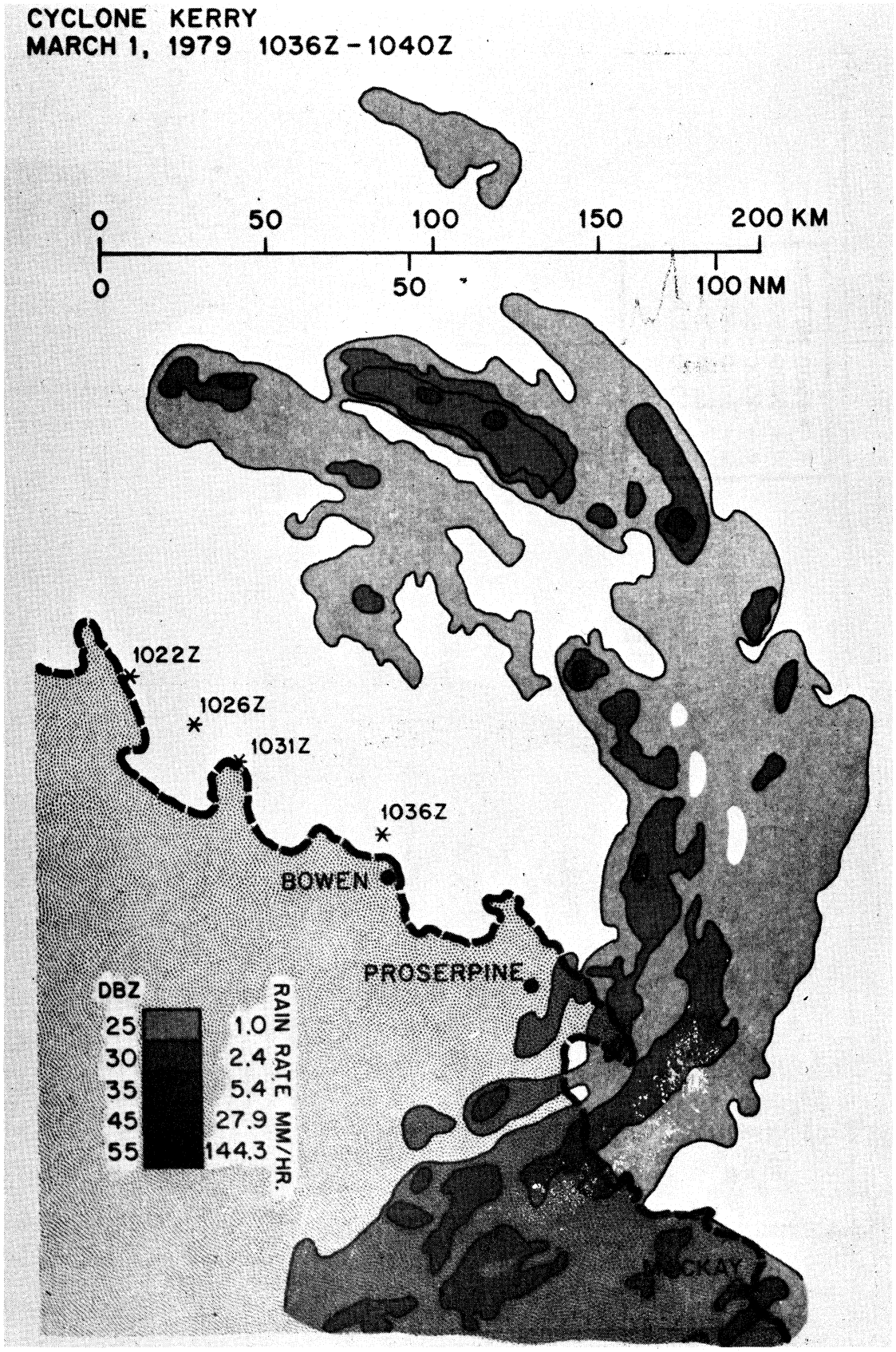

Figure 77. Digitized Plan Position Indicator radar depiction of Tropical Cyclone Kerry compositied from 1036 Z to 1040 Z on March 1, 1979.

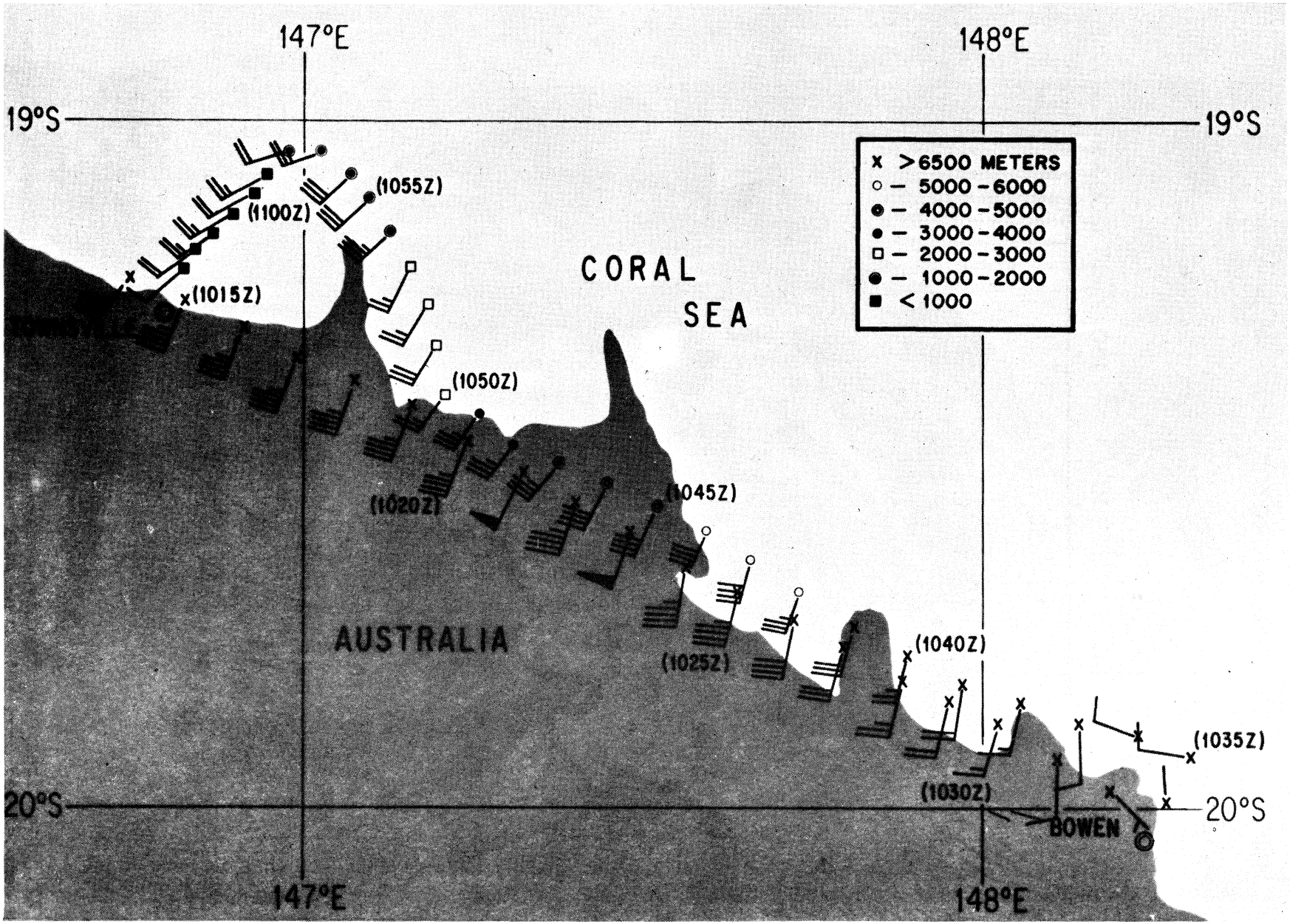

Figure 78. Plan view of aircraft position and actual winds along northeast Australian coast from 1014 Z to 1104 Z on March 1, 1979. (Altitudes of observations are indicated by symbols.)

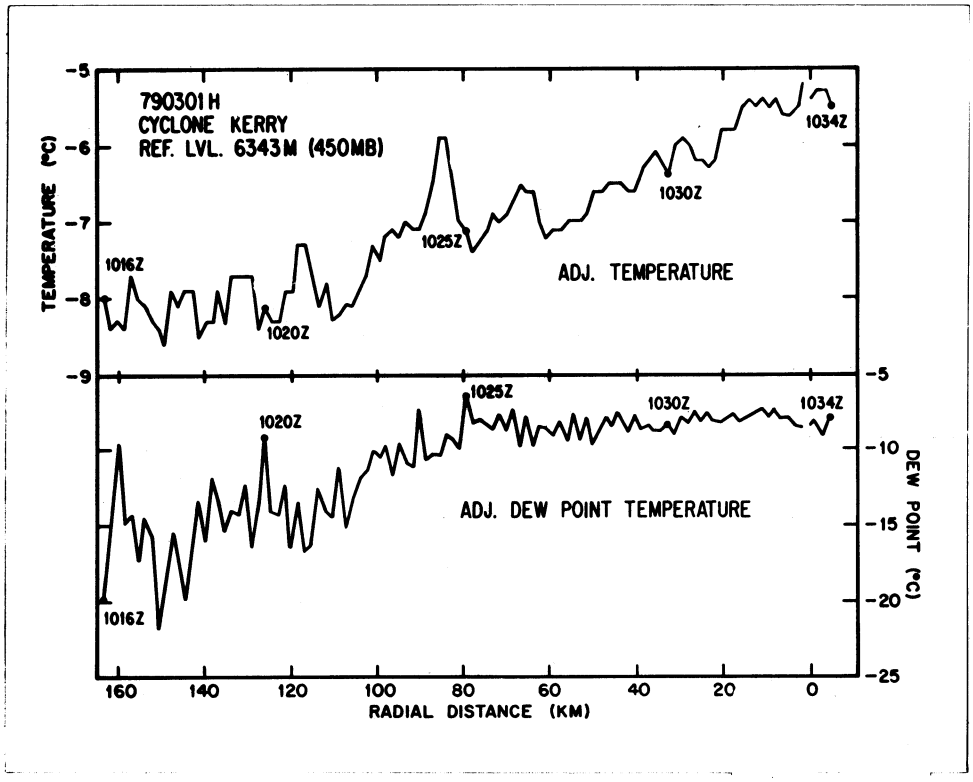

Figure 79. Profiles of adjusted temperature (top) and adjusted dew point temperature (bottom) versus radial distance corresponding to the pass from 1014 Z to 1034 Z in figure 78 at a reference pressure altitude of 6343 m (450 mb).

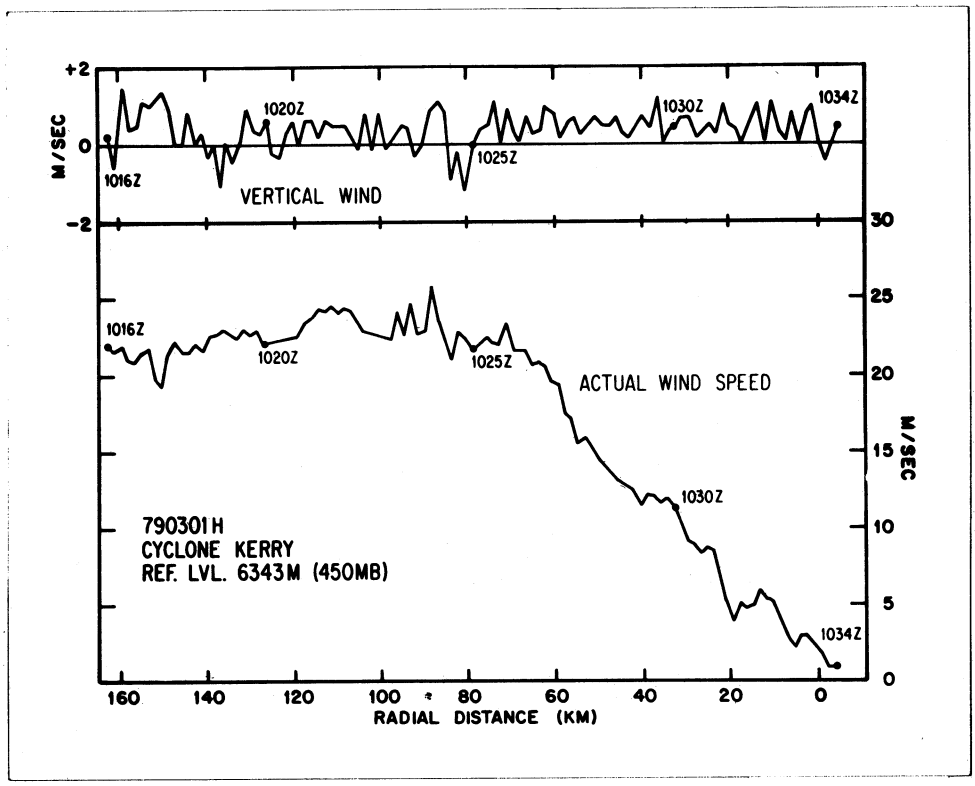

Figure 80. Same as figure 79, except for vertical wind (top) and actual wind (bottom).

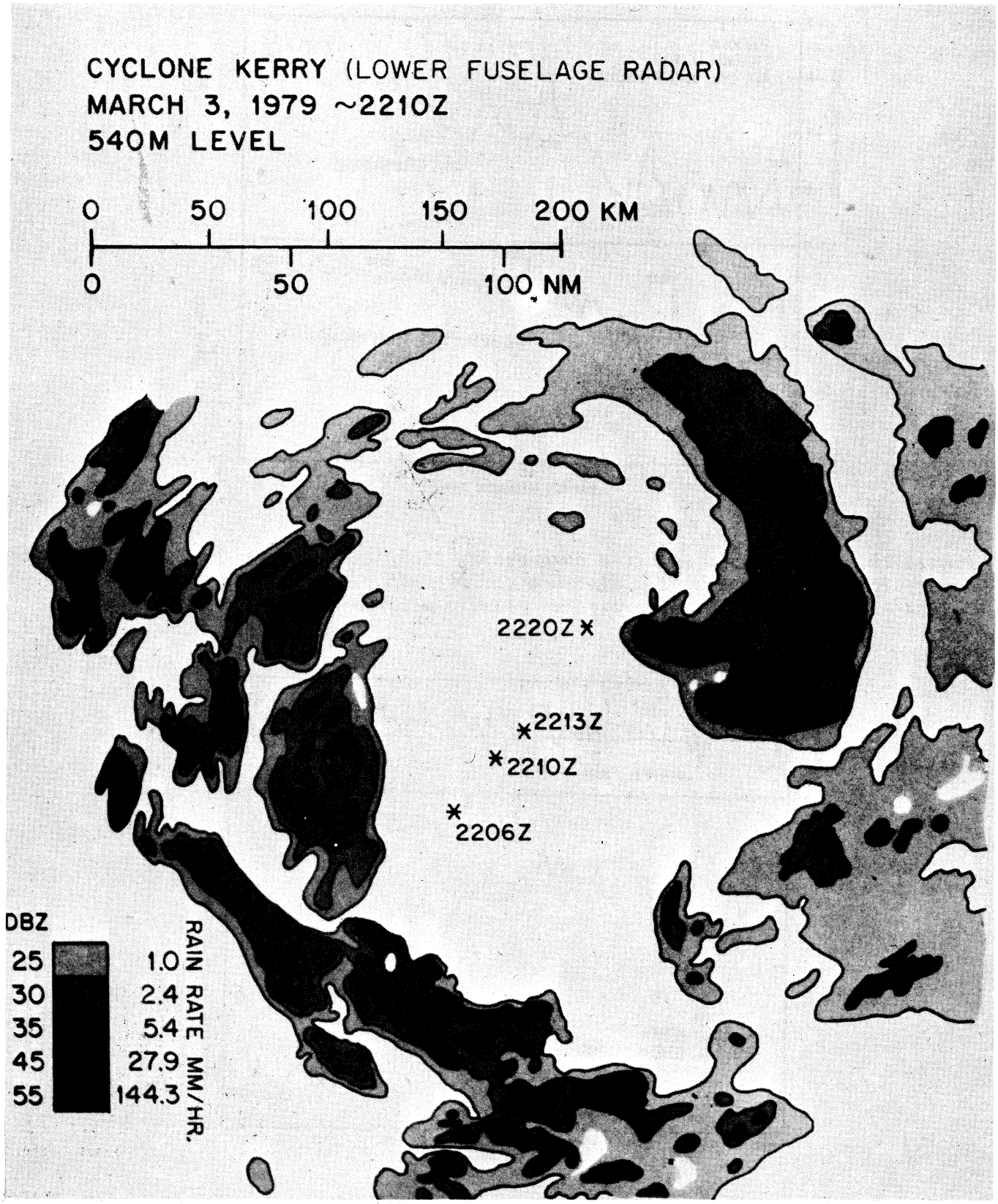

Figure 81. Digitized Plan Position Indicator radar depiction of Tropical Cyclone Kerry compositied from 2206 Z to 2220 Z on March 3, 1979.

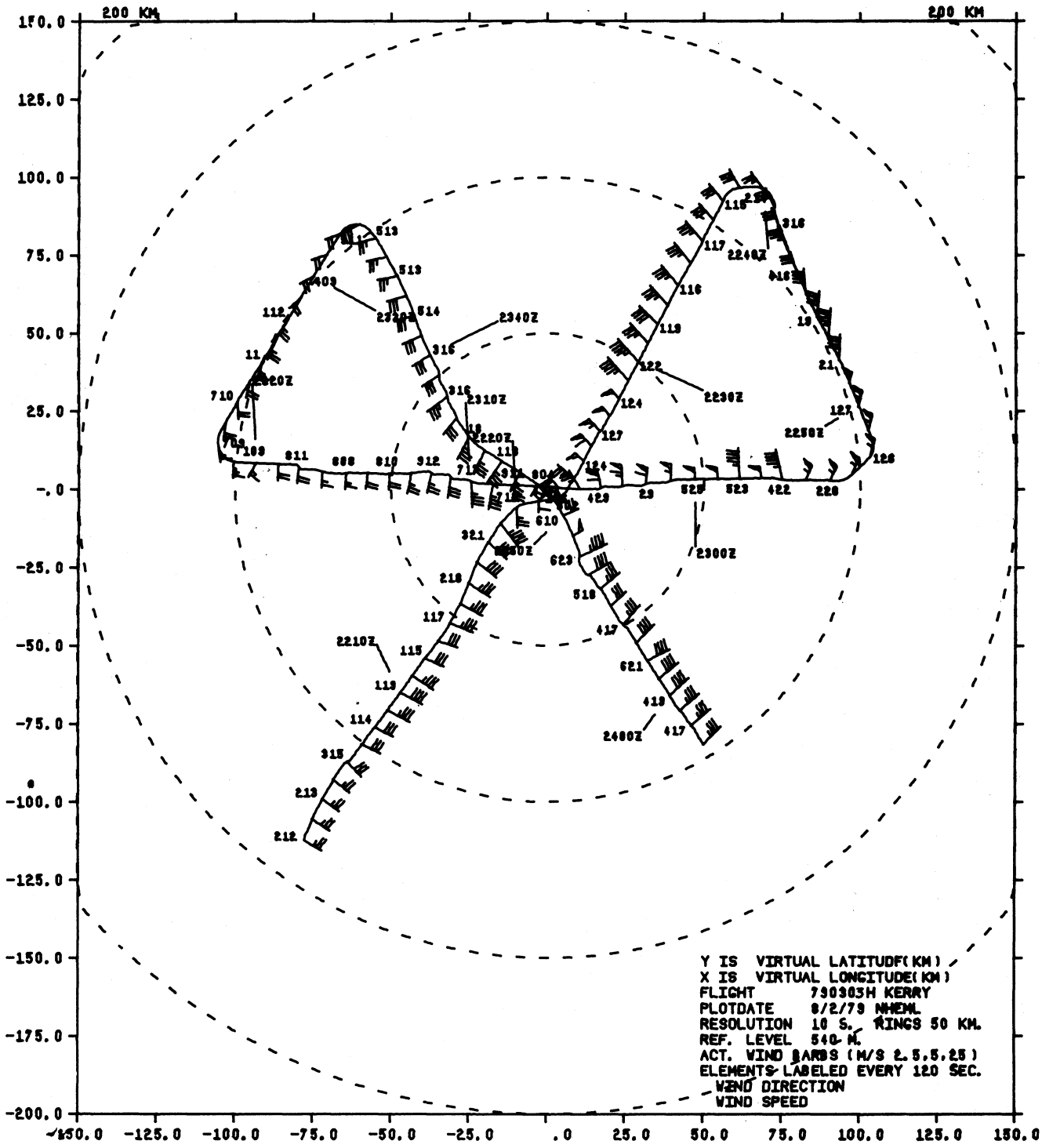

Figure 82. Plan view of aircraft poisition and actual winds relative to the center of Tropical Cyclone Kerry from 2202 Z on March 3 to 0003 Z on March 4, 1979, at an altitude of 540 m.

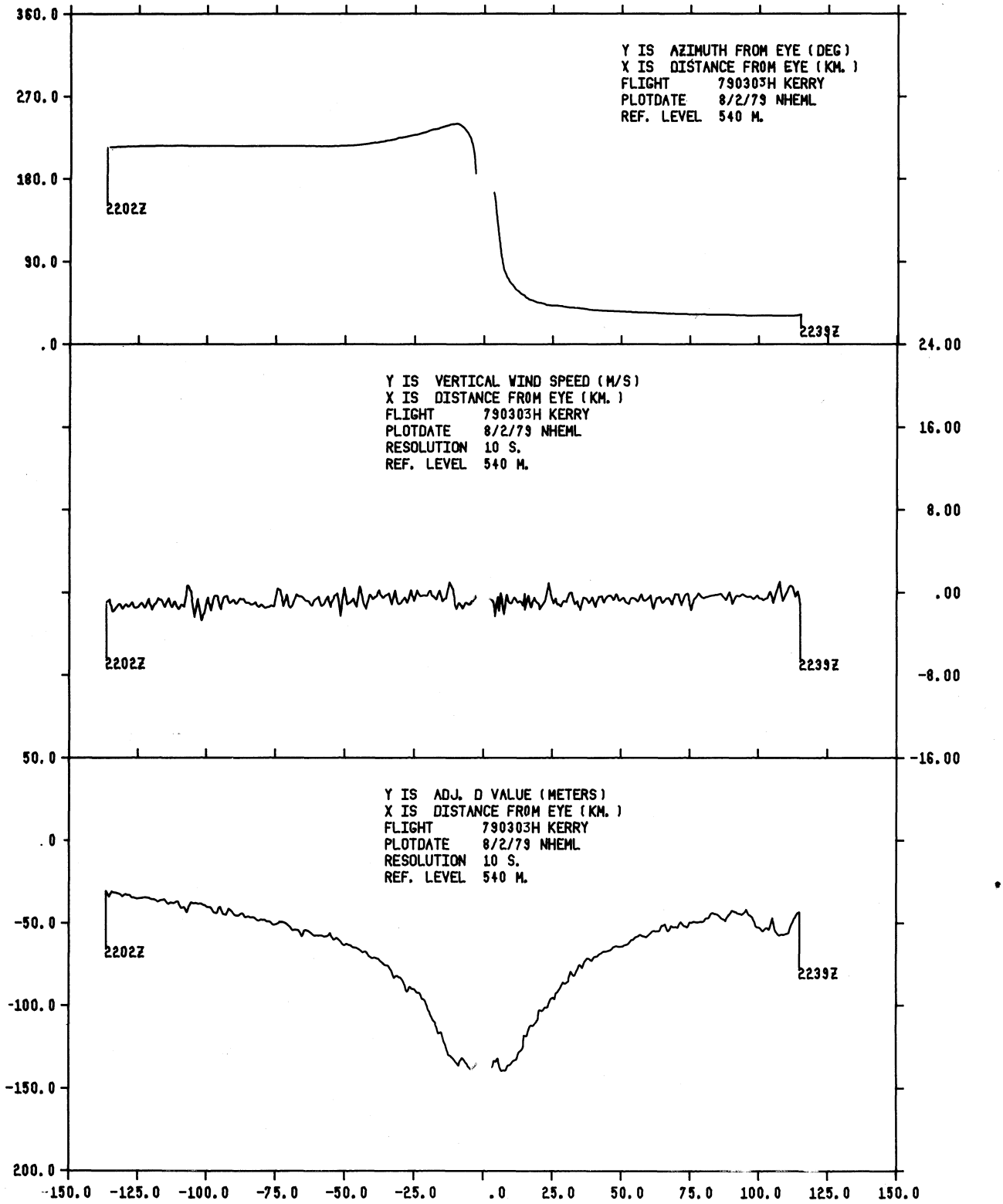

Figure 83. Profiles of the aircraft position (observation point) from the storm center in degrees (top), vertical wind (middle), and adjusted "D" value (bottom) versus radial distance from the storm center. Profiles correspond to the southwest-to northeast pass in figure 81 from 2202 Z to 2239 Z with a reference pressure altitude of 540 m (950 mb).

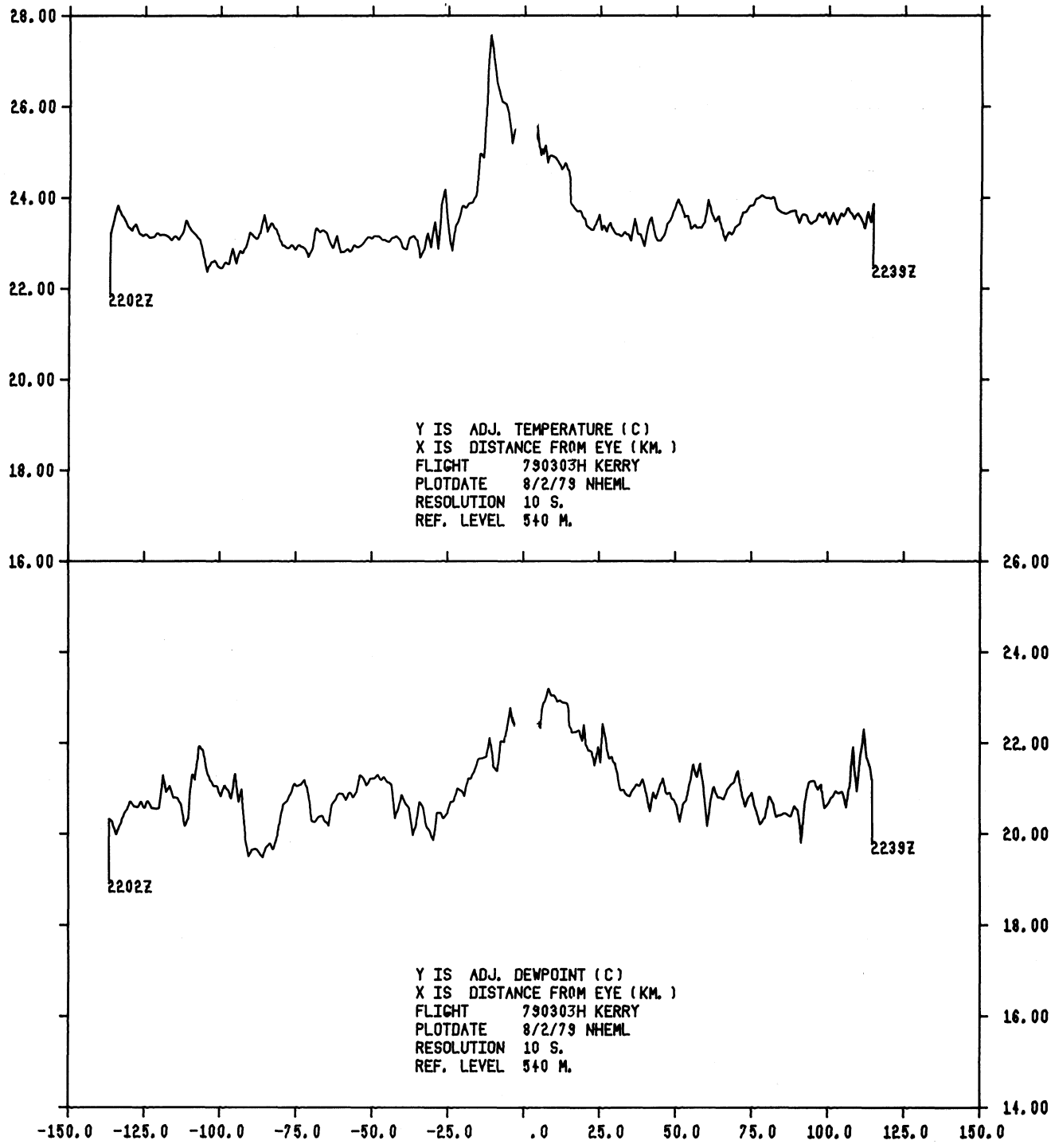

Figure 84. Same as figure 82, except for adjusted temperatures (top) and adjusted dew point temperatures (bottom).

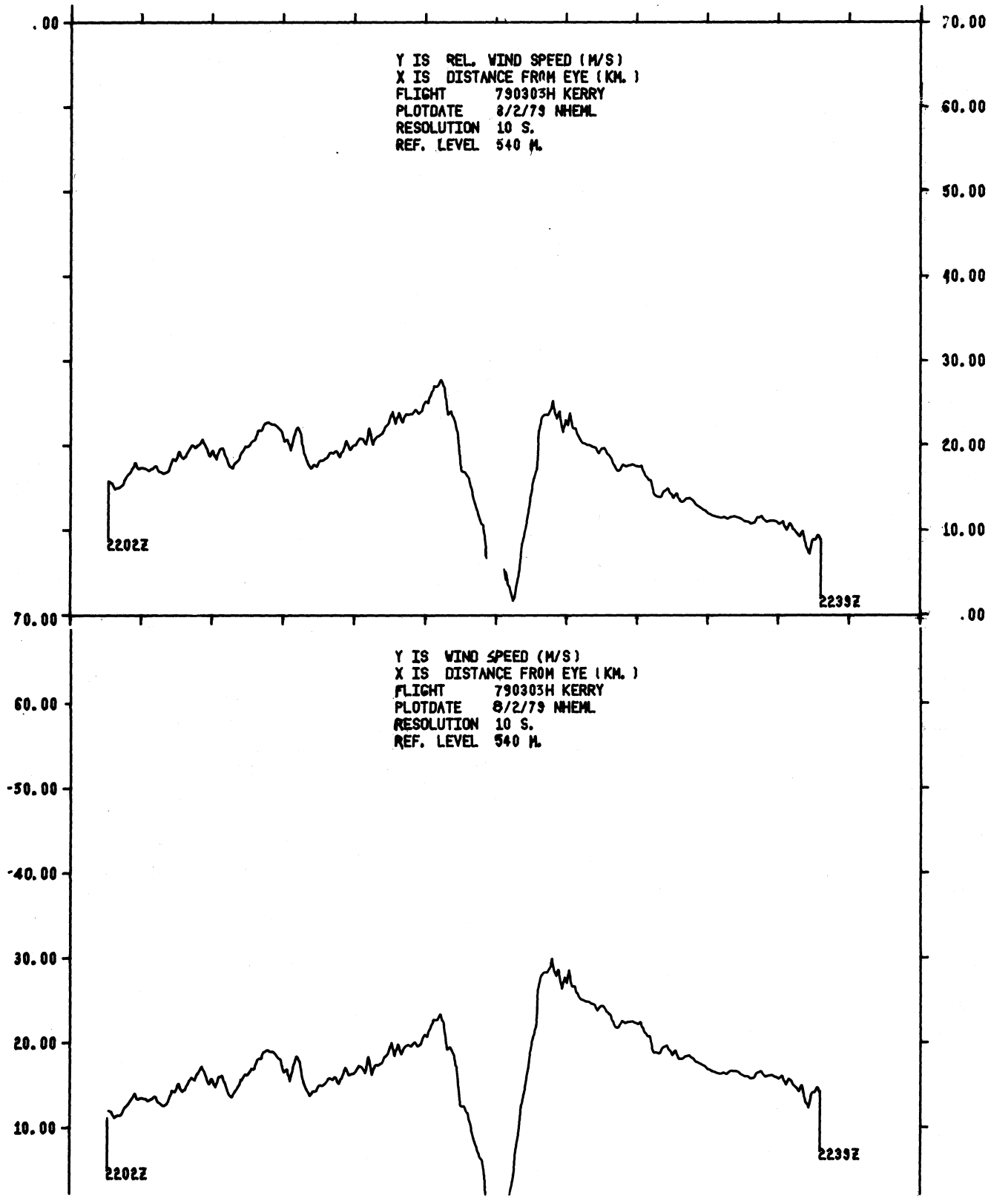

Figure 85. Same as figure 82, except for relative wind speed (top) and actual wind speed (bottom).

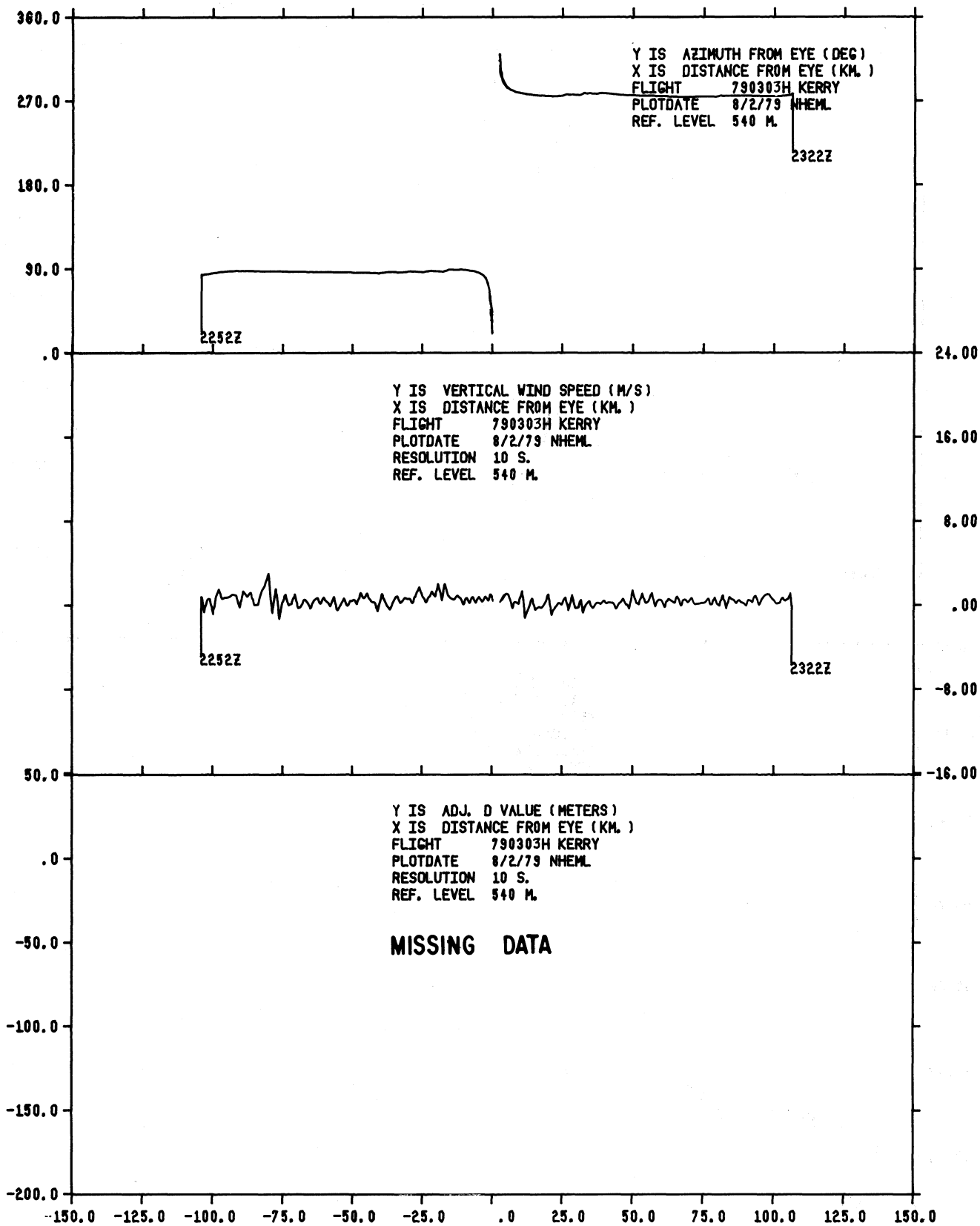

Figure 86. Same as figure 82, except for west-to-east pass in figure 81 from 2252 Z to 2322 Z.

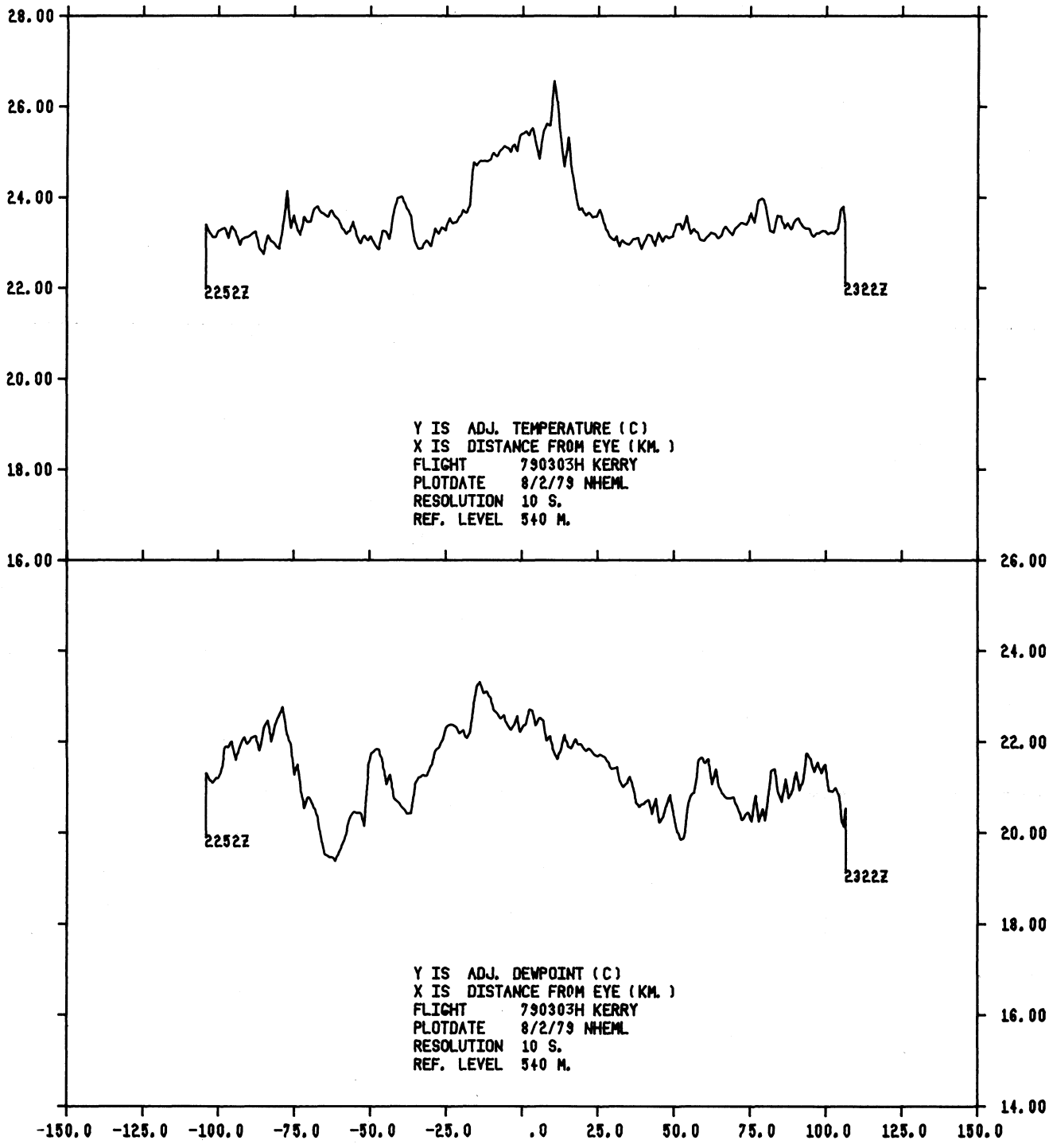

Figure 87. Same as figure 85, except for adjusted temperatures (top) and adjusted dew points (bottom).

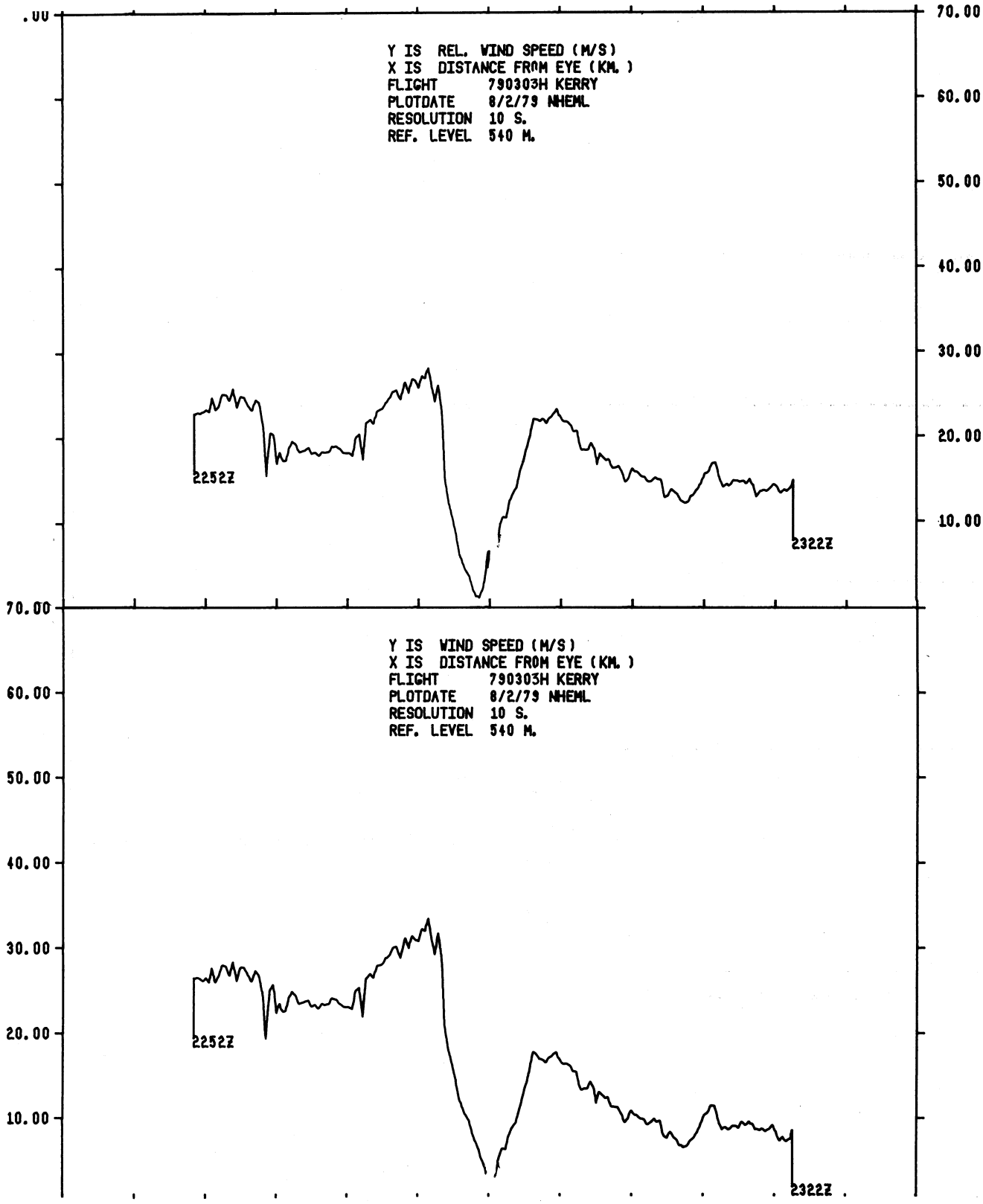

Figure 88. Same as figure 85, except for relative wind speed (top) and actual wind speed (bottom).

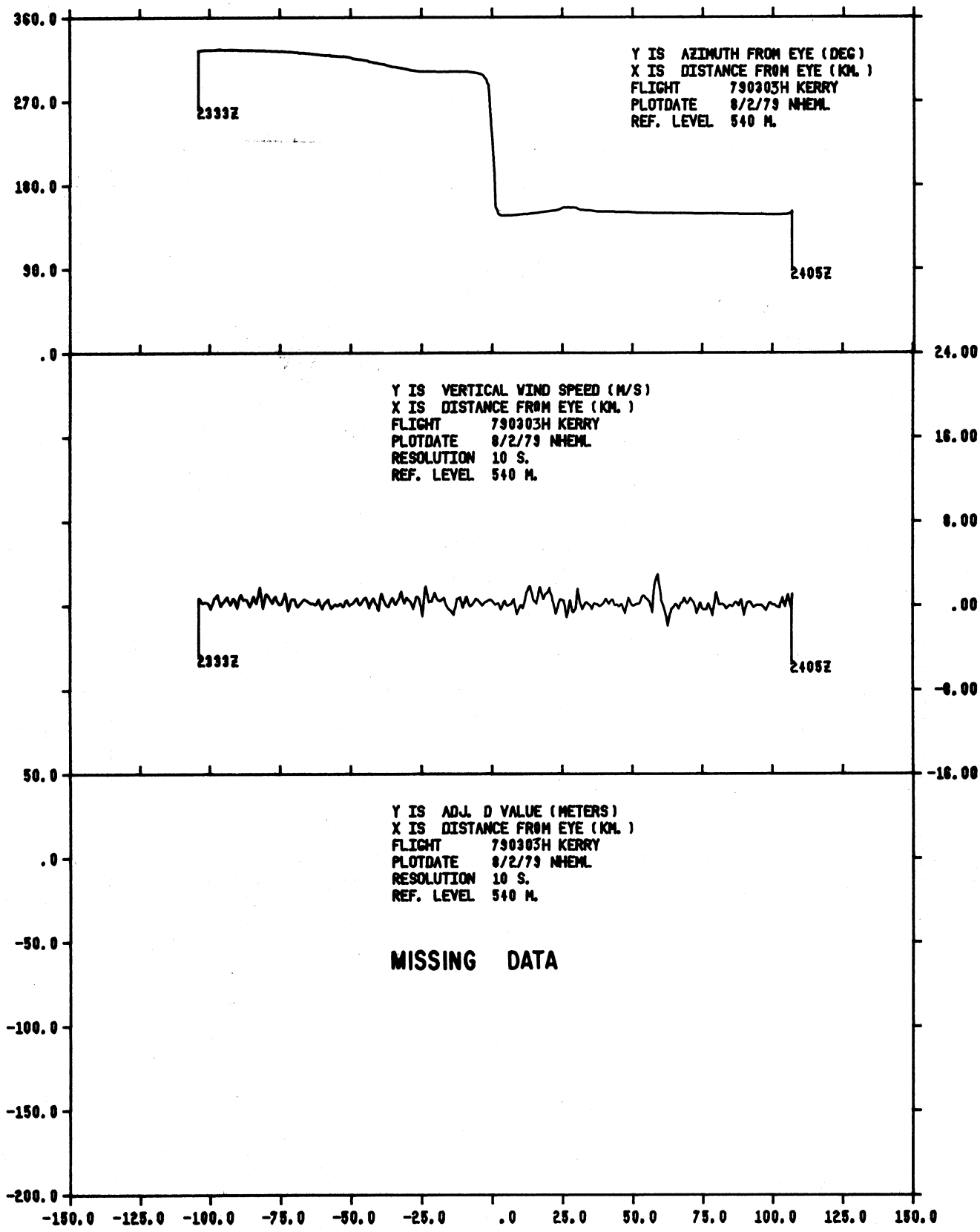

Figure 89. Same as figure 82, except for northwest-to-southeast pass in figure 81 from 2333 Z on March 3 to 0005 Z on March 4, 1979.

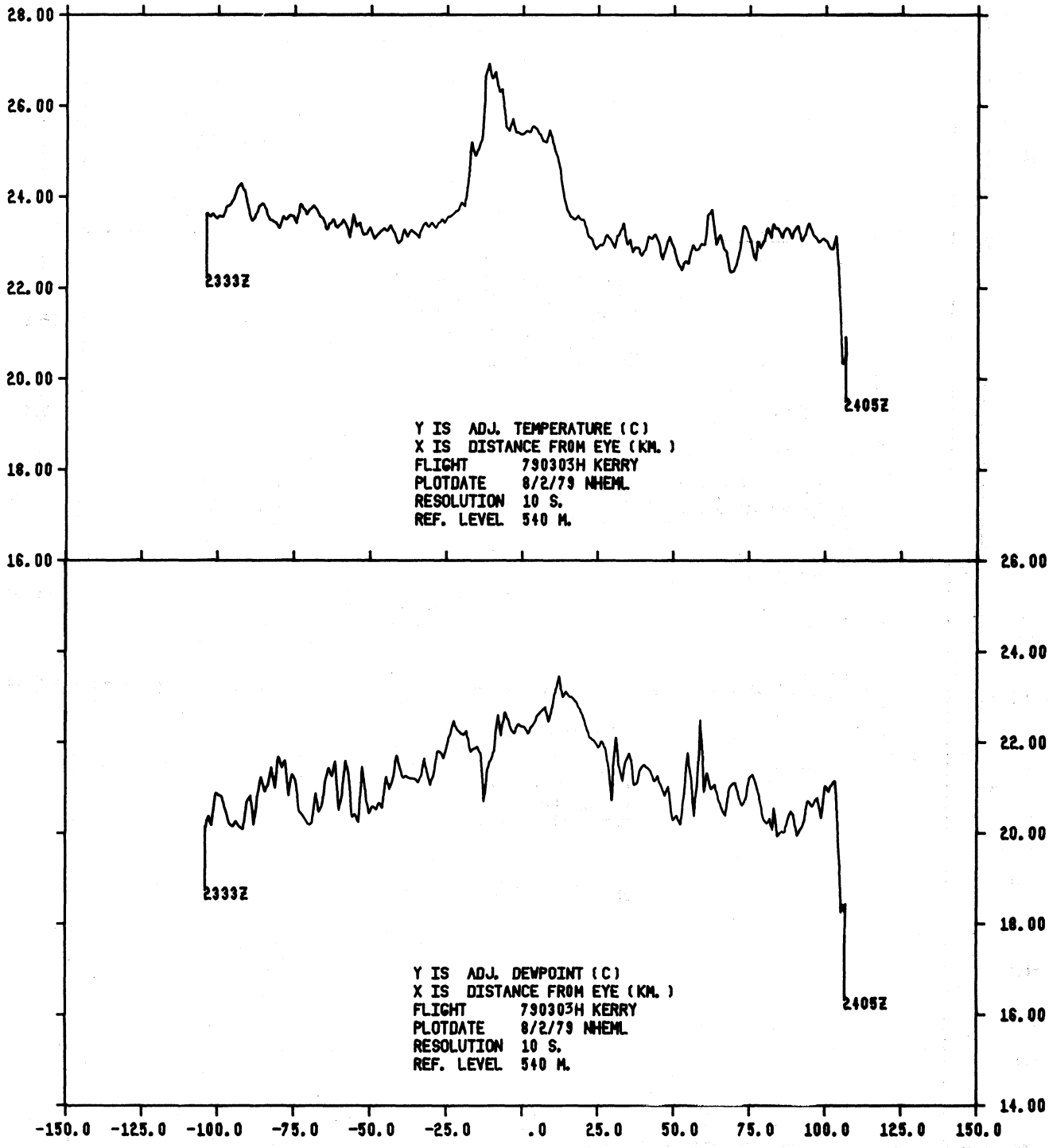

Figure 90. Same as figure 88, except for adjusted temperatures (top) and adjusted dew points (bottom).

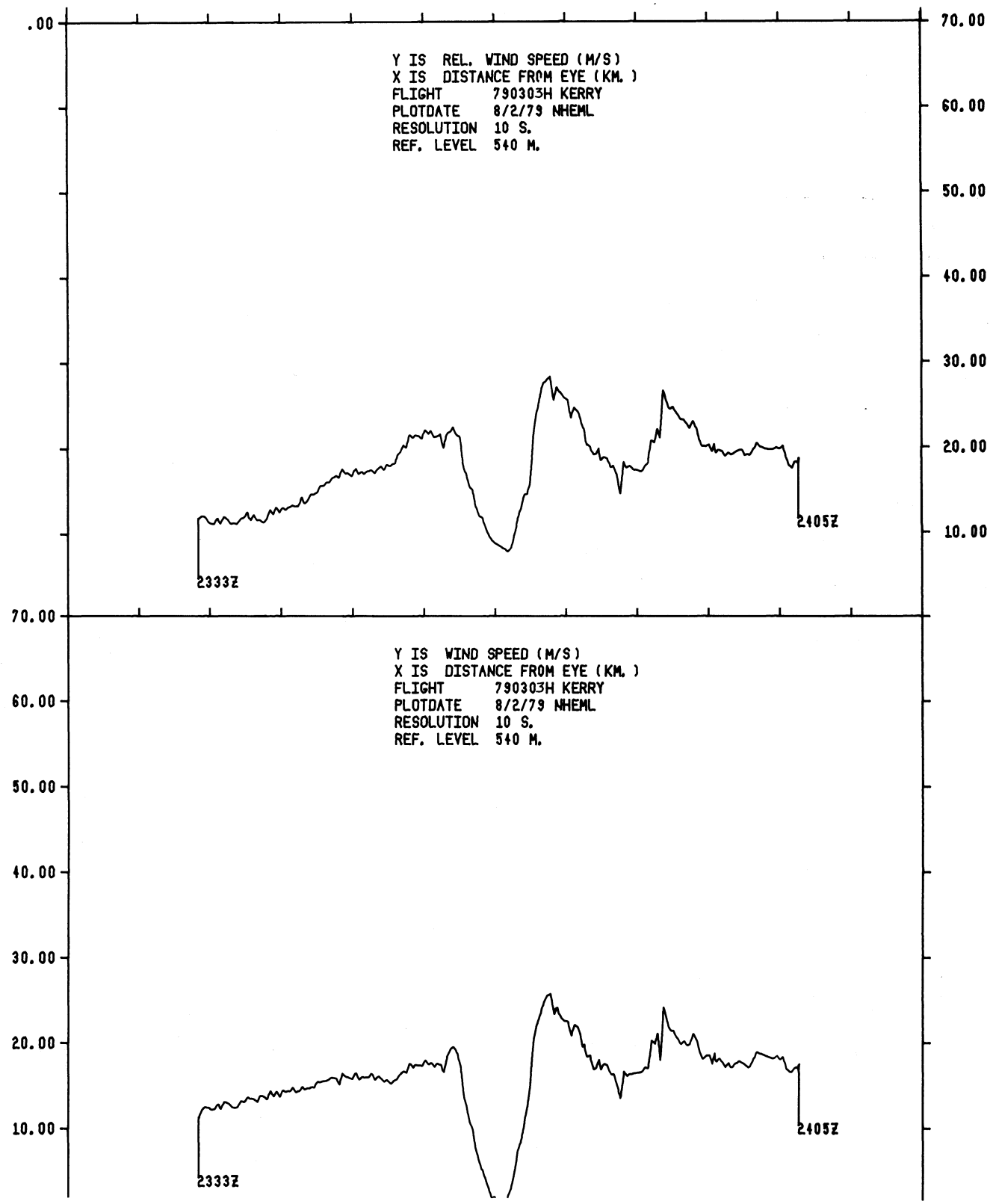

Figure 91. Same as figure 88, except for relative wind speed (top) and actual wind speed (bottom).

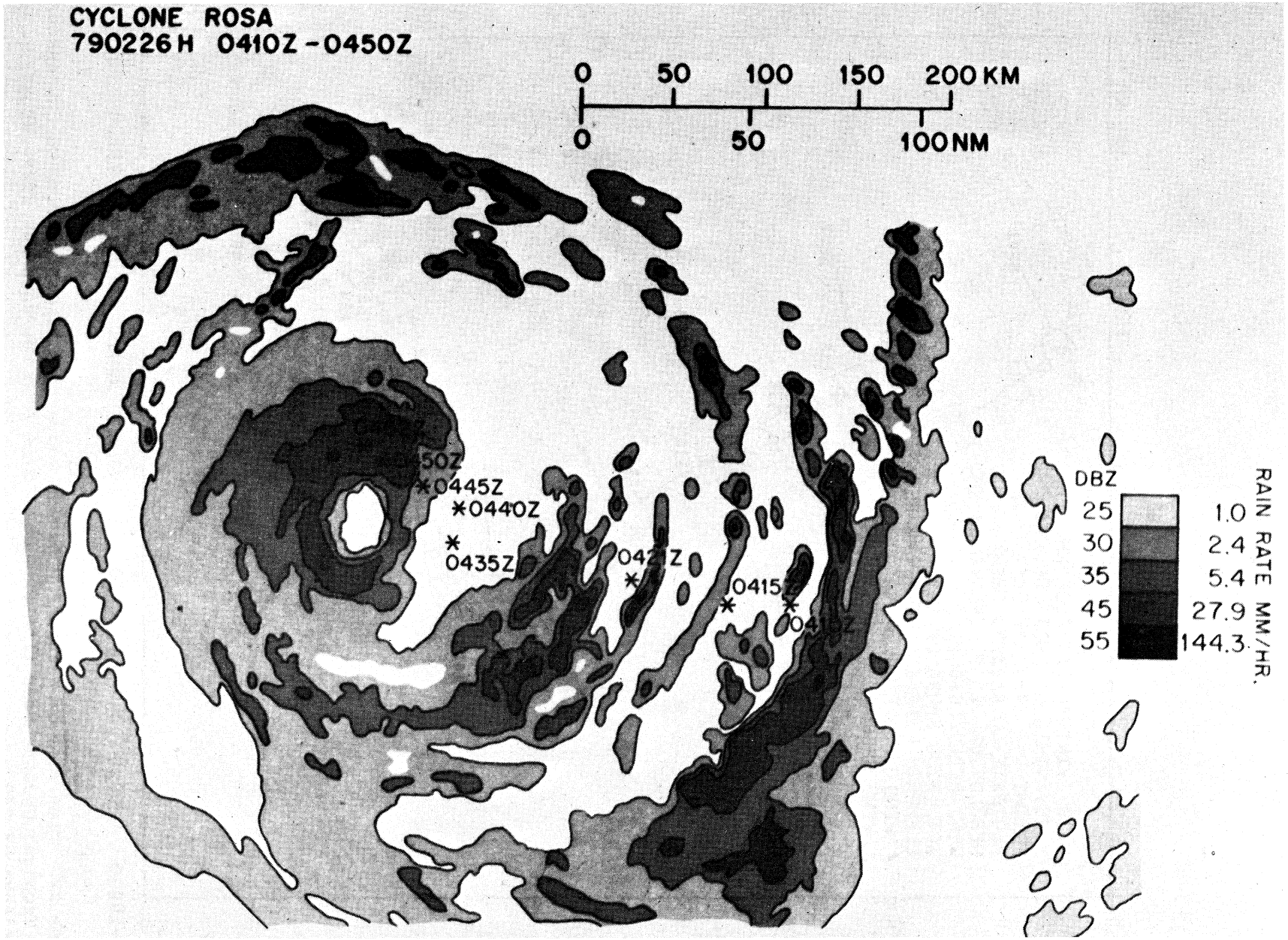

Figure 92. Digitized Plan Position Indicator radar depiction of Tropical Cyclone Rosa composited from 0410 Z to 0453 Z on February 26, 1979.

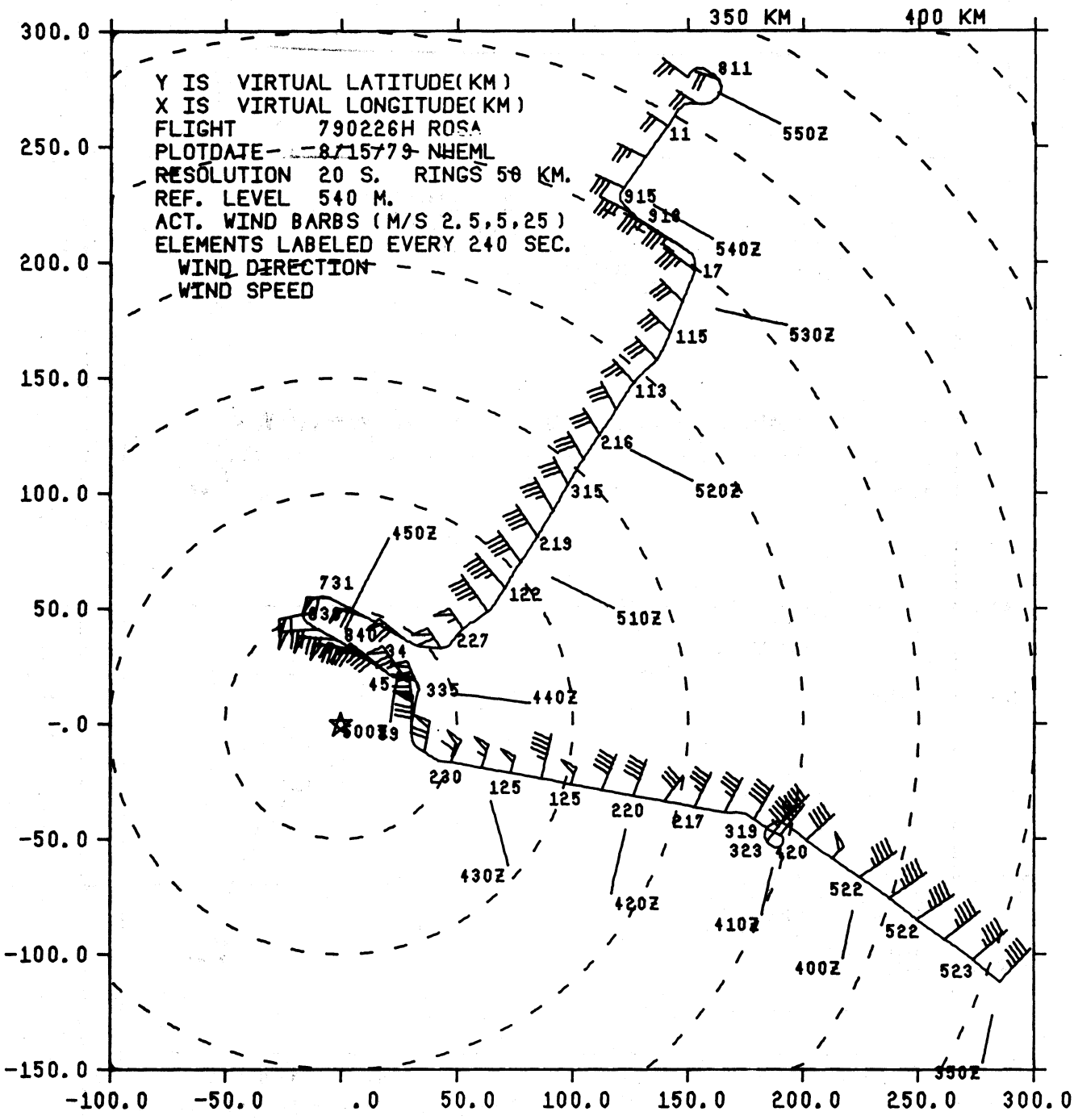

Figure 93. Plan view of aircraft position and actual winds relative to the center of Tropical Cyclone Rosa from 0350 Z to 0554 Z on February 26, 1979, at an altitude of 540 m.

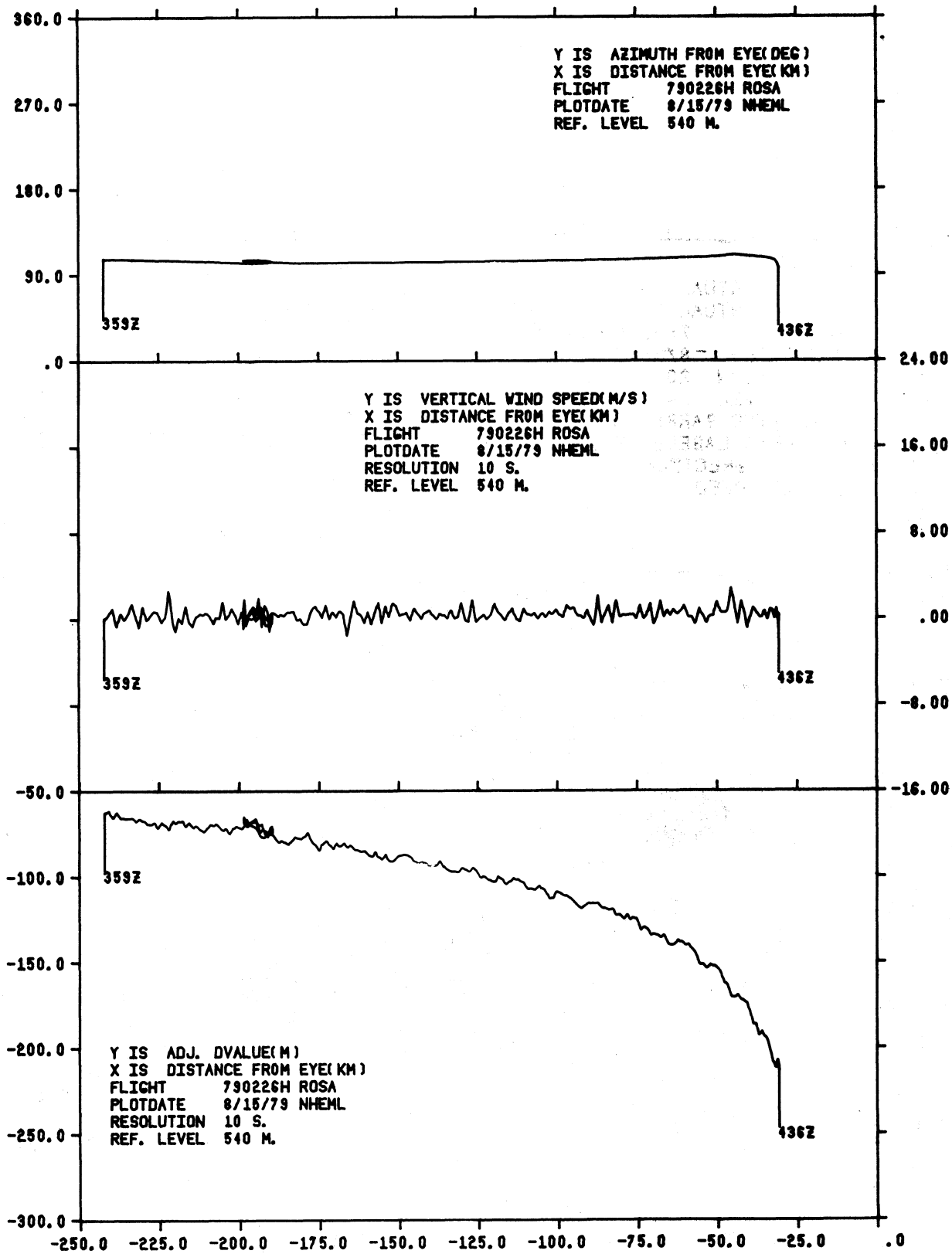

Figure 94. Profiles of the aircraft position (observation point) from the storm center in degrees (top), vertical wind speed (middle), and adjusted "D" value (bottom) versus radial distance from the storm center. Profiles correspond to the southeast-to-near-storm center pass in figure 93 from 0359 Z to 0436 Z with a reference pressure altitude of 540 m (950 mb).

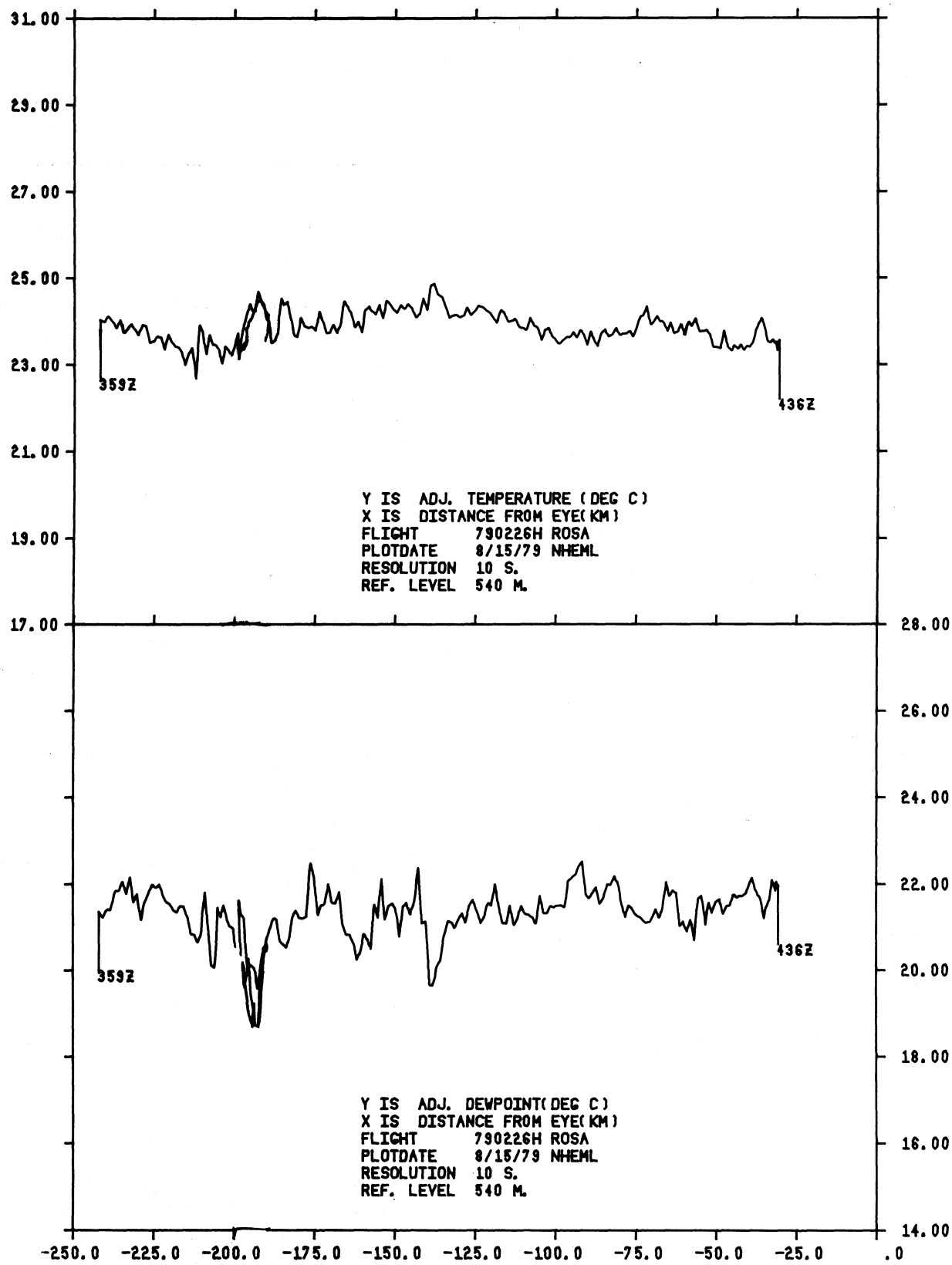

Figure 95. Same as figure 94, except for adjusted temperatures (top) and dew point temperatures (bottom).

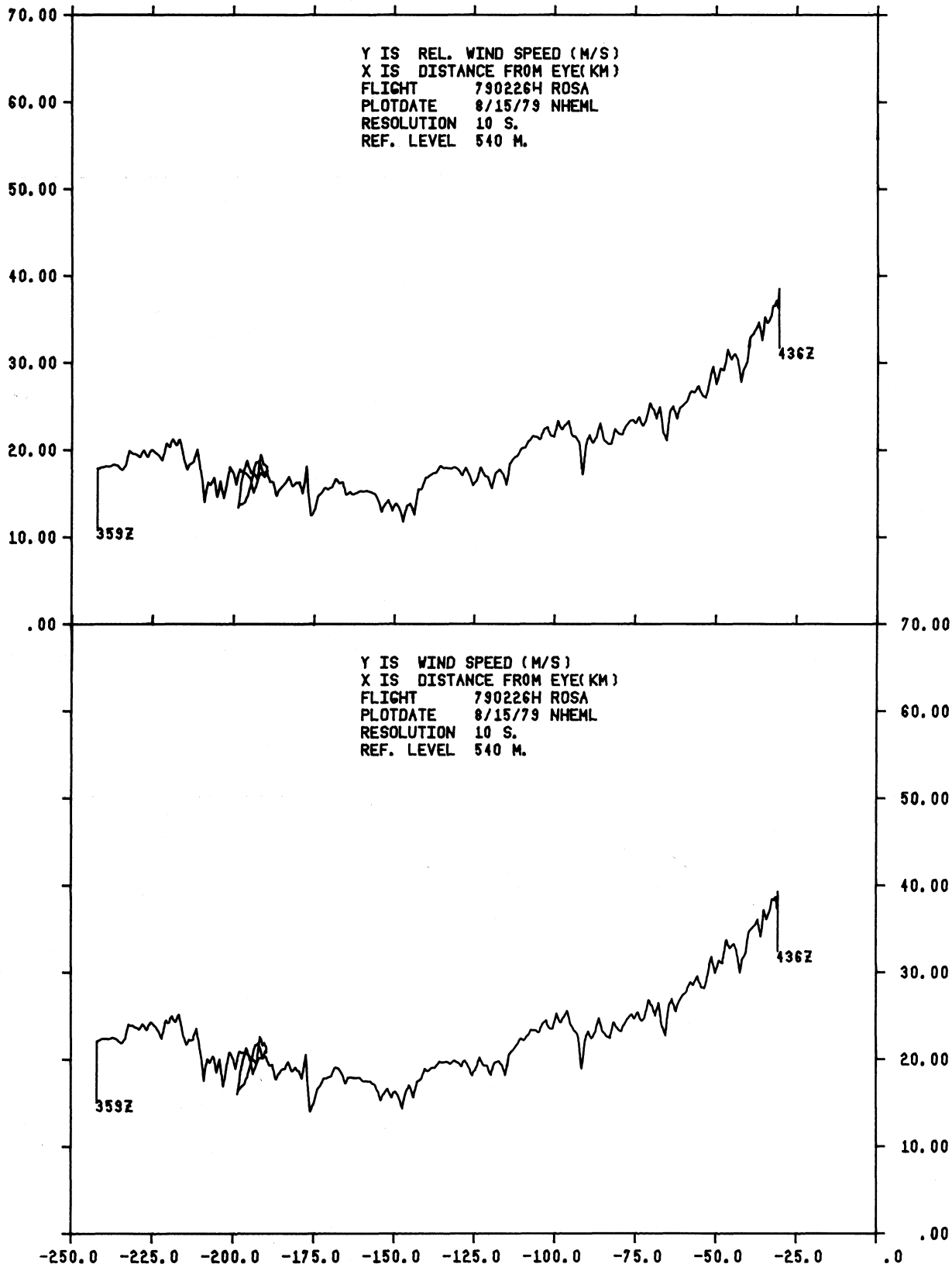

Figure 96. Same as figure 94, except for relative wind speed (top) and actual wind speed (bottom).

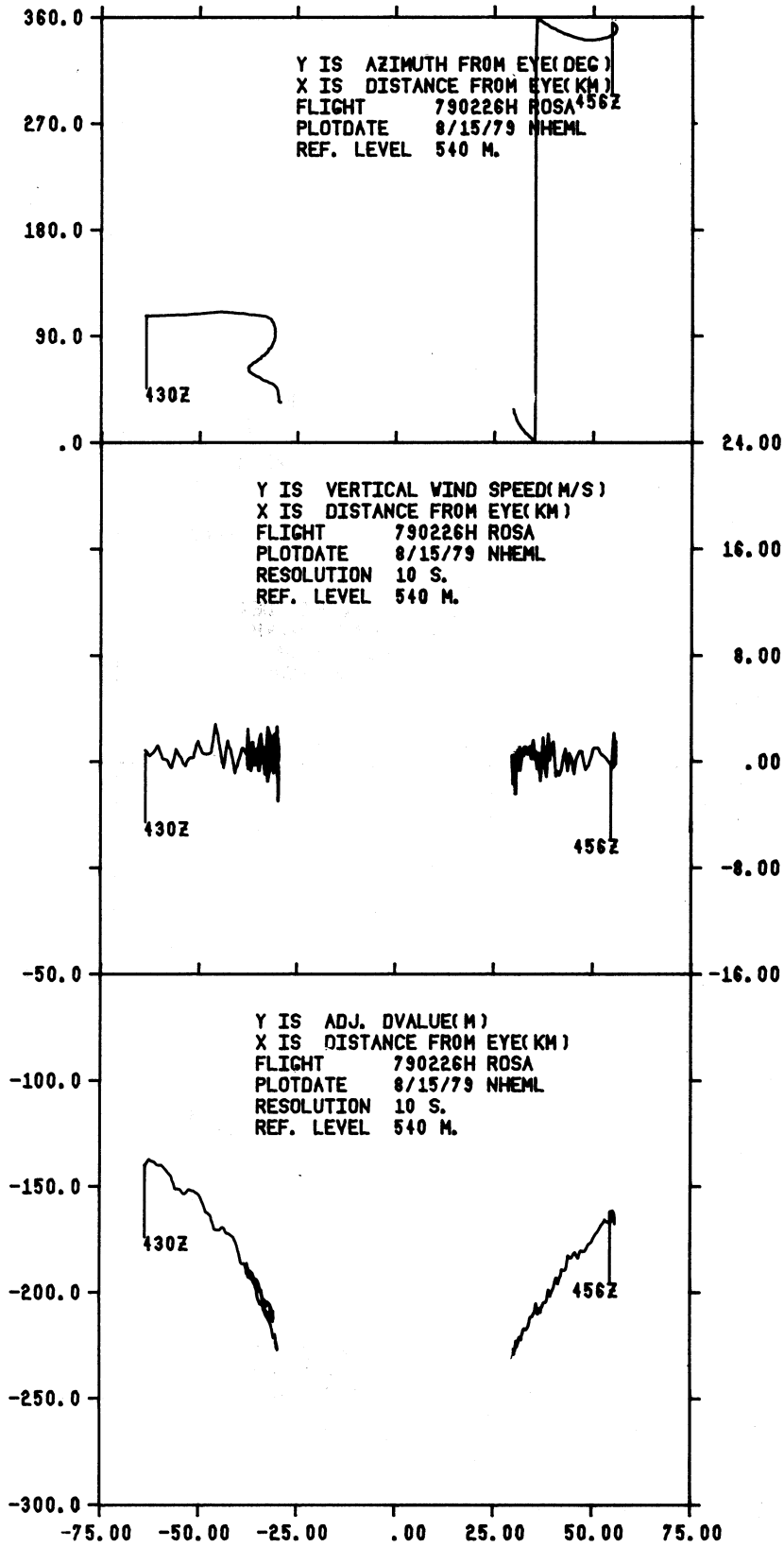

Figure 97. Same as figure 94, except for passes west and northwest of the storm center in figure 93 from 0430 Z to 0456 Z.

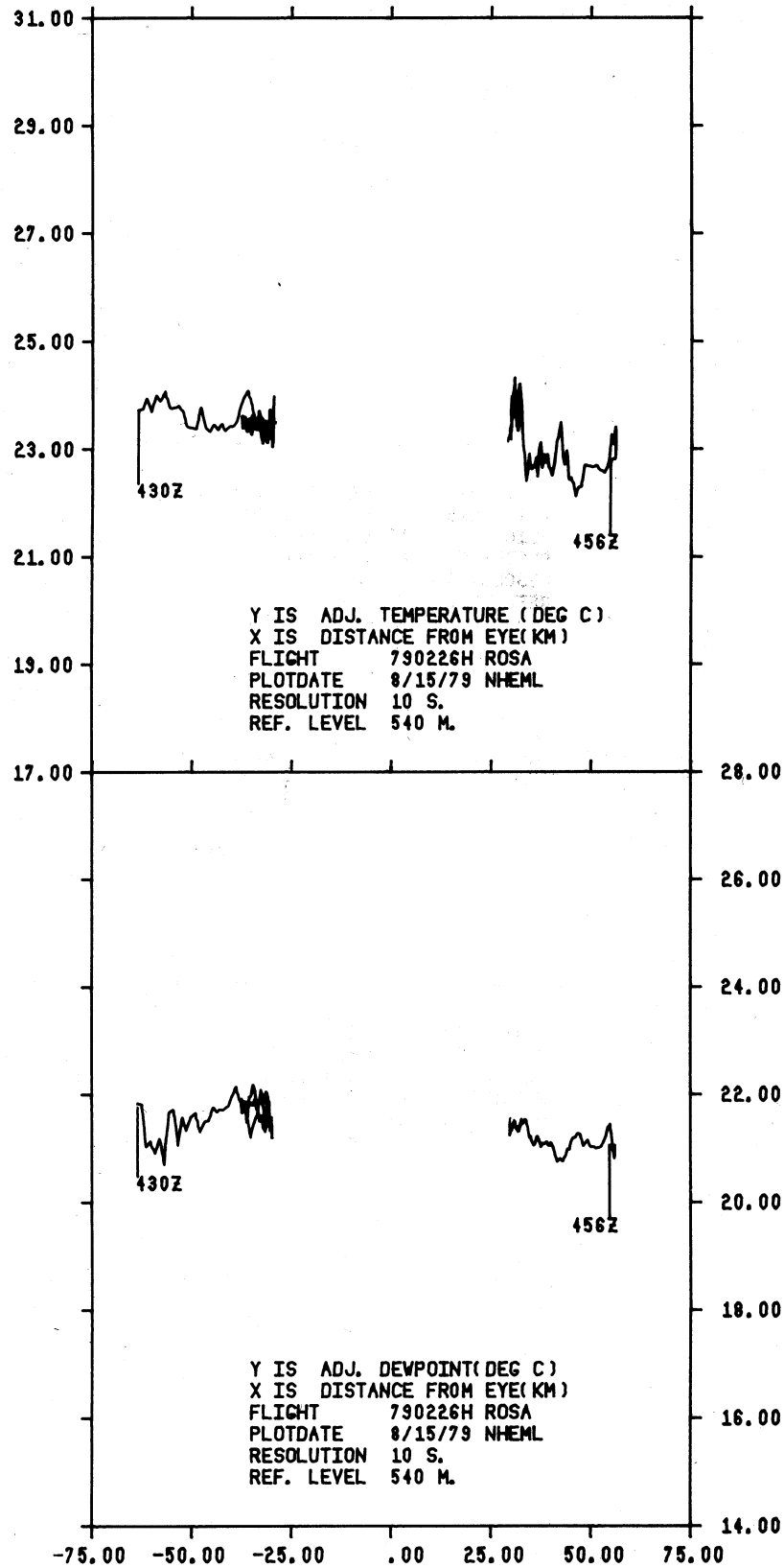

Figure 98. Same as figure 97, except for adjusted temperatures (top) and adjusted dew point temperatures (bottom).

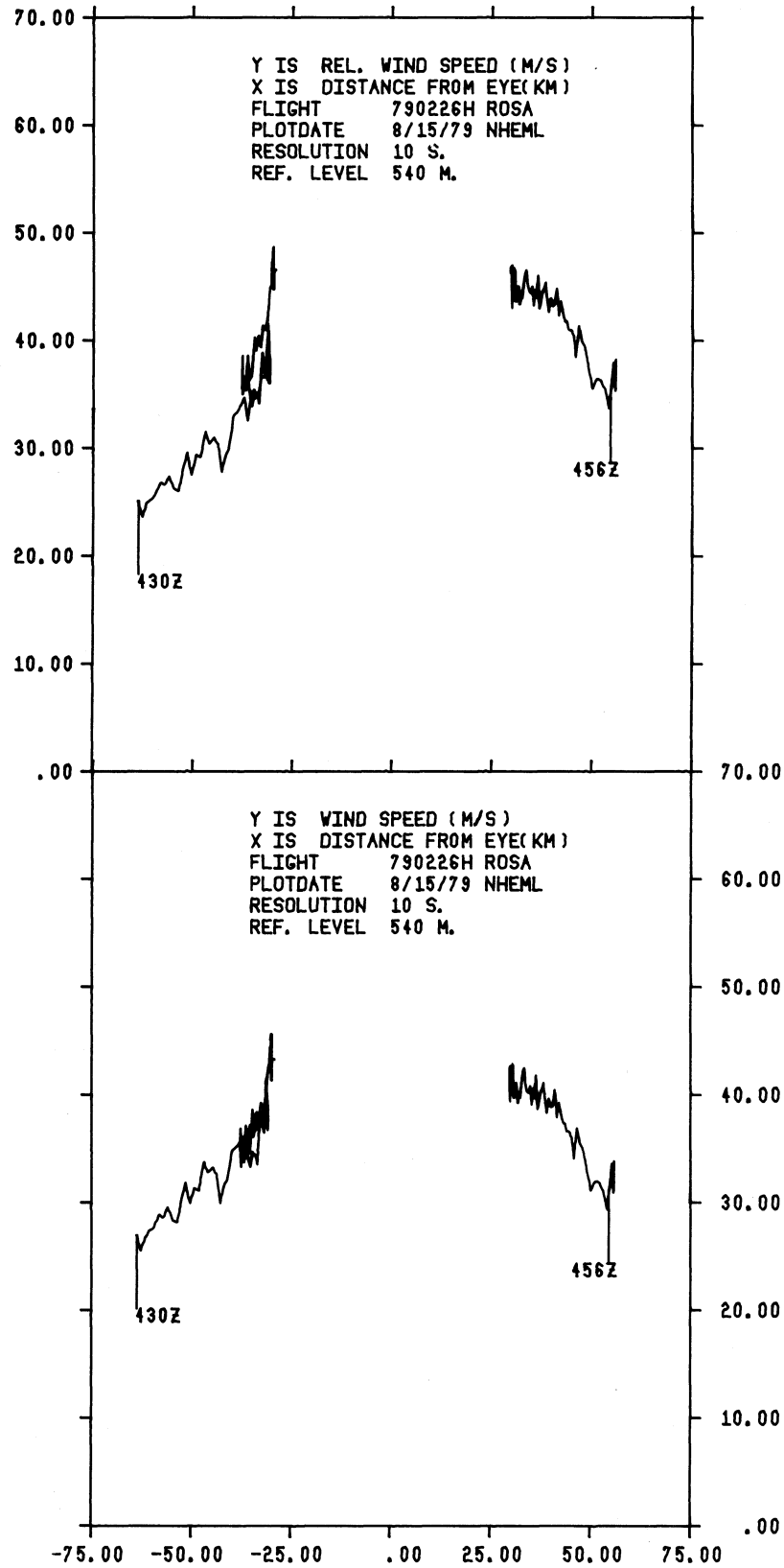

Figure 99. Same as figure 97, except for relative wind speed (top) and actual wind speed (bottom).

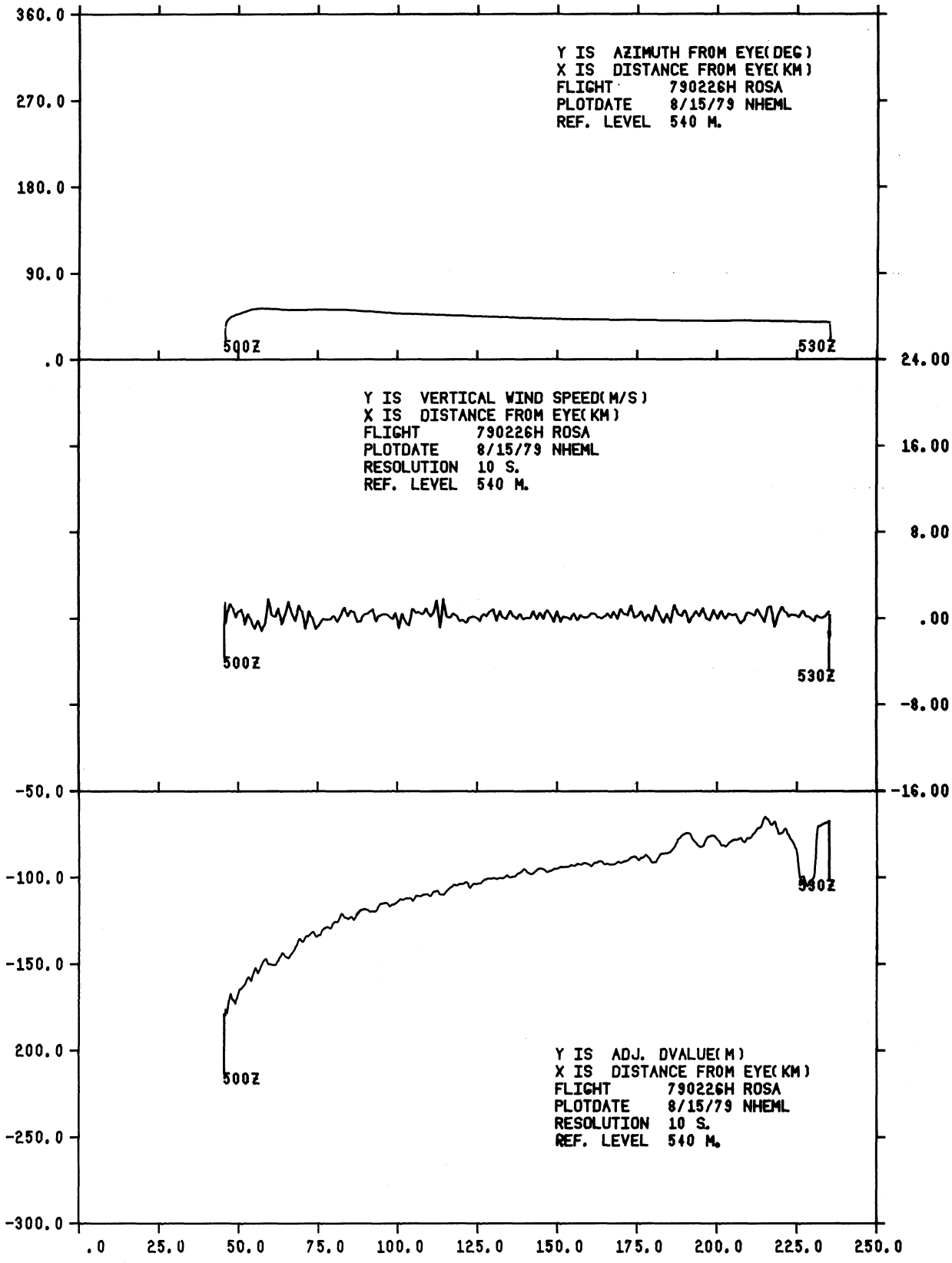

Figure 100. Same as figure 94, except for northeast pass from near the storm center in figure 93 from 0500 Z to 0530 Z.

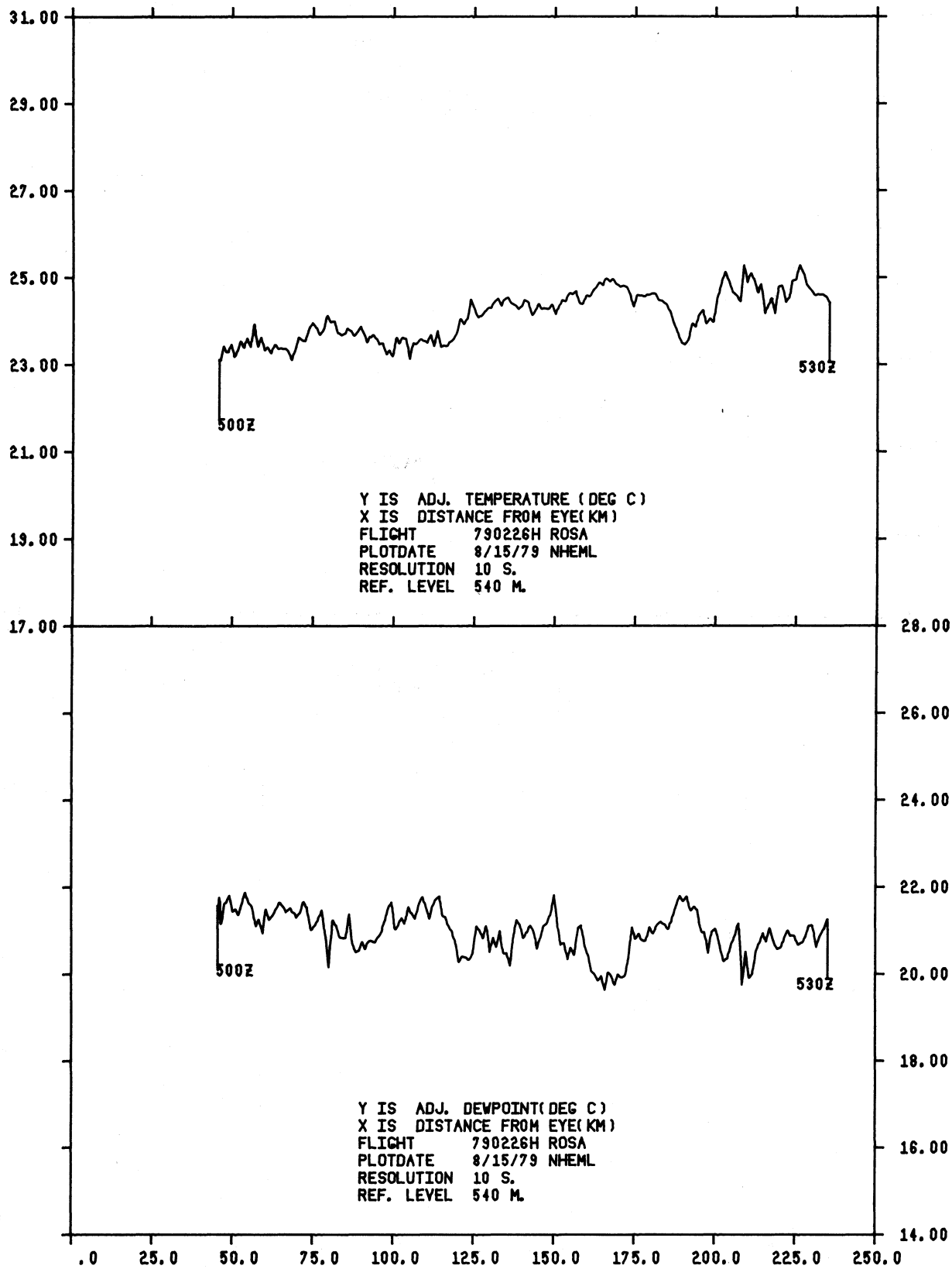

Figure 101. Same as figure 100, except for adjusted temperatures (top) and adjusted dew point temperatures (bottom).

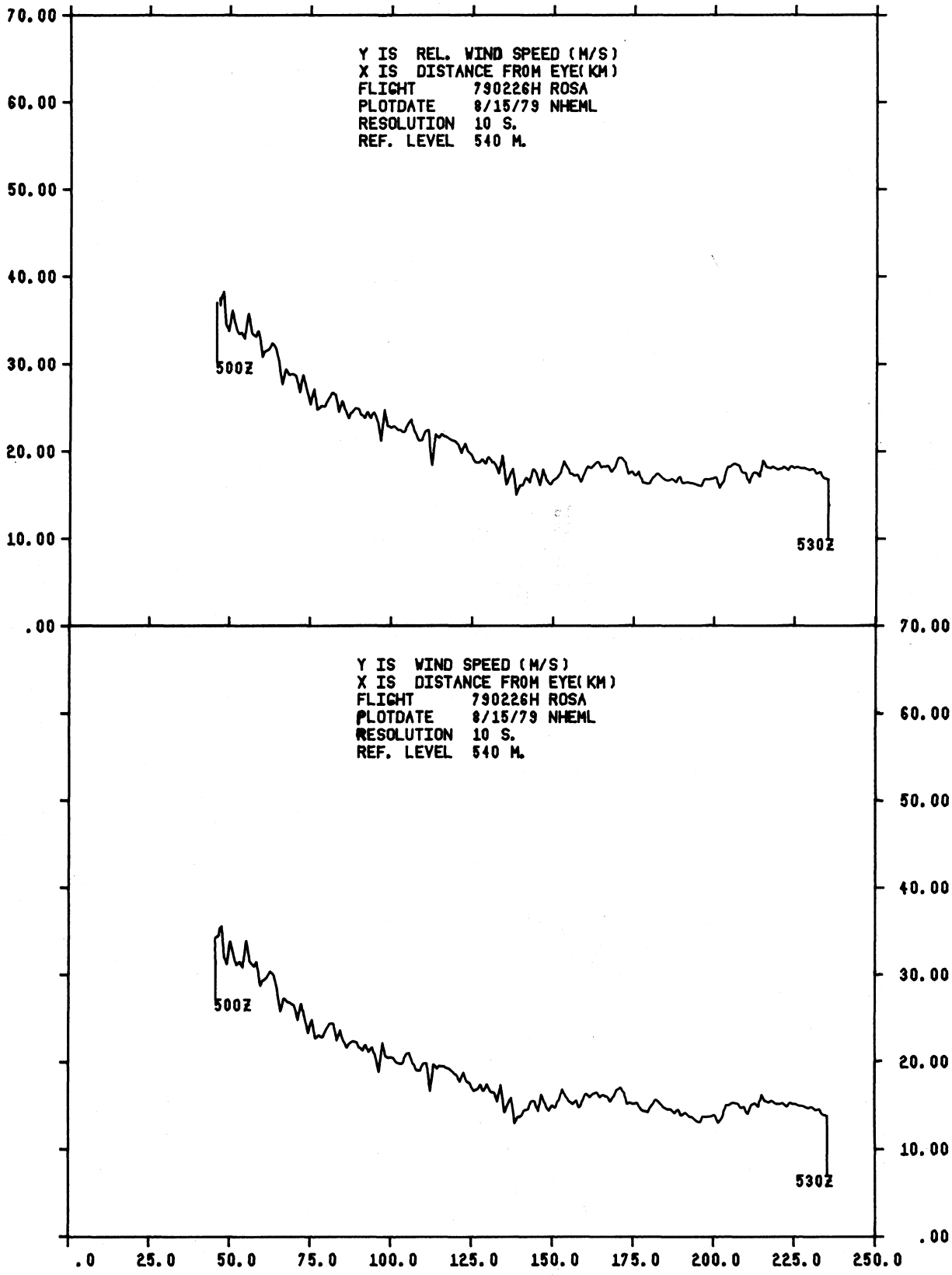

Figure 102. Same as figure 100, except for relative wind speed (top) and actual wind speed (bottom).

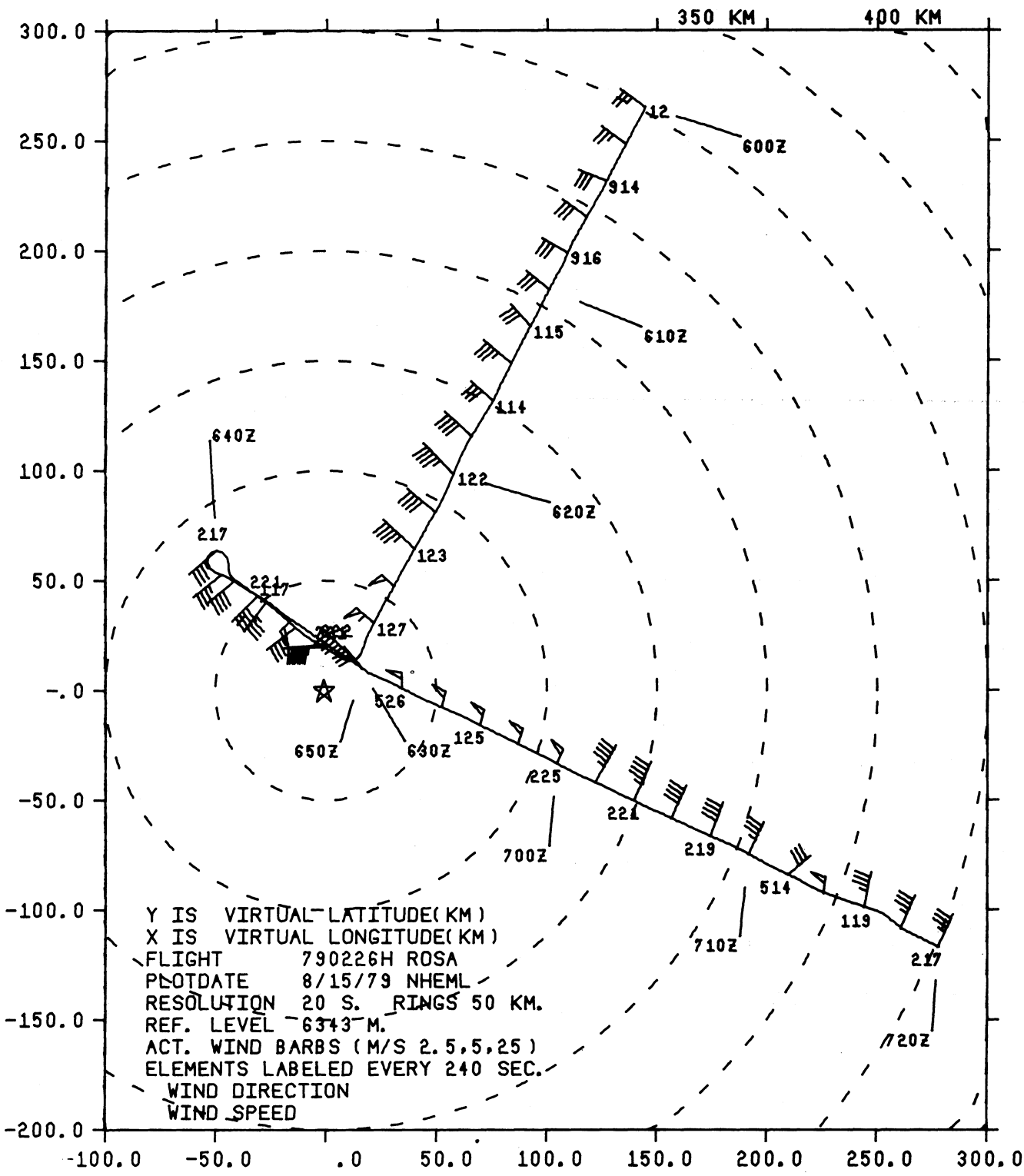

Figure 103. Plan view of aircraft position and acutal winds relative to the center of Tropical Cyclone Rosa from 0600 Z to 0720 Z on February 26, 1979, at a pressure altitude of 6343 m (450 mb).

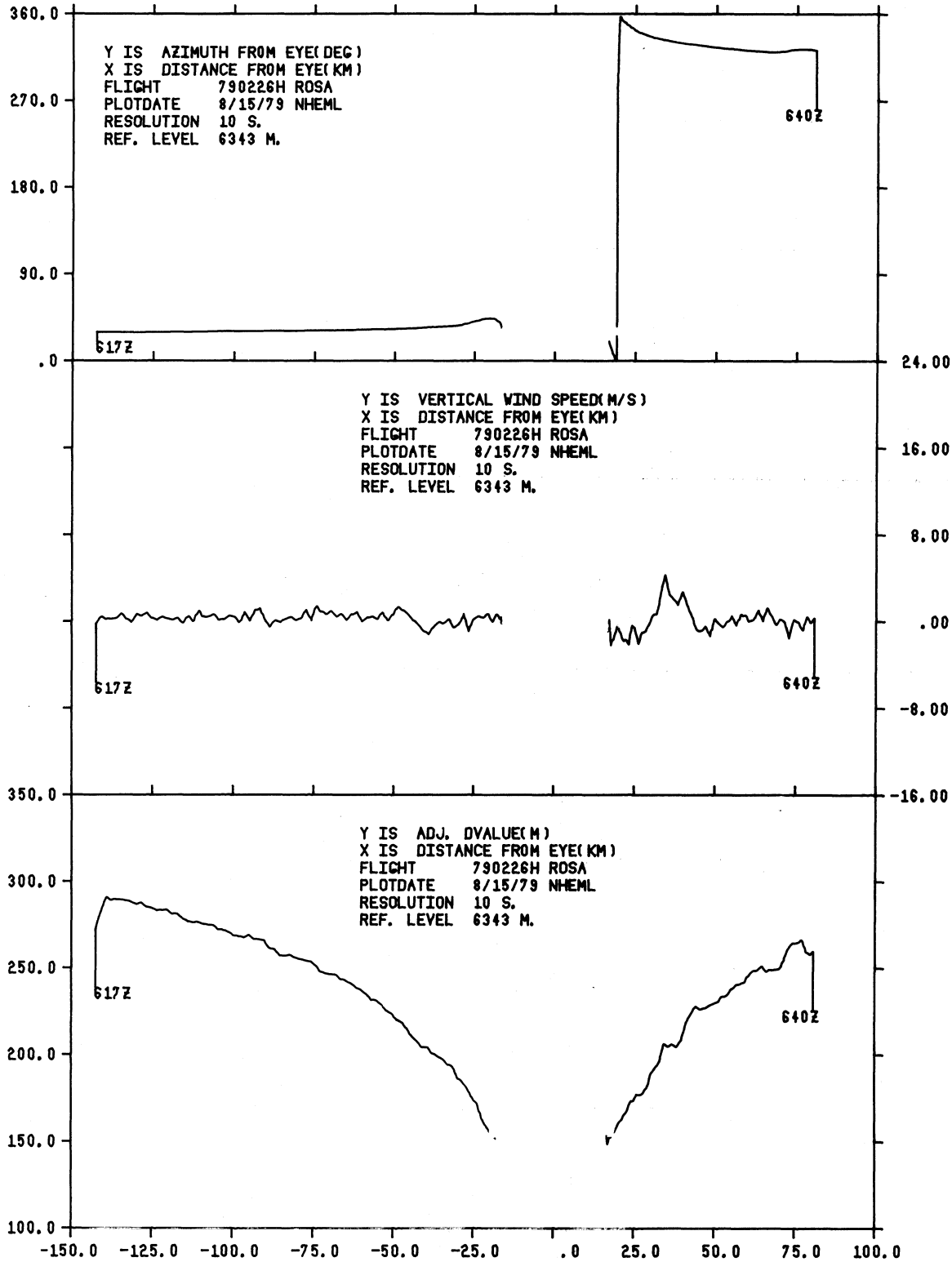

Figure 104. Profiles of the aircraft position (observation point) from the storm center in degrees (top), vertical wind speed (middle), and adjusted "D" value (bottom) versus radial distance from the storm center. Profiles correspond to the northeast-to-near-storm center, then to northwest pass in figure 103 from 0617 Z to 0640 Z.

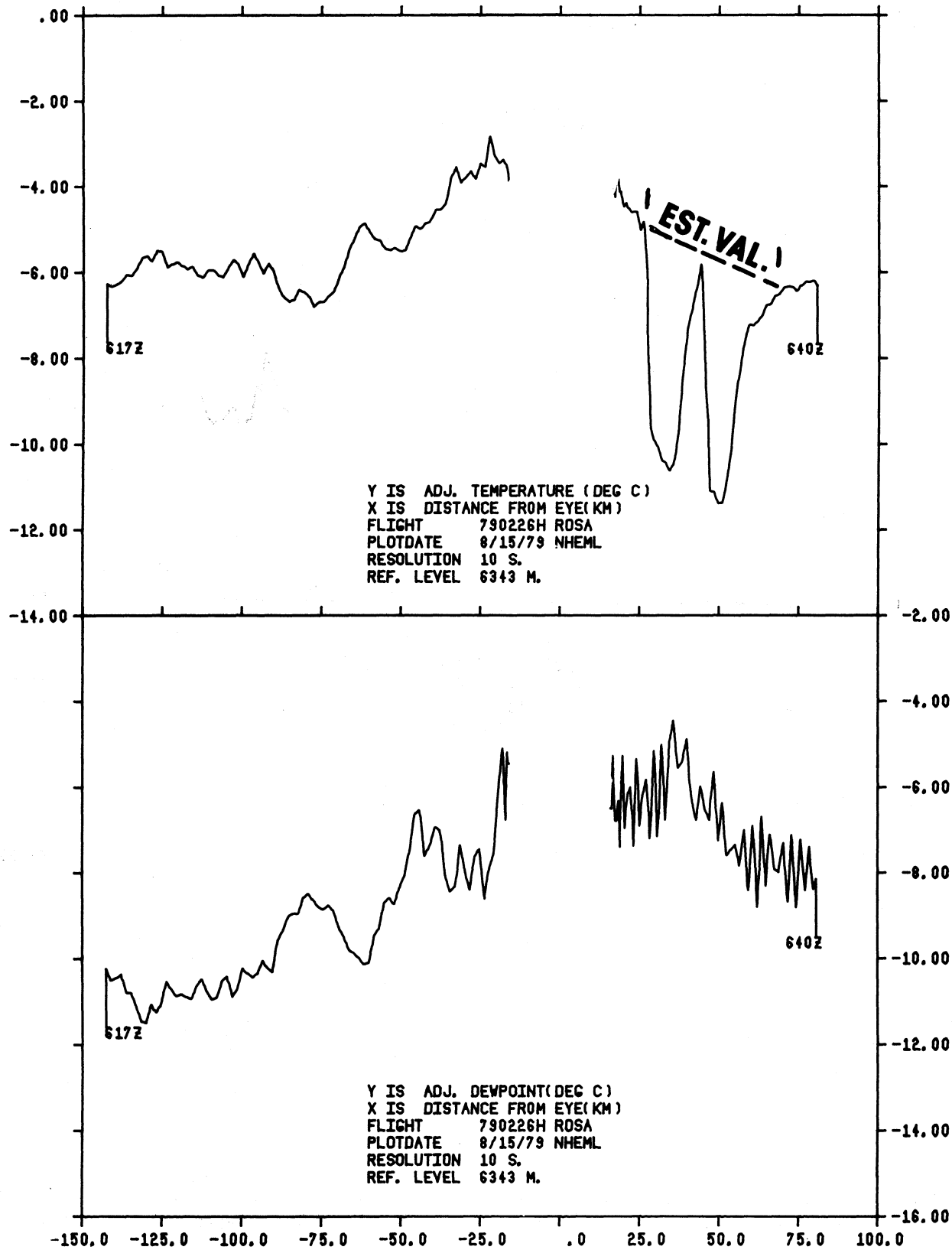

Figure 105. Same as figure 104, except for adjusted temperatures (top) and adjusted dew point temperatures (bottom). (Note comments in section 3.1.)

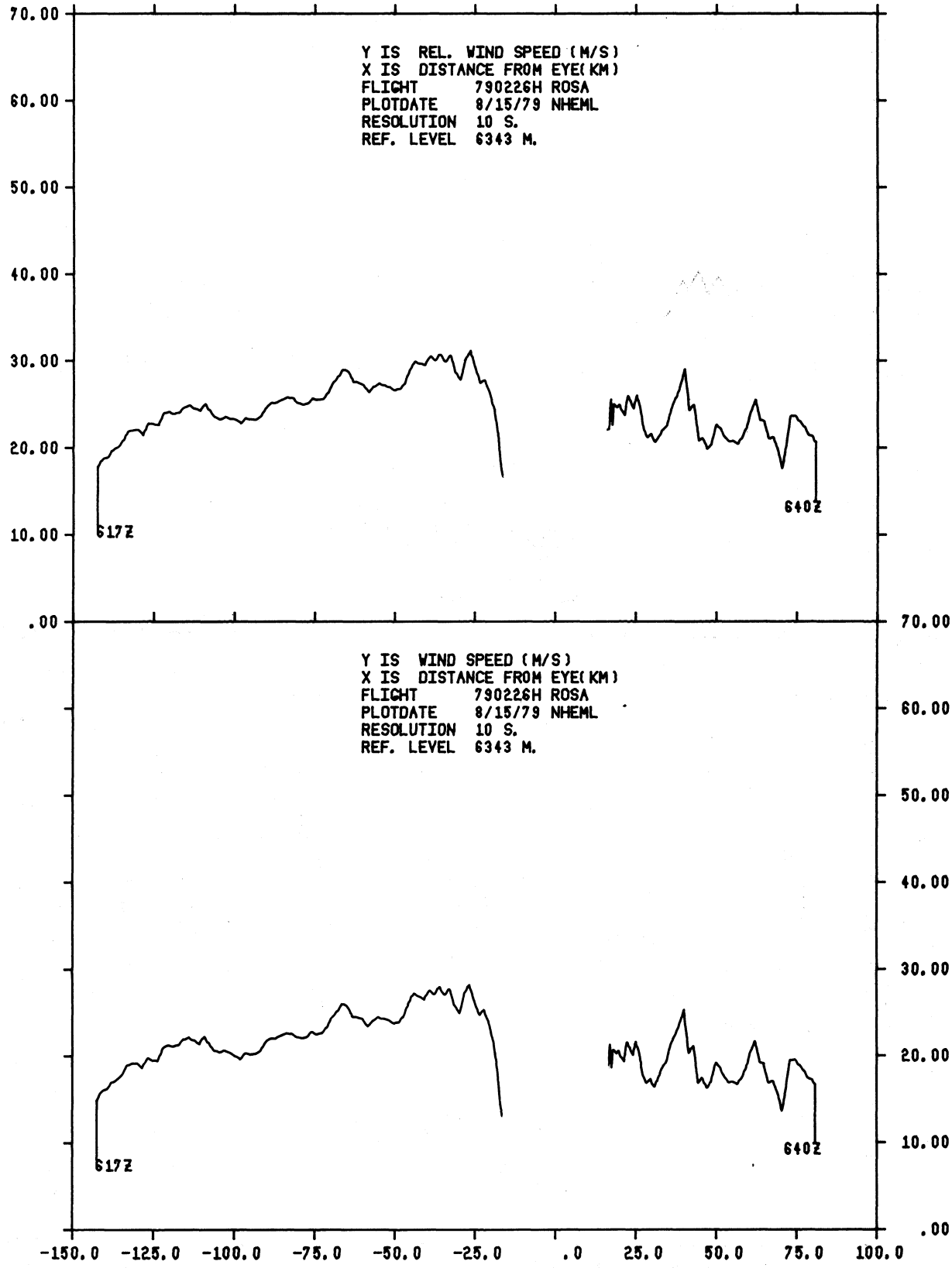

Figure 106. Same as figure 104, except for relative wind speed (top) and actual wind speed (bottom).

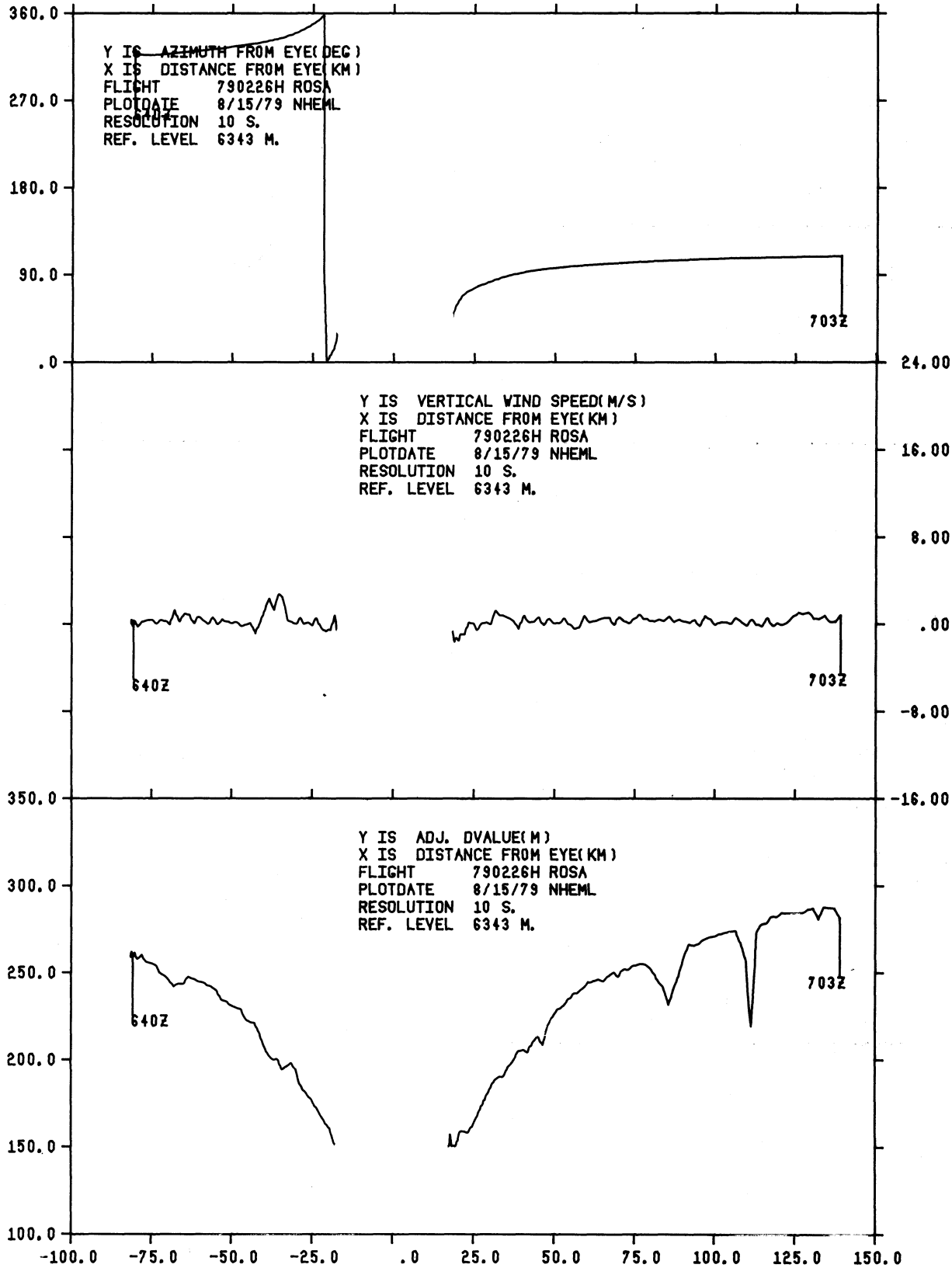

Figure 107. Same as figure 104, except for northwest to southeast pass in figure 103 from 0640 Z to 0703 Z.

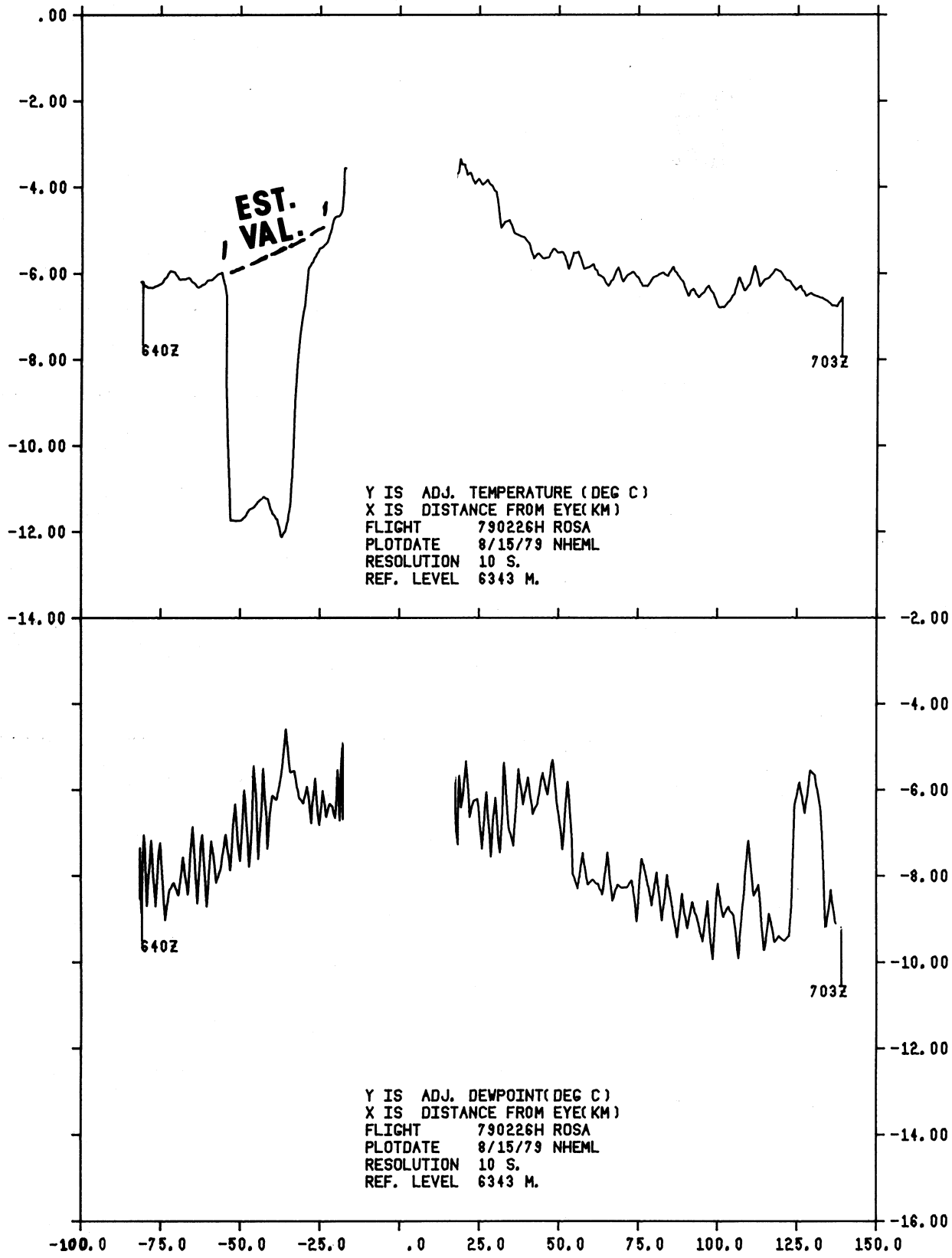

Figure 108. Same as figure 107, except for adjusted temperatures (top) and adjusted dew point temperatures (bottom). (Note comments in section 3.1.)

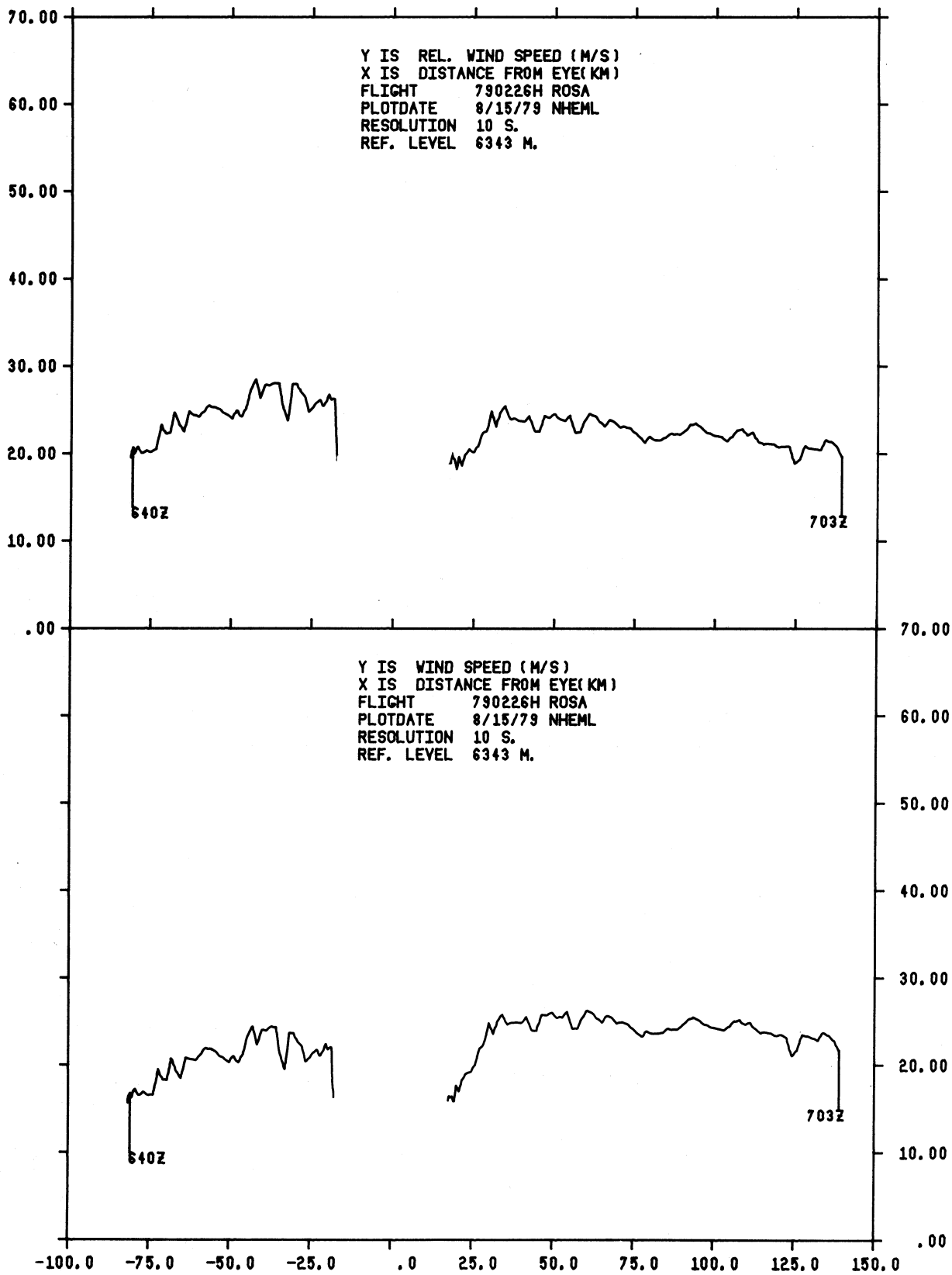

Figure 109. Same as figure 107, except for relative wind speed (top) and actual wind speed (bottom).

☆ U. S. GOVERNMENT PRINTING OFFICE 1981 - 777-002/1264 Reg. 8